FUNCTIONAL CHARACTERISTICS OF NITRIC OXIDE RECEPTOR ISOFORMS

Victoria Sarah Mary Wykes

A thesis presented to the University of London
for the degree of Doctor of Philosophy

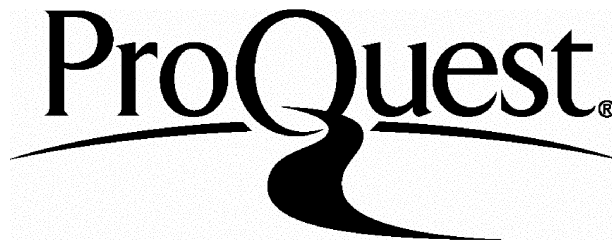The Wolfson Institute for Biomedical Research
University College London

ProQuest Number: U643331

ProQuest U643331

To Mum and Dad

Abstract

Physiologically, nitric oxide (NO) signal transduction occurs through activation of guanylyl cyclase (GC)-coupled receptors, which catalyse cGMP formation. The accumulation of cyclic guanosine 3'-5' monophosphate (cGMP) engages a number of downstream targets to trigger various biological effects, and is ultimately degraded by phosphodiesterases. Unlike with many neurotransmitter receptors, knowledge of the functional characteristics of the NO receptors is limited. The aim of the present research was to begin to address this deficiency by examining the kinetics of the activation of the native receptor and of heterologously-expressed receptor isoforms in intact cells or cell lysates.

In cells from a brain region that is enriched in the NO-cGMP signalling pathway, namely the striatum, NO-evoked cGMP accumulation was located in a neuronal subpopulation and the receptor activity displayed a rapidly-desensitizing profile similar to that found previously in cerebellar astrocytes. To determine if this pattern of activity is peculiar to particular receptors, the two known heterodimeric isoforms, $\alpha 1\beta 1$ and $\alpha 2\beta 1$, were expressed in COS-7 cells. NO was applied in fixed concentrations using a recently-developed method based on balancing NO release from a donor with NO inactivation by red blood cells. The two isoforms were highly sensitive to NO, half-maximal cGMP accumulation occurring at concentrations of about 1 nM in both cases. Furthermore, the NO-evoked activity of both receptors desensitized with very similar kinetics.

To circumvent limitations of the method for NO delivery used in the initial experiments, particularly problems of haemolysis, a new technique, in which a chemical NO scavenger was substituted for the red blood cells, was evaluated and found to be superior in several respects. The new method was used to determine the kinetic parameters of the receptor purified from bovine lung and, for comparison, cell lysates containing the two isoforms. Half-maximal activity in all cases required about 1 nM NO. In addition, the Hill slopes were close to 1, questioning a previous conclusion that receptor activation requires binding of more than one NO molecule per receptor. Contrasting with another previous study which suggested that membrane association sensitizes the receptor to NO, comparison of cytosolic and membrane preparations of two different tissues (cerebellum and platelets) revealed that their sensitivities to NO were indistinguishable when studied using fixed concentrations.

Acknowledgements

Table of contents

List of figures

List of tables

Abbreviations

aCSF	Artificial cerebral spinal fluid
ACh	Acetylcholine
ADP	Adenosine diphosphate
AMPA	α-amino-3-hydroxy-5-methylisoxazole-4-propionic acid
ARL-17477	α-fluro-N-(3-(aminomethyl)-phenyl)-acetamidine
ATP	Adenosine triphosphate
BCA	Bicinchonic acid
BH_4	Tetrahydrobiopterin
BSA	Bovine serum albumin
Ca^{2+}	Calcium
CaM	Calmodulin
cAMP	Cyclic adenosine 3'-5' monophosphate
cDNA	Complementary/copy deoxyribonucleic acid
CFTR	Cystic fibrosis transmembrane conductance regulator
cGK / PKG	cGMP-dependent protein kinase
cGMP	Cyclic guanosine 3'-5' monophosphate
CNG	Cyclic nucleotide gated
CNS	Central nervous system
COS-7	African green monkey kidney fibroblast cells
CPTIO	Carboxy-2-phenyl-4,4,5,5-tetramethylimidazoline-1-oxyl-3-oxide
DAPI	4',6 diamidino-2-phenylindole
DEA/NO	2-(N,N-Diethylamino)-diazenolate-2-oxide
DETA/NO	(Z)-1-[2-(2-Aminoethyl)-N-(2-ammonioethyl)amino]diazen-1-ium-1,2-diolate
dH_2O	Distilled water
DMEM	Dulbecco's modified Eagles Medium
DMSO	Dimethylsulphoxide
DNA	Deoxyribonucleic acid
DTT	Dithiothreitol
EC_{50}	Effective concentration for 50% maximal response
E.coli	*Escherichia coli*
EDRF	Endothelium-derived relaxing factor
EDTA	Ethylenediaminetetraacetic acid
EGTA	Ethylene glycol-bis(beta-aminoethyl ether)-N,N,N',N'-tetraacetic acid
EHNA	Erythro-9-(2-hydroxy-3-nonyl_adenine hydrochloride
eNOS	Endothelial nitric oxide synthase
FAD	Flavin adenine dinucleotide
FITC	Fluorescein isothiocyanate
FMN	Flavin mononucleotide
GABA	γ-aminobutyric acid
GAF	cGMP-regulated PDEs, cyanobacterial *Anabaena* adenylate cyclase, Fh1A protein (a bacterial transcriptional factor)
GC	guanylate cyclase
GDP	Guanosine diphosphate
GFAP	Glial fibrillary acid protein
GTP	Guanosine triphosphate
Hb	Haemoglobin
HEPES	N-(2-hydroxyethyl)piperazine-N'-(2-ethanesulfonic acid)
His	Histidine

IBMX	3-Isobutyl-1-methylxanthine
iNOS	Inducible nitric oxide synthase
IP$_3$R	Inositol 1,4,5-trisphosphate receptor
Kd	Equilibrium dissociation constant
Km	Michaelis constant
KO	Knock out
Kp	Apparent Michaelis constant
L-NA	L-Nitroarginine
LPS	Lipopolysaccharide
LTD	Long term depression
LTP	Long term potentiation
L-VNIO	N5-(1-imino-3-butenyl)-L-ornithine
MAP-2	Micro-tubule associated protein 2
Mb	Myoglobin
MPTP	1-methyl 4-phenyl-1,2,3,6-tetrahydropyridine
mRNA	Messenger ribonucleic acid
NADPH	Reduced nicotinamide adenine dinucleotide phosphate
NANC	Non-adrenergic, non-cholinergic
NeuN	Neurone specific nuclear protein
NMDA	*N*-methyl-D-aspartate
nNOS	Neuronal nitric oxide synthase
NO	Nitric oxide
NO$_{GC}$R	Nitric oxide-guanylyl cyclase coupled receptor
NOS	Nitric oxide synthase
ODQ	1-*H*-[1,2,4]oxadiazolo[4,3-*a*]quinoxalin-1-one
PBS	Phoshate buffered saline
PSD	Post-synaptic density protein
PDE	Cyclic 3'-5' mononucleotide phosphodiesterase
PDZ	PSD-95 discs large/Z0-1 homology
RBC	Red blood cell
sGC	Soluble guanylyl cyclase
SOD	Superoxide dismutase
TAE	Tris-acetate-EDTA
TBS	Tris-buffered saline
Tris	Trichloroacetic acid
TRITC	Tetramethyl rhodamine
VASP	Vasodilator stimulated phosphoprotein
vd	Rate of degeneration
Vmax	Maximal apparent rate of enzyme activity
Vp	Apparent maximal rate of enzyme activity
vs	Rate of synthesis
1400W	(+)cis-4-methyl-5-pentylpyrollidin-2-imine
YC-1	3-(5-hydroxymethyl-2-furyl)-1-benzylindazole

Chapter 1

General introduction to the NO-cGMP signalling pathway

1.1 Historical background

For decades NO gas was considered simply as a common air pollutant and one of the components of acid rain. However, during the late 1980's the biological significance of NO was realised. Research in three separate areas led to the discovery that NO was a mechanism for cell signalling in mammalian systems, and in 1992 the journal Science declared NO the "molecule of the year" (Koshland, Jr., 1992). The importance of NO was highlighted in 1998, when the Nobel Prize in Physiology and Medicine was awarded to three scientists who contributed to the discovery of this signalling molecule (R.F. Furchgott, L.J. Ignarro and F. Murad). The role of NO in both physiological and pathological processes is currently being assessed, and clinical studies are increasingly involved in the search for new strategies for therapeutics.

Soluble guanylyl cyclase (White and Aurbach, 1969) and its product cGMP (Ashman et al., 1963) were identified in the 1960s, and later shown to be activated by exogenously applied NO gas and by NO released from vasodilators such as nitroglycerine and nitroprusside (Katsuki et al., 1977). However at this point NO was not considered to play a role in biological systems. After the discovery that endogenously synthesised NO was a signalling molecule, soluble guanylyl cyclase was identified as the major physiological NO receptor. Since its initial discovery, the enzyme has been found to associate with cellular membranes (Arnold et al., 1977; Gibb et al., 2003; Russwurm et al., 2001; Zabel et al., 2002). Thus the original name of soluble guanylyl cyclase is mis-leading, and so from here on the enzyme will be termed the NO-guanylyl cyclase-coupled receptor ($NO_{GC}R$).

The aim of this chapter is to:

-provide an overview of the cross-disciplinary approaches leading to the identification of NO.

-outline the structural and functional characteristics of NO and its major effector $NO_{GC}R$.

-discuss the physiological importance of this signalling pathway.

Immunology

Early studies indicated that mammals excrete more nitrate than they ingest. This nitrate biosynthesis was initially attributed to microbe metabolism in the intestinal tract (Green et al., 1981a; Tannenbaum et al., 1978). Further studies demonstrated that both germ-free and conventional rats generated nitrate (Green et al., 1981b). During a metabolic study, one of the human subjects consuming a low nitrate diet developed fever and diarrhoea (Wagner and Tannenbaum, 1983). Their urinary nitrate excretion increased to a level 10 fold higher than that measured prior to the onset of symptoms, and it was later shown that rats injected with agents which trigger an immune response (e.g. bacterial lipopolysaccharide (LPS)) developed a similar increase in urinary nitrate excretion (Wagner et al., 1983). Experiments using cultured cells, and a LPS-stimulated mouse model using several mouse strains with specific genetic immunocellular defects, demonstrated that macrophage cells were the major source of nitrate, and that this process may be involved in cytotoxicity (Stuehr and Marletta, 1985). Macrophage cytotoxicity was later reported to require L-arginine (but not D-arginine), and generate citrulline as a co-product of nitrite synthesis. This synthesis was found to be inhibited by the arginine analogue L-NMMA (Hibbs, Jr. et al., 1987). The mechanism by which arginine was converted to citrulline and nitric oxide was not identified until later, as a result of research in a different field.

Regulation of vascular tone

On January 18, 1879, the Lancet published an article entitled "Nitro-glycerine as a remedy for angina pectoris" (Murrel, 1879). The author, William Murrell, a physician lecturer at Westminster hospital described the therapeutic properties of this compound, already well known at that time as an explosive. One of his colleagues, Lauder Brunton, had discovered some years before that amyl nitrite inhaled during an anginal attack provided immediate relief from pain. It took more than a century before the mechanism of action was determined.

Ignarro and his collegues reported that NO and nitroprusside caused relaxation of vascular smooth muscle and that the muscle produced cyclic GMP (cGMP; Gruetter et al., 1979). Furthermore, they demonstrated that in order to produce vasodilation, organic nitrates and nitrites needed to be metabolised to NO and form nitrosothiols (Ignarro et al., 1981). Despite discussing at the time that NO would be an ideal candidate as an endogenous regulator of blood flow this theory was rejected as it was thought that NO was not synthesised by mammalian cells.

13

A serendipitous finding led to the first report that relaxation responses of vascular smooth muscle required the presence of an intact endothelium. Strips of rabbit thoracic aorta in which the endothelium were rubbed during preparation, did not respond to acetylcholine (ACh). In contrast, ACh evoked a concentration-dependent relaxation of rabbit aorta rings, in which the endothelium remained intact (Furchgott and Zawadzki, 1980). This relaxation was blocked by atropine implying that ACh was acting via endothelial cell ACh receptors to stimulate the production of an endothelium-derived relaxing factor (ERDF) that could diffuse to the smooth muscle and initiate relaxation.

During the early 1980's experiments established the similarities between the properties of NO and those of EDRF. In 1987 two studies were published, providing evidence that NO was EDRF. EDRF derived from the pulmonary artery by bioassay, had identical vasodilating properties to NO applied directly to the vascular smooth muscle (Ignarro et al., 1987). Endothelial cells in culture were shown to release an unstable vasorelaxant molecule in response to ACh, with identical biological activity to EDRF. Using a chemiluminescence technique it was demonstrated that the vasoactive molecule was either NO or NO_2^- (Palmer et al., 1987). Shortly thereafter, mass spectrometry studies using ^{15}N-labelling showed that the NO is derived from the terminal guanidine nitrogen of L-arginine (Palmer et al., 1988b), and that vascular endothelial cells can synthesise NO (Palmer et al., 1988a). Since then NO synthesis has been shown to play an important role in regulation of vascular tone under normal physiological conditions.

Neuronal signalling

Studies in the peripheral nervous system showed that electrical field stimulation of nerves in the rodent anococcygeus and bovine retractor penis muscles (in the presence of adrenergic blockers) caused the muscles to relax. This effect could not be attributed to any of the known non-adrenergic, non-cholinergic (NANC) transmitters (Gillespie and Martin, 1980). Once EDRF had been identified as NO and NOS inhibitors became available to demonstrate that a biological response was mediated by NO, it was demonstrated that the electrical stimulation of these NANC nerves was activating NOS and that NO was mediating the inhibitory response in these muscles (Gillespie et al., 1989).

The discovery that NO can also act as a neuronal messenger in the brain came from studies in the Garthwaite laboratory. It had long been known that glutamate evoked large increases in

cGMP concentration in the CNS (Ferrendelli et al., 1974; Garthwaite and Balazs, 1981). These increases were particularly prominent in the cerebellum, and were primarily mediated by a specific population of glutamate receptor (Garthwaite and Balazs, 1981). N-methyl-D-aspartate (NMDA) receptor activation was found to induce the release of a diffusible factor that had remarkable similarities to EDRF, and that this intracellular messenger mediated the activation of guanylyl cyclase (Garthwaite et al., 1988). The cells on which the NMDA receptors were localised were found to be different from those in which cGMP was synthesized (Garthwaite and Garthwaite, 1987). This was the first description of the intercellular molecule that links NMDA activation to cGMP production and established NO as a signalling molecule in the brain.

1.2 Nitric Oxide Synthases

Isoforms and expression

Nitric oxide is produced by a haem containing enzyme termed nitric oxide synthase (NOS) which was first isolated and purified from rat brain (Bredt and Snyder, 1990). Mammalian systems contain three distinct isoforms. In mammals, the NOS isoforms exhibit about 60% homology, and are classified according to the cell type or conditions under which they were first identified. The NOS isoforms are products of different genes, have different cellular locations and biochemical characteristics summarised in Table 1.

Isoform	Neuronal NOS (nNOS)	Inducible NOS (iNOS)	Endothelial NOS (eNOS)
Human chromosomal location	12	7	17
Cellular location	Neurones	Macrophages	Endothelial cells
Subcellular location	Cytosolic/ particulate in varying proportions	Predominantly cytosolic	Predominantly particulate
Protein size (kDa)	161	133	131
Expression	Constitutive	Inducible	Constitutive
Ca^{2+} dependence	Yes	No	Yes

Table 1: Characteristics of the nitric oxide synthase isoforms

Neuronal NOS (nNOS) is predominantly expressed in the central and peripheral nervous system but also in other tissues such as skeletal tissue, macula-densa, and the placenta. During excitatory neurotransmission in the brain, the post-synaptically located NMDA-subtype of glutamate receptors are activated triggering Ca^{2+} influx into the cell (Collingridge and Bliss, 1995), so activating nNOS. Phosphorylation of nNOS at Ser^{847} by calmodulin (CaM) kinases results in a decrease in enzyme activity (Komeima et al., 2000). NO may act as a retrograde messenger to produce sustained glutamate release from pre-synaptic nerve terminals resulting in long-term potentiation (LTP) in brain areas such as the hippocampus (Bon et al., 1992; Garthwaite and Boulton, 1995). LTP is a form of synaptic plasticity in which neurotransmission is enhanced for hours or days in response to repetitive stimulation of pre-synaptic terminals. This phenomenon is thought to be involved in learning and memory (Huang, 1997).

Endothelial NOS (eNOS) is predominantly found in vascular endothelial cells where it is activated by hormones or in response to physical stimuli such as blood flow and shear stress (Ayajiki et al., 1996). This triggers phosphorylation of Ser^{1179} within eNOS by protein kinase Akt (Dimmeler et al., 1999), and results in a calcium-independent increase in enzyme activity (Corson et al., 1996). The NO produced by the endothelium relaxes the vasculature and inhibits adhesion and aggregation of platelets (Moncada et al., 1991).

The inducible isoform (iNOS) is not constituently expressed. *De novo* synthesis is triggered by inflammatory mediators (e.g. interferon, tumour necrosis factor) and bacterial toxins (LPS), in a number of cell types including macrophages, smooth muscle, cardiomyocytes and microglia. iNOS also has a CaM-binding site, and binds CaM tightly even in the presence of low levels of Ca^{2+}. Thus iNOS is primed for activity and acts as a high-output system generating substantial amounts of NO required for killing bacteria, viruses and other pathogens. Over expression of iNOS may contribute to the tissue injury and severe hypotension occurring in inflammatory diseases (Nathan and Xie, 1994).

Structure and catalytic mechanism of NOS

The three main NOS isoforms share structural similarities and have nearly identical catalytic mechanisms (Alderton et al., 2001). They all require a number of co-factors and prosthetic groups for activity, including flavin adenine dinucleotide (FAD), flavin mononucleotide (FMN), haem which binds oxygen, CaM, and tetrahydrobiopterin (BH_4). The NOS isoforms share a

common dimeric structure containing three domains neccesary for catalytic activity: The oxygenase domain, calmodulin-binding domain and the reductase domain. The structure of nNOS is typical of the NOS isoforms but has an additional N-terminal PDZ (PSD-95 discs large/Z0-1 homology) domain (Figure 1).
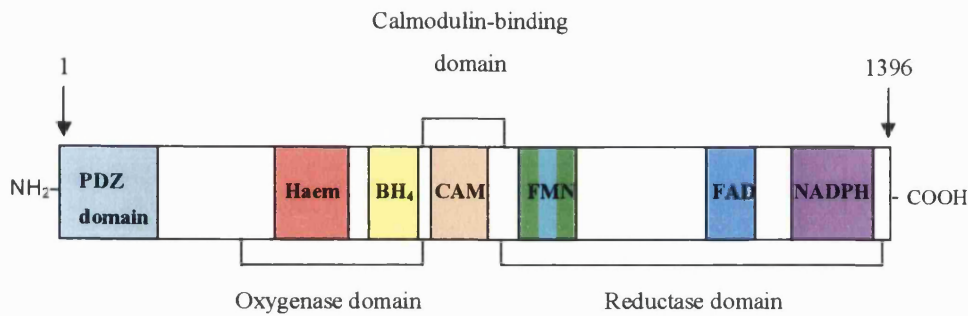
Figure 1: Structure of nNOS

The N-terminal contains a PDZ domain, which provides binding sites for interacting proteins such as post-synaptic density protein (PSD-95). The oxygenase domain binds haem and tetrohydrobiopterin (BH_4). A CaM-binding site links the oxygenase domain to the reductase domain. The C-terminal contains binding sites for flavin adenine mononucleotide (FMN), flavin adenine dinucleotide (FAD) and nicotinamide adenine dinucleotide phosphate (NADPH).

Commencing at the N-terminus the 'oxygenase domain' contains binding sites for L-arginine and the cofactors haem and BH_4, and is linked by a CaM recognition site to the 'reductase domain'. The reductase domain contains binding sites for FMN, FAD and NADPH. This reductase domain is similar to cytochrome P450 reductase, and transports electrons from NADPH, FAD, and FMN to the oxygenase domain where oxidation of L-arginine occurs. Biosynthesis of NO involves a two step oxidation of L-arginine to L-citrulline. The reaction consumes 1.5 mol of NADPH, and 2 mol of oxygen per mol of L-citrulline formed (Figure 2).

17

$$H_2N-\overset{+}{\underset{NH}{C}}-NH_2 \quad \xrightarrow[\substack{1\ NADPH \\ H_2O}]{O_2} \quad H_2N-\overset{+}{\underset{NH}{C}}-\overset{H}{\underset{|}{N}}-OH \quad \xrightarrow[\substack{0.5\ NADPH \\ H_2O}]{O_2} \quad O=\overset{}{\underset{NH}{C}}-NH_2 \quad + \quad \cdot N=O$$

L-Arginine   N^G-Hydroxy-L-arginine   L-Citrulline   Nitric Oxide
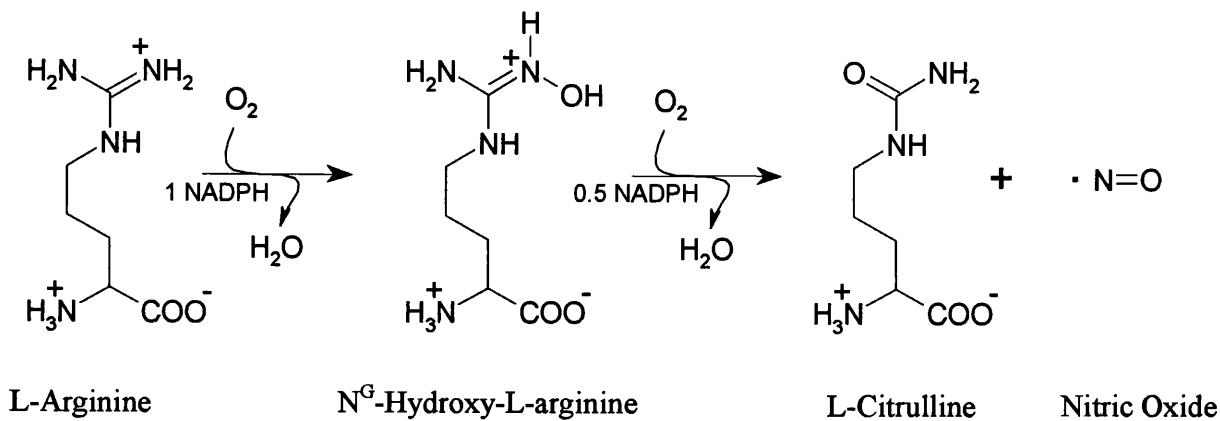
Figure 2: NO synthesis by NOS

NOS is found in both the cytosolic and particulate fractions of cell lysates. Intracellular targeting of the isoforms is determined by the variable N-terminal region. In nNOS, the N-terminal 220 amino acids are unique to this isoform and encode a PDZ domain which facilitates interactions with scaffolding proteins such as the neural post synaptic density protein (PSD 93, and PSD 95), and the muscle protein α-syntrophin (Brenman et al., 1996) (Figure 1). PSD-95 links nNOS to the NMDA receptors at the plasma membrane so that agonist binding results in Ca^{2+} influx through the channel to which nNOS is anchored (Christopherson et al., 1999). The N-terminus of eNOS contains myristoylation and palmitoylation sequences which targets eNOS to membranes or caveolae respectively (Shaul et al., 1996), again localising them to the vicinity of Ca^{2+} influx from plasma membrane channels and endoplasmic reticulum stores. iNOS lacks these N-terminal consensus sequences and is considered to be primarily a cytosolic enzyme.

1.3 Nitric oxide synthase inhibitors

Excessive NO synthesis by different isoforms of NOS has been implicated in several clinical disorders. The NO-cGMP pathway is suggested to be involved in the pathology of a number of clinical disorders including acute (stroke) and chronic (Alzheimer's, Parkinson's, schizophrenia and AIDS dementia) neurodegenerative diseases, convulsions and pain. Sustained NO

production by iNOS has been implicated in septic shock, rheumatoid arthritis and tissue damage following inflammation (Moncada et al., 1991). Selective inhibitors of the individual isoforms may provide useful therapeutic approaches and will be valuable pharmacological tools in the laboratory setting. Since the discovery of the NO signalling pathway numerous NOS inhibitors have been developed. The most commonly used are N-methyl-L-arginine, N-nitro-L-arginine, N-nitro-L-arginine methyl ester and aminoguanidine. These compounds are L-arginine analogues with similar selectivity between NOS isoforms acting as simple competitive inhibitors at the arginine-binding site, with IC_{50} values in the low μM range (Alderton et al., 2001).

The search for more potent and NOS isoform selective inhibitors, revealed that the inhibitory activity of an amidine group inferred greater selectivity between NOS isoforms and was more potent than previous compounds (Moore et al., 1996; Webber et al., 1998). Two compounds (+)cis-4-methyl-5-pentylpyrollidin-2-imine (1400W) and α-fluro-N-(3-(aminomethyl)-phenyl)-acetamidine (ARL-17477) have been tested in intact tissues. 1400W was found to inhibit iNOS 5000-fold more effectively than eNOS, and 200-fold more effectively than nNOS (Garvey et al., 1997). ARL-17477 exhibits at least a 100-fold selectivity for nNOS over both iNOS and eNOS. To date enzymatic studies have found that the most selective nNOS inhibitor is vinyl-L-NIO (N5-(1-imino-3-butenyl)-L-ornithine; L-VNIO) (Babu and Griffith, 1998). The precise mechanism of inhibition is unknown, but spectral analysis suggests that the nNOS haem co-factor is lost or modified. The recent elucidation of iNOS and eNOS crystal structures may aid in the discovery of more potent and selective NOS inhibitors (Li et al., 1999; Raman et al., 1998).

1.4 Nitric oxide synthase knockout mice

Targeted disruption of each of the NOS genes has been achieved in mice and result in viable, fertile knockout (KO) animals. These serve as useful models for NOS deficiencies, as their phenotypes reflect the functions of each isoform.

In nNOS KO mice, the absence of nNOS in the myenteric plexus causes pyloric stenosis and subsequent enlargement of the stomach (Huang et al., 1993). This is consistent with NO playing an important role in gastric motility and pyloric relaxation. Male nNOS KOs display exaggerated aggression which is also observed in mice treated with a nNOS selective inhibitor: 7-nitroindazole (Demas et al., 1997). In cerebral ischaemia, nNOS appears to contribute to tissue

19

damage (Panahian et al., 1996), whereas eNOS is important in preserving cerebral blood flow (Lo et al., 1996).

The aortic rings from eNOS KO mice do not relax in response to ACh, verifying that eNOS is required for EDRF activity (Huang et al., 1995) and these mice are hypertensive confirming a role for basal eNOS activity, in regulation of blood pressure and vascular tone. Furthermore in eNOS KO spontaneous angiogenesis following limb ischaemia was found to be severely reduced in comparison to the wild type (Murohara et al., 1998).

iNOS KO mice are more sensitive to certain infections, but are resistant to sepsis-induced hypotension (Wei et al., 1995). There are criticisms of studies on mice with gene targeted deletions as the gene product is missing throughout development when crucial processes including activation of redundancy and compensatory mechanisms may be affected. The phenotype observed may not be solely due to the mutation and may arise from up or down regulation of other genes and proteins (at both the transcriptional and translational level).

1.5 Cellular targets of NO

At low nanomolar concentrations, NO selectively engages the $NO_{GC}R$, the activation of which results in cellular accumulation of cGMP (see next section for more detail). However, when NO is present in high enough concentrations there is another ubiquitous target, the terminal complex (complex IV) of the mitochondrial respiratory chain cytochrome c oxidase. Using electrons from cytochrome c the oxidase couples the reduction of oxygen to the pumping of electrons out of the mitochondrial matrix. It is now well established that in vitro NO reversibly inhibits mitochondrial cytochrome c oxidase. NO competes with oxygen (Brown and Cooper, 1994; Koivisto et al., 1997), resulting in an increase in the Km of cytochrome c oxidase for oxygen so modulating mitochondrial respiration (Brown, 1995). Various studies have reported that endogenously produced NO can decrease O_2 consumption in vitro (Clementi et al., 1999; Loke et al., 1999; Poderoso et al., 1998; Shen et al., 1995), and in vivo (Shen et al., 1994; Shen et al., 1995). It remains possible that cGMP may mediate some of these effects (Gong et al., 1998; Shen et al., 1995). Furthermore the sensitivity of $NO_{GC}R$ is at lease two orders of magnitude higher than that of cytochrome c oxidase (Bellamy et al., 2002a). Whether NO regulates cellular respiration in vivo remains to be determined (Cooper, 2002; Moncada and Erusalimsky, 2002).

Irreversible damage to cytochrome c oxidase has also been reported following prolonged NO exposure of mitochondria (Poderoso et al., 1996) and cells (Bolanos et al., 1996). It has been suggested that the diffusion limited reaction of NO with superoxide ($O2^{\bullet-}$) to form highly toxic species peroxynitrite ($ONOO^-$) may be responsible (Beckman and Koppenol, 1996). $ONOO^-$ has also been implicated in causing DNA damage, activation of poly(ADP-ribose) polymerase, protein nitration and lipid peroxidation (for a review see Keynes and Garthwaite, 2004).

Guanylyl Cyclases: Isoforms and expression

Soon after the discovery of the cyclic nucleotide cyclic adenosine 3'-5' monophosphate (cAMP), cGMP was detected in rat urine and shown to be formed in nearly all mammalian tissues (Ashman et al., 1963). cAMP is synthesised by adenylyl cyclases (AC) which are associated with the plasma membrane in eukaryotic cells (with the exception of cytosolic AC in sperm). In contrast the cGMP-forming guanylyl cyclases exist as both soluble and membrane-bound forms. Both the soluble and membrane guanylyl cyclases were found to be activated by NO (Arnold et al., 1977), and later it was found that the membrane form is also activated by natriuretic peptides (Chinkers and Garbers, 1989). To date NO is the only known physiological activator of the $NO_{GC}R$.

The first purification of $NO_{GC}R$ was achieved from rat lung (Garbers, 1979) long before NO was recognised as a physiological messenger. $NO_{GC}R$ was identified as a dimer, consisting of two subunits $\alpha1$ (73-80 kDa) and $\beta1$ (70 kDa), and requires a divalent cation as a co-factor (originally proposed to be Mn^{2+}, but later deduced to be Mg^{2+}). The primary amino acid sequence was identified and cDNA was cloned for both the α- (Koesling et al., 1988; Nakane et al., 1988) and the β-subunits (Koesling et al., 1990; Nakane et al., 1990). Homology screening revealed the existence of alternative subunits of the $NO_{GC}R$: $\alpha2$ (Behrends et al., 1995; Harteneck et al., 1991) and $\beta2$ (Yuen et al., 1990). $\alpha3$ and $\beta3$ were later described in human brain (Giuili et al., 1992) but are likely to represent variants of the $\alpha1$ and $\beta1$ subunits rather than different isoforms (Zabel et al., 1998). Subunits corresponding to the mammalian $\alpha1$ and $\beta1$ have also been found in animals other than mammals including fish (Mikami et al., 1999) and insects (Nighorn et al., 1999; Shah and Hyde, 1995) implying that the $NO_{GC}R$ is well conserved though evolution.

In summary two types of α and two types of β NO$_{GC}$R subunits have been identified, from which a total of four different NO$_{GC}$R isoforms (α1β1, α2β1, α1β2 and α2β2) may occur. Only two isoforms have been shown to exist at the protein level *in vivo*. α1β1 has a widespread tissue distribution. α2β1 was originally identified in human placenta, and has since been found in the rat brain, where it associates with synaptic scaffolding proteins (Russwurm et al., 2001). At the mRNA level, β2 was originally found in the kidney with lower expression in the liver (Yuen et al., 1990). *In situ* hybridisation reveals that α2 mRNA is widely expressed in the brain with particular abundance in the cerebellum and hippocampus; however β2 mRNA was not detected (Gibb and Garthwaite, 2001). However a more sensitive RT-PCR method revealed that the β2 mRNA was expressed in the cerebellum. Interestingly the relative concentrations of α1 and β1 in this brain region and elsewhere are not necessarily expressed in a 1:1 ratio but the physiological importance of this is unclear.

Expression experiments revealed that the α1 or β1 subunit transfected alone into cells, or a combination of the cytosolic fractions from each separately expressed subunit, did not result in enzyme activity (Buechler et al., 1991; Harteneck et al., 1990). Co-expression of the α1β1 and α2β1 subunits in these cells produced NO-sensitive enzymes and it has been speculated that a physiological equilibrium between homo- and heterodimers may regulate NO$_{GC}$R activity in cells (Zabel et al., 1999). A combination of α1 and β2 tagged with green fluorescent protein was reported to generate cGMP when expressed transiently in COS-7 cells (Gupta et al., 1997); however this was regarded contentious as the results could not be repeated in other laboratories. The role of β2 was further complicated by the discovery of a variant β2, which contains an additional 60 amino acids at the N terminus, adjacent to the haem-binding domain. This protein was reported to function as a homodimer with a 10-fold higher affinity for NO than the α1β1 heterodimer (Koglin et al., 2001). However, the physiological relevance of the variant β2 subunit remains questionable as enzyme activity required a non-physiological concentration (4 mM) of Mn^{2+} (rather than the usual Mg^{2+}).

Structure of the NO$_{GC}$R

The primary structure of the NO$_{GC}$R subunits can be divided into three domains: a haem-binding domain at the N-terminal, a central dimerisation domain and a C-terminal catalytic domain (Figure 3). A single haem moiety is incorporated within the haem-binding site of the heterodimer. Presence of this prosthetic haem group was shown to be essential for NO-induced enzyme activity, as removal of the haem abolished enzyme activation, which could be reversed following reconstitution with haem (Foerster et al., 1996; Ignarro et al., 1986). Both the α1 and β1 subunits are required for correct binding and orientation of the haem group (Foerster et al., 1996), and sequential truncation studies demonstrated that the β1 subunit plays a more important role in haem binding (Koglin and Behrends, 2003). A histidine residue (His-105) of the β1 subunit was shown to form a covalent link with the Fe^{2+} centre of the haem iron, thereby acting as a proximal ligand (Wedel et al., 1994; Zhao et al., 1998). Mutation of this histidine generated an NO-insensitive, haem-depleted enzyme with only basal activity (Wedel et al., 1994).

Two cysteines adjacent to the His-105 on the β1 subunit appear to assist in the formation of the proper haem pocket. When these were mutated the enzyme failed to bind haem (Friebe et al., 1997). In other haemoproteins such as myoglobin (Mb) or haemoglobin (Hb), the reaction of NO with O_2 results in oxidation of the haem iron and nitrate formation. This does not occur in the NO$_{GC}$R as the haem environment does not bind O_2 (Gerzer et al., 1981a), allowing NO to freely associate and dissociate with the NO$_{GC}$R. This means that in the aerobic environment of a cell, the NO$_{GC}$R activity will not be influenced by competition between NO and O_2.
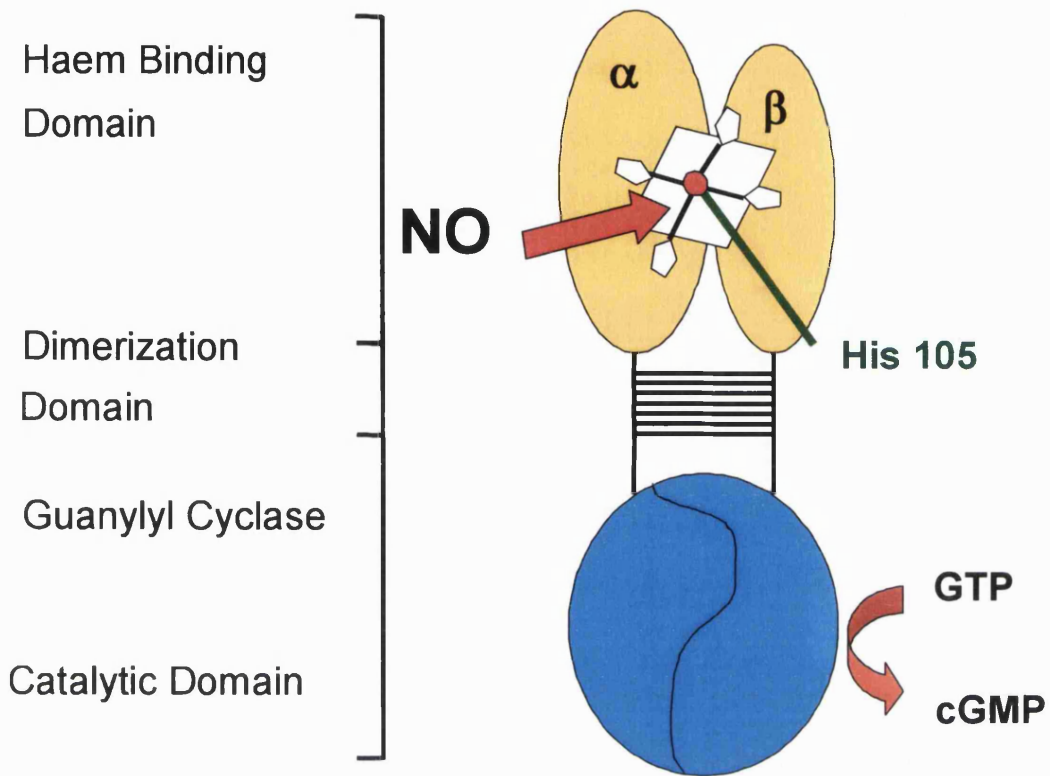
Figure 3: Structure of the NO$_{GC}$R

The β subunit contains histidine 105 which attaches the ferrous haem group (●) to which NO binds. The resulting change in conformation activates the catalytic domain to synthesise cGMP.

1.6 Kinetics of purified $NO_{GC}R$

Out of the three redox forms of NO (NO^-, $NO^•$, and NO^+) only the uncharged radical ($NO^•$) significantly activates the $NO_{GC}R$ (Dierks and Burstyn, 1996). The mechanism of $NO_{GC}R$ activation is centred on the haem group, and the shift in the UV-visible absorbance maximum (known as the Soret band) of the different haem species has proved invaluable in investigating this process. Under resting conditions, the haem group of the $NO_{GC}R$ is five-coordinated, with a His-105 as the axial ligand at the fifth coordinating position, as indicated by an absorbance maximum of 431 nm (Stone and Marletta, 1994). It is widely accepted that activation of the $NO_{GC}R$ is initiated by NO binding to the sixth coordination position of the haem, resulting in the cleavage of the proximal histidine-iron bond. The formation of a five-coordinate nitrosyl Fe^{2+} complex induces a shift in the absorbance maximum towards 398 nm. The resulting conformational change is thought to be propagated to the catalytic site and cause a 200 fold increase in the rate of cGMP synthesis from GTP (Sharma and Magde, 1999).

The initial rate of NO association with the haem group of the $NO_{GC}R$ is very rapid (bimolecular rate constant of 10^7-10^8 $M^{-1}s^{-1}$), and is of an order of magnitude approaching that of a diffusion-limited reaction (Zhao et al., 1999). The subsecond kinetics of $NO_{GC}R$ activation were investigated using stopped-flow spectroscopy (Zhao et al., 1999). The transition from the six-coordinate to the five-coordinate complex was found to be rate limiting for activation; proceeded with second order kinetics (k=2.4 x 10^5 $M^{-1}sec^{-1}$ at 4 °C); and was dependant on the NO concentration. This result suggested $NO_{GC}R$ activity was a more complex event, whereby NO not only activates the enzyme by binding to the haem, but also regulates the velocity of activation by binding to a second site. However, reinterpretation of the data suggested that it is compatible with the simple binding event of activation, and the postulated additional NO binding site was deemed unnecessary (Bellamy et al., 2002b). These models are currently under dispute (Ballou et al., 2002; Bellamy et al., 2002b).

A recent study analysed the effect of both biochemical and genetic removal of the haem, and its reconstitution on the activity of the $NO_{GC}R$ (Martin et al., 2003). When detergent was used to remove the haem from human wild type $\alpha 1\beta 1$ enzyme, a several fold activation of the enzyme was observed. This activation was inhibited following reconstitution of the haem. Furthermore, a haem-deficient mutant enzyme, in which the $\alpha 1\beta 1$ His-105 was substituted for a cysteine, was

found to be constitutively active at a level comparative to the activity of the wild type enzyme activated by NO. When this mutant enzyme was reconstituted with haem the enzyme activity was significantly reduced. This work suggests that the haem moiety, via its coordination with His-105 of the β subunit acts as an endogenous inhibitor of the $NO_{GC}R$. The authors propose that disruption of the haem-coordinating bond induced by binding of NO releases the restriction imposed by this bond, allowing the formation of an optimally organised catalytic centre in the heterodimer.

To date the $NO_{GC}R$ crystal structure remains unknown. Recent crystallographic studies of cytochrome *c'* from the microbe *Alicaligenes xylosoxidans* revealed an unexpected NO binding profile. The NO-bound crystal structure of cytochrome *c'* was found to bind NO on the proximal (rather than distal) face of the haem (Lawson et al., 2000). Progression from the 6-coordinate species to the stable 5-coordinate species proceeded via displacement of the proximal histidine and distal NO by a second NO molecule, which forms a bond in the proximal position (Mayburd and Kassner, 2002). This transition was found to be dependant on NO concentration (Andrew et al., 2002), analogous to findings on $NO_{GC}R$ (Zhao et al., 1999). Cytochrome *c'* is similar to $NO_{GC}R$ in regard to its ligand binding properties (exclusion of O_2, a 5 co-ordinate ferrous resting haem, and a 5-coordinate nitrosyl complex yet 6-coordinate carboxyl complex; Andrew et al., 2002) and so this new finding is likely to provoke the re-examination of many of the assumptions regarding NO activation of the $NO_{GC}R$.

The rate of NO dissociation from purified $NO_{GC}R$ is much faster (half-time = seconds-minutes; Brandish et al., 1998; Kharitonov et al., 1997), than the spontaneous dissociation of NO from the $NO-Fe^{2+}$ bond in the majority of haem-containing proteins (half time = hours-days; Kharitonov et al., 1997). Deactivation of the $NO_{GC}R$ was measured as a decrease in catalytic activity by examining the rate at which cGMP synthesis declined to zero after removal of NO by addition of Hb. The dissociation of NO from its receptor was found to be fastest in the presence of GTP and Mg^{2+} (Kharitonov et al., 1997). Deactivation was found to proceed with a half-life of ~20 s at 20 °C. It is assumed that at the physiological temperature of 37 °C, that this would reduce to a few seconds (Bellamy and Garthwaite, 2002). More work is required to determine the rate of deactivation of purified $NO_{GC}R$.

The kinetics of catalysis have been examined in the purified form of the $NO_{GC}R$ (Gerzer et al., 1981b; Stone and Marletta, 1994). Under conditions of excess activator (NO) and substrate

(GTP) the enzyme exhibits linear Michaelis-Menton kinetics i.e. cGMP accumulates at a constant rate over time, indicating that in the purified state the enzyme is not subject to feedback inhibition. The Michaelis constant of the $NO_{GC}R$ for Mg^{2+}-GTP has been found to be within the range of 40-130 μM in the absence of NO (Denninger et al., 2000; Tomita et al., 1997) and in the range of 14-20 μM in the presence of NO. The maximal observed rate of cGMP synthesis has been measured as 10-100 nmol $cGMP.mg^{-1}.min^{-1}$ in the absence and 10-40 μmol $cGMP.mg^{-1}.min^{-1}$ in the presence of NO (Stone and Marletta, 1995; Tomita et al., 1997).

1.7 Kinetics of the $NO_{GC}R$ in cells

Recent studies examined the behaviour of the $NO_{GC}R$ in cells, and revealed for the first time that within its natural physiological environment the enzyme acts very differently to how it acts when in a purified state. The first major difference was the rate of deactivation of cGMP synthesis. The NO scavenging ability of Hb was exploited to instantly remove all free NO from the medium surrounding the cells. Hb is cell impermeable. Direct measurement of the rate of decline in cGMP synthesis after removal of free NO provides a measure of the rate at which NO dissociates from the $NO_{GC}R$, diffuses through the cell and is quenched by Hb. In immature cerebellar cell suspensions complete $NO_{GC}R$ deactivation occurred within a few seconds or less (Bellamy et al., 2000). A novel method for rapid quenching of cell suspensions was developed to examine the deactivation kinetics in greater detail (Bellamy and Garthwaite, 2001b). Deactivation was found to proceed in a more complex manner than predicted for by a simple decline in levels of active $NO_{GC}R$. The simplest operational description of deactivation was an exponential decline (rate constant $3.7 sec^{-1}$) following an immediate 0.4 fractional loss of activity.

The same technique was applied to investigate the activation kinetics of cellular $NO_{GC}R$ following photolysis of a caged derivative of NO. The rate of $NO_{GC}R$ activation was too rapid to be measured even at a sampling interval of 200 ms. It is unknown whether the rate of activation measured for purified enzyme applies to the receptor within cells. Estimates for the potency (EC_{50}) of NO required for activation of the purified enzyme range from ~80 nM (Schmidt et al., 1997; Schrammel et al., 1996) to 250 nM (Stone and Marletta, 1996), whereas in cells the EC_{50} (measured 100 ms after photolysis of caged NO) is almost two-fold lower ~ 45 nM (Bellamy and

Garthwaite, 2001b). This implies that in a cellular environment an enhanced rate of deactivation does not compromise the potency of NO activation. It has been suggested that the rate of activation must also be equally higher, as the potency of NO is determined by the rate constant for deactivation over the rate constant of activation (Bellamy et al., 2002b).

The concentration of intracellular cGMP is governed simply by a combination of the rate of cGMP synthesis by the $NO_{GC}R$, and the rate of degradation by PDE (Bellamy et al., 2000). How these enzymes contribute to the measured cGMP profile has in the past proved difficult to assess, as a method for measuring one or other of the enzymes activity is required. The non-specific PDE inhibitor IBMX (1 mM) was shown not to fully block cGMP degradation (Mayer et al., 1992). However, the Hb technique proved a useful method to rapidly arrest $NO_{GC}R$ activity (Bellamy et al., 2000). cGMP degradation was followed and fitted with the Michaelis-Menten equation so that a quantitative measurement of PDE activity could be made (Bellamy and Garthwaite, 2001a). Using this description of how the rate of cGMP degradation contributed to the observed cGMP profile, the contribution of cGMP synthesis could be extrapolated.

In rat cerebellar astrocytes and human platelets the $NO_{GC}R$ displayed a rapidly desensitizing profile of activity (Bellamy and Garthwaite, 2001a). This means that the rate of cGMP synthesis wanes despite the continued presence of NO as the $NO_{GC}R$ becomes inactivated or desensitized. Desensitization is a characteristic of numerous neurotransmitter receptors, but its role in neurotransmission is still unknown (Jones and Westbrook, 1996). This response in intact cells was far from the response predicted by the simple kinetics of the purified receptor. Depletion of substrate (GTP), feedback inhibition of the receptor by cGMP or pyrophosphate (the by-product of the synthesis of cGMP from GTP), or active export of cGMP from the cells were considered as alternative explanations for the reduction in $NO_{GC}R$ activity over time. However, these could not account for the desensitization profile observed in cerebellar cells (Bellamy et al., 2002b).

The time constant for desensitization was found to be 6.9 s at ~70 nM NO and fell to 5.4 s at a 10 fold higher NO concentration (Bellamy and Garthwaite, 2001b) indicating that NO accelerates desensitization. A concentration-response curve of cellular $NO_{GC}R$ to NO becomes increasingly bell-shaped over time. This causes difficulty in assessing the potency of NO for its receptor as the maximal $NO_{GC}R$ activity becomes truncated by desensitization. The longer the enzyme is exposed to NO, the greater the potency of NO for its receptor. Measurement of

cellular levels of cGMP over a time course of minutes will yield an EC_{50} value of a lower magnitude than estimates based on activation of the purified receptor.

The recovery from desensitization of cellular $NO_{GC}R$ was found to be much slower than the rate of onset (Bellamy et al., 2000). Cerebellar cells were exposed to a supra-maximal concentration of NO to provoke desensitization, and then deactivated by Hb. NO was re-applied at different times at a concentration great enough to saturate the Hb and fully stimulate the $NO_{GC}R$. The half-time for recovery was found to be ~ 1.5 min.

1.8 Pharmacological modulation of the $NO_{GC}R$

The NO/haem-mediated activation of the $NO_{GC}R$ is now well established but two other mechanisms of activation have been identified which may be of future therapeutic benefit. 3-(5'-hydroxymethyl-2'furyl)-1-benzylindazole (YC-1) was first identified as an activator of the $NO_{GC}R$ in platelets (Ko et al., 1994). Further studies demonstrated that YC-1 caused a 10-fold activation of the purified receptor (Mulsch et al., 1997). YC-1 acts by increasing the maximal catalytic rate of the receptor in an NO independent manner, as shown by the inability of the NO scavenger oxyHb to inhibit activation. Furthermore, YC-1 sensitizes the enzyme towards its activators by binding to an allosteric site other than the haem group, so causing a reduction in ligand dissociation from the haem (Friebe and Koesling, 1998). To date the binding site for YC-1 remains ellusive.

Recently BAY 41-2272 was identified as a compound similar to YC-1, but with a two fold higher potency, and higher specificity as it does not inhibit phosphodiesterases (Stasch et al., 2001). Photoaffinity labelling identified that two cysteines (at Cys 238 and Cys 243) in the $\alpha 1$ $NO_{GC}R$ subunit, act as the target for this new class of stimulator (Stasch et al., 2001). Deletion studies revealed that a similar region in the $\alpha 2$ subunit also acts as a binding site for BAY 41-2272. *In vivo* studies in a canine model of congestive heart failure showed potential use for BAY 42-2272 for treatment of cardiovascular diseases (Boerrigter et al., 2003).

Several compounds are found to inhibit the $NO_{GC}R$. The quinoxalin derivative 1H-[1,2,4]oxadiazolo[4,3-a]- quinoxalin-1-one (ODQ) has been shown to be a potent and selective $NO_{GC}R$ inhibitor in brain slices (Garthwaite et al., 1995). Studies on the purified $NO_{GC}R$ reveal that ODQ binds in an NO-competitive manner and irreversibly inhibits NO-stimulated activity,

leaving basal activity unaltered. Spectral analysis suggests that the inhibitory effect of ODQ is caused by slow reversible oxidation of the haem iron in cells (Schrammel et al., 1996; Zhao et al., 2000).

1.9 Cellular targets of the second messenger cGMP

Phosphodiesterases

Cyclic nucleotide phosphodiesterases (PDEs) regulate all pathways that utilise cGMP or cAMP as second messengers. PDEs catalyse the hydrolysis of 3',5' cyclic nucleotides to 5' monophosphates, and so are important in regulating intracellular concentrations of and, consequently biological responses to, these signalling molecules. So far 11 PDE gene families have been identified in mammalian tissue, which differ in substrate specificity (cGMP or cAMP), kinetic characteristics, tissue distribution, pharmacological profiles and amino acid sequence homology. The C terminal possesses a conserved PDE catalytic domain (270-300 residues) whereas the N terminal confers specific properties to the PDE family. Multiple splice variants, some of which exist in a tissue-specific manner or are expressed in response to a particular stimulus are found in most families.

PDE families 2, 5, 6, 10 and 11, contain one or two highly homologous regulatory domains in their N-terminal regions. These domains have been termed GAF A or GAF B based on their sequence homology to similar motifs of a wide group of proteins. The first members of this group included the cGMP-regulated PDEs, the cyanobacterial *Anabaena* adenylate cyclase and the Fh1A protein (a bacterial transcriptional factor). The first letters of these group names were used to derive the acronym (Aravind and Ponting, 1997). GAFs are one of the largest families of small molecule binding domains found in proteins involved with cyclic nucleotide signalling. The ligands for most GAF domains remain to be identified but amongst PDEs, cGMP is the only known ligand to bind to this domain (PDE 2, 5, 6). Crystalisation studies of the regulatory sequence of mouse PDE2A has revealed the structure of two GAF domains with different structures: GAF-A functions as a dimerisation locus and GAF-B possesses a 11-residue fingerprint sequence for cGMP binding which is found to be highly conserved in other PDE families expressing GAF domains (Martinez et al., 2002). Variance in sequence homology between GAF domains results in changes of affinity to small-molecule ligands e.g. cAMP-

binding GAF-B domain in *Anabaena* cyanobacterium (Figure 4) and contributes to the enormous diversity in regulatory mechanisms in which GAF domains are involved.
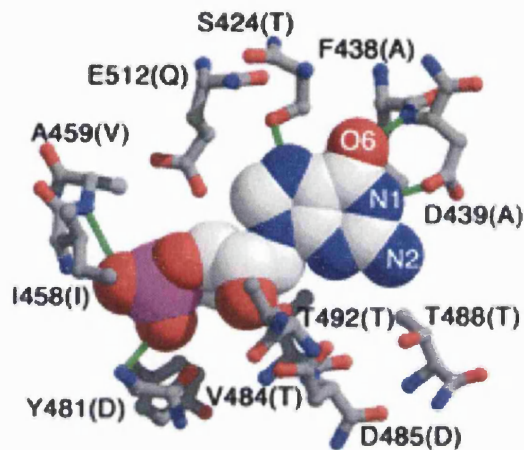
Figure 4: cGMP bound to the GAF-B domain of murine PDE2

Taken from www.stke.org/cgi/content/full/sigtrans;2003/164/pe1

The space-filling representation illustrates cGMP. The ball-and-stick representation shows the 11 fingerprint residues of PDE2 which are essential for cGMP specificity. In parenthesis are the replacement fingerprint residues which infer cAMP-binding in the GAF-B domain of an adenylyl cyclase in *Anabaena* cyanobacterium. The molecules are represented by nitrogen (blue), oxygen (red), phosphorous (magenta), carbon (grey), hydrogen bonds (green).

PDE2 is a dual substrate isoform hydrolysing both cGMP and cAMP (but with a higher affinity to cGMP). On incubation with cGMP the enzyme affinity for cAMP is enhanced, hence the alternative name of the "cGMP stimulated PDE" (Juilfs et al., 1999). This modulatory effect offers an important mechanism in mediating cross talk between cGMP and cAMP regulated pathways. PDE2 is a homodimer of two 105 kD subunits and exists in soluble and membrane-bound forms. This family was first identified in liver, heart adrenal glands and has been shown to be expressed in the brain, especially in the limbic system (reviewed in Manganiello et al., 1995a).

PDE5 (the cGMP-binding, cGMP-specific PDE) and PDE6 (the photoreceptor cGMP PDE) have relatively high affinity for cGMP, and hydrolyse cAMP very poorly. The PDE5 isoform is the target of the selective drug Viagra (sildenafil citrate; Turko et al., 1999). Crystal structures of the PDE5 catalytic domain bound to different inhibitors will provide information to design more potent and selective inhibitors (Sung et al., 2003). Binding of cGMP (or sildenafil) at the catalytic site of PDE 5 stimulates cGMP binding to the PDE5 GAF domains and leads to phosphorylation of a specific serine residue in the N-terminal, by cGMP and cAMP kinases (Thomas et al., 1990; Turko et al., 1998). Phosphorylation induces a conformational change which increases the cGMP affinity of the GAF-A domain ten-fold (Francis et al., 2002) and in purified enzyme increases catalytic activity nearly two fold (Corbin et al., 2000). These changes represent a negative feedback pathway which regulates cGMP levels within cells. Interestingly these effects also imply that by elevating cGMP, sildenafil increases its own binding affinity, so providing positive feedback for effectiveness of the drug (Corbin et al., 2002).

The retinal photoreceptor PDE6 is a membrane bound heterodimer composed of an α and β subunit. In the dark PDE6 activity is blocked by two inhibitory Pγ subunits (McLaughlin et al., 1995). This inhibition is removed by light stimulation of rod and cone cells, which triggers PDE6 activation. cGMP hydrolysis results in the closure of cGMP-gated channels and hyperpolarization of the photoreceptor cell (Beavo, 1988). Mutations in the GAF or catalytic domains in either of the PDE subunits is responsible for about 4 % of recessive autosomal retinitis pigmentosa cases, a progressive retinal degeneration disorder (McLaughlin et al., 1995), and a substitution of the GAF domain in the β subunit (H258N) results in autosomal dominant congenital stationary night blindness as found in the Rambusch family in Denmark (Gal et al., 1994).

PDE10 and PDE11 have only recently been described (Fawcett et al., 2000; Fujishige et al., 1999b; Soderling and Beavo, 2000). PDE10 mRNA expression is limited to the striatum and testis (Fujishige et al., 1999b) and this isoform exhibits dual substrate catalytic activity for cAMP and cGMP. However, PDE10 binds cAMP with a higher affinity than cGMP, and hydrolyses cAMP less effectively and so it has been suggested that PDE10 acts as a cAMP-inhibited cGMP PDE (analogous to PDE3 but with different nucleotide specificity Fujishige et al., 1999a). PDE11 is also a dual substrate PDE, and is expressed predominantly in human prostate and skeletal muscle.

PDE1 is another dual substrate PDE that hydrolyses both cAMP and cGMP (Beavo, 1988). Competitive inhibition of cGMP degradation occurs at elevated cAMP concentrations and vice versa. The PDE1 family is activated by Ca^{2+}/CaM binding and is found abundantly in the mouse brain (Yan et al., 1994). nNOS is also activated by Ca^{2+}/CaM binding, and is found abundantly throughout the CNS. It is hypothesised that a rise in intracellular Ca^{2+} (caused by glutamate receptor activation) simultaneously stimulates nNOS activity and PDE1 activity (Baltrons et al., 1997). This means that cGMP accumulation in the stimulated cells is inhibited, but neighbouring cells with low cytosolic Ca^{2+} are free to respond (Mayer et al., 1993). However, pharmacological characterisation of the PDE constitution of cells accumulating cGMP in cell suspensions from eight day old rat cerebellum (Bellamy and Garthwaite, 2001a) and striatum (Wykes et al., 2002) found no evidence that PDE1 was contributing to cGMP degradation.

PDE3 is a dual substrate isoform and is also referred to as the cGMP inhibited isoform (Degerman et al., 1997). cGMP is hydrolysed about 10 fold less effectively than cAMP and so when bound to the catalytic site cGMP acts as a competitive inhibitor to cAMP degradation. Residues in the N-terminal have recently been shown to be important for membrane association (Shakur et al., 2001) and phosphorylation by protein kinases (Kitamura et al., 1999). Thus subcellular location could influence the specificity of protein kinase interactions of PDE3.

PDE4, 7 and 8 are "cAMP specific" and so these PDE families are not thought to play a role in cGMP signalling. PDE8 and 9 are not inhibited effectively by the non specific PDE inhibitor, IBMX. PDE9 has the highest affinity for cGMP so far recorded (K_m =0.07 μM; Soderling et al., 1998) and so is thought to be important in maintaining basal cGMP levels at low concentrations. At the mRNA level it is highly expressed in the kidney and is thought to participate in the atrial natriuretic peptide-mediated diuresis pathway (Soderling et al., 1998).

cGMP-dependent protein kinases

Two major types of cGMP dependent protein kinases (cGK) or protein kinase G (PKG) have been identified in mammalian tissues: the cytoplasmic type I and the membrane-bound type II. cGK I is a homodimer of two identical subunits approximately 76 kDa each existing in two isoforms designated α and β (Francis and Corbin, 1994), whereas cGK II is an 86 kDa monomer (De Jonge, 1981). Types I and II are not known to be co-expressed in any tissue. The highest

33

concentrations of cGK I are found in cerebellar Purkinje cells (Lohmann et al., 1981), smooth muscle cells and platelets (Walter, 1989). cGK II was originally identified in intestinal microvilli (De Jonge, 1981) but at the mRNA level was shown to have a wide distribution in the brain (el Husseini et al., 1995). For a summary see Table 2.

Isoform	Predominant location	Substrate	Function
cGK I	Brain/neurones Primarily in cerebellar Purkinje cells. Also in spiny striatal neurones, dorsal root ganglion, olfactory bulb and epithelium	AMPA IP$_3$R G-substrate PDE5	Regulation of neuronal excitability and synaptic plasticity
	Smooth muscle cells	VASP, IP$_3$R,	$\downarrow$ [Ca^{2+}]$_i$ contractility
	Platelets	VASP, IP$_3$R	$\downarrow$[Ca^{2+}]$_i$, adhesion, aggregation, secretion, cytoskeleton reorganisation
cGK II	Intestinal mucosa	CFTR	$\uparrow$ Cl$^-$ secretion (via CFTR)
	Brain High levels in brainstem, locus ceruleus, pontine nucleus Low levels in striatum, cerebellum, hippocampus	??	Neurotransmitter release $\downarrow$ Vasopressin release
	Kidney	??	$\downarrow$ Renin secretion
	Bone	??	$\uparrow$ Growth

Table 2: Cellular location, substrate and potential physiological function of the cGMP-dependent protein kinases

VASP = Vasodilator stimulated phosphoprotein, IP$_3$R = Inositol 1,4,5-trisphosphate receptor, CFTR = Cystic fibrosis transmembrane conductance regulator. ?? = Not yet known. Modified from Francis and Corbin, 1994 and Lohmann et al., 1997.

Analysis of the functional significance of the cGK is under investigation using both KO mice carrying null-mutations of cGK I or cGK II and double KO mice. Mice lacking cGK I from only their Purkinje cells exhibited almost complete absence of cerebellar long term depression (LTD; Feil et al., 2003). LTD is the activity dependent attenuation of synaptic transmission. In the cerebellum LTD has been implicated in a specific form of motor learning, the adaption of the vestibular-ocular reflex (de Zeeuw et al., 1998). It has been reported that cGK I can phosphorylate a number of proteins in Purkinje neurons, including AMPA receptors (Nakazawa et al., 1995), IP_3 receptors (Haug et al., 1999), G-substrate (Endo et al., 1999) and PDE5 (Shimizu-Albergine et al., 2003). The roles of AMPA and IP_3 receptors in LTD are well established (Ito, 2001), however as yet the functional significance of their phosphorylation by CGK I has not been determined. G-substrate (a 24 kDa protein) is specifically expressed in Purkinje cells, and when phosphorylated is found to be an effective protein phosphatase inhibitor ($K_i = 1.5$ μM for protein phosphatase 1; $K_i = 0.3$ μM for protein phosphatase 2A). In its unphosphorylated form G-substrate had no significant effect on either protein phosphatase. It has been proposed that by inhibiting endogenous phosphatase activities, phosphorylated G-substrate may control different signal transduction pathways including protein kinase C, protein tyrosine kinases or mitogen-activated protein kinases (Ito, 2001), or affect clathrin-mediated internalisation of AMPA receptors which appears to be important for cerebellar LTD (Wang and Linden, 2000). Phosphorylated PDE5 occurs at the peak of cGMP-CGK I activation, and has been proposed to provide a negative feedback regulation of cGMP concentration in all Purkinje neurons, thereby attenuating the duration of LTD response (Shimizu-Albergine et al., 2003). A subpopulation of Purkinje neurons was found to also contain PDE1B and the authors emphasise the importance of identifying the PDE composition of individual cells (especially for electrophysiological studies) as this may greatly affect the Purkinje cell response to NO-cGMP stimulation during LTD.

The cGKs belong to the serine/threonine kinase family and share common structural features. The N-terminus contains an auto-inhibitory domain with two autophosphorylation sites. The regulatory domain contains two cGMP binding sites arranged in tandem: one with high cGMP binding affinity and one with low affinity, and finally the Mg^{2+}/ATP binding site and target protein interaction domains in the catalytic C-terminal. Activation of the enzyme is thought to

depend on a conformational change, as detailed below. This results in the removal of a pseudo-substrate region of the autoinhibitory domain which occupies the catalytic site under basal conditions (Francis and Corbin, 1994). Initial studies demonstrated that cGMP binding to one or both of the two regulatory binding sites, or autophosphorylation of residues in the N-terminus resulted in the conformational change associated with cGK I activation (Chu et al., 1998). Further studies suggest a simple two-state model where cGMP binding to the low affinity binding site causes "elongation" but full activation is only achieved when cGMP is simultaneously bound to the high affinity binding site (Wall et al., 2003).

The catalytic function of cGK is similar to the cAMP kinases. Both enzymes transfer the γ-phosphate of ATP to a serine or threonine residue of the target protein. The cGK I isoforms have been extensively studied and the structure of cGK II is thought to be similar but with a single cGMP binding site. A leucine zipper in the N terminus of cGK I is responsible for dimerisation; whereas this region in cGK II contains myristoylation sites which targets the protein to membranes in different subcellular localisations.

Cyclic nucleotide gated ion channels

Cyclic nucleotide gated (CNG) channels couple electrical and/or Ca^{2+} signals to cyclic nucleotide concentration. CNG channels are non-selective cation channels which are Na^+ and Ca^{2+} permeable, and opening is dependent on cGMP or cAMP binding to the channel complex. CNG channels were first identified in the visual and olfactory transduction systems, and have a widespread distribution (Zagotta and Siegelbaum, 1996). *In situ* hybridisation shows that CNG channel mRNA is expressed throughout the CNS (Strijbos et al., 1999) in a similar distribution to the NO/cGMP system (Kingston et al., 1999). Expression studies indicate that the CNG channels are constructed of 3α and 1β subunits in a tetrameric configuration (Zhong et al., 2002). Each of the four subunits contributes to the central pore (Figure 5a). Both the α and β subunit contains 6 transmembrane domains and intracellular cGMP or cAMP binding domains (Figure 5b). The difference between α and β subunits is that when expressed as homomeric channels in Xenopus oocytes the α subunit forms functional ion channels, while the β subunits do not but rather, appear to modulate the characteristics of the α subunit (Kaupp et al., 1989).

a

b

Extracellular

1 2 3 4 5 6

+
+
+
+
+

P domain

Intracellular

NH₂

COOH

Cyclic nucleotide
binding site
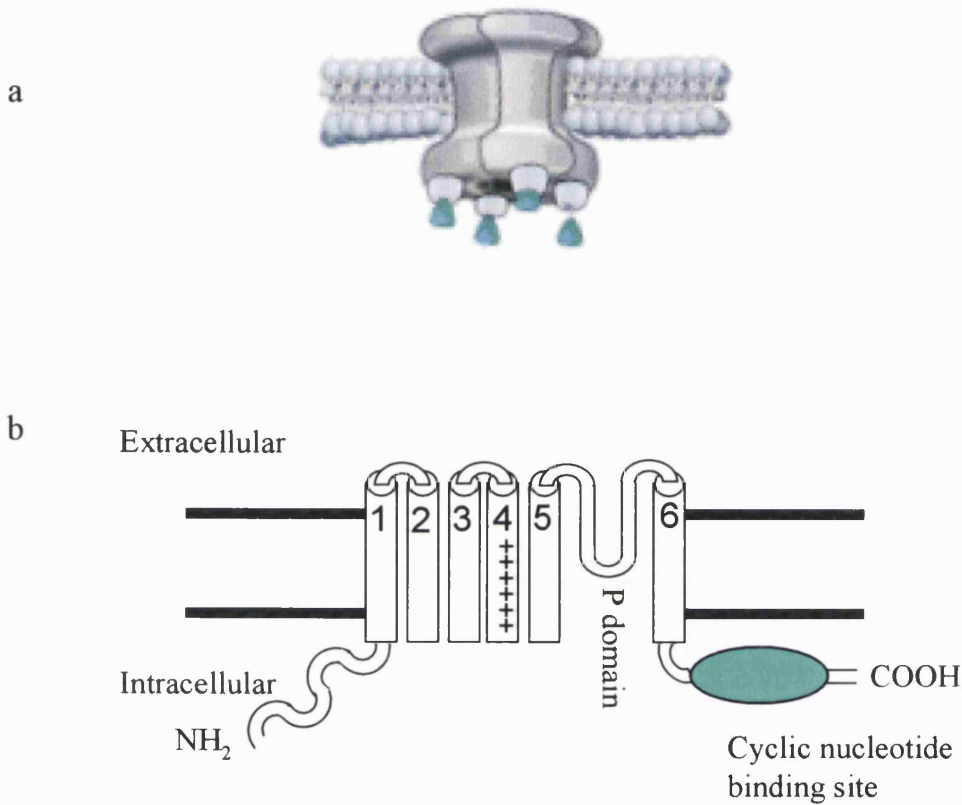
Figure 5: Cyclic-nucleotide gated ion channel

Adapted from Kramer and Molokanova, 2001. a) Three-dimensional structure of a CNG channel.
The four subunits are arranged to form a central pore. b) The primary structure of the α-subunit.
Cylinders represent hydrophobic segments of membrane-spanning domains. The S4 segment is
the voltage sensor for voltage-dependent transition in these channels; the region between S5 and
S6 is thought to be part of the channel pore. The cyclic nucleotide-binding site is in green.

1.10 The physiological role of NO

NO signalling in the CNS

Since its discovery, NO has been considered an unorthodox signalling molecule in the CNS. The classical amino acid and peptide neurotransmitters e.g. glutamate, have well defined synthesis, storage, release, and termination pathways. Release from pre-synaptic structures and diffusion to postsynaptic densities, evoke either excitatory or inhibitory changes in membrane potential which can be mimicked by application of exogenous agonists. However in the CNS, NO plays a more modulating role in cells where synaptic signalling is mediated by neurotransmitters such as glutamate.

The NO signalling pathway is found throughout the mammalian CNS. Briefly, under normal conditions the binding of glutamate to NMDA-type receptors results in the influx of Ca^{2+} into the cell triggering synthesis of NO (Figure 6). NO exhibits rapid diffusability through lipid and aqueous environments, allowing three-dimensional spread of signal across cell membranes. It is estimated that a single point source emitting NO for 1-10 s will influence an area with a diameter of 200 µm containing neurones (around 2 million synapses) glia and vasculature (Wood and Garthwaite, 1994). As described earlier NO acts on its major GC-coupled receptor and the resulting accumulation of cGMP in the target cell modulates the activity of cGK, ion channels, and PDE to bring about changes in cell function. The brain has the highest NOS activity of all the tissues in the body, and with its widespread sphere of influence could be involved in many aspects of CNS function including development, synaptic plasticity, modulation of neurotransmitter release and regulation of blood flow (Garthwaite and Boulton, 1995).
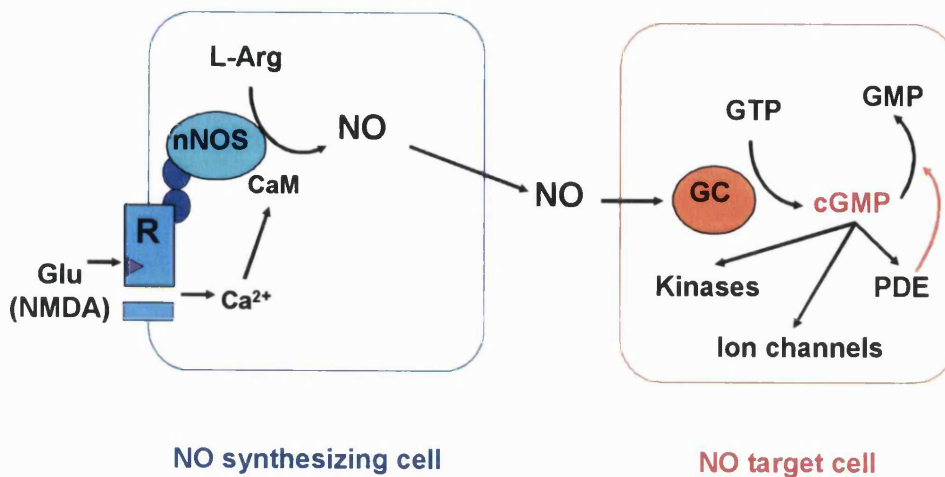
Figure 6: The NO-cGMP signalling pathway in the CNS

NO and CNS development

The NO signalling pathway may represent a potentially important mechanism underlying the timing and co-ordination of neuronal connections within the developing nervous system (Gibbs, 2003). For example, NO is involved in establishing the patterning of retinal inputs in the visual system of the ferret, chick and mouse (Cramer et al., 1996; Wu et al., 1994; Wu et al., 2000). In these systems NO synthesised in cells interacts with newly arrived retinal inputs to regulate the location and number of synaptic connections. In the ferret, development of the visual system is orchestrated by NO acting on the $NO_{GC}R$ (Leamey et al., 2001). Cyclic nucleotides are known regulators of neuronal growth cone migration (Song et al., 1998). The mechanism is poorly understood, but CNG channels are thought to be involved, as immunohistochemical staining reveals that they are expressed in growth cones of cultured hippocampal neurones during development (Zufall et al., 1997).

In the developing brain of the *Xenopus laevis* tadpole, NO regulates cell number (Peunova et al., 2001). In this system NOS inhibition causes an increase in the total number of cells, resulting in a profound distortion of the overall cellular organisation. Conversely, increased levels of NO reduce cell division, resulting in a decreased brain size. This is consistent with NO acting as an anti-proliferative agent to regulate the switch between proliferating neuronal precursors and differentiated cells within the developing brain. It has been proposed that NO inhibits cell division by activating the p53 and Rb signalling pathways (Gibbs, 2003).

39

NO and synaptic plasticity

The most widely studied function of NO in the CNS, is its involvement in the activity-dependent changes in synaptic strength of LTP and LTD. Although the chain of events resulting in increased synaptic strength is unknown, a post-synaptic Ca^{2+} influx is generally agreed to be a minimal requirement for LTP induction. An unresolved issue in LTP research is the site of its expression. The increase in synaptic strength mediated by LTP may be due to either an enhancement of pre-synaptic transmitter release, or post-synaptic transmitter sensitivity, or a combination of both scenarios. Evidence for the pre-synaptic change underlying LTP came from the finding that there was an enhanced release of transmitters from pre-synaptic terminals during LTP induction (Larkman and Jack, 1995). NO was postulated as the retrograde messenger that transmitted the signal triggered by an influx of Ca^{2+} in the post-synaptic cell to pre-synaptic cells (Bohme et al., 1991; Schuman and Madison, 1991). This initial work was based on the strategies of applying NOS inhibitors, NO scavengers or exogenous NO to either inhibit or mimic the endogenous pathway. Gene targeting suggests that both nNOS and neuronally located eNOS are implicated in LTP. In nNOS or eNOS KO mice LTP is only slightly reduced (O'Dell et al., 1994), whereas animals deficient in both NOS isoforms exhibit substantially reduced LTP (Son et al., 1996). There is still much controversy surrounding the importance of NO in LTP (Huang, 1997), but it has now been accepted that LTP can be established by multiple, independent effector mechanisms some of which are NO-dependant while others are NO-independent (Sanes and Lichtman, 1999).

LTD has been predominantly studied in the cerebellum, though can also be observed in other brain regions (Calabresi et al., 1999). In the cerebellum LTD is characterised by a long lasting depression of parallel fibre synapses following repeated excitation of the climbing fibres of Purkinje cells. The reduction in synaptic strength appears to be caused by a diminished sensitisation of the postsynaptic alpha-amino-3-hydroxy-5-methylisoxazole-4-proprionic acid (AMPA) receptors. This process appears to be mediated by the NO-cGMP signalling pathway (Daniel et al., 1993), and has been proposed as a model for the learning of motor movements. The role of NO in both forms of synaptic plasticity appears to involve interaction with PSD-95, as both LTP and LTD are significantly modified in mice with targeted disruption of PSD-95 (Migaud et al., 1998).

1.11 NO and neuropathology

There is much interest in the role that NO plays in the pathogenesis of chronic neurodegenerative diseases such as Alzheimer's (Dorheim et al., 1994; Gahtan and Overmier, 1999), Parkinson's (Hirsch and Hunot, 2000; Liberatore et al., 1999) multiple sclerosis (Smith and Lassmann, 2002), and more acute brain injury such as in cerebral ischaemia (Iadecola, 1997; Keynes and Garthwaite, 2004; Murphy, 1999). Expression of iNOS has been found in the chronic neurodegenerative diseases. In Parkinson's disease post-mortem examination reveals that the loss of dopaminergic neurones in the substantia nigra is associated with a massive astrogliosis and the presence of activated microglia (McGeer et al., 1988). In mice that are rendered Parkinsonian by 1-methyl 4-phenyl-1,2,3,6-tetrahydropyridine (MPTP), microglial iNOS-derived NO has been shown to play a deleterious effect in domaminergic neurones, suggesting that iNOS inhibitors may have a role in future therapies (Liberatore et al., 1999).

Energy failure especially at the level of the mitochondria respiratory chain has been suggested as an important factor in the mechanism of NO mediated neurotoxicity (Stewart and Heales, 2003). As previously described NO may inhibit respiration reversibly at cytochrome c oxidase, or irreversibly following prolonged exposure, at multiple sites including complex I (Stadler et al., 1991) and (after NO has been converted to other reactive nitrogen species such as $ONOO^-$; Cassina and Radi, 1996). NO may directly shift the mitochondrial electron chain into a more reduced state, enhancing formation $O_2^{\bullet-}$. Alternatively, NO or other reactive nitrogen species may trigger induction of the mitochondrial permeability transition pore which results in mitochondrial swelling, calcium release and cell death (Jordan et al., 2003). Different pathways of cell death may then be activated such as apoptosis or necrosis.

One mechanism of oxidative cellular injury is the nitration of protein tyrosine residues, mediated by peroxynitrite, a reaction product of nitric oxide and superoxide radicals. Postmortem tissue samples from patients with Parkinson's (Good et al., 1998), Alzheimer's disease (Smith et al., 1997) and amyotrophic lateral sclerosis (Beal et al., 1997) have all demonstrated nitrotyrosine residues indicating the presence of $ONOO^-$. In cerebral ischaemia NO may also cause damage by enhancing synaptic transmission. *In vivo* experiments showed that the majority of hippocampal CA1 neurons destined to die following ischaemic reperfusion, exhibited potentiated synaptic transmission (Gao et al., 1999). Other reports suggest that the pathology may occur further down the NO-cGMP pathway. Recently, striatal PDE mRNA and protein

levels were found to be reduced in transgenic Huntington's disease mice prior to the onset in loss of motor control (Hebb et al., 2004). As with many areas of research into NO there is considerable conflicting data in the literature. However, with the development of new techniques to apply constant known concentrations of NO to experimental models, and realising the potential for artifacts especially in tissue culture (Keynes et al., 2003; Keynes and Garthwaite, 2004), a better understanding of NO role in these disorders will hopefully be achieved.

1.12 Aims of the project

Over the course of this chapter the discovery of NO has been described and the importance of the NO-cGMP signalling pathway has been highlighted. The $NO_{GC}R$ plays a pivotal role in the transduction of inter- and intra-cellular signals conveyed by NO, and cGMP regulates a plethora of biological functions depending on location and cell type. Due to the ubiquitous nature of the NO-cGMP pathway, signal transduction by the $NO_{GC}R$ also has a profound pathophysiological significance. It is crucial that the NO-cGMP transduction system is understood in its entirety, to provide the greatest opportunity for the design and development of therapeutics. However, despite the numerous advances made in this field since the initial discovery of soluble guanylyl cyclase in 1969, many aspects of this enzyme and the transduction mechanism remain incompletely understood. This study aims to address some of the fundamental questions that are still ambiguous regarding the functional characteristics of the $NO_{GC}R$ isoforms:

1) Is the desensitizing profile of $NO_{GC}R$ activation a common feature of the receptor in cells?
2) Does the molecular makeup of the receptor influence the kinetics of activation?
3) Is NO sensitivity different between isoforms?
4) How many binding sites does the $NO_{GC}R$ have?
5) Is the NO sensitivity of the $NO_{GC}R$ influenced by cellular location?

For the $NO_{GC}R$ there appears much ambiguity and incoherency in the literature regarding these questions. One of the major reasons for this, is that NO is unstable in aerobic solutions, and so many of the previous studies have been done using varying NO levels. Thus a new method has been developed to deliver NO at constant concentrations.

Chapter 2

Materials and methods

2.1 Materials

Compounds

Compounds	Abbreviation	Vehicle	Source
Bovine serum albumin (fractionV)	BSA	—	Sigma
Creatine kinase (type I; from rabbit muscle 324 U/mg/protein)		dH_2O	Sigma
Creatine phosphate		dH_2O	Sigma
Cilostamide		DMSO	Sigma
2-(4-carboxyphenyl)-4,4,5,5-tetramethylimidazoline-1-oxyl-3-oxide.	CPTIO	dH_2O	Alexis
D(-)-2-amino-5-phosphoropentanoic acid	D-AP5	10 mM NaOH	Sigma
Deoxyribonuclease 1 (type IV; from bovine pancreas 2500 Kunitz U/mg/protein)	DNase	—	Sigma
Diethylamine NONOate	DEA/NO	10 mM NaOH	Alexis
2,2'-(Hydroxynitrosohydrazono)bis-ethanimine NONOate	DETA/NO	10 mM NaOH	Sigma
Dimethyl sulfoxide	DMSO	—	Sigma
Dulbeccos minimal essential medium	DMEM	—	InVitrogen
Erythro-9-(2-Hydroxy-3-nonyl)adenine Hydrochloride	EHNA	DMSO	Sigma
Ethylene glycol-bis (β-aminethyl ether)-N,N,N',N'-tetraacetic acid	EGTA	Equimolar NaOH	Sigma
Foetal calf serum	FCS	—	InVitrogen
Guanosine 5'-triphosphate	GTP	dH_2O	Sigma

Haemoglobin from bovine erythrocytes	Hb	—	Sigma
Hepes		—	Sigma
3-Isobutyl-1-methylxanthine	IBMX	—	Sigma
Milrinone		DMSO	Sigma
Nicardipine		DMSO	Sigma
L-Nitroarginine	L-NA	10 mM NaOH	Tocris
Penicillin		—	InVitrogen
Phosphate buffered saline	PBS	dH_2O	Sigma
Rolipram		DMSO	Tocris
RO 20-1724		DMSO	Calbiochem
Sildenafil		DMSO	Chemistry/WIBR
Sodium Hydroxide	NaOH	—	BDH
Soybean trypsin inhibitor		—	Sigma
Spermine NONOate	SPER/NO	10 mM NaOH	Alexis
Streptomycin		—	InVitrogen
Cu/Zn Superoxide dismutase from bovine erythrocytes	SOD	dH_2O	Sigma
Tris (hydroxymethyl)aminomethane	Tris HCl	—	Sigma
Triton X-100		dH_2O	
Trypsin (type I; bovine pancreas 10100 U/mg/protein)		—	Sigma
Uric acid		60 mM NaOH	Sigma

dH_2O Double distilled water, filtered though a 0.22 μm milliQ filter (Millipore, Watford UK)

— Diluted in buffer, or used as indicated in the text.

Antibodies for immunohistochemistry

1st Antibody	1st Host	Conc.	2nd Host	Conc.	Linked
cGMP (kind gift from Dr. J. de Vente, Maastricht, Netherlands)	Sheep	1:8000	Donkey	1:200	Rhodamine (Chemicon)
Neurone-specific nuclear protein (NeuN; Chemicon)	Moucse	1:100	Horse	1:200	Fluoroscein (Vector)
Glial Fibrillary Acidic Protein (GFAP; Chemicon)	Mouse	1:800	Horse	1:200	Fluoroscein (Vector)
Micro-tubule associated protein 2 (MAP-2; Chemicon)	Mouse	1:2000	Horse	1:200	Fluoroscein (Vector)

Suppliers

Alexis   Alexis Biochemicals, Nottingham, UK

BDH   Merck Ltd., Leicestershire, UK

Calbiochem   Calbiochem-Novabiochem (UK) Ltd., Nottingham, UK

Chemicon   Chemicon, Temecula, California, USA

Chemistry   Chemistry Division, Wolfson Institute for Biomedical Research, University College London, UK

Millipore   Millipore Ltd., Watford, UK

InVitrogen   InVitrogen Ltd., Paisley, UK

Tocris   Tocris Cookson Ltd., Bristol UK

Vector   Vector Laboratories, Ltd., Orton Southgate, Peterborough, UK

All other chemicals were from **Sigma-Aldrich**, Hertfordshire, UK

Animal suppliers

Sprague-Dawley rats were obtained from Charles River, Margate, UK

Data manipulation and statistics

The computer package used was Origin™ version 6.1; Aston Scientific Ltd, Stoke Mandeville, UK

2.2 General solutions

Artificial cerebral spinal fluid (aCSF)

aCSF contained in (mM): NaCl (120), KCl (2), $NaHCO_3$ (26), $MgSO_4$ (1.2), KH_2PO_4 (1.2), glucose (11) $CaCl_2$ (2) and was continuously gassed with 95 % O_2 and 5 % CO_2 at pH 7.4 for a minimum of 1 h prior to use. The aCSF also contained L-nitroarginine (L-NA; 0.1), to prevent possible complications from endogenous NO synthesis.

Incubation Buffer

Containing (mM): NaCl (130), KCl 3, $MgSO_4$ (1.2), Na_2HPO_4 (1.2), Tris HCl (15), $CaCl_2$ (2), glucose (11), and L-NA (0.1), pH 7.4. If required the buffer also contained IBMX (1 mM). This buffer was used for the resuspension of striatal, COS-7 cells and red blood cells (RBC). In the latter case the buffer also contained 0.5 % bovine serum albumin (BSA).

Inactivation Buffer

In (mM): Tris-HCl (50), EDTA (4), pH 7.4.

CPTIO-containing assay buffer
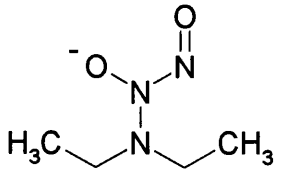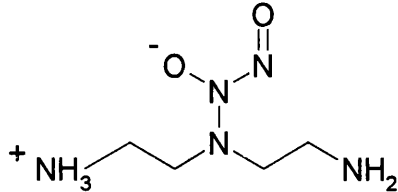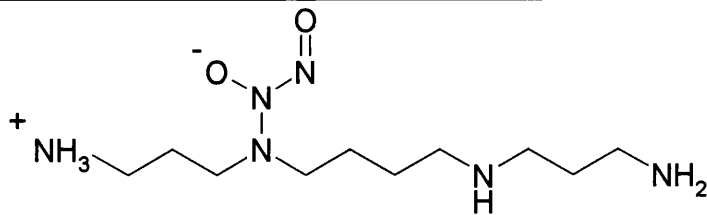
Immediately prior to use a fresh stock of the following buffer was prepared (in mM): Tris-HCl (50) $MgCl_2$ (0.1), EGTA (0.1), DTT (0.01), BSA (0.05), pH 7.4 at 37 °C. Just before each experimental run the following compounds were added to the buffer: superoxide dismutase (SOD; 1000 units/ml) and in (mM) CPTIO (0.2), uric acid (0.3), GTP (1), creatine phosphate (5) and creatine kinase (200 µg/ml). The last three compounds were added to ensure that GTP levels were maintained.

All stock compounds were made fresh each day, dissolved in dH_2O and kept on ice, with the exception of the 30 mM uric acid stock which was dissolved in 60 mM NaOH and kept at room temperature.

NO donors

A series of nucleophile/NO adducts known as NONOates have recently been developed (Morley and Keefer, 1993) and are NO-donating compounds. They have major advantages over previous donors as they are stable as solids, but spontaneously degrade in aqueous solution with first order kinetics, to release NO•. The parameters governing decomposition are temperature, pH, and the identitiy of the nucleophile precursor only (Table 3). Thus addition of a NONOate to a solution at physiological temperature and pH results in the release of NO with predictable kinetics.

All NO donor stocks were made in 10 mM NaOH and kept on ice prior to use to prevent donor decomposition.

Donor	Structure	Half life (at 37 ° C, pH 7.4)
DEA/NO		2.1 minutes
DETA/NO		20 hours
SPER/NO		39 minutes

Table 3: NONOates structure and half-life

2.3 General methods

Striatal slice preparation

Sprague Dawley rats (Charles River, Margate, UK) aged postnatal day 8, were killed by decapitation as approved by the British Home Office and the local ethics committee. The brain was removed and a coronal incision was made approximately 5.0 mm behind the olfactory bulb. Coronal slices 400 μm thick were cut in oxygenated aCSF at 10°C using a Vibratome (Campden Instruments Ltd). Slices were discarded until the merger of the corpus callosum could be seen. At this point 3 further 400 μm thick slices were cut and the striatum from each hemisphere was dissected using a microknife as illustrated by the red line in figure 7. The resulting slices were randomized, paired and 3-4 slices were incubated in 20 ml of aCSF. Slices were recovered for at least 1 h in a shaking water bath (37°C) before use. 10 min prior to NO-stimulation slices were transferred into aCSF which also contained IBMX (1 mM) a non-specific phosphodiesterase inhibitor.
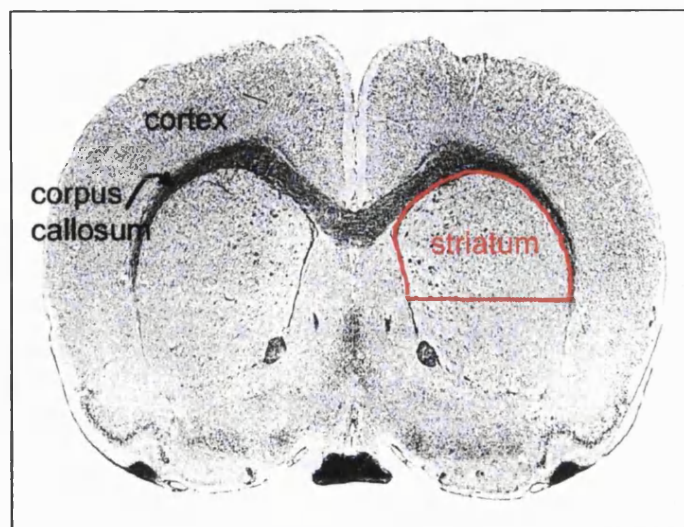
Figure 7: Coronal section of immature rat brain

The red line indicates line of microdissection.

Preparation of striatal cell suspension

The following solutions were required for striatal cell preparation. Solutions 1-6 were gassed under 95% O_2 and 5% CO_2 at room temperature.

Solution	
1	Ca^{2+} free aCSF
2	200 ml (1) + 0.6 mg/ml BSA (fraction V)
3	50 ml (2) + 25 mg trypsin (~8000 U/mg)
4	30 ml (2) + 15.6 μg soybean trypsin inhibitor, 2.5 mg DNase, 46.5 μl $MgSO_4$ (1 M), 30 μl D-AP5 (100 mM stock in 0.1 M NaOH)
5	42 ml (2) + (4) 8 ml
6	25 ml (2) + 2.5 μl $CaCl_2$ (1 M) + 31 μl $MgSO_4$ (1 M)
Incubation buffer	In (mM); Tris-HCl (15), NaCl (130), KCl (3), $MgSO_4$ (1.2), Na_2HPO_4 (1.2), $CaCl_2$ (1.5) glucose (11), L-NA (0.1), pH 7.4 at 37 °C
Wash buffer	(Incubation buffer) without added Ca^{2+} or L-NA.
4% BSA solution	10 ml (1) + 0.4 g BSA fraction V

10-15 Sprague Dawley rats aged postnatal day 8-9 were decapitated, and the brain removed. A thick (1.6 mm) slice of brain was first cut in the coronal plane, starting just behind the merger of the corpus callosum. The striatum from each hemisphere was dissected out and cut in both the coronal and parasagittal planes into 400 μm cubes using a McIlwain tissue chopper. The cubes were washed into 15 ml tubes containing 10 ml of solution (2; cooled in a water bath at 10 °C), and gently dispersed using a Pasteur pipette. The tubes were centrifuged at 100 *g* for a few seconds and the supernatant aspirated.

The pellets were resuspended in 10 ml of solution (3), transferred to a conical flask, and trypsinised for 15 min under carbogen in a gently shaking water bath at 37 °C. The trypsin was neutralised by adding 10 ml of solution (5) and the cells transferred to a 50 ml tube and centrifuged at 100 *g* for a few seconds. The supernatant was aspirated and resuspended in 2 ml of solution (4). The blocks were dispersed by mechanical trituration, passing them up and down

50

through a Pasteur pipette for 10-15 cycles. After settling, the supernatant containing dispersed cells was added to 3 ml of solution (6). Again 2 ml of solution (4) was added to the blocks and the trituration cycle was repeated for 3 cycles or until the blocks had dispersed. Any clumps contaminating the collected cells were removed and the suspension was adjusted to 9 ml with solution (6). The cells were underlaid with 1 ml of 4 % BSA solution (using a syringe with a long needle) and centrifuged at 100 g for 5 min to remove cellular debris. The supernatant was aspirated and the cell pellet resuspended in 5 ml of wash buffer. After centrifugation (100 g, 3 min) the supernatant was aspirated and cells resuspended in incubation buffer.

Cell viability and number was assessed using the trypan blue method. The cell suspension was counted at a 1:5 dilution in trypan blue using a haemocytometer. The yield of striatal cells was approximately 0.5 million cells/rat. Cells were allowed to recover for at least 1 h in a shaking water bath set at 37 °C, at a final concentration of 1 x 10^6 cells/ml. The cells were incubated in the presence of the nitric oxide synthase (NOS) inhibitor L-NA (0.1 mM) to prevent possible complications arising from endogenous NO synthesis.

Tissue inactivation

At the end of experiments brain tissue slices or cell suspensions (50-100 μl) were inactivated for 3 min in 200 μl of boiling hypotonic inactivation buffer. Inactivated slices were homogenised by sonication and a sample removed for protein assay. The remaining sample was then centrifuged at 10,000 g for 5 min to remove tissue debris and the supernatant was analysed for cGMP content.

Protein assay

Protein was measured using a bicinchoninic acid (BCA) protein assay (Perbio Science, UK). The assay is based on the reduction of Cu^{2+} to Cu^{1+} in the presence of protein under alkaline conditions. A reagent containing BCA forms a purple water-soluble complex with Cu^{1+}. This can be measured colourimetrically at the peak absorbance of 562 nm, which is proportional to protein concentration over the range 20-2000 μg/ml. Briefly, BSA protein standards ranging from 0-1 mg/ml were prepared. 10 μl aliquots (in triplicate) of either standards or samples were dispensed into a 96 well plate followed by 0.2 ml of the BCA reagent. After 30 min incubation at 37°C the absorbance was measured at 562 nm using a Spectra max 250 (Molecular Devices,

California, USA) spectrometer. The absorbance increased linearly over the 0-1 mg/ml protein range, allowing the amount of sample protein to be calculated from the standard curve.

cGMP radioimmunoassay

cGMP in the inactivated samples was quantified using a standard ^{3}H-cGMP radioimmunoassay, based on a commercially available kit (Amersham Pharmacia Biotech, Hertfordshire, UK).

Immunohistochemistry

Cell suspensions and slices were fixed in paraformaldehyde (4 %) in 0.1 M phosphate buffer, pH 7.4, for either 1 h (slices) or 20 min (cell suspensions) at room temperature. Cell suspensions were then dried onto gelatine-coated slides, stored at -20 °C, and rehydrated with dH$_2$0 immediately before staining.

Slices were cryoprotected by incubating overnight at 4 °C in phosphate buffer (0.1 M) and 20 % sucrose. The slices were then incubated for 30 min initially in 1:1 solution of 20 % sucrose and OCT embedding material (RALAMB Ltd, East Sussex, U.K), then 30 min in OCT alone, frozen in OCT over dry-ice and stored at -80 °C. 10 μm sections were cut using a cryostat, dried onto gelatine coated slides, and microwaved for 1 min at medium power, in a pre-warmed buffer containing trisodium citrate (10 mM) and EDTA (1 mM).

Slides (with adhering cell suspensions or sections) were rehydrated in dH$_2$O and permeabilized with Tris-buffered saline (TBS) containing 1 % Triton X-100, for 15 min. After rinsing with TBS containing 0.1 % Triton X-100, 0.2 % BSA, slides were incubated with normal rabbit and horse sera for 30 min at room temperature, and then overnight at 4 °C with the primary antibodies: sheep anti-cGMP (1:8000) and either mouse anti-microtubule associated protein 2 (MAP-2; 1:2000), mouse anti-glial fibrillary acidic protein (GFAP,1:800) or mouse anti-neurone-specific nuclear protein (NeuN, 1:100 found by optimisation of the technique). MAP-2 was used to identify neurones in cell suspensions. However, in slices staining of the neuropil masks individual cells, and so NeuN was used as an alternative. Slides were rinsed three times in TBS and incubated with a secondary antibody (anti-sheep Tetramethyl rhodamine isothiocyanate (TRITC) or anti-mouse Fluoroscein isothiocyanate (FITC) for 1 h at room temperature, mounted in Vectorshield with DAPI (4',6-Diamidino-2-phenylindole; Vector)

nuclear stain, and viewed under fluorescence optics or laser scanning confocal microscope (Leika Microsystems, Milton Keynes, UK).

The percentage of cells accumulating cGMP was determined by exposing 4 seperately prepared striatal cell suspensions to DEA/NO (1 μM) for 30 s in the presence of EHNA (300 μM), and processing for immunohistochemistry as above. A random selection of at least three fields per slide (containing between 80-150 cells) were counted for cells that co-stained with cGMP and the nuclear marker DAPI.

Preparation of ferrous haemoglobin

This method is based on a method by (Martin et al., 1985). A 1 mM stock of haemoglobin (Hb; type 1) was prepared in dH_2O. Excess sodium dithionate (10 mM) was added and mixed for a few seconds until the Hb solution became bright red indicating the reduction of Fe^{3+} to Fe^{2+}. To remove the reducing agent 10 ml of the solution was transferred to pre-soaked dialysis tubing (12 kDa cut-off) and dialysed against 2 L dH_2O at 4 °C. After 1 h the dialysis tubing was transferred to a second volume of 2 L of dH_2O and left overnight to dialyse. The Hb was collected, frozen and stored at -20 °C until use.

NO probe

NO concentrations were recorded in buffer (1 ml) in either a sealed or open, stirred vessel at 37 °C, equipped with an NO electrode (Iso-NO, World Precision Instruments, Stevenage, UK).

Red blood cell preparation

This method is based on Liu el al., 1998. Whole blood was withdrawn from 8 day old rats and added to ice-cold phosphate buffered saline (PBS; pH 7.4). Red blood cells (RBC) were pelleted by centrifuging at 2300 *g* for 10 min. The buffy coat and plasma were discarded and the RBC were washed 3 times in PBS. After the final wash, RBC were resuspended at 2 million RBC/ml in incubation buffer containing 0.5 % BSA and IBMX (1 mM).

DNA preparation

cDNAs encoding α1, α2 and β1 NO$_{GC}$R subunits were originally obtained by RT-PCR using total RNA from rat tissue and subcloned into the expression vector pCMV (Gibb and Garthwaite, 2001). The vectors were transformed into *Escherichia coli* (E. coli) DH5α and stored as glycerol (15 %) stocks at -80 °C (kindly given by Barry Gibb). E. coli were streaked out onto 90 mm Petri dishes containing Lennox L-agar (InVitrogen), supplemented with 50 µg/ml kanamycin (Sigma) and incubated overnight at 37 °C.

Single colonies containing the plasmid of interest were picked and grown for a maximum of 16 h at 37 °C at 200 RPM in 5 ml Lennox L-broth supplemented with 50 µg/ml kanamycin. At the end of the growth period, bacteria were pelleted at 16 000 *g* for 1 min and the supernatant discarded. The plasmid DNA was purified from these pellets using a commercially available kit, QIAprep miniprep kit (Qiagen West Sussex, UK) as described by the manufactures instructions.

The DNA for each subunit was pooled and a sample from each was analysed by electrophoresis on 1 % agarose gels. Gels were prepared by adding 1 g agarose (InVitrogen) to 100 ml Tris-Acetate-EDTA (TAE) buffer and heated in a microwave. Ethidium bromide (0.55 µg/L; Sigma) was added to the molten gels and mixed. Gels were poured into the casting trays of a horizontal electrophoresis tank with the appropriate combs inserted. Gels were allowed to set and TAE buffer added to cover the gel.

DNA samples (2-10 µl) were mixed with an appropriate volume of loading buffer prior to loading. Agarose gels were electrophoresed at a constant voltage of 80 V for 40 min and DNA was visualised under ultra-violet light. DNA molecular weight standards of known amount were used to quantify the DNA. Plasmid DNA concentrations were normalised by dilution if necessary so that an equal volume containing similar amounts of DNA could be transfected into mammalian cells.

Tissue culture and transfection

African green monkey kidney fibroblast cells (COS-7, catalogue number 87021302 from the European Collection of Cell Cultures, Salisbury, UK) were cultured in Dulbecco's modified Eagles medium (DMEM), supplemented with 10 % foetal calf serum and 100 units/ml of both penicillin and streptomycin (InVitrogen, Paisley, UK). Cells were maintained in a humidified

54

incubator at 37 °C with 5 % CO_2 for up to a maximum of 30 passages to limit alteration of the cell genotype.

For transfection, cells were plated so that a confluency of 40-60% was achieved at the time of transfection. This ensured that the cell density was not too high and that the cells were growing optimally. To examine individual receptor isoforms, COS-7 cells were transfected with combinations of either the $\alpha 1$ and $\beta 1$ subunits, or $\alpha 2$ and $\beta 1$ subunits. Transfection conditions were optimised and performed using the transfection reagent Effectene (Qiagen, West Sussex, UK) according to manufacturer's instructions, and efficiency was routinely 40 %. Studies were performed on the recombinantly expressed receptors 48 h post transfection to allow for optimal expression of the protein.

Prior to use, cells were harvested by trypsinisation, pooled, pelleted at 1500 g for 5 min. For studies of the receptor isoforms in intact cells, the cells were resuspended at 1 mg protein/ml in incubation buffer.

Preparation of COS-7 homogenate

COS-7 cells were prepared as above except that after pooling and pelleting the cells were resuspended at 3 mg protein/ml in ice-cold lysis buffer (pH 7.4) containing in (mM): Tris HCl (50), DTT (0.1) and a protease inhibitor cocktail (Complete mini EDTA-free; Roche, East Sussex, UK). After addition of glycerol (5 %) the homogenate was frozen until use.

The $\alpha 1 \beta 1$ protein purified from bovine lung

"Soluble guanylyl cyclase" is available from Alexis, and is diluted in a buffer (pH 7.4) containing in (mM): Tris HCl (50), DTT (0.1) and 0.5 % BSA to give a stock concentration of 5 µg/ml. This was stored on ice and subsequently diluted 1:100 into CPTIO-containing assay buffer maintained at 37 °C.

Preparation of perfused heart and cerebellum

Adult female Sprague-Dawley rats were anaesthetised with pentobarbitone (60 mg/kg, i.p.) as approved by the British Home office and the local ethics committee. The animals were perfused through the left ventricle with PBS until the returning buffer ran clear. The hearts and cerebella were swiftly removed and immersed in ice-cold PBS. Adhering connective tissue and

visible vasculature were discarded under a dissecting microscope and the tissues were then cut into 1 mm cubes using a McIlwain tissue chopper, before being frozen on dry ice and homogenised (while frozen) using a stainless steel pestle and mortar, both pre-chilled on ice.

The heart tissue was resuspended to a total volume of 5 ml in ice-cold buffer A containing (mM) NaCl (137), $MgCl_2$ (0.5), NaH_2PO_4 (0.55), KCl (2.7), Hepes (25), glucose (5.6) and a protease inhibitor cocktail (Complete mini EDTA-free; Roche East Sussex, UK), pH 7.4.

The cerebellar tissue was resuspended in 5 ml of buffer as before (Bellamy et al., 2000), containing Tris HCl (50 mM) and DTT (0.1 mM). Preparations were then centrifuged for 5 min at 500 g to remove cellular debris.

Platelet homogenate preparation

Whole blood was collected from 4 adult Sprague-Dawley rats and added to acid citrate dextrose (12.5 %). The platelet rich-plasma was aspirated and re-centrifuged to eliminate residual red and white blood cells. The supernatant was centrifuged for 10 min at 2000 g and the platelet pellet resuspended at a final concentration of 1 mg protein/ml in buffer A (see above). The platelets were lysed by addition of an equal volume of ice-cold distilled water containing protease inhibitor cocktail and 0.2 mM DTT, followed by sonication. The lysate was kept on ice.

Separation of cellular membrane and cytosol fractions

Approximately 3 ml of each homogenate were centrifuged for 1 h at 100,000 g at 4 °C. The supernatants (cytosol) were removed and kept on ice, and the pellets (crude membrane fractions) resuspended in the corresponding homogenisation buffers. The homogenate protein concentrations were determined using the BCA method. For platelets and cerebellum, protein was measured in samples prepared in parallel but lacking DTT (which interferes with the protein assay).

Data analysis

Results are given as the mean cGMP levels (unless otherwise indicated) from n independently treated populations ± SEM, and analysed using the unpaired Student's t-test (two-tailed) or, where stated, analysis of variance using Dunnett's multiple comparison test. Significance was assumed when $p < 0.05$.

Chapter 3

Kinetics of the NO-cGMP signalling in CNS cells

3.1 Introduction

Knowledge of the temporal and amplitude characteristics of NO-evoked cGMP responses is critical to understand how NO signals are decoded. These characteristics are governed by the interplay of the activation kinetics of GC-coupled receptors by NO, and by how the subsequent cGMP responses are shaped by PDE to engage downstream targets.

Previous studies demonstrate that the kinetics of catalysis, of the $NO_{GC}R$ purified from bovine lung, follow the simple Michaelis-Menten model. When the GC-coupled receptor is stimulated with NO, the enzyme is maximally activated and produces cGMP linearly over time, until substrate depletion becomes a limiting factor. However in a more physiological environment for example in intact cerebellar astrocytes, addition of NO causes the GC-coupled receptor to become activated but it then displays a rapidly desensitizing profile (Bellamy et al., 2000). This means that the rate of cGMP synthesis wanes despite the continued presence of NO, as the GC-coupled receptor becomes inactivated or desensitised. Furthermore cellular $NO_{GC}R$ also deactivates rapidly (subsecond time scales) on removal of NO, suggesting that the enzyme in cells behaves in a much more dynamic manner than previously thought.

Unlike the purified $NO_{GC}R$, during sustained NO exposure the rapid desensitization of the enzyme in astrocytes causes the steady-state level of activity to be about 10% of the peak. In these particular cells, the PDE activity is low. The combination of this and $NO_{GC}R$ desensitization leads to a high amplitude plateau of cGMP being produced in response to NO. It is predicted that in cells with high PDE activity, the same NO input signal would result in a low amplitude cGMP transient, a shape that may be tuned to engage different downstream effectors from those in cerebellar astrocytes. Some evidence for this was obtained in human platelets (Bellamy et al., 2000), but this hypothesis has not yet been tested in other CNS cell types that are recognised NO targets, particularly neurones (Southam and Garthwaite, 1993).

NO signalling pathway in the striatum

The striatum forms part of the basal ganglia a brain region associated with movement, and cognitive and emotional aspects of behaviour. It acts as an integrative centre receiving excitatory inputs from the cortex and thalamus, and inhibitory input from the substantia nigra and globus pallidus (Kawaguchi, 1997). The striatum evaluates the inputs, interacts with related brain areas and feeds forward to the cortex. Staining of striatal sections, for acetylcholinesterase (AChE) reveal that it has a patchy appearance. The "matrix" contains cells that stain for AChE and represents about 85% of the total cell volume. Within the matrix are islands of "striasomes" which represent patches of low AChE staining neurones. Further cytological investigation revealed a mosaic of highly organised neuronal connections which have marked differences in their neurotransmitter and receptor distribution (Table 4).

Neuronal Morphology	Type	Transmitter Content	Proportion	Diameter (μm)
Spiny	Projection	GABA, substance P, dynorphin	90-95%	Medium (10-20)
		GABA, enkephalin		Medium (10-20)
Aspiny	Interneurone	ACh	~ 1%	Large (20-50)
		GABA, parvalbumin	3-5%	Medium (10-35)
		GABA, somatostatin, NO, neuropeptide Y	1-2%	Medium (10-35)

Table 4: Striatal neurone subtypes

Adapted from (Kawaguchi, 1997).

The striatum is enriched in the NO-cGMP pathway. Endogenous NO is produced from a small population of interneurones (1-2% of total striatal cells) containing two neuropeptides: somatostatin and neuropeptide Y (Vincent and Johansson, 1983) and probably GABA (Kubota et al., 1993). These aspiny neurones receive inputs from the cortex (Rudkin and Sadikot, 1999) and nigral dopaminergic neurones (Fujiyama and Masuko, 1996), and make synaptic contacts with medium spiny GABAergic projection neurones (Kharazia et al., 1994). Nitrergic neurones also synapse on cholinergic striatal neurones (Vuillet et al., 1992) which receive glutamatergic fibres and in turn innervate projection neurones themselves. Thus endogenous NO may differentially modulate striatal release of ACh, and serotonin, glutamate, γ-aminobutyric acid (GABA), and dopamine (DA) (Trabace and Kendrick, 2000). nNOS positive aspiny neurones express low levels of mRNA for the NMDA receptor subunit NMDAR1 (Price, Jr. et al., 1993) and are immunoreactive for the subunits NR1 and gluR5-7 (Chen et al., 1996). As elsewhere NO production was found to be coupled to NMDA receptors (East et al., 1996).

The striatum also contains high GC activity (Greenberg L.H. et al., 1978) and abundantly expresses mRNA for $\alpha 1$ and $\beta 1$ subunits of the enzyme (Furuyama et al., 1993; Gibb and Garthwaite, 2001). Immunochemical studies showed that high levels of the $NO_{GC}R$ were located in the spiny neurones (Ariano, 1983; Ariano and Ufkes, 1983) suggesting that these are the main targets for NO produced by the interspiny nNOS positive neurones. PDE activity in the striatum is the highest of all brain areas (Greenberg L.H. et al., 1978). The Ca^{2+}/calmodulin-dependent PDE1 (Polli and Kincaid, 1994; Yan et al., 1994) PDE2 (Michie et al., 1996) PDE3 (Reinhardt and Bondy, 1996) PDE4 (Cherry and Davis, 1999), PDE7B (Cherry and Davis, 1999; Sasaki et al., 2000) PDE9A (Andreeva et al., 2001) and PDE10A (Fujishige et al., 1999b; Seeger et al., 2003) are all located there although which, if any, is responsible for degrading NO-induced cGMP signals has not been investigated.

Functionally, the striatal NO-cGMP pathway is involved in synaptic plasticity (Calabresi et al., 1999), neurotransmitter release (Trabace and Kendrick, 2000) and excitation of cholinergic interneurones (Centonze et al., 2001). The striatum is particularly vulnerable to acute insults (such as hypoxia, hypoglyceamia, global ischaemia) and chronic degenerative disorders such as Huntingdon's disease. Altered energy metabolism and excessive activation of glutamamte receptors (excitotoxicity) are thought to be responsible for the striatal neurone damage. NO generation following NMDA receptor stimulation was shown to cause delayed neuronal death in

59

cultured striatal neurones (Strijbos et al., 1996). As the striatum is enriched in all aspects of the NO-cGMP pathway, much research is focused on the signal transduction mechanism in the hope that therapeutic agents to prevent cell damage during acute and chronic neuronal insults will be found.

The striatum is enriched in all elements of the NO-cGMP pathway (as described above) however, the functional characteristics of these elements have not yet been determined. In comparison to cerebellar astrocytes, these cells may have different activities of the component enzymes, and possibly also different isoforms. Thus the striatum was considered a suitable brain area for discerning the kinetics of this signalling pathway in a physiologically relevant context, in neurotransmission. Initially pilot experiments on intact slices of rat striatum were carried out, and then cell suspensions derived therefrom were used to determine the distribution, the identity of the PDE and the kinetics of the enzymes involved in the NO evoked cGMP response.

3.2 Methods

Striatal slices and cell suspensions were prepared as described in chapter 2. When used, PDE inhibitors were made up in DMSO and added 10 min prior to DEA/NO addition. At the 1:100 dilution used, DMSO had no effect on the DEA/NO induced cGMP response (not shown). DEA/NO was prepared in 10 mM NaOH, stored on ice until use and added at a 1:100 dilution. DEA/NO was added to striatal slices/cell suspension at $t = 0$, mixed rapidly and slices/aliquots of cells were removed and inactivated by plunging them into boiling hypotonic inactivation buffer. For the 4 s time course data, cells were sucked up into the barrel of a repeater pipette and 50 μl aliquots were inactivated in boiling inactivation buffer every 4 s as timed by a metronome. The repeater pipette was pre-warmed in a 37 °C chamber and during the experiment the barrel was maintained at body temperature by holding it in the palm of the hand. The location of the cGMP response in both suspensions and slices was identified using immunohistochemistry techniques as described in chapter 2.

Quantification of the rate of cGMP degradation

The addition of Hb to a cell suspension exposed to NO leads to the rapid (half life<0.5 ms) removal of NO, and the rapid ($\tau = 0.27$ s) deactivation of NO$_{GC}$R (Bellamy and Garthwaite, 2001b). Following cellular accumulation of cGMP to high levels (2 minute exposure to a

60

maximal DEA/NO concentration), this method can be used to almost instantaneously arrest the activity of the $NO_{GC}R$. The rate of cGMP degradation within cells can be measured, fitted with the integrated Michaelis-Menten equation (see below), and an operational description of PDE activity can be found.

$$V_p t = K_p \ln\left(\frac{P_o}{P_t}\right) + (P_o - P_t)$$

Where P_0 = concentration of cGMP immediately before Hb addition, P_t = concentration of cGMP at time t. The apparent Michaelis Menten constants V_p, and K_p were found by iteration (Fernley, 1974) using Microsoft VISUAL BASIC 6™ (Microsoft MSN, London, UK).

Simulation of cGMP accumulation in striatal cells

The desensitizing profile of the $NO_{GC}R$ activity over time was first identified in cerebellar astrocytes (Bellamy et al., 2000), and was found to be well described by a single exponential function (Bellamy and Garthwaite, 2001b). The suitability of this model to striatal neurones was tested by simulating cGMP accumulation over time with a combination of an exponentially declining rate of synthesis (v_s) and a substrate-linked (Michaelis-Menten) rate of degradation (v_d).

$$\frac{dP}{dt} = v_s - v_d$$

and

$$v_s = \left(ae^{-kt} + c\right) \qquad\qquad v_d = \left(\frac{V_p P}{K_p + P}\right)$$

The profile of the cGMP accumulation (P) over time (t) reflects the difference between the rates of cGMP synthesis (v_s) and degradation (v_d). Vp = apparent maximal rate of degradation, Kp = apparent Michaelis constant. The initial rate of synthesis (maximum v_s; non-desensitised GC) = $a + c$ and the final rate (minimum v_s; desensitised GC) = c. The constant k determines the rate at which $NO_{GC}R$ progresses from maximum to minimum activity.

61

3.3 Results

Potency of NO for GC in intact striatal cells

The striatal cell suspension was incubated in the presence of the non-selective phosphodiesterase inhibitor IBMX (1 mM). The basal cGMP level was 3.3 ± 0.8 pmol/10^6 cells (n=7). On exposure to the NO donor, DEA/NO (0.03-3 µM) for 30 s, there was a concentration-dependent accumulation of cGMP. The maximal cGMP levels of about 60 pmol/10^6 cells were found at 1 µM DEA/NO, and the NO concentration giving half-maximal activation (the EC_{50}) was approximately 0.1 µM (Figure 8).
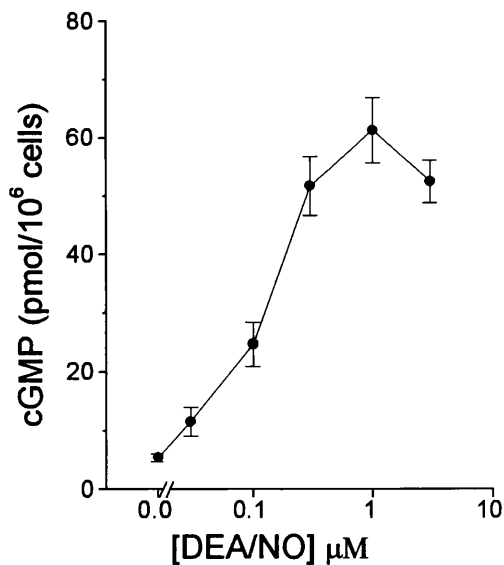
Figure 8: Potency of DEA/NO in striatal cell suspension

The concentration-cGMP accumulation curve was obtained by using a 30 s DEA/NO exposure in the presence of the non-specific PDE inhibitor IBMX (1 mM) and NOS inhibitor L-NA (100 µM); n = 9-12.

Location of cGMP accumulation

The cell suspension is a heterogenous mix of all the cell types present in the striatum. Immunohistochemistry was used to locate the NO evoked cGMP accumulation. Cells stimulated with DEA/NO (1 μM) for 30 s (in the presence of a selective PDE 2 inhibitor; see below) were fixed with paraformaldehyde (4%) and dried onto slides. The percentage of cells accumulating cGMP was determined by counting the number of cells that co-localise cGMP and the nuclear stain DAPI, and represented a subpopulation of spherical cells (6.7 ± 1.3% of the total; 4 separate cell suspensions) with a mean diameter of 7.7 ± 0.4 μm (n=18). Cells accumulating cGMP (Figure 9b) were amongst those that expressed the neuronal MAP-2 (Figure 9a), but were unstained for the astrocytic marker GFAP (Figure 9d) indicating that the target cells were neurones. cGMP immunostaining was not seen in unstimulated cell suspension (data not shown).

To check that the NO-evoked cGMP accumulation in neurones was not a non-physiological consequence of cell dissociation, immunohistochemistry was repeated on intact striatal slices. Following a 2 min exposure to DEA/NO (10 μM; a maximal concentration) in the presence of IBMX (1 mM) high levels of cGMP staining was observed in bundles of fibres running throughout the striatum. Lower levels of cGMP staining were seen in a network of varicose fibres (Figure 9e) in agreement with previous work (Markerink-van Ittersum et al., 1997). A small population of cell bodies stained brightly and these were identified as neurones using NeuN (Figure 9e arrows). It was assumed that these cells in the slice were the same cGMP and MAP-2 positive in the striatal cell suspension.
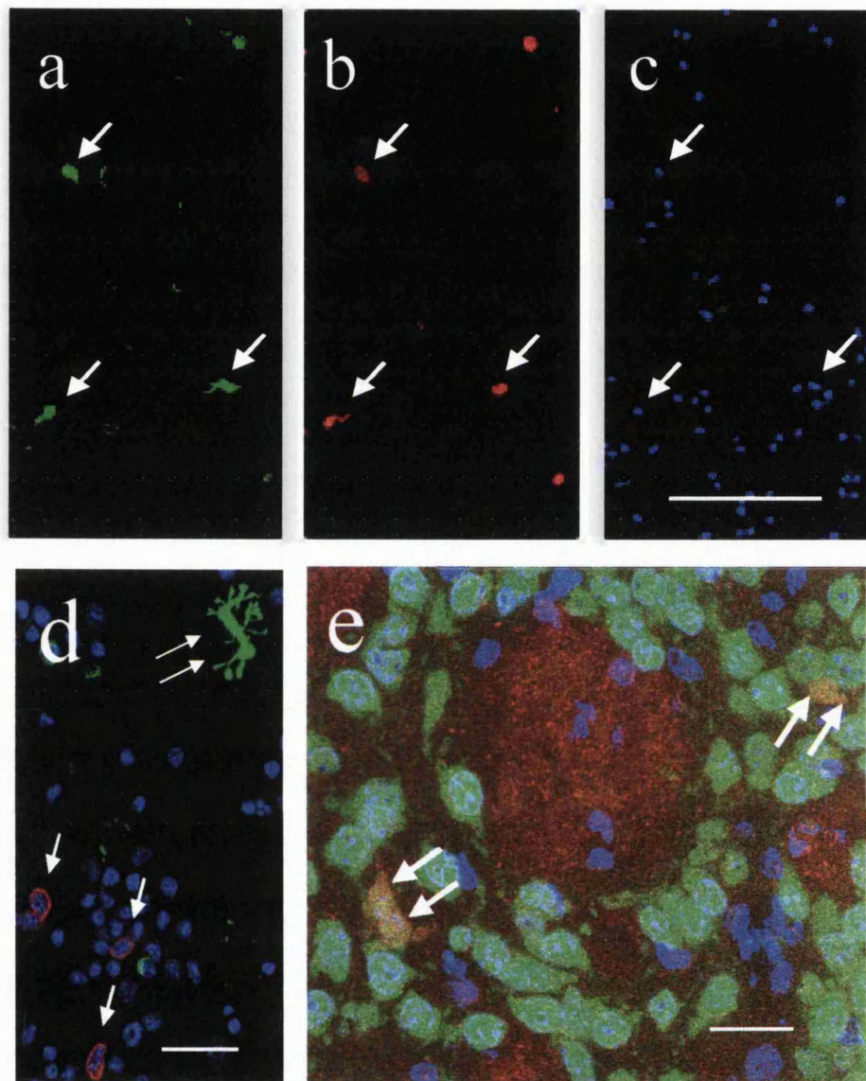
Figure 9: Location of NO stimulated cGMP accumulation in striatal tissue

(a-d) Cell suspension fixed following 30 s exposure to DEANO (1 μM) in the presence of EHNA (300 μM) and stained for MAP-2 (a) cGMP (b); and cell nuclei (DAPI stain) (c). In (d) cells are stained for GFAP (green), cGMP (red) and nuclei (blue). Single arrows indicate cGMP positive cells and double arrows indicate GFAP positive cells. e) Slices were fixed after 2-min exposure to DEA/NO (10 μM) in the presence of IBMX (1 mM), and stained for NeuN (green), cGMP (red) and nuclei (blue). Co-stained cells (orange) are marked with double arrows and fibre bundles (fb). Calibration bar = 100 μm (a-c), 20μm (d-e).

Pharmacological identification of active PDE isoforms

So far 11 distinct families of PDEs have been identified, each with multiple isoforms. PDEs play an important role in shaping cGMP signals so a pharmacological approach was used to identify the PDEs responsible for degrading cGMP in the striatal cells. Inhibitors selective for different PDE families were screened by determining their ability to enhance cGMP accumulation in response to a 30 s exposure to DEA/NO (0.3 μM). In control cells (no PDE inhibitor) cGMP accumulation was 9.8 ± 0.9 pmol/10^6 cells whereas, in the presence of the non-specific PDE inhibitor IBMX (1 mM) the response was 57 ± 4 pmol/10^6 cells. The PDE1-selective inhibitors nicardipine (300 μM; Agullo and Garcia, 1997; Bellamy et al., 2000) and 8-methoxymethyl-IBMX (300 μM; Ahn et al., 1989), the PDE3-selective inhibitors cilostamide (100 μM; Manganiello et al., 1995a) and milrinone (300 μM; Manganiello et al., 1995b; Schudt et al., 1996a), the PDE4-selective inhibitors rolipram and Ro-20-1724 (300 μM; Schudt et al., 1996b), and the PDE5-selective inhibitor sildenafil (300 μM; Turko *et al.* 1999), all failed to augment cGMP accumulation (Figure 10). The only isoform-selective inhibitor that was effective was the PDE2-selective compound erythro-9-(2-hydroxy-3-nonyl)adenine (EHNA, 300 μM; Michie et al., 1996; Podzuweit et al., 1995) which elevated cGMP to levels not significantly different from those found with IBMX (Figure 10). A concentration-response curve for EHNA (3-300 μM) indicated an EC_{50} of around 30 μM and a maximally-effective concentration of ~300 μM (Figure 10 inset). None of the PDE inhibitors significantly influenced cGMP levels in cells not treated with DEA/NO (not shown) which presumably reflected the lack of a synaptic network in the cell suspension.
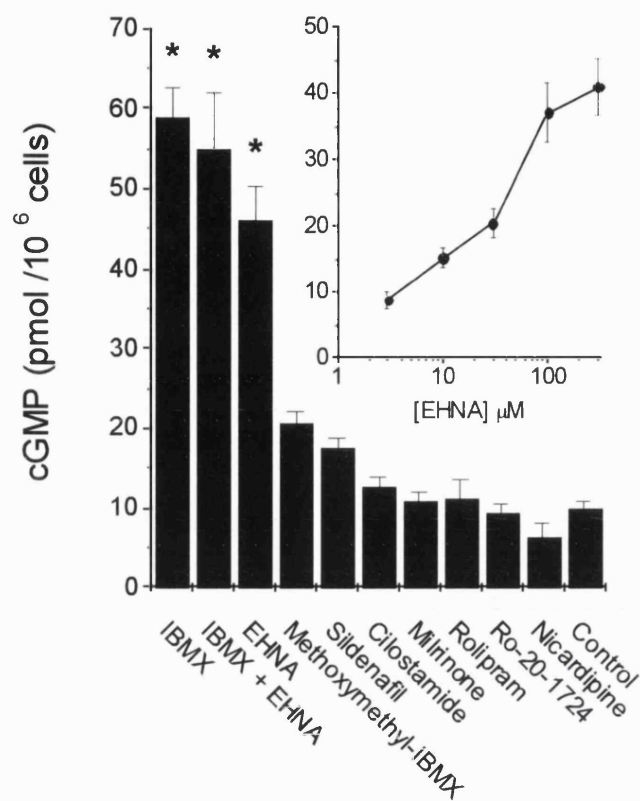
Figure 10: Effect of different PDE inhibitors on cGMP level

Data represent the total cGMP levels remaining 30 s after addition of DEA/NO (30 μM; n = 4-9). All PDE inhibitors were tested at a concentration of 300 μM with the exception of IBMX (1 mM) and cilostamide (100 μM). * $p<0.05$ versus control (analysed using Dunnett's test). Inset: EHNA concentration, cGMP accumulation curve following 30 s exposure to DEA/NO (0.3 μM; n=3).

Kinetic analysis of cGMP synthesis and degradation

The kinetics of $NO_{GC}R$ and PDE in the striatal neurones was investigated by exposing the cells to a maximal concentration of DEA/NO (1 μM), and obtaining detailed time courses in the presence and absence of EHNA (300 μM). A maximal DEA/NO concentration was used so that decay of NO by auto-oxidation was not a limiting factor. In the presence of EHNA, cGMP showed a steep rate of rise to reach a transient plateau after 15 s (Figure 11). At this point the rate of cGMP synthesis is equal to the rate of breakdown. In untreated cells the time course had a similar profile but with a much lower overall level of cGMP, as seen in other cell types containing high PDE e.g. platelets (Bellamy et al., 2000).
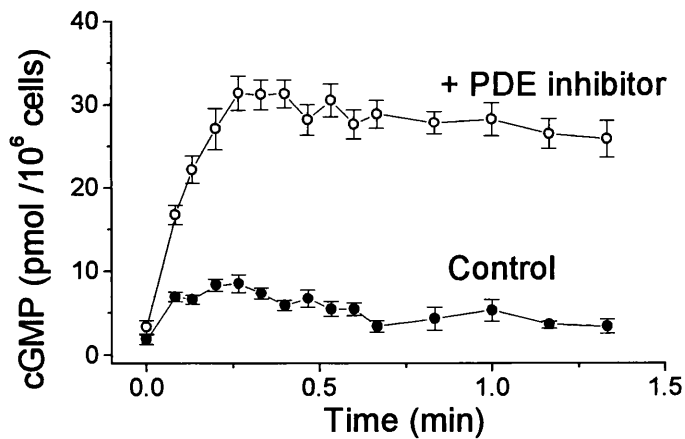
Figure 11: cGMP accumulation in striatal cells

cGMP accumulation was induced by DEA/NO (1 μM) in the presence (o) and absence (•) of the PDE2 inhibitor erythro-9-(2-hydroxyl-3-nonyl)adenosine).

The rate of cGMP accumulation is a result of the difference between the rate of cGMP synthesis (v_s) by $NO_{GC}R$ and the rate of cGMP degradation (v_d) by PDE (or other routes). By measuring the rate of cGMP accumulation v_d and v_s can be calculated. The ability of Hb to scavenge NO (rate constant of ~50 $\mu M^{-1}s^{-1}$ at 37 °C; Eich et al., 1996) was exploited to remove free NO from the cell suspension. The decline in cGMP levels reflects degradation, as NO dissociates from the haem moiety to be trapped by the Hb so abolishing cGMP synthesis. In living cells this has been shown to occur with a half-life of around 200 ms (Bellamy and Garthwaite, 2001b). Under control conditions v_d cannot be accurately measured as it is so high, and so the Michaelis-Menten parameters governing PDE activity were measured in the presence of EHNA (300 μM), which greatly slows the degradation of cGMP. In striatal cells receptor activity was arrested following a 1 min exposure to 1 μM DEA/NO by addition of 10 μM Hb. The decline in cGMP could be satisfactorily fitted with the Michaelis-Menten equation (Figure 12a) allowing the rate of cGMP degradation over the time course of cGMP accumulation to be defined (Figure 12b).

Previous studies using cerebellar cell suspensions stimulated with NO suggested that $NO_{GC}R$ activity declines exponentially over time reflecting desensitization (Bellamy et al., 2000; Bellamy and Garthwaite, 2001b). The suitability of this model in the striatal cell preparation was evaluated by simulating the cGMP response to NO with an exponentially falling v_s and Michaelis-Menten-type degradation. The simulations were then overlaid on experimental data and provided a close fit to the cGMP accumulation in cells incubated with EHNA (Figure 12b). The derived v_s was initially 3.5 pmol/cGMP/10^6 cells/s and then it declined progressively to a 13-fold lower rate (0.26 pmol/cGMP/10^6 cells/s) within around 30 s (n=7). This is similar to the profile derived from rat cerebellar cells (Bellamy et al., 2000) suggesting that the $NO_{GC}R$ expressed in the striatal neurones exhibits similar kinetics to the enzyme in cerebellar astrocytes.
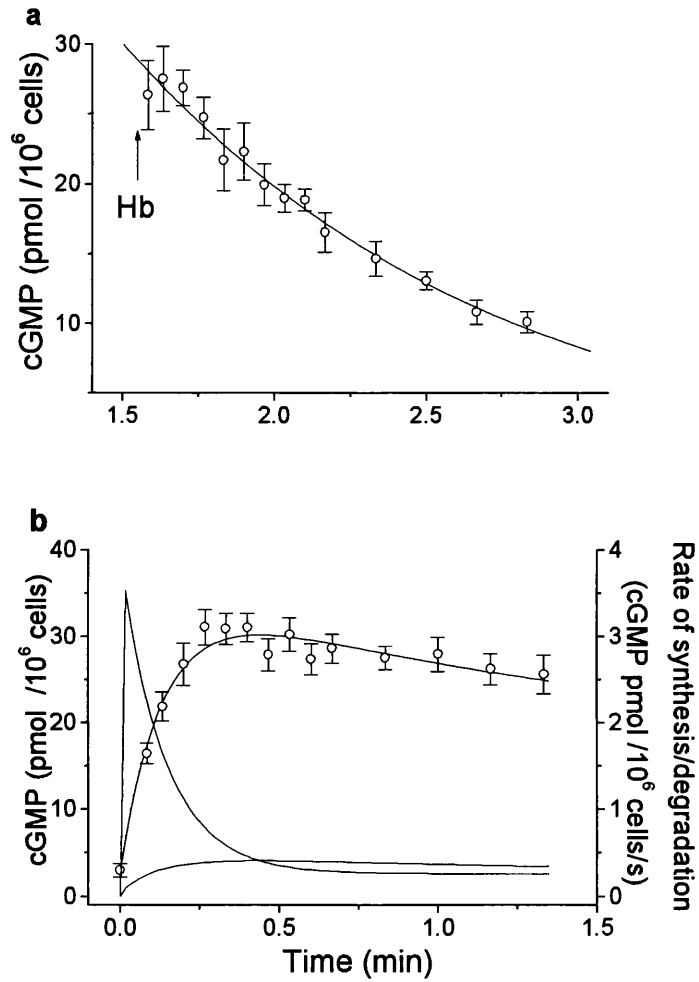
Figure 12: Kinetic analysis of cGMP synthesis and degradation

a) Decay of the cGMP levels after addition of Hb (10 μM) in the presence of PDE inhibitor, fitted by the Michaelis Menten equation to determine v_d. b) cGMP accumulation (o) data from figure 11 fitted by an exponential equation to determine v_s as described in methods.

The simple model of desensitization was then used to investigate whether the profile of cGMP accumulation measured under the control conditions (where parameters for cGMP degradation cannot be measured directly as the PDE activity is so high) can be predicted. The simplest scenario is to predict that in the absence of EHNA v_s is identical, but v_d enhanced. However, when this situation was modeled by reducing the Michaelis Menten parameter K_p (to simulate loss of a competitive inhibitor) no good fit was obtained regardless of the K_p value used (Figure 13a). An explanation for the inaccurate simulation is that cGMP is exported from the cell rendering it unsusceptible to hydrolysis by PDE. To check this, Hb was added to arrest GC activity 16 and 80 s after DEA/NO addition (i.e. at the peak and plateau stages of the time course). At both time points, cGMP rapidly declined to basal levels indicating that it was indeed subject to degradation by PDE throughout (Figure 13b). Consequently, in contrast to the findings in cerebellar cells (Bellamy et al., 2000; Manganiello et al., 1995a), the model fails to predict the control profile of cGMP accumulation. There are two reasons why the model may be inaccurate:

Firstly, the PDE activity does not follow the simple Michaelis-Menten kinetics.
This is not supported by the experimental data. The decline in cGMP following Hb addition to EHNA-treated cells was well described by the Michaelis-Menten equation (Figure 11). It is possible that, at the lower levels of cellular cGMP obtained under control conditions, the PDE activity may be lower than predicted values. Alternatively the PDE activity may vary over time such that the value of v_d is initially high, but then falls to a lower level during the steady state plateau. However, when Hb was added during the plateau (Figure 12b) a rapid fall in cGMP is seen indicating that PDE activity is immeasurably high. Consequently in order to maintain a steady state cGMP concentration $NO_{GC}R$ activity must remain equally high.

Secondly, $NO_{GC}R$ activity varies according to whether PDEs are active or inhibited. This means that the receptor may not desensitize to the same degree under control conditions as when EHNA is present. This model can be simulated by increasing the minimum rate of cGMP synthesis to which the $NO_{GC}R$ desensitizes (the constant "c" in the equation of the methods). This situation provides a much better fit to the experimental data (solid line Figure 13a). The profile of $NO_{GC}R$ activity generating the best fit was desensitization to a level approximately 50% of the peak activity rather than by more than 90% in the presence of EHNA (Figure 13c).

70
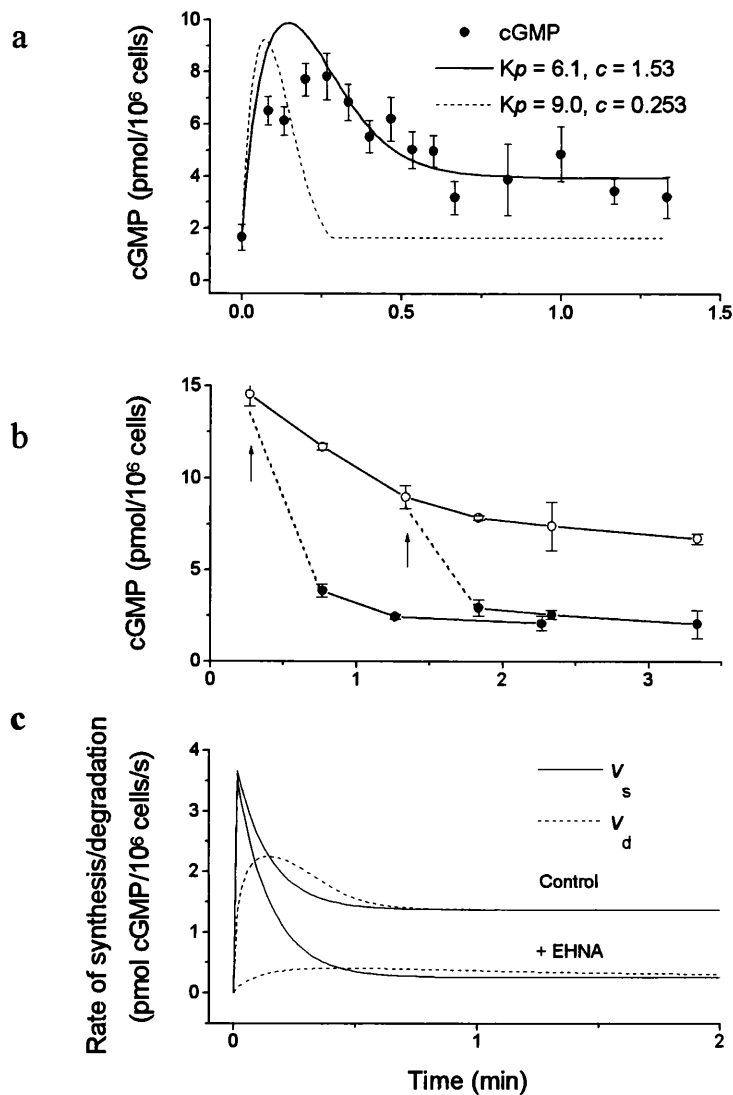
Figure 13: Kinetic analysis of cGMP accumulation in the absence of PDE inhibition

a) Data for the cGMP response to DEA/NO (•) are taken from figure 11. Broken line shows the best fit achieved by taking the profile of cGMP synthesis (v_s) and the value of the apparent maximal rate of cGMP degradation (V_p) giving the fit to the data in figure 12b but decreasing the apparent Michaelis constant (K_p) for cGMP degradation (corresponding to removal of a competitive inhibitor). Solid line shows the better fit achieved by altering both K_p and degree of NO$_{GC}$R desensitization. b) Vulnerability of cGMP to PDE activity. During the normal response to 1 µM DEA/NO (○), Hb (10 µM) was added (arrows) and the cGMP levels followed (●); $n = 4$-6. c) Comparison of profiles of cGMP synthesis and degradation providing the best fits to experimental data obtained in the absence and presence of EHNA.

71

3.4 Discussion

The cGMP response curve for DEA/NO demonstrated that the NO-cGMP pathway was functioning in the cell suspension of the immature rat striatum, as cGMP accumulates in a concentration dependent manner following exposure to NO. The location of cGMP accumulation in striatal slices was in agreement with previous reports (Markerink-van Ittersum et al., 1997). Cell dissociation removed the fibre networks, and the location of the cGMP response was shown to be limited to a sub-population of neurones. These were presumed to be the same neurones that were cGMP- and NeuN-positive in the intact striatal slice.

Due to the similar intensities of cGMP immuno-staining, the restricted range of cell sizes, and the lack of evidence for more than one PDE isoform at work the cells were considered to be a single homogenous population. The exact identity is unknown however previous studies have shown that high levels of GC-coupled receptor are found in striatal spiny neurones (Ariano, 1983; Ariano and Ufkes, 1983).

Several PDE families have been localised to the rat striatum. In situ hybridisation and immunohistochemistry studies have suggested that PDE1, 2, 3, 4, 7, 9, 10 are present in this brain area (see introduction). The PDE isoform that degrades cGMP generated in response to NO in the striatal neurones was found to be sensitive to EHNA, suggesting it to be PDE2 (Podzuweit et al., 1995). An EHNA-sensitive isoform is also found to participate in cGMP hydrolysis in hippocampal slices stimulated with NO (van Staveren et al., 2001). PDE2 is a cGMP-stimulated enzyme which hydrolyses both cAMP and cGMP with similar affinities (10-30 µM respectively) and maximal velocities (Juilfs et al., 1999). In purified PDE2 preparations, submicromolar concentrations of cGMP stimulated cAMP hydrolysis 50-fold suggesting that this enzyme may mediate cross-talk between cGMP and cAMP pathways (Juilfs et al., 1999). The dopamine receptors D_1 and D_2 are prominently expressed in the striatum, and their signals are transmitted by cAMP (adenylyl cyclase is activated by D_1 and inhibited by D_2). Thus cAMP hydrolysis by PDE2 may be regulated by intracellular cGMP levels and so play a role in neuronal signal transduction.

An appreciable PDE activity remained in the striatal cells in the presence of a maximally effective EHNA concentration. This may be due to the participation of another isoform. The pharmacological screen suggested that PDE1, 3, 4, 5 are not significantly involved. Out of the remaining identified PDE families, PDE6 is expressed in the retina and pineal gland (Beavo,

1995; Carcamo et al., 1995), PDE7 and 8 are cAMP specific (Carcamo et al., 1995; Sasaki et al., 2000; Soderling and Beavo, 2000) and PDE11 A appears to have little expression in the CNS (Yuasa 2001). PDE9A and PDE10A are found in the brain (Andreeva et al., 2001; Carcamo et al., 1995; Fujishige et al., 1999b) and can hydrolyse cGMP but the lack of selective inhibitors makes their roles difficult to evaluate. Recently immunohistochemical and Western blot analysis indicated that PDE10A is expressed at high levels in the rat striatum and is detected in the vast majority of cells in the striatum (Seeger et al., 2003). The authors suggest that this is consistent with the enzyme being expressed by the medium spiny neurones, as they account for 90-95% of the total neuronal population. The residual PDE activity in the presence of high EHNA concentrations may also be explained by the fact that the effectiveness of a competitive inhibitor is inherently self-limiting. The greater the inhibition, the more the inhibitor will be out-competed by the build up of accompanying cyclic nucleotide.

Throughout the body different cells exhibit very different patterns of NO stimulated cGMP accumulation ranging from slow developing waves typical of modulatory effects to fast spike-like transients analogous to neurotransmission. The pattern, i.e. both the dynamics and the amplitude of intracellular cGMP accumulation may be modified physiologically by altering either the kinetics of the cGMP synthesising enzyme or by altering the different levels of PDE activity within cells. Previous work in cerebellar astrocytes (cells with low PDE activity) showed that a slowly developing plateau of cGMP accumulates in these cells. It can be predicted that in cells with high PDE, a transient cGMP accumulation will be observed following stimulation with NO. This was seen in the control cGMP accumulation in figure 11. However in the presence of the EHNA the cells were effectively transformed into a low PDE state. The NO-stimulated cGMP accumulation was deconvoluted in order to measure the rate of synthesis of GC (v_s). In striatal neurones the rate of cGMP synthesis peaked within ~5 s of NO application, and then declined to a 13 fold lower steady-state. This desensitizing profile is not seen in the purified enzyme, but is similar to $NO_{GC}R$ kinetics in cerebellar astrocytes and platelets, implying that it is a common feature of the $NO_{GC}R$ in intact cells, and may require an as yet unknown cellular factor.

The simplest model of the $NO_{GC}R$ desensitization assumes that cellular levels of cGMP do not influence either the kinetics or degree of desensitization. A prediction of this model is that the cGMP accumulation under control conditions can be fitted by simply reducing the K_p value

(corresponding to the absence of the competitive inhibitor) and retaining the parameters found in the presence of PDE inhibitors. In the first description of $NO_{GC}R$ desensitization (Bellamy et al., 2000) the simple model provided a good approximation of the experimental data for GC activity in platelets. This simple model was deemed appropriate for the striatal cells as EHNA is a competitive inhibitor (Haynes, Jr. et al., 1996).

However the simulation failed in the striatal cells, implying that this model of desensitization is an over simplification. Repeated simulations showed that a better approximation of the data could be achieved by linking the degree of desensitization to the intracellular cGMP level. Thus $NO_{GC}R$ desensitization is lower in untreated neurones than in those incubated with EHNA (where cGMP levels were 4 fold higher). Feedback inhibition, where the product of receptor or enzyme activity influences its production is a common feature of biological systems, and may also apply to the $NO_{GC}R$ to provide a mechanism whereby cGMP synthesis is under much tighter control.

A recent study provides an alternative explanation as to why the simple model of desensitization failed in the striatal cells. PDE5 was found to be directly activated by cGMP binding to the GAF A domain in a time- and cGMP concentration-dependent manner (Rybalkin et al., 2003). The authors propose that the mechanism of the GAF domain stimulatory effect on the catalytic domain extends to other cGMP-binding PDE and GAF domain- containing proteins. Indeed, when the cAMP-binding GAF domain of the cyanobacteria adenylyl cyclase was replaced with the cGMP-binding GAF A domain from rat cGMP-stimulated PDE2 the chimeric protein was found to be responsive to cGMP stimulation (Kanacher et al., 2002). Thus cGMP binding to the GAF A domain acts like a switch to activate PDE. A much better approximation of the control data in figure 13a would probably be achieved by linking the degree of PDE2 activation and resultant cGMP breakdown with the intracellular cGMP level.

Chapter 4

Characteristics of the $NO_{GC}R$ expressed in cells

4.1 Introduction

It has been shown in both cerebellar astrocytes and striatal neurones that the $NO_{GC}R$ displays a desensitizing profile of activity. To investigate whether this pattern of activity is a peculiarity of these cell types, and how the different molecular combinations work in a cellular environment, the $\alpha 1\beta 1$ and $\alpha 2\beta 1$ isoforms were expressed in COS-7 cells. To date, only these $NO_{GC}R$ isoforms have been found to be expressed at the protein level in the brain and elsewhere, hence only the function of these isoforms was investigated.

In order to develop more realistic models of the NO-cGMP signalling pathway, the NO concentration that engages the $NO_{GC}R$ needs to be measured. Currently there is much confusion and incoherency surrounding this issue, and widely differing estimates of the potency of NO on its receptors have been made (Table 5). Early dose response curves of NO in aqueous solutions applied to coronary circulation of isolated guinea-pig hearts suggested that the NO concentration giving half-maximal activation (the EC_{50}) is approximately 5 nM (Kelm and Schrader, 1990). However, studies on the purified receptor from bovine lung (predominantly $\alpha 1\beta 1$) suggested that the EC_{50} is 250 nM (Stone and Marletta, 1996), and using the $NO_{GC}R$ extracted from rat aorta the EC_{50} value was reported to be 1.6 μM (Artz et al., 2001). These results corroborated the idea that the EC_{50} value lies in the hundred nM range. Studies using the NONOate DEA/NO appeared to support this range, as in standard assays the EC_{50} value was found to be about 300 nM (Koglin et al., 2001; Russwurm et al., 1998; Schrammel et al., 1996), and this was thought to be the potency of NO (Russwurm et al., 1998; Russwurm et al., 2002). In intact cells from the brain, the EC_{50} values ranged from 2-20 nM (Bellamy and Garthwaite, 2001b; Griffiths and Garthwaite, 2001).

75

| Preparation	EC$_{50}$ value	Reference
Cultured endothelial cells	5 nM NO	(Kelm et al., 1988)
Constant-flow-perfused guinea pig hearts	5-10 nM NO	(Kelm and Schrader, 1990)
Purified enzyme from bovine lung	$\approx$ 250 nM NO	(Stone and Marletta, 1996)
Rat aorta homogenate	1.6 μM NO	(Artz et al., 2001)
Purified enzyme from bovine lung	4 nM	(Bellamy et al., 2002a)
Purified enzyme from bovine lung	$\approx$ 100 nM DEA/NO	(Schrammel et al., 1996)
$\alpha 1\beta 1$ expressed in Sf9 cells and purified	$\approx$ 300 nM DEA/NO	(Russwurm et al., 1998)
Rat cerebellar cells	< 20 nM	(Bellamy et al., 2000)
$\alpha 1\beta 1$ expressed in Sf9 cytosol lysate	$\approx$ 400 nM DEA/NO	(Koglin et al., 2001)

Table 5: EC$_{50}$ values of NO or DEA/NO for the NO$_{GC}$R in different preparations

Many of the previous estimates of potency have been made with varying NO levels. In several of the early studies NO was prepared in anaerobic solutions and diluted into aerobic solutions. NO is unstable in aerobic solutions as it is consumed by reaction with oxygen (autoxidation) at a rate that is proportional to the square of the NO concentration (Ford et al., 1993). The development of the NONOate NO donors provided more flexibility as these compounds are stable as solids, but spontaneuosly decompose to release NO with predictable kinetics in aqueous solution (Keefer et al., 1996). However, on addition to solutions, the NO concentration rises (at a rate governed by the half-life) and then falls as the rate of autoxidation exceeds the rate of NO release (Schmidt et al., 1997). Furthermore autoxidation causes additional problems as it results in the formation of reactive nitrosating agents (NO_2, and N_2O_3; Augusto et al., 2002). In this study NO was applied in fixed concentrations using a recently-developed method based on balancing NO release from a donor with NO inactivation by red blood cells (Bellamy et al., 2002a).

4.2 Methods

COS-7 cells were co-transfected with either the $\alpha1\beta1$ or $\alpha2\beta2$ $NO_{GC}R$ as described in the methods section. 48 hours after transfection, COS-7 cells from 35 mm wells were trypsinised, pooled and spun at 1500 g for 5 min. The supernatant was aspirated and the cells were resuspended in incubation buffer containing IMBX (1 mM), at a protein concentration of 1 mg/ml. For the DEA/NO concentration response curves the cell suspensions were immediately incubated at 37 °C for 10 min prior to use, and DEA/NO was added at t=0 for 2 min. For cells that were exposed to constant NO concentrations, cells were resuspended in incubation buffer that also contained 0.5% BSA and again were pre-warmed for 10 min.

The method for delivering clamped NO concentration is based on the principle that a fixed NO concentration will be formed when a constant source of NO comes into equilibrium with a sink that consumes it (Figure 14). DETA/NO was used as an NO source, as it decomposes slowly (half-life = 20 h at 37 °C) with first order kinetics. Thus the rate of NO release is effectively constant over many hours. For a sink, the ability of oxyhaemoglobin located within RBC to consume NO was exploited. Oxyhaemoglobin consumes NO at an appropriate first order rate to form met-haemoglobin and nitrate (Liu et al., 1998).
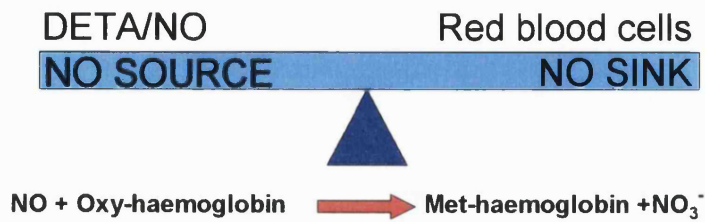
Figure 14: Method for delivering fixed NO concentrations

Clamped concentrations of NO were achieved by allowing a dynamic equilibrium to exist between NO release from the donor DETA/NO and NO inactivation by the haem in red blood cells (RBC) (Bellamy et al., 2002a). RBC were prepared as described in the methods section and kept on ice. Before use, RBC were aliquoted into plastic sterilin vials. Superoxide dismutase (SOD) was added to give a final activity of 1000 units/ml to prevent breakdown of NO by free superoxide radicals. The reaction mixture was warmed at 37 °C for 1 min in a shaking water bath. At $t = 0$, a concentration of DETA/NO was added and after 2 min a steady state concentration was established and the pre-warmed COS-7 cells transfected with the $NO_{GC}R$ receptor were added at 80 μl/ml and mixed, and aliquots were inactivated at the appropriate time point.

Fresh RBC/DETA/NO preparations were made on each experimental day and the amplitude of the clamped NO concentration was measured on the NO probe 2 min after addition of DETA/NO (100-500 μM).

4.3 Results

Potency of NO for GC in NO$_{GC}$R –transfected COS-7 cells

Exposure of a suspension of $\alpha1\beta1$ NO$_{GC}$R co-transfected COS-7 cells to DEA/NO caused a concentration-dependent increase in cGMP over 2 min. A maximal effect was observed at 100 nM which produced a high-amplitude cGMP response peaking at 300-600 pmol/mg protein (Figure 15). The half–maximal response was approximately 7 nM. The $\alpha2\beta1$ receptor was found to have both the magnitude and characteristics of a previously measured cGMP response (Gibb et al., 2003). It has been suggested that the responsiveness of the NO$_{GC}$Rs to DEA/NO may not be a reliable predictor of their sensitivity to NO (Bellamy et al., 2002a), and so in these experiments the receptor was exposed to NO at constant measured NO concentrations.

Evaluation of the method for delivering clamped NO concentrations

When DETA/NO (100-500 μM) was mixed with a suspension of RBC (2 million/ml) a fixed concentration of NO in the low nM range was produced within 2 min (Figure 16a). NO concentrations were measured with an electrochemical probe at 37 °C in an open stirred chamber. An addition artefact was observed each time a volume was added into the open NO probe chamber. Simply placing a Hamilton pipette or Pasteur pipette in the probe had no effect on the NO trace. However, when a volume was added to the NO chamber using either pipette type, a negative deflection proportional to the volume added was observed. This occurred whether distilled water, buffer or NO donor were added (data not shown).

A linear relationship between the DETA/NO concentration and the resultant amplitude of the NO steady-state concentration was observed (Figure 16b). This means that DETA/NO at a concentration within this range can be added and the resulting NO steady state concentration produced can be predicted. When DETA/NO levels higher than 500 μM were used, the NO sink became exhausted typically after 2 min (data not shown). Presumably this was caused by oxidation of oxyHb. The aim of these studies was to test the NO$_{GC}$R sensitivity to low nM concentrations of NO, and so the duration of the clamp was adequate for the time period of the experiment (1-2 min). Additions of pre-warmed, small volumes to the pre-equilibrated mixture did not affect the NO concentration. In this study COS-7 cells co- transfected with the $\alpha1\beta1$ or

α2β1 heterodimers of the $NO_{GC}R$ were added to the pre-equilibriated DETA/NO RBC mixture as indicated by the red box in figure 16a.
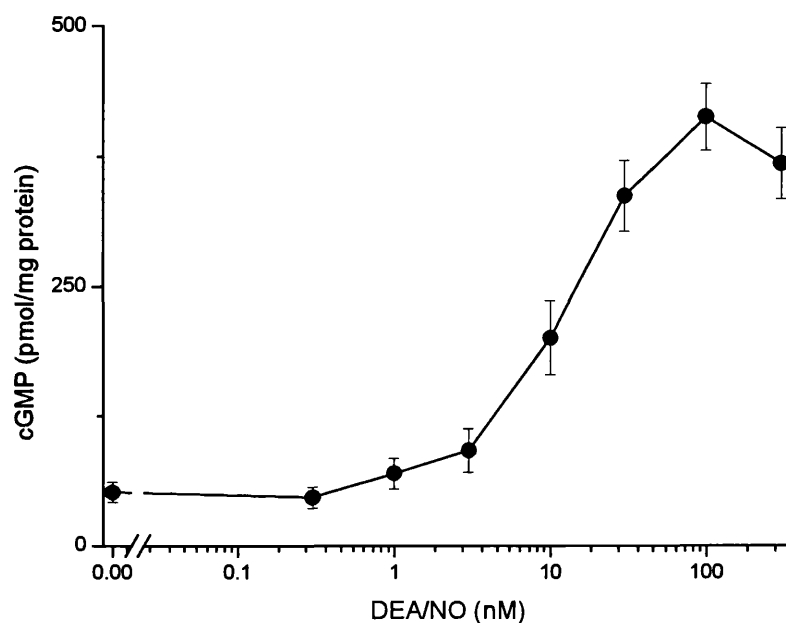
Figure 15: Concentration-curve for DEA/NO on COS-7 cells co-transfected with the α1β1 $NO_{GC}R$ isoform

Cells were exposed to different concentrations of DEA/NO for 2 min ($n=12$).
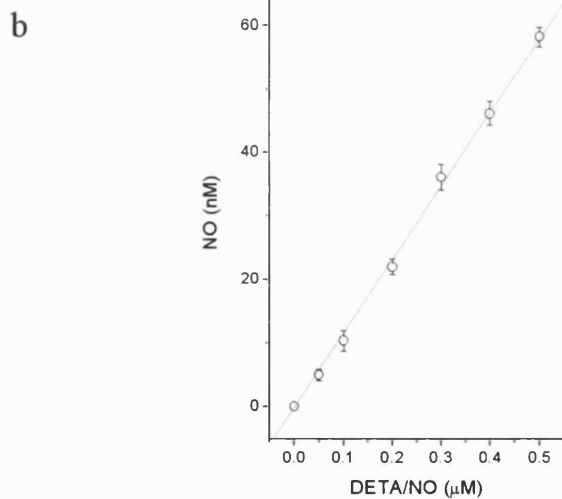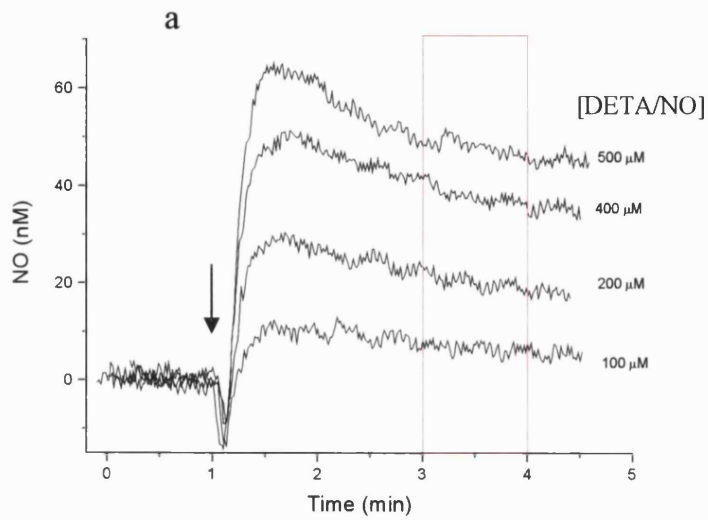
Figure 16: The delivery of a clamped NO concentration

Recordings of the NO concentration profile following addition of a range of DETA/NO concentrations (indicated by the arrow) to a suspension of red blood cells (2 million/ml). b) Plot of the amplitude of the NO concentration measured 2 min after addition of DETA/NO) versus DETA/NO addition. Data are mean ± SEM (n=3) from the experiment shown in part a. Data in parts a and b are from a typical experiment that was conducted in parallel each time the method was used to analyse the activity of the $NO_{GC}R$ using the same batch of RBC and DETA/NO. COS-7 cells co-transfected with the $NO_{GC}R$ subunits were added to the pre-equilibrated mixture as indicated by the red box (a).

Comparison of the sensitivities of α1β1 and α2β1 NO_{GC}Rs to NO at known, constant concentrations

Steady state concentration-cGMP response curves were obtained for both receptors using a 1 min exposure to different clamped NO concentrations (Figure 17). Both curves show a threshold of about 0.5 nM NO and maximum at 10 nM. They were also bell shaped such that higher concentrations (30-70 nM NO) generated lower cGMP levels. The rising portions of the curves were fitted to the Hill equation and showed that the α1β1 receptor has an EC_{50} of 1.2 ± 0.1 nM and a Hill co-efficient of 1.8 ± 0.3, whereas the α2β1 receptor has an EC_{50} of 2.2 ± 0.2 nM and a Hill co-efficient of 1.2 ± 0.1. To evaluate the contribution of the red blood cells to the cGMP concentration, the basal and stimulated levels were measured. cGMP levels in unstimulated cells were 2.2 ± 0.3 pmol/2 million RBC, and in cells stimulated with 500 nM NO were 2.4 ± 0.3 pmol/2 million RBC ($n = 10$). A t-test revealed that these values are not significantly different at the $p=0.5$ level ($p>0.6$).

Kinetic profile of the NO_{GC}R exposed to a maximal clamped NO concentration

The kinetic profile of the α1β1 NO_{GC}R was examined by measuring a detailed time course of the cGMP accumulation in cells exposed to a clamped, maximal NO concentration of 10 nM (Figure 18). cGMP levels rose rapidly over the first 20 s and the rate of accumulation then slowed to reach a plateau after around 60 s. In order to interpret the kinetic profile, the PDE activity of the COS-7 cells must be determined (Figure 19). Cells were allowed to maximally accumulate cGMP following a maximal DEA/NO concentration of 100 nM for 2 min in the presence and absence of IBMX.

After 2 min, 10 µM Hb was added to remove all free NO and cGMP levels were measured over the next 3 min. Under control conditions, cGMP levels fell to approximately a quarter of the maximum within 3 min. In the presence of 1 mM IBMX the level of cGMP fell only slowly, indicating that the phosphodiesterase activity was negligible over the relevant time period. Consequently the observed profile must be caused by time-dependent changes in cGMP synthesis.

The profile of GC activity can be extracted from the cGMP accumulation data by fitting it with a simple hyperbolic function and then differentiating (dotted line figure 18). The NO_{GC}R kinetics are rapid, with a peak activity occurring within 2 s followed by reduction to 50 % of

maximum by 12 s. This profile obtained using the α1β1 isoform was representative of that

obtained using the α2β1 isoform (data not shown).
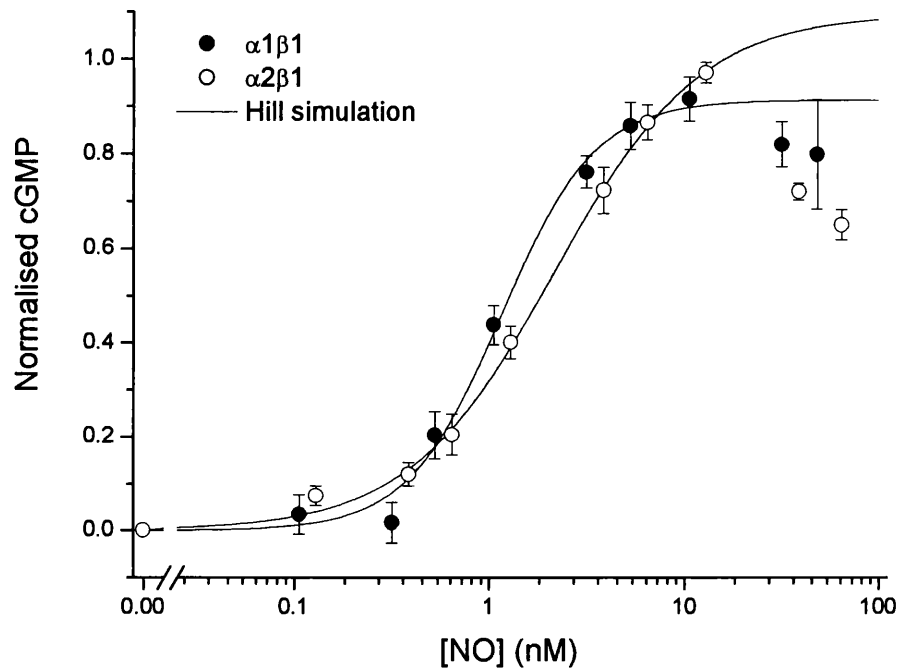
Figure 17: Concentration-cGMP response curves of cells expressing α1β1 and α2β1 receptors

COS-7 cells were exposed to fixed NO concentrations for 1 min. The data are normalised to the maximum cGMP response observed in each experiment (range 300-500 pmol/mg protein) and represent the means ± SEM (n=6-9). The solid lines are fits of the rising portions of the curves to the Hill equation.
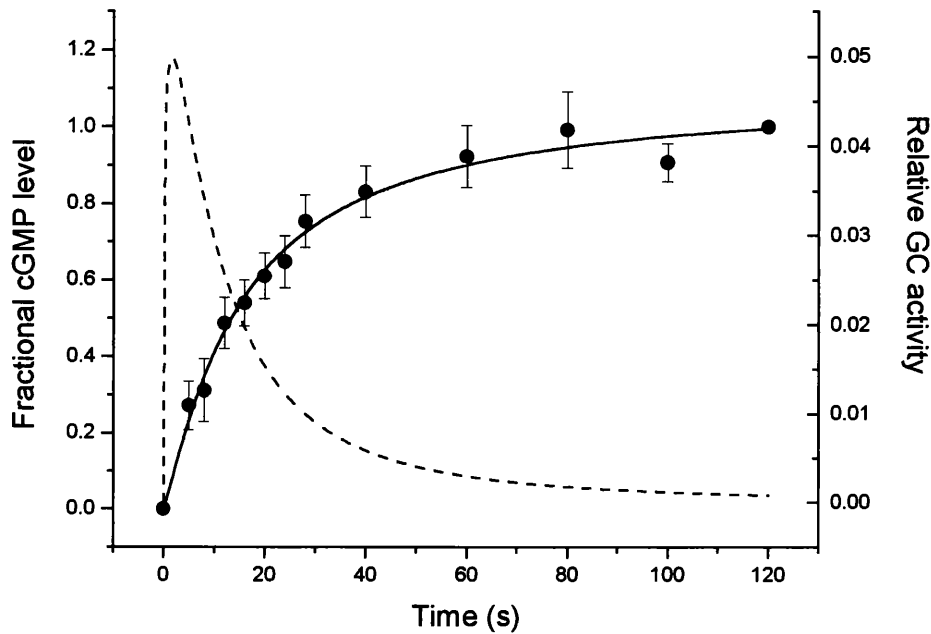
Figure 18: Kinetics of α1β1 NO$_{GC}$R exposed to clamped NO concentrations

COS-7 cells expressing the α1β1 receptor were exposed to 10 nM NO at t=0 and cGMP levels were followed over time. Each data point represents the mean ± SEM of data normalised to the cGMP level found after 120 s exposure. In different experiments this cGMP level ranged from 400-700 pmol/mg protein (*n*=6). The solid line through the data is a fit to a hyperbolic function which, when differentiated gives the indicated profile of NO$_{GC}$R activity (broken line; right axis).
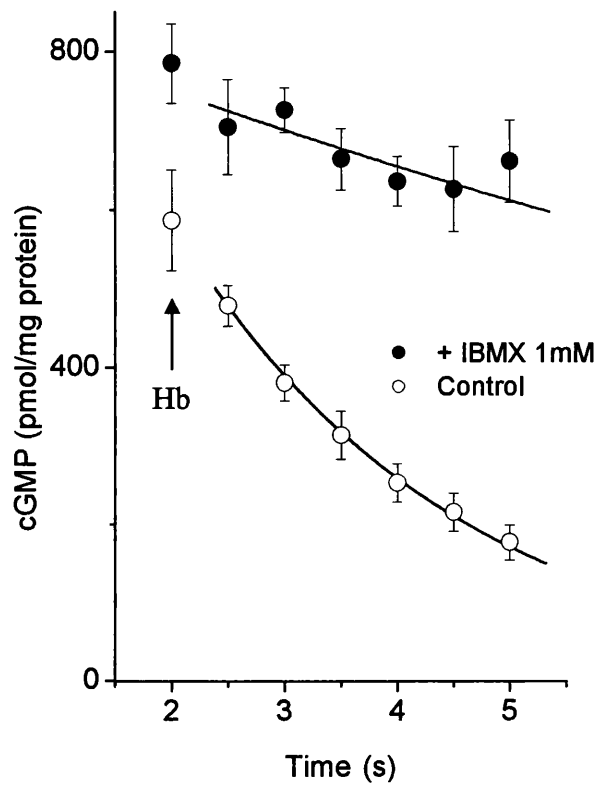
Figure 19: Phosphodiesterase activity in COS-7 cells

COS-7 cells expressing $\alpha 1\beta 1$ $NO_{GC}R$ were stimulated for 2 min with 100 nM DEA/NO concentration to maximally accumulate cGMP. At 2 min (indicated by the arrow) excess Hb was added to quench NO. cGMP levels were followed in the absence (○) and presence (●) of IBMX.

4.4 Discussion

The $\alpha1\beta1$ $NO_{GC}R$ in cells acts as a highly sensitive NO detector, with an EC_{50} value for DEA/NO of 7 nM over a 2 min exposure and is similar to the $\alpha2\beta1$ subunit (Gibb et al., 2003). These EC_{50} values for DEA/NO are 10-100 fold lower than previous reports, in which the receptors were used either from cell lysates or as purified enzymes (Koglin et al., 2001; Russwurm et al., 1998; Schrammel et al., 1996). In these studies the receptor was exposed to varying DEA/NO concentrations for 10-15 min. An explanation for the higher EC_{50} values obtained has been suggested (Bellamy et al., 2002a). In one study dithiothreitol (3 mM) was present in the incubation buffer (Russwurm et al., 1998), and dithiothreitol is known to react with NO (Bellamy et al., 2002a). It is unlikely that the loss of NO by this mechanism was accounted for in the study by Russwurm et al.. Furthermore the NO profile produced by 300 nM DEA/NO was found to peak at 50 nM after 2 min and then fall below the detection limit of the probe after 5-6 min. This translates to the NO concentration being only at an active level for approximately half of the duration of the experiment. Thus the responsiveness of the $NO_{GC}R$ to DEA/NO may not be a reliable indicator of their absolute or relative sensitivities to NO as the NO concentration is changing over time. In order to remedy this technical problem a method was developed to produce constant clamped NO concentrations.

Using clamped NO concentrations, the EC_{50} values for $\alpha1\beta1$ and $\alpha2\beta1$ were found to be 1 and 2 nM respectively, and the maximal responses occurred at 10 nM. A recent publication suggests that when the purified $\alpha1\beta1$ receptor was exposed to constant NO concentrations, the EC_{50} was found to be 4 nM (Bellamy et al., 2002a). The value is approximately 3 fold higher than reported here in cells expressing the $\alpha1\beta1$ isoform. This is consistent with the idea that in cells the receptor undergoes desensitization which truncates the concentration-response curve (Bellamy and Garthwaite, 2001b). The bell-shaped curves for both the DEA/NO and clamped NO induced responses of the receptor in cells are also characteristic of a rapidly desensitizing receptor (Paternain et al., 1998).

The shape of the curve provides further information about the receptor. The simple model of $NO_{GC}R$ activation is that a single NO molecule binds to the haem prosthetic group (Koesling and Friebe, 1999), and predicts a Hill coefficient of 1. The curves, especially that for $\alpha1\beta1$ appear steep (Hill coefficient = 1.8). The simplest explanation for a Hill coefficient greater than 1, is

that two or more molecules of NO cooperatively bind to each receptor. This has been a matter of some debate in the literature as analysis of the activation kinetics of the $NO_{GC}R$ suggested the possibility of more than one binding site (Zhao et al., 1999). It was later argued by work in the Garthwaite laboratory that the data could be fit with the simple model of agonist binding (Bellamy et al., 2002b). However the shape of the concentration-response curve for the purified receptor was found to be best fit with a Hill coefficient of 2.1. This value is similar to that reported here using intact cells. Whether this also applies to the $\alpha2\beta1$ receptor (Hill coefficient = 1.2) is ambiguous. This parameter may be compromised by GC desensitization. To eliminate this complication, studies on the purified enzyme are essential (see chapter 5).

A recent study reported that NO plays a role in RBC deformability (Bor-Kucukatay et al., 2003). The mechanism responsible for this effect is currently unknown. Both the particulate and soluble cyclases (Petrov and Lijnen, 1996), and an ATP-dependent, low affinity cGMP transporter (Sundkvist et al., 2002) have been found to exist in human RBC. Thus the NO-cGMP pathway appears to be present in RBC, but when stimulated with a supramaximal concentration of DEATA/NO the cGMP level was not significantly different from basal levels. Previous work suggests that cGMP independent effects also contribute to RBC deformability (Bor-Kucukatay et al., 2003).

Studies on the native $NO_{GC}R$ in cells e.g. cerebellar astrocytes and striatal neurones suggest that the enzyme activity declines exponentially with time reflecting desensitization (Bellamy and Garthwaite, 2001b; Bellamy and Garthwaite, 2002; Wykes et al., 2002). This behaviour is characteristic of neurotransmitters (Jones and Westbrook, 1996), but in the case of the $NO_{GC}R$ is not observed in cell free preparations. When expressed in COS-7 cells and exposed to constant clamped NO concentrations (10 nM), the rate of synthesis peaked within 2 s, followed by desensitization to 50 % of the maximal response by about 12 s. Thus heterologous expression of the $\alpha1\beta1$ isoform displays a rapidly desensitizing profile of activity similar to that reported for the native enzyme in cerebellar and striatal cells. In preliminary experiments the $\alpha2\beta1$ isoform was found to behave in a similar manner.

In summary, the $NO_{GC}R$ receptors containing the $\beta1$ subunits are highly sensitive NO detectors with EC_{50} values in the low nM range. Both the $\alpha1\beta1$ and $\alpha2\beta1$ isoforms display a rapidly desensitizing profile of activity, similar to each other and to the native enzyme. Thus the $\beta1$ containing isoforms maybe considered functionally similar. However recent reports suggest

87

that $\alpha1\beta1$ is associated with cellular membranes in a calcium-dependent manner (Zabel et al., 2002) and the $\alpha2\beta1$ receptor associates with membranes through synaptic scaffolding proteins which also binds neuronal nitric oxide synthase (Russwurm et al., 2001). Thus the different molecular makeup of the $NO_{GC}Rs$ may have evolved for targeting different sub-cellular locations.

Chapter 5

Development of a new method to deliver constant NO concentrations

5.1 Introduction

The method for applying clamped concentrations of NO using red blood cells as an NO sink (as described in the previous chapter) is subject to several inherent limitations, and so a new chemical method was developed. The limitations of using RBC as a NO sink are chiefly:

1) Having to prepare a washed RBC suspension for each experiment.

2) The rise of NO to plateau concentration (60 s) is slow, so that for rapid kinetics experiments additions needed to be made to a pre-equilibrated mixture in a small enough volume not to disturb the equilibrium, thus limiting the scope of the experiment.

3) Any lysis of RBC could compromise the experiment as Hb inactivates NO at a much higher rate than when protein is packaged in RBC (Liu et al., 1998)

4) Possible interference from bioactive substances that may be taken up into, or released from the RBC.

To obtain clamped NO concentrations after the release of NO from a donor the following reaction scheme was considered:

$$Donor \xrightarrow{K_a} NO \xrightarrow{K_b} products$$
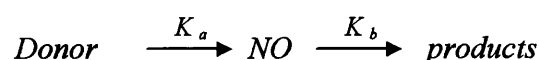
When $k_b >> k_a$ the steady state NO concentration is given by

$$[NO] = (k_a / k_b) [Donor]$$

SPER/NO was chosen as a source of NO as it releases NO at a steady state over the time scale of a few minutes. The half-life of this NONOate is 39 min at 37 °C (Keefer et al., 1996). The sink must have the capacity to consume NO quite rapidly over the requisite time-scale without significant exhaustion. The chemical NO scavenger carboxy-2-phenyl-4,4,5,5-tetramethylimidazoline-1-oxyl-3-oxide (CPTIO; 200 μM) was chosen for this purpose (Figure

20). The reaction between NO and CPTIO forms the NO$_2$ radical (NO$_2$•). This reactive oxidising species rapidly combines with other radicals such as NO (Augusto et al., 2002), so must be scavenged. Urate, an endogenous antioxidant (Becker, 1993) that converts NO$_2$ into NO$_2^-$ was used at the physiological plasma concentration of 300 µM.
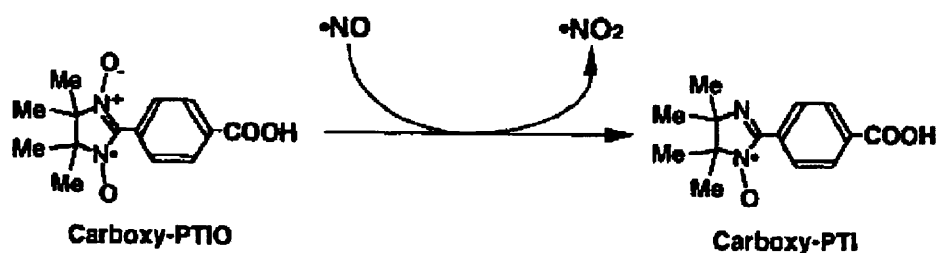
Figure 20: The reaction between NO and CPTIO forms the NO$_2$ radical (NO$_2$•) and carboxy-PTI

(Taken from (Amano and Noda, 1995)).

In order to evaluate the ability of the SPER/NO-CPTIO couple to deliver clamped NO concentrations, the rate constants of the chemical reactions were incorporated into a mathematical model. A comparison between the predicted and measured NO clamped concentrations was carried out and a correlation was found (Griffiths et al., 2003). The next step was to explore the utility of the method for biological purposes. This was achieved by investigating the kinetics of activation by NO of its GC-coupled receptor purified from bovine lung and, for comparison, COS-7 cell lysates containing the two physiological isoforms α1β1 and α2β1.

5.2 Methods

Experiments were carried out in CPTIO-containing assay buffer, except when DEA/NO was used, in which case the CPTIO (200 μM) was omitted.

Receptor protein purified from bovine lung ("soluble guanylyl cyclase) was prepared, stored on ice and diluted 1:100 into CPTIO-containing assay buffer. Homogenates of the COS-7 cells expressing the α1β1 or α2β1 NO$_{GC}$R were prepared as described in the methods. Prior to use the homogenates were thawed, stored on ice and diluted 1:10 into CPTIO-containing assay buffer pre-equilibrated at 37 °C.

SPER/NO was added to achieve varying steady-state NO concentrations (as measured on the NO probe) and 2 min later aliquots of the reaction mixture were inactivated and cGMP measured as described in the methods.

5.3 Results

Application of the method to activation of the $NO_{GC}R$

The CPTIO-containing assay buffer contained components required for $NO_{GC}R$ activation, and was thus more complex than the original mixture used to evaluate the method. The first step was to check that this new buffer did not cause any unexpected effects. The SPER/NO-CPTIO couple generated stable NO concentrations over a 2 min period that were linearly related to the SPER/NO concentrations (Figure 21a). Additions of receptor protein had no affect on NO concentration (data not shown).

Possible unwanted effects of the new approach were investigated by comparing the time-course of GC activity over 2 min at a maximally-effective NO concentration produced by the SPER/NO-CPTIO couple (50 nM), with that occurring on addition of a supramaximal concentration of DEA/NO (1 μM). The GC-activity in each case was linear with time and the slopes were not significantly different (about 10 μmoles cGMP/mg protein/min; $p > 0.05$; Figure 21b). With DEA/NO, receptor activity cannot be monitored usefully at submaximal concentrations as the NO concentration changes rapidly and continuously (Bellamy et al., 2002a). In contrast using the SPER/NO-CPTIO couple, GC activity remained linear with time at the low NO concentration of 2 nM (Figure 21b). Addition of a further 2 nM NO after 1 min increased the rate from 4.4 to 6.4 μmoles/mg protein/min whereas addition of Hb to scavenge NO led to an immediate cessation of GC-activity (Figure 20c), indicating that if any biologically significant variation in the NO concentration had occurred over time it would have been detected.

The concentration-response relationship was studied using a 2 min exposure to a range of clamped NO concentrations. The curve had a threshold of approximately 0.1 nM NO and displayed maximal activity at about 12 nM (Figure 21d). It was well fitted by the Hill equation, with an EC_{50} of 1.7 nM and a Hill coefficient of 1.0.
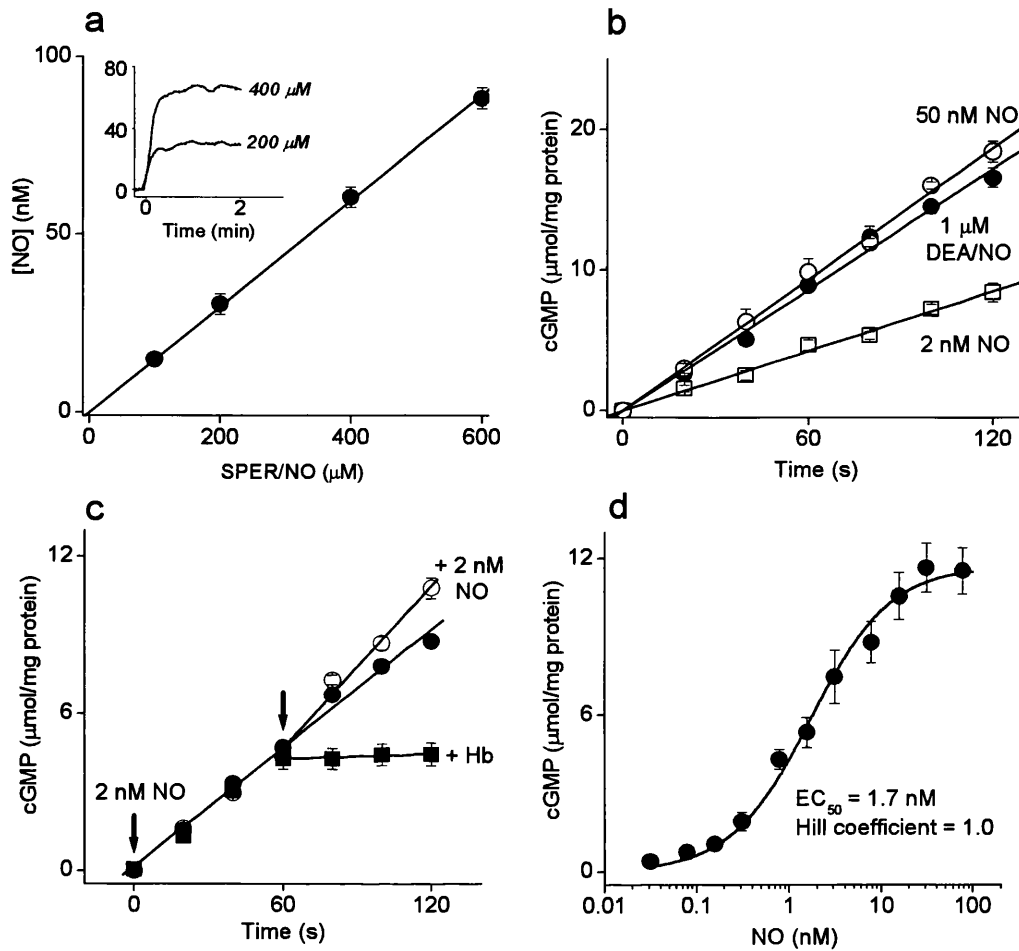
Figure 21: Activation of the NO$_{GC}$R under steady state conditions

a) The mean NO concentrations present 45-75 s after the addition of SPER/NO in a range of concentrations to CPTIO (200 μM)-containing assay buffer are plotted against the SPER/NO concentration and fit with a linear function ($n = 4$). Inset, representative traces of the NO concentration profile with 200 and 400 μM SPER/NO, smoothed by adjacent averaging (5 s bins). b) Time-course of cGMP produced by the receptor protein following exposure either to a SPER/NO-CPTIO mixture giving steady-state NO concentrations of 2 nM (open squares) and 50 nM (open circles), or to 1 μM DEA/NO (filled circles). Data are fit with a linear function and are the means ± SEM of 3 independent runs. c) cGMP accumulation following exposure of the receptor protein to 2 nM NO without further addition (filled circles) or with addition after 60 s

93

(arrow) of either 25 μM haemoglobin (Hb, filled squares) or a further 2 nM NO (open circles), n = 11-12. d) Equilibrium concentration-response curve for NO on the GC activity of the purified receptor protein. cGMP levels were measued following a 2 min exposure to a range of NO concentrations generated by adding various SPER/NO concentrations to a CPTIO-containing assay buffer (n = 4). Data are fit to the Hill equation, giving an EC_{50} of 1.7 nM and a Hill coefficient of 1.0.

To check that the concentration-response curve obtained for the purified receptor (Figure 22) was not peculiar to the use of SPER/NO as the donor, we evaluated the combination of diethylenetriamine/NO (DETA/NO, half-life 20 h) and CPTIO for the same purpose. To avoid the use of excessive DETA/NO concentrations, the concentration of CPTIO was lowered to 50 μM, allowing steady-state NO concentrations to be achieved in 4 s. As with SPER/NO, there was a linear relationship between the concentrations of DETA/NO and NO (data not illustrated). When the mixture was used to investigate the concentration-response curve for NO on purified lung GC (2 min exposure), the results (EC_{50} = 1.4 nM; Hill coefficient = 1.0) were indistinguishable from those obtained using SPER/NO (Figure 21d).

The established GC-coupled NO receptors are αβ heterodimers and the lung may contain both known isoforms, α1β1 and α2β1, with the former predominating (Mergia et al., 2003). Accordingly, the response of the purified lung protein may be a composite one. To examine the sensitivity of the separate isoforms to NO, they were expressed in COS-7 cells and the NO-evoked GC activity followed in cell lysates. The resultant maximal activity of the two isoforms was similar (Figure 23a,b). Moreover, the EC_{50} values for NO were also comparable, being 0.9 nM for α1β1 and 0.5 nM for α2β1. The slopes of both curves were described by a Hill coefficient of 1.1.
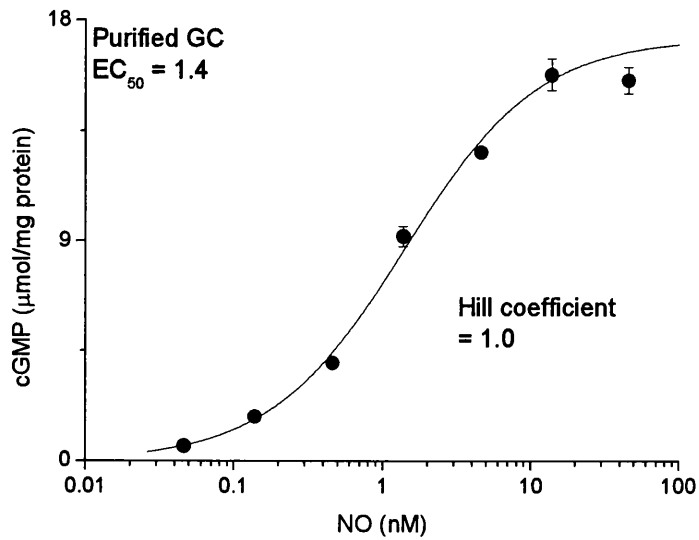
Figure 22: Equilibrium concentration-response curve for NO on the GC activity of the purified receptor protein

cGMP levels were measured following a 2 min exposure to a range of NO concentrations generated by adding various DETA/NO concentrations to a reaction mixture containing 50 μM CPTIO ($n = 4$). Data are fit to the Hill equation, giving an EC_{50} of 1.4 nM and a Hill coefficient of 1.0.
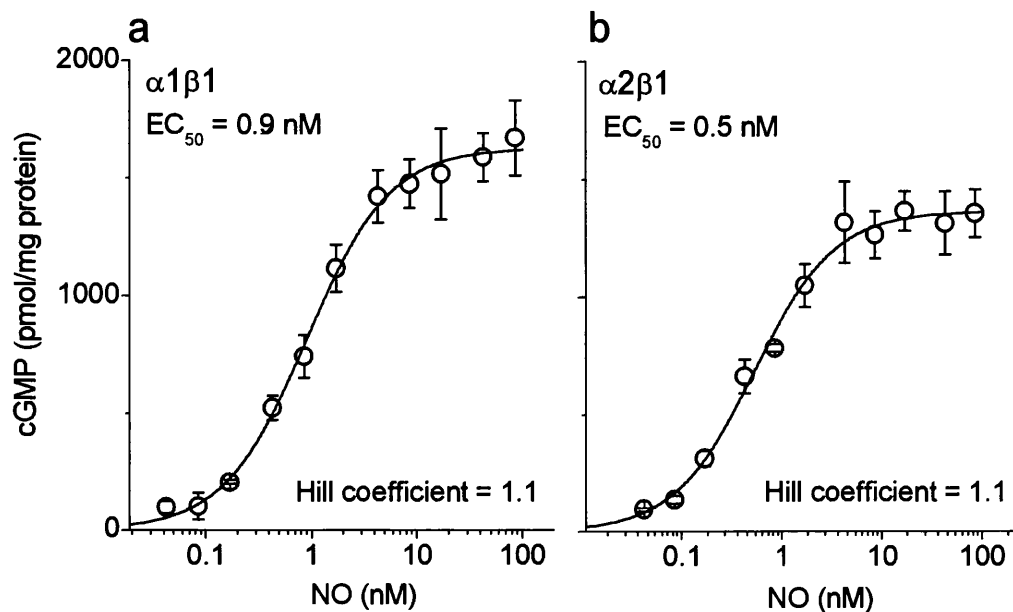
Figure 23: Equilibrium concentration-response curves for NO on the GC activity of the (a) α1β1 and (b) α2β1 receptor isoforms in lysates of transfected COS-7 cells

Data (means ± SEM, n = 3) were obtained following a 2 min exposure to a range of NO concentrations generated by adding various SPER/NO concentrations to a reaction mixture containing 200 μM CPTIO. Data are fit to the Hill equation, giving EC_{50} values of 0.9 nM for α1β1, 0.5 nM for α2β1 and a Hill coefficient of 1.1 for both.

5.4 Discussion

The results support the utility of the SPER/NO-CPTIO method for delivering clamped physiological concentrations of NO to biological preparations. The benefits of this system are that it requires chemicals that are commercially available at relatively low cost, and is far simpler to use than other recently described methods (Zhelyaskov and Godwin, 1999). However it is worth noting that, as with all newly developed systems both real and potential limitations may exist. Out of the nitronyl nitroxides, CPTIO is the least cell-permeable and was used for this reason, so that the risk of possible unwanted intracellular effects when used with intact cells was minimised. CPTIO has been frequently used as an NO scavenger in previous studies and no undesirable side-effects have so far been reported. SPER/NO is a member of the well characterised and much used NONOate family. The carrier nucleophile/NO adduct is spermine which is an endogenous polyamine with biological activity (Bachrach et al., 2001). It has been suggested that the rate of NO release from SPER/NO may depend on donor concentration (Davies et al., 2001). However in this study this did not appear to be a problem. An identical profile of $NO_{GC}R$ activation was observed when DETA/NO, another donor that was reported not to exhibit this behaviour (Davies et al., 2001) was used. Urate was used at a concentration found in plasma to scavenge NO_2, and can be regarded as a physiological ingredient. However the reactivity of the resulting urate radical is unclear so the production was kept at a minimum. NO_2^- is produced by the reaction of NO_2 with urate and is formed at the same rate as CPTIO is consumed. The human plasma concentration of NO_2^- in the body is 0.5-210 μM (Augusto et al., 2002), and is relatively unreactive at neutral pH and thus is unlikely to cause problems.

As previously described in the introduction to chapter 4, the lack of control over NO concentrations has led to widely differing estimates of the potency of NO on its GC coupled-receptors. An initial estimate of the EC_{50} value, based on addition of NO from concentrated solutions was ≤ 250 nM (Stone and Marletta, 1996). Standard GC assays using the NONOate DEA/NO found that the potency was similar (approximately 300 nM; Russwurm et al., 1998). This sustained the idea that physiological NO signalling involved NO concentrations in the 100 nM range. The profile of NO release was followed over the time course of such assays and it was found that a measured EC_{50} value of 300 nM was compatible with the true potency of NO being in the low nM range that had been suggested in previous studies in intact cells from the brain

(Bellamy et al., 2002a). In this study, using the red blood cell technique to maintain constant NO concentrations, an EC_{50} value of 4 nM was measured for the purified bovine lung GC-coupled receptor (Bellamy et al., 2002a). This suggests that the high potency of NO in cells does not reflect some peculiarity of the protein in an intracellular environment. Furthermore, the slope of the concentration-response curve was unexpectedly steep (Hill co-efficient of 2) which, if correct would suggest cooperative binding of two or more molecules of NO to each receptor is required for receptor activation.

Using the new method of NO delivery re-examination of these issues supported the potency of NO for its receptor in lung being in the low nM range, although the actual EC_{50} value ($\sim$ 1.5 nM) was approximately 2-fold lower that that obtained using the red blood cell method (Bellamy et al., 2002a). More importantly, the Hill coefficient was of the value 1 which is indicative of a single NO binding site. This discrepancy is best attributed to differences in methodology, and especially to the former use of red blood cells. Any lysis of cells in the suspension would result in release of free Hb, which binds NO far more avidly than when encapsulated in red blood cells (Liu et al., 1998). There was no evidence for free Hb, at the NO concentrations measured on the electrochemical probe ($\geq$ 5-10 nM). Significant lysis (calculated to be >0.1%) would preferentially impact on the lower NO concentrations that could not be measured. If this occurred, the lower half of the concentration-response curve would be artificially steepened, and give rise to an over-estimate of the Hill coefficient. This effect would also explain the higher EC_{50} value obtained in the earlier study.

There had been no previous side-by-side comparison of the relative or absolute NO sensitivities of the individual $\alpha 1 \beta 1$ and $\alpha 2 \beta 1$ receptor isoforms in cell-free preparations. Concentration-response curves to DEA/NO were reported to be similar (Russwurm et al., 1998). However this result was suggested to be equivocal (Bellamy et al., 2002a). A direct comparison using the new method indicated that the EC_{50} values for NO are closely comparible to each other (about 1 nM) and to the value obtained for the purified receptor protein from lung. These values were similar in absolute potency of NO towards the two isoforms when expressed in COS-7 cells (see Chapter 4;Gibb et al., 2003). However these estimates were complicated by receptor desensitization and bell-shaped concentration curves observed with the receptors in intact cells.

In conclusion the results support the utility of the SPER/NO-CPTIO method for delivering physiological concentrations of NO to biological preparations in a reliable and reproducible

manner. The direct comparison of the kinetic parameters for activation of the GC-coupled receptor derived in this study, are likely to be more reliable than those determined previously using the RBC method. The EC_{50} values of the $\alpha1\beta1$ and $\alpha2\beta1$ isoforms are very similar to each other (≈ 1 nM) and to the value obtained for the purified receptor isoform. The slopes of the concentration-response curves were shallower (Hill coefficient of 1) than previously reported, questioning the need to consider binding of more than one molecule for receptor activation

Chapter 6

Membrane-association and the sensitivity of the guanylyl-cyclase coupled receptors to nitric oxide

6.1 Introduction

The known GC-coupled receptors are $\alpha\beta$–heterodimers of which two isoforms, $\alpha1\beta1$ and $\alpha2\beta1$, are widely expressed at the mRNA and protein levels (Friebe and Koesling, 2003). So far, the two isoforms have appeared functionally and pharmacologically similar, whether studied in intact cells or in cell lysates (Friebe and Koesling, 2003; Gibb et al., 2003; Griffiths et al., 2003). However, complexity might arise from differences in subcellular location. In this respect, early data showed that NO-evoked GC activity was present in varying amounts in the soluble (cytosolic) and insoluble (particulate) fractions of several tissues (Arnold et al., 1977) and recent evidence indicates that the $\alpha1\beta1$ receptor translocates to membranes in response to a Ca^{2+} signal (Zabel et al., 2002) whereas, in the brain, the $\alpha2\beta1$ isoform is targeted to membrane-linked synaptic scaffold proteins (Russwurm et al., 2001).

From a study using heart tissue, association with membranes was reported to sensitize the receptors to (Zabel et al., 2002). If correct, this conclusion might be important because it could provide a device for modulating cellular responsiveness to NO and/or for concentrating NO signal transduction into discrete subcellular domains analogous to those mediating conventional synaptic transmission. The result was based on differences in the concentrations of the NO donor, diethylamine/NO adduct (DEA/NO) needed to evoke GC activity in cytosol and membrane fractions. DEA/NO degrades to release NO with a half-life of 2.1 min (37 °C). The amplitude, shape, and duration of the resulting NO concentration profile, however, is dependent on several factors, including pH and the rate of consumption of NO. Without rigorous checks, therefore, a shift in the DEA/NO concentration-response curve is difficult to interpret (Bellamy et al., 2002a). Accordingly we have evaluated the veracity of the result using a method for delivering NO in known, fixed concentrations (Griffiths et al., 2003)

6.2 Methods

The heart, cerebellar and platelet homogenates were prepared as described in the Materials and Methods section. Crude fractions were used in order to replicate the experiments of Zabel (2002). The protein concentrations (measured using the bicinchoninic acid method) of the cytosols of platelets, heart and cerebellum were, respectively, 0.13, 13 and 1.4 mg/ml; and the corresponding values for the membranes were 0.4, 5 and 2.9 mg protein/ml. Previously it was shown that cGMP production is linear with the protein concentrations used in this study (Troyer E.W. et al., 1978).

The activity of the $NO_{GC}R$ in the different preparations was measured by exposing them to constant concentrations of NO, using the SPER/NO-CPTIO method. Aliquots of the tissue fractions were diluted 1:10 into CPTIO-containing assay buffer. SPER/NO was added from concentrated stock solutions to achieve varying steady-state NO concentrations (achieved within about 1 s) and, 2 min later, 100 μl of the reaction mix was removed and inactivated in boiling hypotonic buffer.

To scrutinize the results obtained by Zabel (2002), the GC reaction mixture was changed to the one they used (with 1000 U ml^{-1} superoxide dismutase as an additional ingredient) and DEA/NO was used as the donor. The methods otherwise were as detailed above except that the tissue fractions were diluted 1:100 into the reaction mixture and aliquots were sampled for cGMP determination at 1 min intervals for a total of 10 min.

cGMP was measured using radioimmunoassay. Each concentration-response curve was fitted to the Hill equation (in Origin™ version 6.1; Aston Scientific Ltd, Stoke Mandeville, UK) to obtain values of the EC_{50} and Hill coefficient.

6.3 Results

Comparison of the sensitivity of GC-coupled NO receptors in membrane and cytosol fractions

NO-evoked GC activity is found in varying amounts in the insoluble (particulate) fractions of several tissues (Arnold et al., 1977). For the present purposes, we initially selected tissue from a brain region (the cerebellum) in which the NO-cGMP pathway is highly expressed (Garthwaite and Boulton, 1995). NO elicited GC activity in both cytosolic and membrane fractions of cerebellum, with the former dominating (Figure 24a). Concentration-response curves were constructed using NO delivered in known, constant concentrations (Griffiths et al., 2003). In both fractions, the threshold NO concentration required to stimulate GC activity was 50-100 pM and the maximum response occurred at about 10 nM (Figure 24a). The concentrations giving half-maximal activity (the EC_{50} values) were very similar (0.94 ± 0.09 nM in the cytosol and 1.09 ± 0.15 nM in the membranes, $n = 4$; $p > 0.4$), as were the Hill slopes (1.1 ± 0.1 and 0.9 ± 0.1; $p > 0.2$). Accordingly, when normalized, the two curves were superimposable (Figure 24b).

In case the cerebellum behaved unusually, the experiments were repeated using blood platelets, a well-known target for NO (Schwarz et al., 2001). The concentration-response curves for cytosol and membrane fractions were again closely similar (Figure 25a, b). The respective EC_{50} values (0.90 ± 0.12 nM and 1.23 ± 0.04 nM; n = 3-4) were not significantly different from each other ($p > 0.07$), nor from the corresponding values in cerebellum ($p > 0.7$ and 0.4). The Hill slopes (1.2 ± 0.2 and 1.1 ± 0.03) were also no different from each other ($p > 0.6$) or from the cerebellar values ($p > 0.3$ and $p > 0.1$).

The experiments leading to the general conclusion that membrane association sensitises the receptors to NO were conducted on the rat heart (Zabel et al., 2002). In view of the above negative findings, we began to investigate the possibility that the phenomenon might be peculiar to the heart. However, it soon became evident that such an undertaking would be compromised. A homogenate of 3 rat hearts (previously perfused thoroughly *in situ* to wash out red blood cells) in 5 ml buffer was used to prepare concentrated membrane and cytosol fractions. The membrane fraction was its usual milky-white colour but the cytosol was bright red-pink due to the presence of myoglobin, a cytosolic protein expressed in sufficient abundance to give the heart its gross colour (Garry et al., 1998). NO reacts very rapidly with myoglobin, forming nitrate and metmyoglobin (Eich et al., 1996); consequently, the presence of significant quantities of

myoglobin in the cytosol will reduce the amount of NO available for activating GC-coupled receptors. Hence, more NO would have to be added to match the degree of receptor activation taking place in the absence of myoglobin.

In order to evaluate this simple explanation for the results of Zabel et al. (Zabel et al., 2002), recordings were made of the NO concentration profiles following addition of the NONOate diethylamine/NO adduct (DEA/NO), which was used to supply NO in the experiments of Zabel et al. The DEA/NO concentration selected (0.5 μM) was one evoking approximately half-maximal activation of GC-coupled NO receptors in the heart cytosol preparations during a 10 min incubation (Zabel et al., 2002). In buffer, the NO concentration rose to a peak of approximately 400 nM after about 3 min (Figure 26). The dilution of heart cytosol used in the study of Zabel et al. was not disclosed but when DEA/NO was added to a 1:100 dilution of the cytosol (giving a final protein concentration equivalent to that used for assaying GC activity in the cerebellar cytosol), NO was undetectable for a period of about 2 min. Afterwards, the concentration rose to reach a plateau about 3-fold lower than was observed in buffer. When the test was repeated on the membrane fraction (similarly diluted), the NO profile was the same as in buffer.

The method of assaying GC activity used by (Zabel et al., 2002) was then applied to the heart fractions, except that the activity was followed at 1 min intervals for 10 min rather than at only a single time point (10 min). With a maximal DEA/NO concentration (10 μM; Zabel et al., 2002) cGMP accumulated fairly linearly over the 10 min period in both fractions, with the GC activity being more than 10-fold higher in the cytosol than in the membranes (Figure 27). In the membranes, DEA/NO concentrations spanning the EC_{50} value reported by Zabel et al., namely 0.1 and 0.3 μM, gave cGMP levels after 10 min that were, respectively, about 50 % and 70 % of the maximum. In the cytosol, the corresponding levels at this time were lowered to about 0 % and 22 %. These relative values are all closely similar to those reported by Zabel et al. (although, unfortunately, they did not also disclose the absolute values). Inspection of earlier time points at the 0.3 μM concentration, however, showed that, in the membranes, there was near-maximal GC activity over the first 2 min (when the rate of NO release is highest), followed by a decline. In contrast, in the cytosol, there was no measurable GC activity for the same initial period, with a slow rise occurring afterwards. Measurement of the NO concentration under the same conditions gave the same result as before (Figure 26): on addition of DEA/NO (0.3 μM), NO rose

immediately in the diluted membranes but was undetectable for about 2 min in the diluted cytosol (results not illustrated).
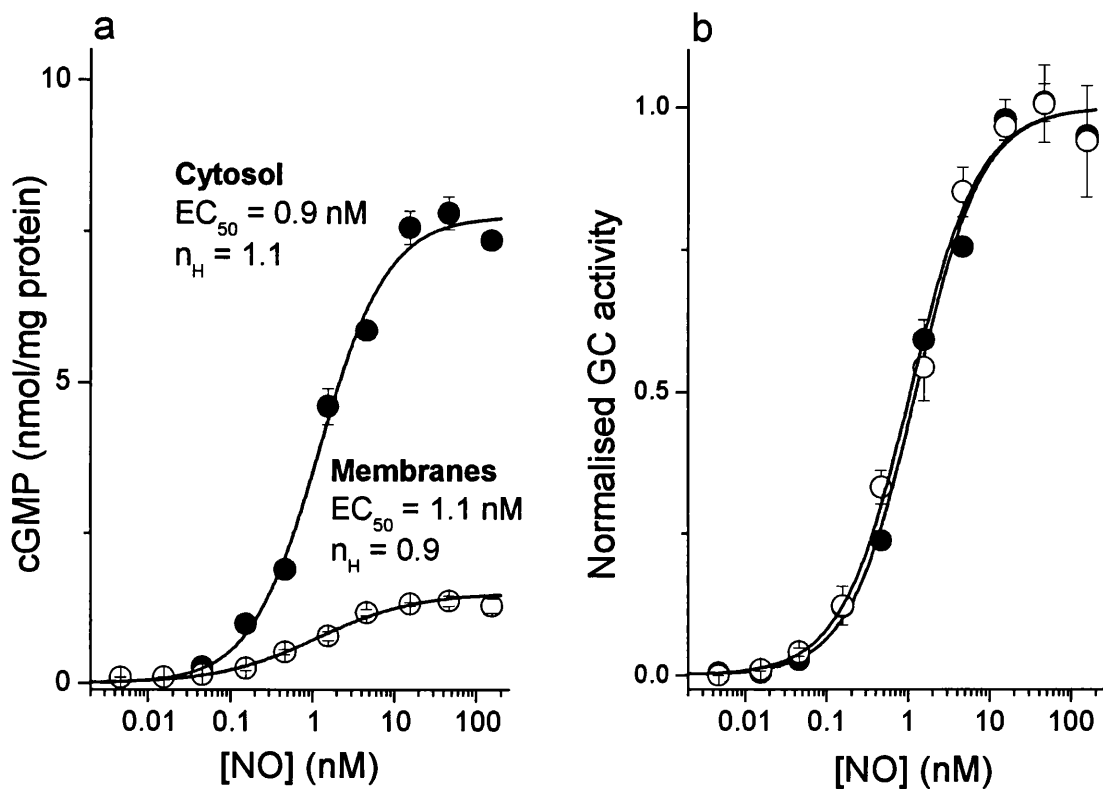
Figure 24: Comparison of the sensitivity of GC-coupled NO receptors in membrane and cytosol fractions of rat cerebellum

(a) Raw concentration-cGMP response curves for NO in cytosol (●) and membrane (○) fractions; $n = 3$-4. The solid lines fit the data to the Hill equation; n_H signifies the Hill coefficient. (b) The same data normalized to the mean maximal GC activity in each case (derived from the Hill fits). Protein concentrations were 140 μg/ml (cytosol) and 290 μg/ml (membranes).
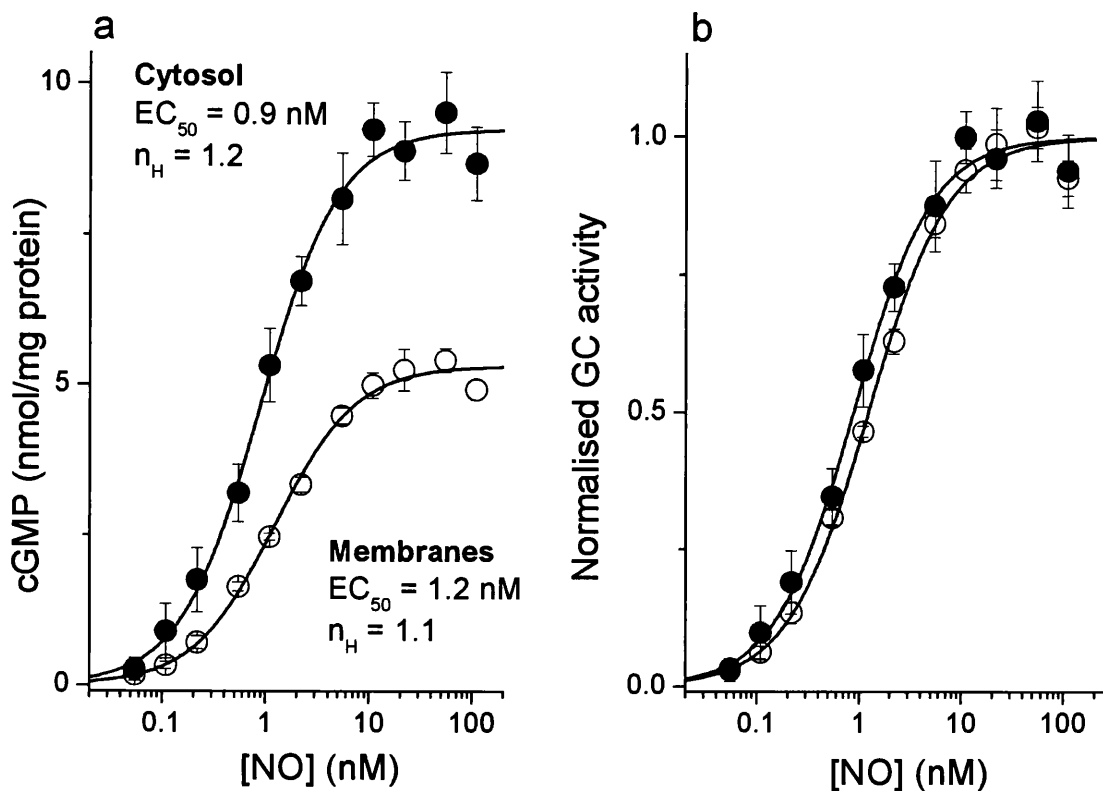
Figure 25: Comparison of the sensitivity of GC-coupled NO receptors in membrane and cytosol fractions of rat platelets

(a) Raw concentration-cGMP response curves for NO in cytosol (●) and membrane (○) fractions; $n = 4$. The solid lines fit the data to the Hill equation; n_H signifies the Hill coefficient. (b) The same data normalized to the mean maximal GC activity in each case (derived from the Hill fits). Protein concentrations were 13 μg/ml (cytosol) and 40 μg/ml (membranes).
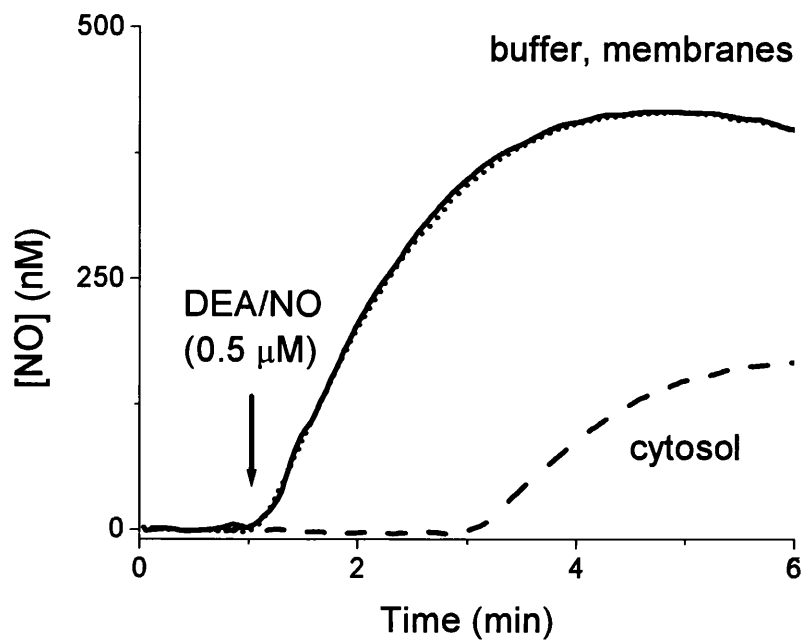
Figure 26: Consumption of NO by heart cytosol

Data are recordings of the NO concentration profiles over time resulting from addition of DEA/NO (0.5 μM; arrow) in buffer alone (solid line), or buffer containing the membrane fraction (dotted line) or the cytosolic fraction (dashed line) from rat heart. The traces are means of 2 runs and were smoothed by adjacent averaging (10 s bins). Protein concentrations were 130 μg/ml (cytosol) and 50 μg/ml (membranes).
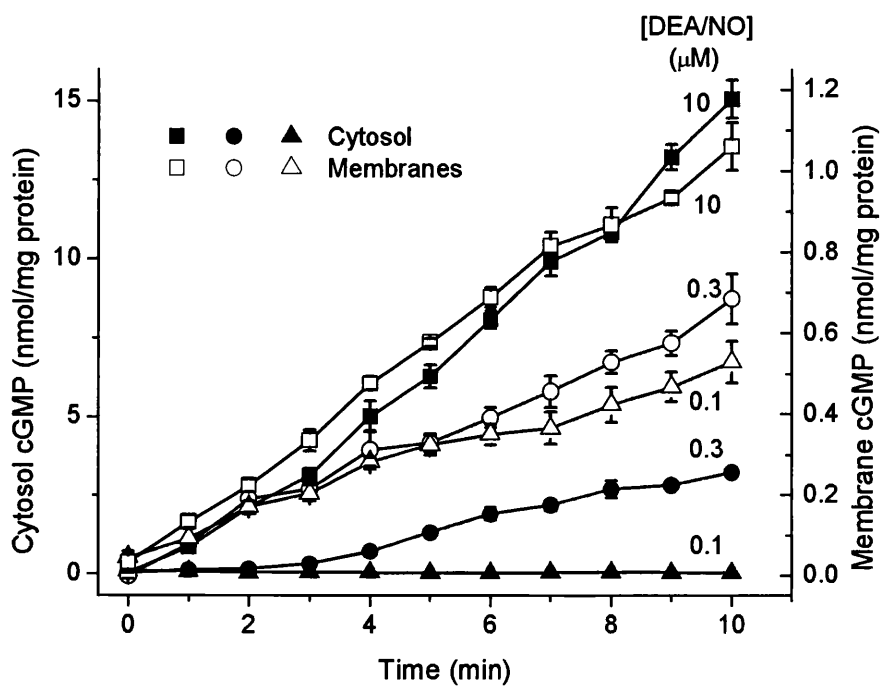
Figure 27: DEA/NO-induced cGMP accumulation in heart membranes and cytosol

The data show cGMP levels over time in response to addition of DEA/NO in concentrations of 10 µM (squares), 0.3 µM (circles) and 0.1 µM (triangles) in membranes (open symbols) or cytosol (filled symbols) from rat heart; $n = 4$. Protein concentrations were 86 µg/ml (cytosol) and 66 µg/ml (membranes).

6.4 Discussion

From the two different tissues examined in detail, we conclude that there is no discemable alteration in NO sensitivity of membrane-associated versus cytosolic GC-coupled receptors and that previous evidence that the two differ is spurious because, in the tissue examined (heart), the exposures to NO in the two fractions were different.

The concentration of myoglobin in heart is about 200 μmoles (kg wet weight)$^{-1}$ (Godecke et al., 1999) from which it can be estimated that the diluted cytosol used in our experiments would contain the protein in the upper 100 nM range. At the concentration of DEA/NO tested in figure 26 (0.5 μM) NO would be released at an initial rate of about 2.8 nM s^{-1} (assuming a half-life of 2.1 min and 1 mole of NO released per mole of DEA/NO; (Schmidt et al., 1997). To scavenge NO for the period observed (2 min) would require 250 nM myoglobin, a concentration well within the range predicted to be present, even allowing for some of the protein being in its oxidized, unreactive, form (metmyoglobin). A similar period of NO consumption was observed at a lower DEA/NO concentration (0.3 μM) in another experiment (the one whose cGMP results are reported in figure 27), which is explained by the protein concentration also being lower (see legends to figures. 26 and 27): assuming a proportionate reduction in myoglobin concentration (to 165 nM) it can be calculated that NO released from 0.3 μM DEA/NO would be grounded for 2 min, as was observed. The same myoglobin concentration would consume all NO releasable from 0.1 μM DEA/NO.

The presence of such a powerful NO scavenger means, of course, that the receptor cannot become activated until the scavenger is exhausted, which explains why, in the heart cytosol, there was no GC activity for 2 min following addition of 0.3 μM DEA/NO and no activity at all during a 10 min exposure to 0.1 μM DEA/NO whereas, with no scavenger (in the heart membranes), these same concentrations were sufficient to evoke half-maximal, or greater, net GC activity. Unfortunately, the problem imposed by myoglobin in the heart cytosol would also apply to the other NO delivery method used here for the cerebellum and platelets (NO reacts with myoglobin 1000-fold faster than with CPTIO); a method for removing myoglobin is needed to conduct the experiment meaningfully.

Rather than regulate their sensitivity to NO, the subcellular distribution of the GC-coupled NO receptors may reflect a physical compartmentation of the signal transduction cascade,

108

although the possibility that functional differences exist when the proteins are in their normal cellular environment *in vivo* cannot be excluded.

Chapter 7

General Discussion

During this study the functional characteristics of the physiologically expressed $NO_{GC}R$ were examined.

7.1 The cGMP response to NO in striatal cells

In order to examine the kinetics of activation of the natively expressed receptor in the striatum, the NO-cGMP signalling pathway first had to be characterised. Some of the key players in the pathway were identified. The cellular distribution of cGMP accumulation in response to NO was explored using immunohistochemical techniques in both striatal suspension and slices. It was found that the accumulation of cGMP was limited to cells expressing microtubule-associated protein 2, and neurone-specific nuclear protein. Thus neurones constitute the major site for cGMP responses to NO in the striatum, a finding that was consistent with earlier findings in striatal slices (Ariano and Matus, 1981; de Vente et al., 2000; Markerink-van Ittersum et al., 1997). Another cell type may also accumulate low levels of cGMP, which are dwarfed by the neuronal response, as the distribution of subunit mRNA of the $NO_{GC}R$ in the striatum is apparently widespread (Gibb and Garthwaite, 2001). However it is reasonable to assume that the experimentally measured increase in cGMP resulting from NO exposure accurately reflects the cGMP levels within neurones.

7.2 Degradation of cGMP by phosphodiesterases in the striatum

Using a pharmacological screen of inhibitors selective for different PDE families (1, 2, 3, 4, 5) the ability to potentiate the cGMP accumulation in response to a 30 s exposure to DEA/NO was measured. It was found that the major component of cGMP breakdown was though PDE2 as the PDE2 selective inhibitor EHNA blocked cGMP hydrolysis in the cells, with high potency ($IC_{50} = 30$ μM). PDE2 is "cGMP stimulated" and is a dual

110

substrate isoform hydrolysing both cGMP and cAMP, but with a higher affinity to cGMP (K_m cGMP = 10 µM; K_m cAMP = 30 µM) with similar maximum velocities (Juilfs et al., 1999). Interestingly PDE2 is also a target of cGMP so it acts as a negative feedback pathway to enhance cGMP degradation (Figure 28) and so produce a more transient cGMP response.

Striatal neurons

NO target cell
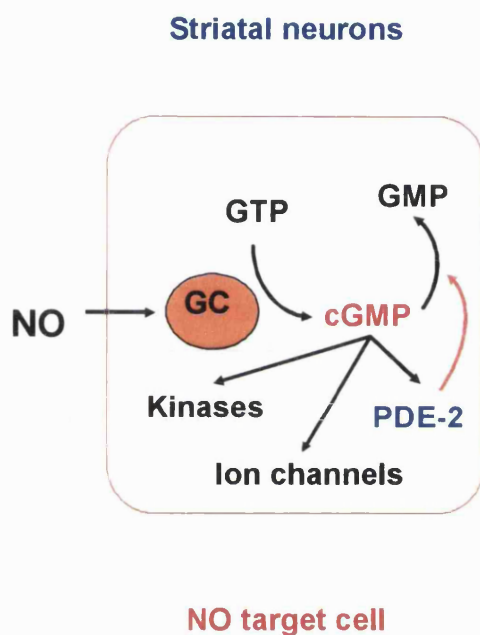
Figure 28: The NO-cGMP signalling pathway in the striatum

PDE2 is responsible for the degradation of cGMP in the striatum. However the activity of this isoform is also influenced by the ambient cGMP concentrations. The "cGMP stimulated" isoform acts to feedback to increase cGMP degradation.

7.3 The kinetics of cellular NO$_{GC}$R

Previous studies have revealed that within its natural, physiological environment the NO$_{GC}$R in cerebellar astrocytes acts more like a receptor than when in cell-free or purified preparations (Bellamy et al., 2000). Using the same method as previously

reported (Bellamy and Garthwaite, 2001b), the time course of cGMP accumulation has been "deconvoluted" to reveal the rates of cGMP synthesis and degradation. As in cerebellar astrocytes the receptor in striatal neurones was found to undergo a rapidly desensitizing profile following agonist exposure. However in the striatal cells the model of desensitization was more complicated, as the degree of desensitization appeared to be linked to the cGMP level. Thus as intracellular cGMP levels rose, the $NO_{GC}R$ desensitization became more pronounced. This feedback inhibition is a common mechanism of control in biology, but due to the lack of desensitization in homogenate it is difficult to investigate. As an alternative, recovery from desensitization, starting at different cGMP concentrations was investigated in cerebellar cells (for convenience) (Wykes et al., 2002). The initial rate of $NO_{GC}R$ activity was inversely correlated with cGMP, and when PDE inhibition was used to deliberately slow down the decline of cGMP levels, the recovery of $NO_{GC}R$ activity was also slowed. Thus cGMP appears to maintain the receptor in is desensitised state, and so may also initiate and regulate the extent of desensitization. This hypothesis is consistent with the data obtained with the striatal cells. cGMP alone (up to 1 mM) does not inhibit the purified $NO_{GC}R$ (Lee et al., 2000), and so desensitization may be triggered by an accumulation of cGMP, which in turn acts through an additional inhibitory factor (s). On cellular lysis, the $NO_{GC}R$ desensitization profile is lost, which could be due to dilution of this inhibitory desensitizing factor (Bellamy et al., 2000). An endogenous protein inhibitor of the $NO_{GC}R$ has been partially purified from bovine lung, but has not yet been fully characterised (Kim and Burstyn, 1994).

Recent work questioned the validity of taking the $NO_{GC}R$ activity profile obtained in the presence of PDE inhibitors and applying it to the normal cGMP response. In human platelets, the $NO_{GC}R$ activity was found to remain similarly active throughout the time course of NO exposure, implying lack of receptor desensitization (Mullershausen et al., 2001). Furthermore, the biphasic cGMP response observed over time was found to be associated with phosphorylation, and up-regulation of PDE5 activity, but no quantitative analysis was performed. It was also speculated that the desensitizing profile of the $NO_{GC}R$ in the presence of PDE inhibitors could be due to depletion of intraplatelet GTP levels, resulting in a lack of receptor substrate. However, pharmacological manipulation

112

of the activity of the NO$_{GC}$R in cerebellar cells, over a ten fold range (using the receptor activiator YC-1, and inhibitor ODQ) did not change the profile of receptor desensitization (Bellamy et al., 2000).

The lack of receptor desensitization in normal platelets (in the absence of PDE inhibitor) observed by Mullerhausen *et al.* (2001) is not inconsistent with the hypothesis that we present here, namely that cGMP regulates desensitization. In normal platelets, NO evoked cGMP accumulation peaks within 5-10 s and with a subsequent decrease to plateau at the basal level over the next minute. Thus the cGMP levels in these cells, is negligible following the brief spike of cGMP, and NO$_{GC}$R desensitization is minimal (Mullershausen et al., 2001). In the striatal neurones the cGMP levels are intermediate and the model of medium desensitization fits the data (Wykes et al., 2002), whereas in cerebellar astrocytes cGMP levels are high and desensitization is marked (Bellamy et al., 2000). Indeed when the platelets and striatal cells are incubated with PDE inhibitors to raise the cGMP levels, receptor desensitization is pronounced and exhibits a similar profile to that observed in cerebellar cells. Thus the hypothesis presented here accommodates the available data, but it is likely that alterations in PDE activity over time may also shape cGMP responses in some cells. Recent studies support this dual control of shaping cGMP signals. PDE5 activation is paralleled by phosphorylation of CGK I, which increases the cGMP affinity of the GAF-A domain (Francis et al., 2002). A comparison of PDE5 phosphorylation evoked by NO stimulation was absent in CGK I KO verses wild type mice, implying that this kinase is responsible for PDE5 activation (Shimizu-Albergine et al., 2003). Whether this mechanism is widespread in the NO-cGMP signalling remains to be investigated.

Changes in the phosphorylation state of a receptor are well established mechanisms of desensitization, including for the related membrane bound guanylyl cyclases (Potter and Garbers, 1994; Potter, 1998). Dephosphorylation of the β subunit of the NO$_{GC}$R by a phosphatase has been reported to inhibit the NO$_{GC}$R activity in bovine chromaffin cells under normal resting conditions (Ferrero et al., 2000). Activation NO$_{GC}$R results in the elevation of cGMP levels and activation of PKG which in turn dephosphorylates the NO$_{GC}$R causing a marked decrease in NO-evoked cGMP accumulation. In contrast a more recent study in smooth muscle, suggested that intracellular cGMP accumulation

stimulates CGK phosphorylation of the NO$_{GC}$R, resulting in an inhibition of the synthetic activity of the enzyme (Murthy, 2001). However, the cGMP accumulation in a cerebellar cell suspension was unaffected by two different CGK inhibitors or a broad-spectrum phosphatase inhibitor, suggesting that protein phosphorylation/ dephosphorylation are unlikely to be responsible for NO$_{GC}$R desensitization (Wykes et al., 2002). In comparison with other receptors, especially the adenylyl cyclases and other guanylyl cyclases there may be multiple regulatory factors awaiting identification (Chem, 2000), and these may be unique to different cell types.

7.4 Functional importance of NO$_{GC}$R desensitization

Desensitization of the NO$_{GC}$R plays an important physiological role in cells. The signal produced using the NO$_{GC}$R requires the consumption of GTP. This molecule is an important in the production of energy for the cell and is maintained in equilibrium with ATP. The most "cost effective" way for the cell to sustain a cGMP steady state is to allow the NO$_{GC}$R to initially have a high rate of cGMP synthesis thus ensuring that the steady state is achieved followed by desensitization which means considerably less GTP is consumed. This represents a mechanism by which cells can preserve GTP levels during prolonged NO exposures which may occur in chronic inflammation (Nathan and Xie, 1994) or during periods of LTP (Garthwaite and Boulton, 1995). The varying activity of the NO$_{GC}$R (and PDEs) result in different patterns of cGMP accumulation ranging from a large sustained plateaux to brief low amplitude transients. These diverse signals introduce selectivity as to which target is engaged. For example cyclic gated nucleotide channels are activated by high NO concentrations (μM), protein kinases are activated by low concentrations (nM) and PDE within the intermediate range.

7.5 NO sensitivity of the β1-containg NO$_{GC}$R isoforms

Having established that the NO$_{GC}$R undergoes a desensitizing profile in activity in these brain cells namely neurones, the next aim was to examine whether the different physiologically expressed isoforms exhibited different profiles of activation. Using a

114

recently developed technique to balance the rate of NO release with NO inactivation by red blood cells, clamped levels of NO were achieved. NO evoked cGMP accumulation was found to occur in a dose dependent manner with similar curves for both isoforms. The EC_{50} values were in the low nM range indicating that both isoforms are highly sensitive NO detectors. Receptor desensitization and the bell shaped nature of the concentration-response curve compromised interpretation of the data regarding the mechanism of $NO_{GC}R$ activation. To avoid this complication the next step was to investigate the receptor kinetics in cell lysates. This represented a good opportunity to reassess the method of delivery of constant NO concentrations. The biological method using red blood cells to act as a NO scavenger was subject to several limitations and thus was substituted for a chemical scavenger.

7.6 Improvements of the new chemical NO delivery method

The major improvement of the SPER/NO-CPTIO couple to deliver clamped concentrations of NO are manifold. The chemical method is quick, cheap and easy to use. A major advantage is that 95% of the plateaux NO concentration is attained 1 s after addition of the SPER/NO (Griffiths et al., 2003). This provides greater flexibility and accuracy for experiments where the rapid kinetics of receptor activation are investigated.

Using the previous technique where red blood cells were used as the scavenger for NO, a slow rise of the NO to plateau concentrations occurred (around 1 min). This meant that the additions e.g. of the receptor had to be made to the pre-equilibrated mixture in a small enough volume so as not to disturb the equilibrium. Clearly this represents a major limitation of the technique. An inherent problem of the biological NO scavenger is the potential of red blood cell lysis. Free haemoglobin inactivates NO at a much higher rate than when packaged in red blood cells (Liu et al., 1998). This will impact on the low levels of NO that are below the detection level of the electrochemical NO probe. The biological reactivity of the compounds required for the SPER/NO-CPTIO couple and accumulation of interfering products such as NO_2 has been accounted for by the addition of the radical scavenger urate. Validation of the technique and subsequent use, in my

hands and also by colleagues in the laboratory show that it appears to be free of unanticipated side effects.

7.7 NO binding sites for the GC-coupled receptor

Using a new chemical method for delivering constant clamped NO levels (the SPER/NO-CPTIO couple) the parameters of activation of the $NO_{GC}R$ were investigated. The NO concentration-response curve for the purified enzyme from bovine lung preparation indicated that the Hill coefficient was 1, in contrast to the value of 2 obtained using the RBC method (Bellamy et al., 2002a). A recent report suggested that it is likely that the enzyme represented a combination of the different isoforms and so lysates of COS-7 cells co-transfected with the individual subunits were used (Mergia et al., 2003). Again the concentration-response curves for both $\alpha1\beta1$ and $\alpha2\beta1$ were best fit with a Hill coefficient of 1. This clarifies the controversy that has been rife in the NO literature, as it supports the simple model of one NO molecule binding to the receptor to induce activation. Interestingly a recent paper reports that removal of the haem group of the $NO_{GC}R$ by genetic mutagenesis or detergent resulted in a several fold activation of the enzyme (Martin et al., 2003). The group suggest that the haem prosthetic group that is attached via the His105 bond of the β subunit acts as an endogenous inhibitor of the $NO_{GC}R$. Cleavage of the haem-coordinating bond induced by NO binding releases the restriction caused by this bond, allowing the catalytic domain to become activated. Until the crystal structure of the $NO_{GC}R$ has been elucidated, the exact mechanism of receptor activation will remain elusive.

7.8 NO receptor sensitivity

A recent report suggested that localisation of the $NO_{GC}R$ to cellular membranes enhanced its state of NO sensitivity two-fold (Zabel et al., 2002). In order to investigate this finding further, the NO sensitivities of the $NO_{GC}R$ in the membrane and soluble fractions of two different tissue types was investigated. However this phenomenon could not be reproduced. When the experiments were repeated using the tissue in which it was

116

first described, it became apparent that unfortunately an artefact had crept into the experimental design that invalidated the initial finding. However the $\alpha 1\beta 1$ receptor is associated with cellular membranes in a calcium-sensitive manner (Zabel et al., 2002), while the $\alpha 2\beta 1$ isoform associates with membranes through synaptic scaffolding proteins which also bind nNOS (Russwurm et al., 2001). Thus the difference in molecular makeup of the $NO_{GC}R$ isoforms may have evolved for targeting of different sub-cellular locations, but as yet no functional differences have been shown to exist *in vivo*.

7.9 Summary

In this study I have examined the kinetics of activation of the native $NO_{GC}R$ and of the heterologously-expressed receptor isoforms in intact cells and cell lysates. In the striatum the NO-cGMP pathway was characterised and some of the key players were identified: NO induced cGMP accumulation occurs in a subpopulation of neurons and cGMP stimulated PDE2 is responsible for cyclic nucleotide breakdown. PDE2 is target of cGMP but also acts as a feedback pathway to produce a more transient cGMP response. Desensitisation was found to be a common feature of the $NO_{GC}R$ when expressed natively in brain cells (striatal neurones) and transfected COS-7 cells. A comparison of the two known heterodimeric isoforms $\alpha 1\beta 1$ and $\alpha 2\beta 1$ expressed in COS-7 cells, exposed to fixed concentrations of NO demonstrated that both $\beta 1$-containing $NO_{GC}R$ isoforms have similar sensitivities to NO, responding in the low nM range. A new, more versatile chemical method for delivering constant clamped levels of NO was developed to avoid limitations associated with the use of RBC to inactivate NO. Using the new method the kinetic parameters of the receptor purified from bovine lung, and cell lysates containing the two isoforms were determined. In all cases half-maximal activity was about 1 nM. The Hill slopes were close to 1 which questions a previous conclusion that receptor activation requires binding of more that one NO molecule per receptor. To examine whether the location of the $NO_{GC}R$ within the cell influenced the receptor kinetics, cytosolic and membrane preparations from cerebellum and platelets were studied using fixed NO concentrations. In contrast to a previous study their sensitivities

to NO were indistinguishable suggesting that the subcellular distribution of the $NO_{GC}R$ may reflect a physical compartmentation of the signal cascade.

7.10 Future work

Continued investigation of the mechanism responsible for desensitisation is paramount in order to understand and develop therapeutics that will modify the cGMP response. Identification of the factor responsible for $NO_{GC}R$ desensitisation may be achieved by capture of the proteins which interact with the $NO_{GC}R$ under control and desensitising conditions. Immunoprecipitation and gel electrophoresis techniques or a yeast hybrid system with the different subunits of the $NO_{GC}R$ as bait, could be used. Proteomic analysis may identify the proteins which interact with the $NO_{GC}R$, and provide further clues as to how the receptor kinetics can be modulated.

Further work needs to investigate whether dephosphorylation or phosphorylation play a role in $NO_{GC}R$ desensitisation. At the first International Conference on cGMP "NO/sGC Interaction and its Therapeutic Implications; Leipzig 2003" Werner Mueller-Esterl reported that human $NO_{GC}R$ associates with an 89 kDa protein and that this interaction is regulated by reversible tyrosine phosphorylation. Site-directed mutagenesis may shed light on how the phosphorylation status of this protein influences $NO_{GC}R$ desensitisation.

References

1. Agullo L, Garcia A (1997) Ca^{2+}/calmodulin-dependent cyclic GMP phosphodiesterase activity in granule neurons and astrocytes from rat cerebellum. Eur J Pharmacol 323: 119-125.

2. Ahn HS, Crim W, Romano M, Sybertz E, Pitts B (1989) Effects of selective inhibitors on cyclic nucleotide phosphodiesterases of rabbit aorta. Biochem Pharmacol 38: 3331-3339.

3. Alderton WK, Cooper CE, Knowles RG (2001) Nitric oxide synthases: structure, function and inhibition. Biochem J 593-615.

4. Amano F, Noda T (1995) Improved detection of nitric oxide radical (NO.) production in an activated macrophage culture with a radical scavenger, carboxy PTIO and Griess reagent. FEBS Lett 368: 425-428.

5. Andreeva SG, Dikkes P, Epstein PM, Rosenberg PA (2001) Expression of cGMP-specific phosphodiesterase 9A mRNA in the rat brain. J Neurosci 21: 9068-9076.

6. Andrew CR, George SJ, Lawson DM, Eady RR (2002) Six- to five-coordinate heme-nitrosyl conversion in cytochrome c' and its relevance to guanylate cyclase. Biochemistry 41: 2353-2360.

7. Aravind L, Ponting CP (1997) The GAF domain: an evolutionary link between diverse phototransducing proteins. Trends Biochem Sci 22: 458-459.

8. Ariano MA (1983) Distribution of components of the guanosine 3',5'-phosphate system in rat caudate-putamen. Neuroscience 10: 707-723.

9. Ariano MA, Matus AI (1981) Ultrastructural localization of cyclic GMP and cyclic AMP in rat striatum. J Cell Biol 91: 287-292.

10. Ariano MA, Ufkes SK (1983) Cyclic nucleotide distribution within rat striatonigral neurons. Neuroscience 9: 23-29.

11. Arnold WP, Mittal CK, Katsuki S, Murad F (1977) Nitric oxide activates guanylate cyclase and increases guanosine 3':5'-cyclic monophosphate levels in various tissue preparations. Proc Natl Acad Sci U S A 74: 3203-3207.

12. Artz JD, Toader V, Zavorin SI, Bennett BM, Thatcher GR (2001) In vitro activation of soluble guanylyl cyclase and nitric oxide release: a comparison of NO donors and NO mimetics. Biochemistry 40: 9256-9264.

13. Ashman DF, Lipton R, Melcow NM, Price TD (1963) Isolation of adenosine 3',5'-monophosphate and guanosine 3',5'-monophosphate from rat urine. Biochem Biophys Res Commun 11: 330-334.

14. Augusto O, Bonini MG, Amanso AM, Linares E, Santos CC, De Menezes SL (2002) Nitrogen dioxide and carbonate radical anion: two emerging radicals in biology. Free Radic Biol Med 32: 841-859.

15. Ayajiki K, Kindermann M, Hecker M, Fleming I, Busse R (1996) Intracellular pH and tyrosine phosphorylation but not calcium determine shear stress-induced nitric oxide production in native endothelial cells. Circ Res 78: 750-758.

16. Babu BR, Griffith OW (1998) N5-(1-Imino-3-butenyl)-L-ornithine. A neuronal isoform selective mechanism-based inactivator of nitric oxide synthase. J Biol Chem 273: 8882-8889.

17. Bachrach U, Wang YC, Tabib A (2001) Polyamines: new cues in cellular signal transduction. News Physiol Sci 16: 106-109.

18. Ballou DP, Zhao Y, Brandish PE, Marletta MA (2002) Revisiting the kinetics of nitric oxide (NO) binding to soluble guanylate cyclase: the simple NO-binding model is incorrect. Proc Natl Acad Sci U S A 99: 12097-12101.

19. Baltrons MA, Saadoun S, Agullo L, Garcia A (1997) Regulation by calcium of the nitric oxide/cyclic GMP system in cerebellar granule cells and astroglia in culture. J Neurosci Res 49: 333-341.

20. Beal MF, Ferrante RJ, Browne SE, Matthews RT, Kowall NW, Brown RH, Jr. (1997) Increased 3-nitrotyrosine in both sporadic and familial amyotrophic lateral sclerosis. Ann Neurol 42: 644-654.

21. Beavo JA (1988) Multiple isozymes of cyclic nucleotide phosphodiesterase. Adv Second Messenger Phosphoprotein Res 22: 1-38.

22. Beavo JA (1995) Cyclic nucleotide phosphodiesterases: functional implications of multiple isoforms. Physiol Rev 75: 725-748.

23. Becker BF (1993) Towards the physiological function of uric acid. Free Radic Biol Med 14: 615-631.

24. Beckman JS, Koppenol WH (1996) Nitric oxide, superoxide, and peroxynitrite: the good, the bad, and ugly. Am J Physiol 271: C1424-C1437.

25. Behrends S, Harteneck C, Schultz G, Koesling D (1995) A variant of the alpha 2 subunit of soluble guanylyl cyclase contains an insert homologous to a region within adenylyl cyclases and functions as a dominant negative protein. J Biol Chem 270: 21109-21113.

26. Bellamy TC, Garthwaite J (2001a) "cAMP-specific" phosphodiesterase contributes to cGMP degradation in cerebellar cells exposed to nitric oxide. Mol Pharmacol 59: 54-61.

27. Bellamy TC, Garthwaite J (2001b) Sub-second kinetics of the nitric oxide receptor, soluble guanylyl cyclase, in intact cerebellar cells. J Biol Chem 276: 4287-4292.

28. Bellamy TC, Garthwaite J (2002) The receptor-like properties of nitric oxide-activated soluble guanylyl cyclase in intact cells. Mol Cell Biochem 230: 165-176.

29. Bellamy TC, Griffiths C, Garthwaite J (2002a) Differential sensitivity of guanylyl cyclase and mitochondrial respiration to nitric oxide measured using clamped concentrations. J Biol Chem 277: 31801-31807.

30. Bellamy TC, Wood J, Garthwaite J (2002b) On the activation of soluble guanylyl cyclase by nitric oxide. Proc Natl Acad Sci U S A 99: 507-510.

31. Bellamy TC, Wood J, Goodwin DA, Garthwaite J (2000) Rapid desensitization of the nitric oxide receptor, soluble guanylyl cyclase, underlies diversity of cellular cGMP responses. Proc Natl Acad Sci U S A 97: 2928-2933.

32. Boerrigter G, Costello-Boerrigter LC, Cataliotti A, Tsuruda T, Harty GJ, Lapp H, Stasch JP, Burnett JC, Jr. (2003) Cardiorenal and humoral properties of a novel direct soluble guanylate cyclase stimulator BAY 41-2272 in experimental congestive heart failure. Circulation 107: 686-689.

33. Bohme GA, Bon C, Stutzmann JM, Doble A, Blanchard JC (1991) Possible involvement of nitric oxide in long-term potentiation. Eur J Pharmacol 199: 379-381.

34. Bolanos JP, Heales SJ, Peuchen S, Barker JE, Land JM, Clark JB (1996) Nitric oxide-mediated mitochondrial damage: a potential neuroprotective role for glutathione. Free Radic Biol Med 21: 995-1001.

35. Bon C, Bohme GA, Doble A, Stutzmann JM, Blanchard JC (1992) A Role for Nitric Oxide in Long-term Potentiation. Eur J Neurosci 4: 420-424.

36. Bor-Kucukatay M, Wenby RB, Meiselman HJ, Baskurt OK (2003) Effects of nitric oxide on red blood cell deformability. Am J Physiol Heart Circ Physiol 284: H1577-H1584.

37. Brandish PE, Buechler W, Marletta MA (1998) Regeneration of the ferrous heme of soluble guanylate cyclase from the nitric oxide complex: acceleration by thiols and oxyhemoglobin. Biochemistry 37: 16898-16907.

38. Bredt DS, Snyder SH (1990) Isolation of nitric oxide synthetase, a calmodulin-requiring enzyme. Proc Natl Acad Sci U S A 87: 682-685.

39. Brenman JE, Chao DS, Gee SH, McGee AW, Craven SE, Santillano DR, Wu Z, Huang F, Xia H, Peters MF, Froehner SC, Bredt DS (1996) Interaction of nitric oxide synthase with the postsynaptic density protein PSD-95 and alpha1-syntrophin mediated by PDZ domains. Cell 84: 757-767.

40. Brown GC (1995) Nitric oxide regulates mitochondrial respiration and cell functions by inhibiting cytochrome oxidase. FEBS Lett 369: 136-139.

41. Brown GC, Cooper CE (1994) Nanomolar concentrations of nitric oxide reversibly inhibit synaptosomal respiration by competing with oxygen at cytochrome oxidase. FEBS Lett 356: 295-298.

42. Buechler WA, Nakane M, Murad F (1991) Expression of soluble guanylate cyclase activity requires both enzyme subunits. Biochem Biophys Res Commun 174: 351-357.

43. Calabresi P, Gubellini P, Centonze D, Sancesario G, Morello M, Giorgi M, Pisani A, Bernardi G (1999) A critical role of the nitric oxide/cGMP pathway in corticostriatal long-term depression. J Neurosci 19: 2489-2499.

44. Carcamo B, Hurwitz MY, Craft CM, Hurwitz RL (1995) The mammalian pineal expresses the cone but not the rod cyclic GMP phosphodiesterase. J Neurochem 65: 1085-1092.

45. Cassina A, Radi R (1996) Differential inhibitory action of nitric oxide and peroxynitrite on mitochondrial electron transport. Arch Biochem Biophys 328: 309-316.

46. Centonze D, Pisani A, Bonsi P, Giacomini P, Bernardi G, Calabresi P (2001) Stimulation of Nitric Oxide-cGMP pathway excites striatal cholinergic interneurones via Protein Kinase G activation. J Neurosci 21: 1393-1400.

47. Chen Q, Veenman CL, Reiner A (1996) Cellular expression of ionotropic glutamate receptor subunits on specific striatal neuron types and its implication for striatal vulnerability in glutamate receptor-mediated excitotoxicity. Neuroscience 73: 715-731.

48. Chern Y (2000) Regulation of adenylyl cyclase in the central nervous system. Cell Signal 12: 195-204.

49. Cherry JA, Davis RL (1999) Cyclic AMP phosphodiesterases are localized in regions of the mouse brain associated with reinforcement, movement, and affect. J Comp Neurol 407: 287-301.

50. Chinkers M, Garbers DL (1989) The protein kinase domain of the ANP receptor is required for signaling. Science 245: 1392-1394.

51. Christopherson KS, Hillier BJ, Lim WA, Bredt DS (1999) PSD-95 assembles a ternary complex with the N-methyl-D-aspartic acid receptor and a bivalent neuronal NO synthase PDZ domain. J Biol Chem 274: 27467-27473.

52. Chu DM, Francis SH, Thomas JW, Maksymovitch EA, Fosler M, Corbin JD (1998) Activation by autophosphorylation or cGMP binding produces a similar apparent conformational change in cGMP-dependent protein kinase. J Biol Chem 273: 14649-14656.

53. Clementi E, Brown GC, Foxwell N, Moncada S (1999) On the mechanism by which vascular endothelial cells regulate their oxygen consumption. Proc Natl Acad Sci U S A 96: 1559-1562.

54. Collingridge GL, Bliss TV (1995) Memories of NMDA receptors and LTP. Trends Neurosci 18: 54-56.

55. Cooper CE (2002) Nitric oxide and cytochrome oxidase: substrate, inhibitor or effector? Trends Biochem Sci 27: 33-39.

56. Corbin JD, Francis SH, Webb DJ (2002) Phosphodiesterase type 5 as a pharmacologic target in erectile dysfunction. Urology 60: 4-11.

57. Corbin JD, Turko IV, Beasley A, Francis SH (2000) Phosphorylation of phosphodiesterase-5 by cyclic nucleotide-dependent protein kinase alters its catalytic and allosteric cGMP-binding activities. Eur J Biochem 267: 2760-2767.

58. Corson MA, James NL, Latta SE, Nerem RM, Berk BC, Harrison DG (1996) Phosphorylation of endothelial nitric oxide synthase in response to fluid shear stress. Circ Res 79: 984-991.

59. Cramer KS, Angelucci A, Hahm JO, Bogdanov MB, Sur M (1996) A role for nitric oxide in the development of the ferret retinogeniculate projection. J Neurosci 16: 7995-8004.

60. Daniel H, Hemart N, Jaillard D, Crepel F (1993) Long-term depression requires nitric oxide and guanosine 3':5' cyclic monophosphate production in rat cerebellar Purkinje cells. Eur J Neurosci 5: 1079-1082.

61. Davies KM, Wink DA, Saavedra JE, Keefer LK (2001) Chemistry of the diazeniumdiolates. 2. Kinetics and mechanism of dissociation to nitric oxide in aqueous solution. J Am Chem Soc 123: 5473-5481.

62. De Jonge HR (1981) Cyclic GMP-dependent protein kinase in intestinal brushborders. Adv Cyclic Nucleotide Res 14: 315-333.

63. de Vente J, Markerink-van Ittersum M, van Abeelen J, Emson PC, Axer H, Steinbusch HW (2000) NO-mediated cGMP synthesis in cholinergic neurons in the rat forebrain: effects of lesioning dopaminergic or serotonergic pathways on nNOS and cGMP synthesis. Eur J Neurosci 12: 507-519.

64. de Zeeuw CI, Hansel C, Bian F, Koekkoek SK, van Alphen AM, Linden DJ, Oberdick J (1998) Expression of a protein kinase C inhibitor in Purkinje cells blocks cerebellar LTD and adaptation of the vestibulo-ocular reflex. Neuron 20: 495-508.

65. Degerman E, Belfrage P, Manganiello VC (1997) Structure, localization, and regulation of cGMP-inhibited phosphodiesterase (PDE3). J Biol Chem 272: 6823-6826.

66. Demas GE, Eliasson MJ, Dawson TM, Dawson VL, Kriegsfeld LJ, Nelson RJ, Snyder SH (1997) Inhibition of neuronal nitric oxide synthase increases aggressive behavior in mice. Mol Med 3: 610-616.

67. Denninger JW, Schelvis JP, Brandish PE, Zhao Y, Babcock GT, Marletta MA (2000) Interaction of soluble guanylate cyclase with YC-1: kinetic and resonance Raman studies. Biochemistry 39: 4191-4198.

68. Dierks EA, Burstyn JN (1996) Nitric oxide (NO), the only nitrogen monoxide redox form capable of activating soluble guanylyl cyclase. Biochem Pharmacol 51: 1593-1600.

69. Dimmeler S, Fleming I, Fisslthaler B, Hermann C, Busse R, Zeiher AM (1999) Activation of nitric oxide synthase in endothelial cells by Akt-dependent phosphorylation. Nature 399: 601-605.

70. Dorheim MA, Tracey WR, Pollock JS, Grammas P (1994) Nitric oxide synthase activity is elevated in brain microvessels in Alzheimer's disease. Biochem Biophys Res Commun 205: 659-665.

71. East SJ, Parry-Jones A, Brotchie JM (1996) Ionotropic glutamate receptors and nitric oxide synthesis in the rat striatum. Neuroreport 8: 71-75.

72. Eich RF, Li T, Lemon DD, Doherty DH, Curry SR, Aitken JF, Mathews AJ, Johnson KA, Smith RD, Phillips GN, Jr., Olson JS (1996) Mechanism of NO-induced oxidation of myoglobin and hemoglobin. Biochemistry 35: 6976-6983.

73. el Husseini AE, Bladen C, Vincent SR (1995) Molecular characterization of a type II cyclic GMP-dependent protein kinase expressed in the rat brain. J Neurochem 64: 2814-2817.

74. Endo S, Suzuki M, Sumi M, Nairn AC, Morita R, Yamakawa K, Greengard P, Ito M (1999) Molecular identification of human G-substrate, a possible downstream

component of the cGMP-dependent protein kinase cascade in cerebellar Purkinje cells. Proc Natl Acad Sci U S A 96: 2467-2472.

75. Fawcett L, Baxendale R, Stacey P, McGrouther C, Harrow I, Soderling S, Hetman J, Beavo JA, Phillips SC (2000) Molecular cloning and characterization of a distinct human phosphodiesterase gene family: PDE11A. Proc Natl Acad Sci U S A 97: 3702-3707.

76. Feil R, Hartmann J, Luo C, Wolfsgruber W, Schilling K, Feil S, Barski JJ, Meyer M, Konnerth A, de Zeeuw CI, Hofmann F (2003) Impairment of LTD and cerebellar learning by Purkinje cell-specific ablation of cGMP-dependent protein kinase I. J Cell Biol 163: 295-302.

77. Fernley HN (1974) Statistical estimations in enzyme kinetics. The integrated Michaelis equation. Eur J Biochem 43: 377-378.

78. Ferrendelli JA, Chang MM, Kinscherf DA (1974) Elevation of cyclic GMP levels in central nervous system by excitatory and inhibitory amino acids. J Neurochem 22: 535-540.

79. Ferrero R, Rodriguez-Pascual F, Miras-Portugal MT, Torres M (2000) Nitric oxide-sensitive guanylyl cyclase activity inhibition through cyclic GMP-dependent dephosphorylation. J Neurochem 75: 2029-2039.

80. Foerster J, Harteneck C, Malkewitz J, Schultz G, Koesling D (1996) A functional heme-binding site of soluble guanylyl cyclase requires intact N-termini of alpha 1 and beta 1 subunits. Eur J Biochem 240: 380-386.

81. Ford PC, Wink DA, Stanbury DM (1993) Autoxidation kinetics of aqueous nitric oxide. FEBS Lett 326: 1-3.

82. Francis SH, Bessay EP, Kotera J, Grimes KA, Liu L, Thompson WJ, Corbin JD (2002) Phosphorylation of isolated human phosphodiesterase-5 regulatory domain induces an apparent conformational change and increases cGMP binding affinity. J Biol Chem 277: 47581-47587.

83. Francis SH, Corbin JD (1994) Progress in understanding the mechanism and function of cyclic GMP-dependent protein kinase. Adv Pharmacol 26: 115-170.

84. Friebe A, Koesling D (1998) Mechanism of YC-1-induced activation of soluble guanylyl cyclase. Mol Pharmacol 53: 123-127.

85. Friebe A, Koesling D (2003) Regulation of nitric oxide-sensitive guanylyl cyclase. Circ Res 93: 96-105.

86. Friebe A, Wedel B, Harteneck C, Foerster J, Schultz G, Koesling D (1997) Functions of conserved cysteines of soluble guanylyl cyclase. Biochemistry 36: 1194-1198.

125

87. Fujishige K, Kotera J, Michibata H, Yuasa K, Takebayashi S, Okumura K, Omori K (1999a) Cloning and characterization of a novel human phosphodiesterase that hydrolyzes both cAMP and cGMP (PDE10A). J Biol Chem 274: 18438-18445.

88. Fujishige K, Kotera J, Omori K (1999b) Striatum- and testis-specific phosphodiesterase PDE10A. Eur J Biochem 266: 1118-1127.

89. Fujiyama F, Masuko S (1996) Association of dopaminergic terminals and neurons releasing nitric oxide in the rat striatum: an electron microscopic study using NADPH-diaphorase histochemistry and tyrosine hydroxylase immunohistochemistry. Brain Res Bull 40: 121-127.

90. Furchgott RF, Zawadzki JV (1980) The obligatory role of endothelial cells in the relaxation of arterial smooth muscle by acetylcholine. Nature 288: 373-376.

91. Furuyama T, Inagaki S, Takagi H (1993) Localizations of alpha 1 and beta 1 subunits of soluble guanylate cyclase in the rat brain. Brain Res Mol Brain Res 20: 335-344.

92. Gahtan E, Overmier JB (1999) Inflammatory pathogenesis in Alzheimer's disease: biological mechanisms and cognitive sequeli. Neurosci Biobehav Rev 23: 615-633.

93. Gal A, Orth U, Baehr W, Schwinger E, Rosenberg T (1994) Heterozygous missense mutation in the rod cGMP phosphodiesterase beta-subunit gene in autosomal dominant stationary night blindness. Nat Genet 7: 551.

94. Gao TM, Pulsinelli WA, Xu ZC (1999) Changes in membrane properties of CA1 pyramidal neurons after transient forebrain ischemia in vivo. Neuroscience 90: 771-780.

95. Garbers DL (1979) Purification of soluble guanylate cyclase from rat lung. J Biol Chem 254: 240-243.

96. Garry DJ, Ordway GA, Lorenz JN, Radford NB, Chin ER, Grange RW, Bassel-Duby R, Williams RS (1998) Mice without myoglobin. Nature 395: 905-908.

97. Garthwaite J, Balazs R (1981) Excitatory amino acid-induced changes in cyclic GMP levels in slices and cell suspensions from the cerebellum. Adv Biochem Psychopharmacol 27: 317-326.

98. Garthwaite J, Boulton CL (1995) Nitric oxide signaling in the central nervous system. Annu Rev Physiol 57: 683-706.

99. Garthwaite J, Charles SL, Chess-Williams R (1988) Endothelium-derived relaxing factor release on activation of NMDA receptors suggests role as intercellular messenger in the brain. Nature 336: 385-388.

100. Garthwaite J, Garthwaite G (1987) Cellular origins of cyclic GMP responses to excitatory amino acid receptor agonists in rat cerebellum in vitro. J Neurochem 48: 29-39.

101. Garthwaite J, Southam E, Boulton CL, Nielsen EB, Schmidt K, Mayer B (1995) Potent and selective inhibition of nitric oxide-sensitive guanylyl cyclase by 1H-[1,2,4]oxadiazolo[4,3-a]quinoxalin-1-one. Mol Pharmacol 48: 184-188.

102. Garvey EP, Oplinger JA, Furfine ES, Kiff RJ, Laszlo F, Whittle BJ, Knowles RG (1997) 1400W is a slow, tight binding, and highly selective inhibitor of inducible nitric-oxide synthase in vitro and in vivo. J Biol Chem 272: 4959-4963.

103. Gerzer R, Bohme E, Hofmann F, Schultz G (1981a) Soluble guanylate cyclase purified from bovine lung contains heme and copper. FEBS Lett 132: 71-74.

104. Gerzer R, Hofmann F, Bohme E, Ivanova K, Spies C, Schultz G (1981b) Purification of soluble guanylate cyclase without loss of stimulation by sodium nitroprusside. Adv Cyclic Nucleotide Res 14: 255-261.

105. Gibb BJ, Garthwaite J (2001) Subunits of the nitric oxide receptor, soluble guanylyl cyclase, expressed in rat brain. Eur J Neurosci 13: 539-544.

106. Gibb BJ, Wykes V, Garthwaite J (2003) Properties of NO-activated guanylyl cyclases expressed in cells. Br J Pharmacol 139: 1032-1040.

107. Gibbs SM (2003) Regulation of neuronal proliferation and differentiation by nitric oxide. Mol Neurobiol 27: 107-120.

108. Gillespie JS, Liu XR, Martin W (1989) The effects of L-arginine and NG-monomethyl L-arginine on the response of the rat anococcygeus muscle to NANC nerve stimulation. Br J Pharmacol 98: 1080-1082.

109. Gillespie JS, Martin W (1980) A smooth muscle inhibitory material from the bovine retractor penis and rat anococcygeus muscles. J Physiol 309: 55-64.

110. Giuili G, Scholl U, Bulle F, Guellaen G (1992) Molecular cloning of the cDNAs coding for the two subunits of soluble guanylyl cyclase from human brain. FEBS Lett 304: 83-88.

111. Godecke A, Flogel U, Zanger K, Ding Z, Hirchenhain J, Decking UK, Schrader J (1999) Disruption of myoglobin in mice induces multiple compensatory mechanisms. Proc Natl Acad Sci U S A 96: 10495-10500.

112. Gong GX, Weiss HR, Tse J, Scholz PM (1998) Exogenous nitric oxide reduces oxygen consumption of isolated ventricular myocytes less than other forms of guanylate cyclase stimulation. Eur J Pharmacol 344: 299-305.

113. Good PF, Hsu A, Werner P, Perl DP, Olanow CW (1998) Protein nitration in Parkinson's disease. J Neuropathol Exp Neurol 57: 338-342.

114. Green LC, Ruiz dL, Wagner DA, Rand W, Istfan N, Young VR, Tannenbaum SR (1981a) Nitrate biosynthesis in man. Proc Natl Acad Sci U S A 78: 7764-7768.

115. Green LC, Tannenbaum SR, Goldman P (1981b) Nitrate synthesis in the germfree and conventional rat. Science 212: 56-58.

116. Greenberg L.H., Troyer E., Ferrendelli J.A, Weiss B. (1978) Enzymic regulation of the concentration of cGMP in mouse brain. Neuropharmacology 17: 737-745.

117. Griffiths C, Garthwaite J (2001) The shaping of nitric oxide signals by a cellular sink. J Physiol 536: 855-862.

118. Griffiths C, Wykes V, Bellamy TC, Garthwaite J (2003) A new and simple method for delivering clamped nitric oxide concentrations in the physiological range: application to activation of guanylyl cyclase-coupled nitric oxide receptors. Mol Pharmacol 64: 1349-1356.

119. Gruetter CA, Barry BK, McNamara DB, Gruetter DY, Kadowitz PJ, Ignarro L (1979) Relaxation of bovine coronary artery and activation of coronary arterial guanylate cyclase by nitric oxide, nitroprusside and a carcinogenic nitrosoamine. J Cyclic Nucleotide Res 5: 211-224.

120. Gupta G, Azam M, Yang L, Danziger RS (1997) The beta2 subunit inhibits stimulation of the alpha1/beta1 form of soluble guanylyl cyclase by nitric oxide. Potential relevance to regulation of blood pressure. J Clin Invest 100: 1488-1492.

121. Harteneck C, Koesling D, Soling A, Schultz G, Bohme E (1990) Expression of soluble guanylyl cyclase. Catalytic activity requires two enzyme subunits. FEBS Lett 272: 221-223.

122. Harteneck C, Wedel B, Koesling D, Malkewitz J, Bohme E, Schultz G (1991) Molecular cloning and expression of a new alpha-subunit of soluble guanylyl cyclase. Interchangeability of the alpha-subunits of the enzyme. FEBS Lett 292: 217-222.

123. Haug LS, Jensen V, Hvalby O, Walaas SI, Ostvold AC (1999) Phosphorylation of the inositol 1,4,5-trisphosphate receptor by cyclic nucleotide-dependent kinases in vitro and in rat cerebellar slices in situ. J Biol Chem 274: 7467-7473.

124. Haynes J, Jr., Killilea DW, Peterson PD, Thompson WJ (1996) Erythro-9-(2-hydroxy-3-nonyl)adenine inhibits cyclic-3',5'-guanosine monophosphate-stimulated phosphodiesterase to reverse hypoxic pulmonary vasoconstriction in the perfused rat lung. J Pharmacol Exp Ther 276: 752-757.

125. Hebb AL, Robertson HA, Denovan-Wright EM (2004) Striatal phosphodiesterase mRNA and protein levels are reduced in Huntington's disease transgenic mice prior to the onset of motor symptoms. Neuroscience 123: 967-981.

126. Hibbs JB, Jr., Taintor RR, Vavrin Z (1987) Macrophage cytotoxicity: role for L-arginine deiminase and imino nitrogen oxidation to nitrite. Science 235: 473-476.

127. Hirsch EC, Hunot S (2000) Nitric oxide, glial cells and neuronal degeneration in parkinsonism. Trends Pharmacol Sci 21: 163-165.

128. Huang EP (1997) Synaptic plasticity: a role for nitric oxide in LTP. Curr Biol 7: R141-R143.

129. Huang PL, Dawson TM, Bredt DS, Snyder SH, Fishman MC (1993) Targeted disruption of the neuronal nitric oxide synthase gene. Cell 75: 1273-1286.

130. Huang PL, Huang Z, Mashimo H, Bloch KD, Moskowitz MA, Bevan JA, Fishman MC (1995) Hypertension in mice lacking the gene for endothelial nitric oxide synthase. Nature 377: 239-242.

131. Iadecola C (1997) Bright and dark sides of nitric oxide in ischemic brain injury. Trends Neurosci 20: 132-139.

132. Ignarro LJ, Adams JB, Horwitz PM, Wood KS (1986) Activation of soluble guanylate cyclase by NO-hemoproteins involves NO-heme exchange. Comparison of heme-containing and heme-deficient enzyme forms. J Biol Chem 261: 4997-5002.

133. Ignarro LJ, Byrns RE, Buga GM, Wood KS (1987) Endothelium-derived relaxing factor from pulmonary artery and vein possesses pharmacologic and chemical properties identical to those of nitric oxide radical. Circ Res 61: 866-879.

134. Ignarro LJ, Lippton H, Edwards JC, Baricos WH, Hyman AL, Kadowitz PJ, Gruetter CA (1981) Mechanism of vascular smooth muscle relaxation by organic nitrates, nitrites, nitroprusside and nitric oxide: evidence for the involvement of S-nitrosothiols as active intermediates. J Pharmacol Exp Ther 218: 739-749.

135. Ito M (2001) Cerebellar long-term depression: characterization, signal transduction, and functional roles. Physiol Rev 81: 1143-1195.

136. Jones MV, Westbrook GL (1996) The impact of receptor desensitization on fast synaptic transmission. Trends Neurosci 19: 96-101.

137. Jordan J, Cena V, Prehn JH (2003) Mitochondrial control of neuron death and its role in neurodegenerative disorders. J Physiol Biochem 59: 129-141.

138. Juilfs DM, Soderling S, Burns F, Beavo JA (1999) Cyclic GMP as substrate and regulator of cyclic nucleotide phosphodiesterases (PDEs). Rev Physiol Biochem Pharmacol 135: 67-104.

139. Kanacher T, Schultz A, Linder JU, Schultz JE (2002) A GAF-domain-regulated adenylyl cyclase from Anabaena is a self-activating cAMP switch. EMBO J 21: 3672-3680.

140. Katsuki S, Arnold W, Mittal C, Murad F (1977) Stimulation of guanylate cyclase by sodium nitroprusside, nitroglycerin and nitric oxide in various tissue preparations and comparison to the effects of sodium azide and hydroxylamine. J Cyclic Nucleotide Res 3: 23-35.

141. Kaupp UB, Niidome T, Tanabe T, Terada S, Bonigk W, Stuhmer W, Cook NJ, Kangawa K, Matsuo H, Hirose T, . (1989) Primary structure and functional expression from complementary DNA of the rod photoreceptor cyclic GMP-gated channel. Nature 342: 762-766.

142. Kawaguchi Y (1997) Neostriatal cell subtypes and their functional roles. Neurosci Res 27: 1-8.

143. Keefer LK, Nims RW, Davies KM, Wink DA (1996) "NONOates" (1-substituted diazen-1-ium-1,2-diolates) as nitric oxide donors: convenient nitric oxide dosage forms. Methods Enzymol 268: 281-293.

144. Kelm M, Feelisch M, Spahr R, Piper HM, Noack E, Schrader J (1988) Quantitative and kinetic characterization of nitric oxide and EDRF released from cultured endothelial cells. Biochem Biophys Res Commun 154: 236-244.

145. Kelm M, Schrader J (1990) Control of coronary vascular tone by nitric oxide. Circ Res 66: 1561-1575.

146. Keynes RG, Garthwaite J (2004) Nitric oxide and its role in ischaemic brain injury. Curr Mol Med 4: 179-191.

147. Keynes RG, Griffiths C, Garthwaite J (2003) Superoxide-dependent consumption of nitric oxide in biological media may confound in vitro experiments. Biochem J 369: 399-406.

148. Kharazia VN, Schmidt HH, Weinberg RJ (1994) Type I nitric oxide synthase fully accounts for NADPH-diaphorase in rat striatum, but not cortex. Neuroscience 62: 983-987.

149. Kharitonov VG, Russwurm M, Magde D, Sharma VS, Koesling D (1997) Dissociation of nitric oxide from soluble guanylate cyclase. Biochem Biophys Res Commun 239: 284-286.

150. Kim TD, Burstyn JN (1994) Identification and partial purification of an endogenous inhibitor of soluble guanylyl cyclase from bovine lung. J Biol Chem 269: 15540-15545.

151. Kingston PA, Zufall F, Barnstable CJ (1999) Widespread expression of olfactory cyclic nucleotide-gated channel genes in rat brain: implications for neuronal signalling. Synapse 32: 1-12.

152. Kitamura T, Kitamura Y, Kuroda S, Hino Y, Ando M, Kotani K, Konishi H, Matsuzaki H, Kikkawa U, Ogawa W, Kasuga M (1999) Insulin-induced phosphorylation and activation of cyclic nucleotide phosphodiesterase 3B by the serine-threonine kinase Akt. Mol Cell Biol 19: 6286-6296.

153. Ko FN, Wu CC, Kuo SC, Lee FY, Teng CM (1994) YC-1, a novel activator of platelet guanylate cyclase. Blood 84: 4226-4233.

154. Koesling D, Friebe A (1999) Soluble guanylyl cyclase: structure and regulation. Rev Physiol Biochem Pharmacol 135: 41-65.

155. Koesling D, Harteneck C, Humbert P, Bosserhoff A, Frank R, Schultz G, Bohme E (1990) The primary structure of the larger subunit of soluble guanylyl cyclase from bovine lung. Homology between the two subunits of the enzyme. FEBS Lett 266: 128-132.

156. Koesling D, Herz J, Gausepohl H, Niroomand F, Hinsch KD, Mulsch A, Bohme E, Schultz G, Frank R (1988) The primary structure of the 70 kDa subunit of bovine soluble guanylate cyclase. FEBS Lett 239: 29-34.

157. Koglin M, Behrends S (2003) A functional domain of the alpha 1 subunit of soluble guanylyl cyclase is necessary for activation of the enzyme by nitric oxide and YC-1 but is not involved in heme binding. J Biol Chem.

158. Koglin M, Vehse K, Budaeus L, Scholz H, Behrends S (2001) Nitric Oxide Activates the beta 2 Subunit of Soluble Guanylyl Cyclase in the Absence of a Second Subunit. J Biol Chem 276: 30737-30743.

159. Koivisto A, Matthias A, Bronnikov G, Nedergaard J (1997) Kinetics of the inhibition of mitochondrial respiration by NO. FEBS Lett 417: 75-80.

160. Komeima K, Hayashi Y, Naito Y, Watanabe Y (2000) Inhibition of neuronal nitric-oxide synthase by calcium/ calmodulin-dependent protein kinase IIalpha through Ser847 phosphorylation in NG108-15 neuronal cells. J Biol Chem 275: 28139-28143.

161. Koshland DE, Jr. (1992) The molecule of the year. Science 258: 1861.

162. Kramer RH, Molokanova E (2001) Modulation of cyclic-nucleotide-gated channels and regulation of vertebrate phototransduction. J Exp Biol 204: 2921-2931.

163. Kubota Y, Mikawa S, Kawaguchi Y (1993) Neostriatal GABAergic interneurones contain NOS, calretinin or parvalbumin. Neuroreport 5: 205-208.

164. Larkman AU, Jack JJ (1995) Synaptic plasticity: hippocampal LTP. Curr Opin Neurobiol 5: 324-334.

165. Lawson DM, Stevenson CE, Andrew CR, Eady RR (2000) Unprecedented proximal binding of nitric oxide to heme: implications for guanylate cyclase. EMBO J 19: 5661-5671.

166. Leamey CA, Ho-Pao CL, Sur M (2001) Disruption of retinogeniculate pattern formation by inhibition of soluble guanylyl cyclase. J Neurosci 21: 3871-3880.

167. Lee YC, Martin E, Murad F (2000) Human recombinant soluble guanylyl cyclase: expression, purification, and regulation. Proc Natl Acad Sci U S A 97: 10763-10768.

168. Li H, Raman CS, Glaser CB, Blasko E, Young TA, Parkinson JF, Whitlow M, Poulos TL (1999) Crystal structures of zinc-free and -bound heme domain of human inducible nitric-oxide synthase. Implications for dimer stability and comparison with endothelial nitric-oxide synthase. J Biol Chem 274: 21276-21284.

169. Liberatore GT, Jackson-Lewis V, Vukosavic S, Mandir AS, Vila M, McAuliffe WG, Dawson VL, Dawson TM, Przedborski S (1999) Inducible nitric oxide synthase stimulates dopaminergic neurodegeneration in the MPTP model of Parkinson disease. Nat Med 5: 1403-1409.

170. Liu X, Miller MJ, Joshi MS, Sadowska-Krowicka H, Clark DA, Lancaster JR, Jr. (1998) Diffusion-limited reaction of free nitric oxide with erythrocytes. J Biol Chem 273: 18709-18713.

171. Lo EH, Hara H, Rogowska J, Trocha M, Pierce AR, Huang PL, Fishman MC, Wolf GL, Moskowitz MA (1996) Temporal correlation mapping analysis of the hemodynamic penumbra in mutant mice deficient in endothelial nitric oxide synthase gene expression. Stroke 27: 1381-1385.

172. Lohmann SM, Vaandrager AB, Smolenski A, Walter U, De Jonge HR (1997) Distinct and specific functions of cGMP-dependent protein kinases. Trends Biochem Sci 22: 307-312.

173. Lohmann SM, Walter U, Miller PE, Greengard P, De Camilli P (1981) Immunohistochemical localization of cyclic GMP-dependent protein kinase in mammalian brain. Proc Natl Acad Sci U S A 78: 653-657.

132

174. Loke KE, McConnell PI, Tuzman JM, Shesely EG, Smith CJ, Stackpole CJ, Thompson CI, Kaley G, Wolin MS, Hintze TH (1999) Endogenous endothelial nitric oxide synthase-derived nitric oxide is a physiological regulator of myocardial oxygen consumption. Circ Res 84: 840-845.

175. Manganiello VC, Murata T, Taira M, Belfrage P, Degerman E (1995a) Diversity in cyclic nucleotide phosphodiesterase isoenzyme families. Arch Biochem Biophys 322: 1-13.

176. Manganiello VC, Taira M, Degerman E, Belfrage P (1995b) Type III cGMP-inhibited cyclic nucleotide phosphodiesterases (PDE3 gene family). Cell Signal 7: 445-455.

177. Markerink-van Ittersum M, Steinbusch HW, de Vente J (1997) Region-specific developmental patterns of atrial natriuretic factor- and nitric oxide-activated guanylyl cyclases in the postnatal frontal rat brain. Neuroscience 78: 571-587.

178. Martin E, Sharina I, Kots A, Murad F (2003) A constitutively activated mutant of human soluble guanylyl cyclase (sGC): implication for the mechanism of sGC activation. Proc Natl Acad Sci U S A 100: 9208-9213.

179. Martin W, Villani GM, Jothianandan D, Furchgott RF (1985) Selective blockade of endothelium-dependent and glyceryl trinitrate-induced relaxation by hemoglobin and by methylene blue in the rabbit aorta. J Pharmacol Exp Ther 232: 708-716.

180. Martinez SE, Wu AY, Glavas NA, Tang XB, Turley S, Hol WG, Beavo JA (2002) The two GAF domains in phosphodiesterase 2A have distinct roles in dimerization and in cGMP binding. Proc Natl Acad Sci U S A 99: 13260-13265.

181. Mayburd AL, Kassner RJ (2002) Mechanism and biological role of nitric oxide binding to cytochrome c'. Biochemistry 41: 11582-11591.

182. Mayer B, Klatt P, Bohme E, Schmidt K (1992) Regulation of neuronal nitric oxide and cyclic GMP formation by Ca^{2+}. J Neurochem 59: 2024-2029.

183. Mayer B, Koesling D, Bohme E (1993) Characterization of nitric oxide synthase, soluble guanylyl cyclase, and Ca^{2+}/calmodulin-stimulated cGMP phosphodiesterase as components of neuronal signal transduction. Adv Second Messenger Phosphoprotein Res 28: 111-119.

184. McGeer PL, Itagaki S, Boyes BE, McGeer EG (1988) Reactive microglia are positive for HLA-DR in the substantia nigra of Parkinson's and Alzheimer's disease brains. Neurology 38: 1285-1291.

185. McLaughlin ME, Ehrhart TL, Berson EL, Dryja TP (1995) Mutation spectrum of the gene encoding the beta subunit of rod phosphodiesterase among patients with

autosomal recessive retinitis pigmentosa. Proc Natl Acad Sci U S A 92: 3249-3253.

186. Mergia E, Russwurm M, Zoidl G, Koesling D (2003) Major occurrence of the new alpha(2)beta(1) isoform of NO-sensitive guanylyl cyclase in brain. Cell Signal 15: 189-195.

187. Michie AM, Lobban M, Muller T, Harnett MM, Houslay MD (1996) Rapid regulation of PDE-2 and PDE-4 cyclic AMP phosphodiesterase activity following ligation of the T cell antigen receptor on thymocytes: analysis using the selective inhibitors erythro-9-(2- hydroxy-3-nonyl)-adenine (EHNA) and rolipram. Cell Signal 8: 97-110.

188. Migaud M, Charlesworth P, Dempster M, Webster LC, Watabe AM, Makhinson M, He Y, Ramsay MF, Morris RG, Morrison JH, O'Dell TJ, Grant SG (1998) Enhanced long-term potentiation and impaired learning in mice with mutant postsynaptic density-95 protein. Nature 396: 433-439.

189. Mikami T, Kusakabe T, Suzuki N (1999) Tandem organization of medaka fish soluble guanylyl cyclase alpha1 and beta1 subunit genes. Implications for coordinated transcription of two subunit genes. J Biol Chem 274: 18567-18573.

190. Moncada S, Erusalimsky JD (2002) Does nitric oxide modulate mitochondrial energy generation and apoptosis? Nat Rev Mol Cell Biol 3: 214-220.

191. Moncada S, Palmer RM, Higgs EA (1991) Nitric oxide: physiology, pathophysiology, and pharmacology. Pharmacol Rev 43: 109-142.

192. Moore WM, Webber RK, Fok KF, Jerome GM, Connor JR, Manning PT, Wyatt PS, Misko TP, Tjoeng FS, Currie MG (1996) 2-Iminopiperidine and other 2-iminoazaheterocycles as potent inhibitors of human nitric oxide synthase isoforms. J Med Chem 39: 669-672.

193. Morley D, Keefer LK (1993) Nitric oxide/nucleophile complexes: a unique class of nitric oxide- based vasodilators. J Cardiovasc Pharmacol 22 Suppl 7: S3-S9.

194. Mullershausen F, Russwurm M, Thompson WJ, Liu L, Koesling D, Friebe A (2001) Rapid nitric oxide-induced desensitization of the cGMP response is caused by increased activity of phosphodiesterase type 5 paralleled by phosphorylation of the enzyme. J Cell Biol 155: 271-278.

195. Mulsch A, Bauersachs J, Schafer A, Stasch JP, Kast R, Busse R (1997) Effect of YC-1, an NO-independent, superoxide-sensitive stimulator of soluble guanylyl cyclase, on smooth muscle responsiveness to nitrovasodilators. Br J Pharmacol 120: 681-689.

196. Murohara T, Asahara T, Silver M, Bauters C, Masuda H, Kalka C, Kearney M, Chen D, Symes JF, Fishman MC, Huang PL, Isner JM (1998) Nitric oxide

synthase modulates angiogenesis in response to tissue ischemia. J Clin Invest 101: 2567-2578.

197. Murphy MP (1999) Nitric oxide and cell death. Biochim Biophys Acta 1411: 401-414.

198. Murrel W (1879) Vitro-glycerine as a remedy for angina pectoris. Lancet 113: 80-81.

199. Murthy KS (2001) Activation of phosphodiesterase 5 and inhibition of guanylate cyclase by cGMP-dependent protein kinase in smooth muscle. Biochem J 360: 199-208.

200. Nakane M, Arai K, Saheki S, Kuno T, Buechler W, Murad F (1990) Molecular cloning and expression of cDNAs coding for soluble guanylate cyclase from rat lung. J Biol Chem 265: 16841-16845.

201. Nakane M, Saheki S, Kuno T, Ishii K, Murad F (1988) Molecular cloning of a cDNA coding for 70 kilodalton subunit of soluble guanylate cyclase from rat lung. Biochem Biophys Res Commun 157: 1139-1147.

202. Nakazawa K, Mikawa S, Hashikawa T, Ito M (1995) Transient and persistent phosphorylation of AMPA-type glutamate receptor subunits in cerebellar Purkinje cells. Neuron 15: 697-709.

203. Nathan C, Xie QW (1994) Regulation of biosynthesis of nitric oxide. J Biol Chem 269: 13725-13728.

204. Nighorn A, Byrnes KA, Morton DB (1999) Identification and characterization of a novel beta subunit of soluble guanylyl cyclase that is active in the absence of a second subunit and is relatively insensitive to nitric oxide. J Biol Chem 274: 2525-2531.

205. O'Dell TJ, Huang PL, Dawson TM, Dinerman JL, Snyder SH, Kandel ER, Fishman MC (1994) Endothelial NOS and the blockade of LTP by NOS inhibitors in mice lacking neuronal NOS. Science 265: 542-546.

206. Palmer RM, Ashton DS, Moncada S (1988a) Vascular endothelial cells synthesize nitric oxide from L-arginine. Nature 333: 664-666.

207. Palmer RM, Ferrige AG, Moncada S (1987) Nitric oxide release accounts for the biological activity of endothelium-derived relaxing factor. Nature 327: 524-526.

208. Palmer RM, Rees DD, Ashton DS, Moncada S (1988b) L-arginine is the physiological precursor for the formation of nitric oxide in endothelium-dependent relaxation. Biochem Biophys Res Commun 153: 1251-1256.

209. Panahian N, Yoshida T, Huang PL, Hedley-Whyte ET, Dalkara T, Fishman MC, Moskowitz MA (1996) Attenuated hippocampal damage after global cerebral ischemia in mice mutant in neuronal nitric oxide synthase. Neuroscience 72: 343-354.

210. Paternain AV, Rodriguez-Moreno A, Villarroel A, Lerma J (1998) Activation and desensitization properties of native and recombinant kainate receptors. Neuropharmacology 37: 1249-1259.

211. Petrov V, Lijnen P (1996) Regulation of human erythrocyte Na+/H+ exchange by soluble and particulate guanylate cyclase. Am J Physiol 271: C1556-C1564.

212. Peunova N, Scheinker V, Cline H, Enikolopov G (2001) Nitric oxide is an essential negative regulator of cell proliferation in Xenopus brain. J Neurosci 21: 8809-8818.

213. Poderoso JJ, Carreras MC, Lisdero C, Riobo N, Schopfer F, Boveris A (1996) Nitric oxide inhibits electron transfer and increases superoxide radical production in rat heart mitochondria and submitochondrial particles. Arch Biochem Biophys 328: 85-92.

214. Poderoso JJ, Peralta JG, Lisdero CL, Carreras MC, Radisic M, Schopfer F, Cadenas E, Boveris A (1998) Nitric oxide regulates oxygen uptake and hydrogen peroxide release by the isolated beating rat heart. Am J Physiol 274: C112-C119.

215. Podzuweit T, Nennstiel P, Muller A (1995) Isozyme selective inhibition of cGMP-stimulated cyclic nucleotide phosphodiesterases by erythro-9-(2-hydroxy-3-nonyl) adenine. Cell Signal 7: 733-738.

216. Polli JW, Kincaid RL (1994) Expression of a calmodulin-dependent phosphodiesterase isoform (PDE1B1) correlates with brain regions having extensive dopaminergic innervation. J Neurosci 14: 1251-1261.

217. Potter LR (1998) Phosphorylation-dependent regulation of the guanylyl cyclase-linked natriuretic peptide receptor B: dephosphorylation is a mechanism of desensitization. Biochemistry 37: 2422-2429.

218. Potter LR, Garbers DL (1994) Protein kinase C-dependent desensitization of the atrial natriuretic peptide receptor is mediated by dephosphorylation. J Biol Chem 269: 14636-14642.

219. Price RH, Jr., Mayer B, Beitz AJ (1993) Nitric oxide synthase neurons in rat brain express more NMDA receptor mRNA than non-NOS neurons. Neuroreport 4: 807-810.

220. Raman CS, Li H, Martasek P, Kral V, Masters BS, Poulos TL (1998) Crystal structure of constitutive endothelial nitric oxide synthase: a paradigm for pterin function involving a novel metal center. Cell 95: 939-950.

221. Reinhardt RR, Bondy CA (1996) Differential cellular pattern of gene expression for two distinct cGMP- inhibited cyclic nucleotide phosphodiesterases in developing and mature rat brain. Neuroscience 72: 567-578.

222. Rudkin TM, Sadikot AF (1999) Thalamic input to parvalbumin-immunoreactive GABAergic interneurons: organization in normal striatum and effect of neonatal decortication. Neuroscience 88: 1165-1175.

223. Russwurm M, Behrends S, Harteneck C, Koesling D (1998) Functional properties of a naturally occurring isoform of soluble guanylyl cyclase. Biochem J 335 (Pt 1): 125-130.

224. Russwurm M, Mergia E, Mullershausen F, Koesling D (2002) Inhibition of deactivation of NO-sensitive guanylyl cyclase accounts for the sensitizing effect of YC-1. J Biol Chem 277: 24883-24888.

225. Russwurm M, Wittau N, Koesling D (2001) Guanylyl cyclase/PSD-95 interaction: targeting of the nitric oxide-sensitive alpha2beta1 guanylyl cyclase to synaptic membranes. J Biol Chem 276: 44647-44652.

226. Rybalkin SD, Rybalkina IG, Shimizu-Albergine M, Tang XB, Beavo JA (2003) PDE5 is converted to an activated state upon cGMP binding to the GAF A domain. EMBO J 22: 469-478.

227. Sanes JR, Lichtman JW (1999) Can molecules explain long-term potentiation? Nat Neurosci 2: 597-604.

228. Sasaki T, Kotera J, Yuasa K, Omori K (2000) Identification of human PDE7B, a cAMP-specific phosphodiesterase. Biochem Biophys Res Commun 271: 575-583.

229. Schmidt K, Desch W, Klatt P, Kukovetz WR, Mayer B (1997) Release of nitric oxide from donors with known half-life: a mathematical model for calculating nitric oxide concentrations in aerobic solutions. Naunyn Schmiedebergs Arch Pharmacol 355: 457-462.

230. Schrammel A, Behrends S, Schmidt K, Koesling D, Mayer B (1996) Characterization of 1H-[1,2,4]oxadiazolo[4,3-a]quinoxalin-1-one as a heme-site inhibitor of nitric oxide-sensitive guanylyl cyclase. Mol Pharmacol 50: 1-5.

231. Schudt DA, Dent G, Rabe KF (1996a) cGMP-inhibited phosphodiesterases (PDE-3). In: Phosphodiesterase inhibitors pp 89-109. London, UK: Academic Press.

232. Schudt DA, Dent G, Rabe KF (1996b) Interaction of PDE4 inhibitors with enzymes. In: Phosphodiesterase Inhibitors pp 110-126. London, UK: Academic Press.

233. Schuman EM, Madison DV (1991) A requirement for the intercellular messenger nitric oxide in long-term potentiation. Science 254: 1503-1506.

137

234. Schwarz UR, Walter U, Eigenthaler M (2001) Taming platelets with cyclic nucleotides. Biochem Pharmacol 62: 1153-1161.

235. Seeger TF, Bartlett B, Coskran TM, Culp JS, James LC, Krull DL, Lanfear J, Ryan AM, Schmidt CJ, Strick CA, Varghese AH, Williams RD, Wylie PG, Menniti FS (2003) Immunohistochemical localization of PDE10A in the rat brain. Brain Res 985: 113-126.

236. Shah S, Hyde DR (1995) Two Drosophila genes that encode the alph and beta subunits of the brain soluble guanylyl cyclase. J Biol Chem 270: 15368-15376.

237. Shakur Y, Holst LS, Landstrom TR, Movsesian M, Degerman E, Manganiello V (2001) Regulation and function of the cyclic nucleotide phosphodiesterase (PDE3) gene family. Prog Nucleic Acid Res Mol Biol 66: 241-277.

238. Sharma VS, Magde D (1999) Activation of soluble guanylate cyclase by carbon monoxide and nitric oxide: a mechanistic model. Methods 19: 494-505.

239. Shaul PW, Smart EJ, Robinson LJ, German Z, Yuhanna IS, Ying Y, Anderson RG, Michel T (1996) Acylation targets emdothelial nitric-oxide synthase to plasmalemmal caveolae. J Biol Chem 271: 6518-6522.

240. Shen W, Hintze TH, Wolin MS (1995) Nitric oxide. An important signaling mechanism between vascular endothelium and parenchymal cells in the regulation of oxygen consumption. Circulation 92: 3505-3512.

241. Shen W, Xu X, Ochoa M, Zhao G, Wolin MS, Hintze TH (1994) Role of nitric oxide in the regulation of oxygen consumption in conscious dogs. Circ Res 75: 1086-1095.

242. Shimizu-Albergine M, Rybalkin SD, Rybalkina IG, Feil R, Wolfsgruber W, Hofmann F, Beavo JA (2003) Individual cerebellar Purkinje cells express different cGMP phosphodiesterases (PDEs): in vivo phosphorylation of cGMP-specific PDE (PDE5) as an indicator of cGMP-dependent protein kinase (PKG) activation. J Neurosci 23: 6452-6459.

243. Smith KJ, Lassmann H (2002) The role of nitric oxide in multiple sclerosis. Lancet Neurol 1: 232-241.

244. Smith MA, Richey Harris PL, Sayre LM, Beckman JS, Perry G (1997) Widespread peroxynitrite-mediated damage in Alzheimer's disease. J Neurosci 17: 2653-2657.

245. Soderling SH, Bayuga SJ, Beavo JA (1998) Identification and characterization of a novel family of cyclic nucleotide phosphodiesterases. J Biol Chem 273: 15553-15558.

246. Soderling SH, Beavo JA (2000) Regulation of cAMP and cGMP signaling: new phosphodiesterases and new functions. Curr Opin Cell Biol 12: 174-179.

247. Son H, Hawkins RD, Martin K, Kiebler M, Huang PL, Fishman MC, Kandel ER (1996) Long-term potentiation is reduced in mice that are doubly mutant in endothelial and neuronal nitric oxide synthase. Cell 87: 1015-1023.

248. Song H, Ming G, He Z, Lehmann M, McKerracher L, Tessier-Lavigne M, Poo M (1998) Conversion of neuronal growth cone responses from repulsion to attraction by cyclic nucleotides. Science 281: 1515-1518.

249. Southam E, Garthwaite J (1993) The nitric oxide-cyclic GMP signalling pathway in rat brain. Neuropharmacology 32: 1267-1277.

250. Stadler J, Curran RD, Ochoa JB, Harbrecht BG, Hoffman RA, Simmons RL, Billiar TR (1991) Effect of endogenous nitric oxide on mitochondrial respiration of rat hepatocytes in vitro and in vivo. Arch Surg 126: 186-191.

251. Stasch JP, Becker EM, Alonso-Alija C, Apeler H, Dembowsky K, Feurer A, Gerzer R, Minuth T, Perzborn E, Pleiss U, Schroder H, Schroeder W, Stahl E, Steinke W, Straub A, Schramm M (2001) NO-independent regulatory site on soluble guanylate cyclase. Nature 410: 212-215.

252. Stewart VC, Heales SJ (2003) Nitric oxide-induced mitochondrial dysfunction: implications for neurodegeneration. Free Radic Biol Med 34: 287-303.

253. Stone JR, Marletta MA (1994) Soluble guanylate cyclase from bovine lung: activation with nitric oxide and carbon monoxide and spectral characterization of the ferrous and ferric states. Biochemistry 33: 5636-5640.

254. Stone JR, Marletta MA (1995) Heme stoichiometry of heterodimeric soluble guanylate cyclase. Biochemistry 34: 14668-14674.

255. Stone JR, Marletta MA (1996) Spectral and kinetic studies on the activation of soluble guanylate cyclase by nitric oxide. Biochemistry 35: 1093-1099.

256. Strijbos PJ, Leach MJ, Garthwaite J (1996) Vicious cycle involving $Na+$ channels, glutamate release, and NMDA receptors mediates delayed neurodegeneration through nitric oxide formation. J Neurosci 16: 5004-5013.

257. Strijbos PJ, Pratt GD, Khan S, Charles IG, Garthwaite J (1999) Molecular characterization and in situ localization of a full-length cyclic nucleotide-gated channel in rat brain. Eur J Neurosci 11: 4463-4467.

258. Stuehr DJ, Marletta MA (1985) Mammalian nitrate biosynthesis: mouse macrophages produce nitrite and nitrate in response to Escherichia coli lipopolysaccharide. Proc Natl Acad Sci U S A 82: 7738-7742.

139

259. Sundkvist E, Jaeger R, Sager G (2002) Pharmacological characterization of the ATP-dependent low K(m) guanosine 3',5'-cyclic monophosphate (cGMP) transporter in human erythrocytes. Biochem Pharmacol 63: 945-949.

260. Sung BJ, Yeon HK, Ho JY, Lee JI, Heo YS, Hwan KJ, Moon J, Min YJ, Hyun YL, Kim E, Jin ES, Park SY, Lee JO, Gyu LT, Ro S, Myung CJ (2003) Structure of the catalytic domain of human phosphodiesterase 5 with bound drug molecules. Nature 425: 98-102.

261. Tannenbaum SR, Fett D, Young VR, Land PD, Bruce WR (1978) Nitrite and nitrate are formed by endogenous synthesis in the human intestine. Science 200: 1487-1489.

262. Thomas MK, Francis SH, Corbin JD (1990) Substrate- and kinase-directed regulation of phosphorylation of a cGMP-binding phosphodiesterase by cGMP. J Biol Chem 265: 14971-14978.

263. Tomita T, Ogura T, Tsuyama S, Imai Y, Kitagawa T (1997) Effects of GTP on bound nitric oxide of soluble guanylate cyclase probed by resonance Raman spectroscopy. Biochemistry 36: 10155-10160.

264. Trabace L, Kendrick KM (2000) Nitric oxide can differentially modulate striatal neurotransmitter concentrations via soluble guanylate cyclase and peroxynitrite formation. J Neurochem 75: 1664-1674.

265. Troyer E.W., Hall I.A., Ferrendelli J.A. (1978) Guanylate cyclases in CNS: Enzymatic characteristics of soluble and particulate enzymes from mouse cerebellum and retina. J Neurochem 31: 825-833.

266. Turko IV, Ballard SA, Francis SH, Corbin JD (1999) Inhibition of cyclic GMP-binding cyclic GMP-specific phosphodiesterase (Type 5) by sildenafil and related compounds. Mol Pharmacol 56: 124-130.

267. Turko IV, Francis SH, Corbin JD (1998) Binding of cGMP to both allosteric sites of cGMP-binding cGMP-specific phosphodiesterase (PDE5) is required for its phosphorylation. Biochem J 329 (Pt 3): 505-510.

268. van Staveren WC, Markerink-van Ittersum M, Steinbusch HW, de Vente J (2001) The effects of phosphodiesterase inhibition on cyclic GMP and cyclic AMP accumulation in the hippocampus of the rat. Brain Res 888: 275-286.

269. Vincent SR, Johansson O (1983) Striatal neurons containing both somatostatin- and avian pancreatic polypeptide (APP)-like immunoreactivities and NADPH-diaphorase activity: a light and electron microscopic study. J Comp Neurol 217: 264-270.

270. Vuillet J, Dimova R, Nieoullon A, Goff LK (1992) Ultrastructural relationships between choline acetyltransferase- and neuropeptide y-containing neurons in the rat striatum. Neuroscience 46: 351-360.

271. Wagner DA, Tannenbaum SR (1983) Nitrosamines and Human Cancer. In: Nitrosamines and Human Cancer pp 437-443. New York: Cold Spring Harbour.

272. Wagner DA, Young VR, Tannenbaum SR (1983) Mammalian nitrate biosynthesis: incorporation of 15NH3 into nitrate is enhanced by endotoxin treatment. Proc Natl Acad Sci U S A 80: 4518-4521.

273. Wall ME, Francis SH, Corbin JD, Grimes K, Richie-Jannetta R, Kotera J, Macdonald BA, Gibson RR, Trewhella J (2003) Mechanisms associated with cGMP binding and activation of cGMP-dependent protein kinase. Proc Natl Acad Sci U S A 100: 2380-2385.

274. Walter U (1989) Physiological role of cGMP and cGMP-dependent protein kinase in the cardiovascular system. Rev Physiol Biochem Pharmacol 113: 41-88.

275. Wang YT, Linden DJ (2000) Expression of cerebellar long-term depression requires postsynaptic clathrin-mediated endocytosis. Neuron 25: 635-647.

276. Webber RK, Metz S, Moore WM, Connor JR, Currie MG, Fok KF, Hagen TJ, Hansen DW, Jr., Jerome GM, Manning PT, Pitzele BS, Toth MV, Trivedi M, Zupec ME, Tjoeng FS (1998) Substituted 2-iminopiperidines as inhibitors of human nitric oxide synthase isoforms. J Med Chem 41: 96-101.

277. Wedel B, Humbert P, Harteneck C, Foerster J, Malkewitz J, Bohme E, Schultz G, Koesling D (1994) Mutation of His-105 in the beta 1 subunit yields a nitric oxide-insensitive form of soluble guanylyl cyclase. Proc Natl Acad Sci U S A 91: 2592-2596.

278. Wei XQ, Charles IG, Smith A, Ure J, Feng GJ, Huang FP, Xu D, Muller W, Moncada S, Liew FY (1995) Altered immune responses in mice lacking inducible nitric oxide synthase. Nature 375: 408-411.

279. White AA, Aurbach GD (1969) Detection of guanyl cyclase in mammalian tissues. Biochim Biophys Acta 191: 686-697.

280. Wood J, Garthwaite J (1994) Models of the diffusional spread of nitric oxide: implications for neural nitric oxide signalling and its pharmacological properties. Neuropharmacology 33: 1235-1244.

281. Wu HH, Cork RJ, Huang PL, Shuman DL, Mize RR (2000) Refinement of the ipsilateral retinocollicular projection is disrupted in double endothelial and neuronal nitric oxide synthase gene knockout mice. Brain Res Dev Brain Res 120: 105-111.

282. Wu HH, Williams CV, McLoon SC (1994) Involvement of nitric oxide in the elimination of a transient retinotectal projection in development. Science 265: 1593-1596.

283. Wykes V, Bellamy TC, Garthwaite J (2002) Kinetics of nitric oxide-cyclic GMP signalling in CNS cells and its possible regulation by cyclic GMP. J Neurochem 83: 37-47.

284. Yan C, Bentley JK, Sonnenburg WK, Beavo JA (1994) Differential expression of the 61 kDa and 63 kDa calmodulin-dependent phosphodiesterases in the mouse brain. J Neurosci 14: 973-984.

285. Yuen PS, Potter LR, Garbers DL (1990) A new form of guanylyl cyclase is preferentially expressed in rat kidney. Biochemistry 29: 10872-10878.

286. Zabel U, Hausler C, Weeger M, Schmidt HH (1999) Homodimerization of soluble guanylyl cyclase subunits. Dimerization analysis using a glutathione s-transferase affinity tag. J Biol Chem 274: 18149-18152.

287. Zabel U, Kleinschnitz C, Oh P, Nedvetsky P, Smolenski A, Muller H, Kronich P, Kugler P, Walter U, Schnitzer JE, Schmidt HH (2002) Calcium-dependent membrane association sensitizes soluble guanylyl cyclase to nitric oxide. Nat Cell Biol 4: 307-311.

288. Zabel U, Weeger M, La M, Schmidt HH (1998) Human soluble guanylate cyclase: functional expression and revised isoenzyme family. Biochem J 335 (Pt 1): 51-57.

289. Zagotta WN, Siegelbaum SA (1996) Structure and function of cyclic nucleotide-gated channels. Annu Rev Neurosci 19: 235-263.

290. Zhao Y, Brandish PE, Ballou DP, Marletta MA (1999) A molecular basis for nitric oxide sensing by soluble guanylate cyclase. Proc Natl Acad Sci U S A 96: 14753-14758.

291. Zhao Y, Brandish PE, DiValentin M, Schelvis JP, Babcock GT, Marletta MA (2000) Inhibition of soluble guanylate cyclase by ODQ. Biochemistry 39: 10848-10854.

292. Zhao Y, Schelvis JP, Babcock GT, Marletta MA (1998) Identification of histidine 105 in the beta1 subunit of soluble guanylate cyclase as the heme proximal ligand. Biochemistry 37: 4502-4509.

293. Zhelyaskov VR, Godwin DW (1999) A nitric oxide concentration clamp. Nitric Oxide 3: 419-425.

294. Zhong H, Molday LL, Molday RS, Yau KW (2002) The heteromeric cyclic nucleotide-gated channel adopts a 3A:1B stoichiometry. Nature 420: 193-198.

295. Zufall F, Shepherd GM, Barnstable CJ (1997) Cyclic nucleotide gated channels as regulators of CNS development and plasticity. Curr Opin Neurobiol 7: 404-412.

Appendix: Abstracts and publications

Abstracts

Wykes V, Bellamy T, Garthwaite J (January 10, 2003)

Nitric oxide signal transduction through guanylyl cyclase isoforms.

3rd UK Nitric Oxide Forum. London, UK.

Wykes V, Gibb B, Garthwaite J (April 13-16, 2003).

Does the molecular makeup of the guanylyl cyclase coupled nitric oxide receptor

influence its function?

17th National Meeting of the British Neuroscience Association. Harrogate, UK.

Wykes V, Gibb B, Garthwaite J (June 14-16 2003).

Kinetic characteristics of the guanylyl cyclase-coupled receptor.

1st International Conference on cGMP: NO/sGC Interaction and Therapeutic

Implications. Leipzig, Germany.

Wykes V, Griffiths C, Gibb B, Garthwaite J (November 8-12, 2003).

Kinetic characteristics of the guanylyl cyclase-coupled receptor.

Society for Neuroscience 33rd annual meeting. New Orleans, USA.

144

Publications

Wykes V, Bellamy T, Garthwaite J, (2002) Kinetics of Nitric Oxide-cGMP signaling in CNS cells and its possible regulation by cGMP. J Neurochem 83: 37-47.

Gibb B. Wykes V. Garthwaite J (2003) Properties of NO-activated guanylyl cyclases expressed in cells. Br J Pharmacol 139: 1032-1040.

Griffiths C, Wykes V, Bellamy T, Garthwaite J (2003) A new and simple method for delivering clamped nitric oxide concentrations in the physiological range: Application to activation of guanylyl cyclase-coupled nitric oxide receptors. Mol Pharmacol 64: 1349-1356.

Wykes V, Garthwaite J (2004) Membrane-association and the sensitivity of guanylyl cyclase-coupled receptors to nitric oxide. Br J Pharmacol 141: 1087-90.

145

Kinetics of nitric oxide-cyclic GMP signalling in CNS cells and its possible regulation by cyclic GMP

Victoria Wykes, Tomas C. Bellamy[1] and John Garthwaite

Wolfson Institute for Biomedical Research, University College London, London, UK

Abstract

Physiologically, nitric oxide (NO) signal transduction occurs through soluble guanylyl cyclase (sGC), which catalyses cyclic GMP (cGMP) formation. Knowledge of the kinetics of NO-evoked cGMP signals is therefore critical for understanding how NO signals are decoded. Studies on cerebellar astrocytes showed that sGC undergoes a desensitizing profile of activity, which, in league with phosphodiesterases (PDEs), was hypothesized to diversify cGMP responses in different cells. The hypothesis was tested by examining the kinetics of cGMP in rat striatal cells, in which cGMP accumulated in neurones in response to NO. Based on the effects of selective PDE inhibitors, cGMP hydrolysis following exposure to NO was attributed to a cGMP-stimulated PDE (PDE 2). Analysis of NO-induced cGMP accumulation in the presence of a PDE inhibitor indicated that sGC underwent marked desensitization. However, the desensitization kinetics determined under these conditions described poorly the cGMP profile observed in the absence of the PDE inhibitor. An explanation shown plausible theoretically was that cGMP determines the level of sGC desensitization. In support, tests in cerebellar astrocytes indicated an inverse relationship between cGMP level and recovery of sGC from its desensitized state. We suggest that the degree of sGC desensitization is related to the cGMP concentration and that this effect is not mediated by (de)phosphorylation.

Keywords: cyclic GMP, nitric oxide, phosphodiesterase, soluble guanylyl cyclase, striatum.

J. Neurochem. (2002) **83**, 37–47.

Nitric oxide (NO) serves as an intercellular signalling molecule in most tissues. In the central nervous system (CNS) the synthesis of NO is typically linked to activation of the NMDA subtype of glutamate receptors through the Ca^{2+}/calmodulin-dependent activation of neuronal NO synthase (Garthwaite 1991). The major physiological receptor for NO is soluble guanylyl cyclase (sGC), an $\alpha\beta$ heterodimer that catalyses the conversion of GTP to cGMP. The resulting increase of this second messenger modulates the activity of cGMP-dependent protein kinases, phosphodiesterases (PDEs) and ion channels. Activation of sGC appears to be the main pathway through which NO exerts its many physiological effects in the CNS, including synaptic plasticity (Garthwaite 2000), neurotransmitter release (Prast and Philippu 2001) and synaptogenesis (Contestabile 2000). NO is also implicated in cGMP-independent processes, such as neuronal cell death (Dawson *et al.* 1991; Almeida *et al.* 1998).

In order to develop concepts of NO signalling at the cellular and molecular levels, it is necessary to understand the kinetic properties of the activation of sGC by NO and the ways that subsequent cGMP responses are shaped to engage downstream targets. Recent studies on cerebellar cell suspensions have shown that sGC in astrocytes activates and deactivates rapidly (subsecond time scales) on addition and removal of NO, respectively, suggesting that the enzyme behaves in a much more dynamic manner than had appeared to be the case beforehand (Bellamy *et al.* 2000; Bellamy and Garthwaite 2001a). Moreover, unlike with purified sGC, the enzyme in astrocytes

undergoes rapid desensitization to the extent that the steady-state level of activity during sustained NO exposure is about 10% of the peak (Bellamy *et al.* 2000). In these particular cells, the PDE activity is low. The combination of this and sGC desensitization leads to high-amplitude plateaux of cGMP being generated in response to NO. It was predicted that in cells with high PDE activity, the same profile of sGC activity would lead to a low amplitude cGMP transient, a shape that may be tuned to engage different downstream mechanisms from those in cerebellar astrocytes. Some evidence for this was obtained for human platelets (Bellamy *et al.* 2000), but this hypothesis remains to be tested in other CNS cell types that are recognized NO targets, notably neurones (Southam and Garthwaite 1993).

The striatum is enriched in all elements of this signalling pathway. NO synthase is expressed in interneurones and in dense fibre networks (Vincent and Kimura 1992) and, as elsewhere, NO production is coupled to NMDA receptor activity (East *et al.* 1996). The striatum also contains high sGC activity (Greenberg *et al.* 1978) and expresses abundantly mRNA for both $\alpha 1$ and $\beta 1$ subunits of the enzyme (Furuyama *et al.* 1993; Gibb and Garthwaite 2001). The striatum also has one of the highest levels of PDE activity in the brain (Greenberg *et al.* 1978). The Ca^{2+}/calmodulin-dependent PDE 1 (Polli and Kincaid 1994; Yan *et al.* 1994), PDE 2 (Michie *et al.* 1996), PDE 3 (Reinhardt and Bondy 1996), PDE 4 (Cherry and Davis 1999), PDE 7B (Sasaki *et al.* 2000), PDE 9A (Andreeva *et al.* 2001) and PDE 10A (Fujishige *et al.* 1999) are all located there although which, if any, is responsible for degrading NO-induced cGMP signals has not been investigated. Functionally, the striatal NO-cGMP pathway is involved in synaptic plasticity (Calabresi *et al.* 1999), neurotransmitter release (Trabace and Kendrick 2000) and excitation of cholinergic interneurones (Centonze *et al.* 2001).

This information suggested that the striatum would represent a suitable brain area for discerning the kinetics of the NO-cGMP signalling pathway in cells that have different activities of the component enzymes, and possibly also different isoforms, compared with cerebellar astrocytes. To this end, we used cell suspensions from the striatum to determine how the interplay between sGC and PDE activities regulates the levels of the effector molecule, cGMP.

Experimental procedures

Striatal slice preparation

Sprague–Dawley rats (aged postnatal day 8) were killed by decapitation as approved by the British Home Office and the local ethics committee. The brain was removed and coronal slices (400-μm thick) containing the striatum were cut using a Vibroslice (Campden Instruments). The striatum from each hemisphere was dissected out and the resulting slices incubated in Krebs–Henseleit

buffer gassed with 5% CO_2 and 95% O_2 (pH 7.4) containing (in mM): NaCl (120), KCl (2), NaHCO$_3$ (26), MgSO$_4$ (1.2), KH$_2$PO$_4$ (1.2), glucose (11) and CaCl$_2$ (2) together with L-nitroarginine (0.1) to prevent possible complications from endogenous NO synthesis. Slices were recovered for at least 1 h in a shaking water bath (37°C) before use.

Preparation of cell suspensions

For striatal cell suspensions, a thick (1.6 mm) slice of brain was first cut in the coronal plane, starting just behind the merger of the corpus callosum. The striatum from each hemisphere was dissected out and cut into 400 μm cubes using a McIlwain tissue chopper. Cell suspensions were prepared from these cubes, and from analogous tissue prepared from the cerebellum, following mild trypsinization and trituration as previously described (Garthwaite 1985). The cells were counted using a haemocytometer in the presence of trypan blue (1 : 5 dilution, to determine viability which was always > 95%) and then incubated in an air-equilibrated medium (pH 7.4) containing (mM): NaCl (130), KCl (3), MgSO$_4$ (1.2), NaH$_2$PO$_4$ (1.2), Tris-HCl (15), glucose (11), CaCl$_2$ (1.5) and L-nitroarginine (0.1). The yield of striatal cells was approximately 0.5 million/rat and they were incubated at a final concentration of 1×10^6 cells/mL. Reflecting a much higher cell density in the cerebellum, the yield therefrom was much higher (about 20 million/rat) and they were used at a final concentration of 20×10^6 cells/mL. The use of differing cell concentrations is unlikely to introduce complications because the response to NO is independent of this parameter (Garthwaite and Garthwaite 1987).

Exposure to NO

Slices and cell suspensions were exposed to the NO donor diethylamine/NO adduct (DEA/NO), which has a half-life of 2.1 min at 37°C. When used, PDE inhibitors, kinase and phosphatase inhibitors were made up in dimethyl sulphoxide (DMSO) and added 10 min prior to addition of DEA/NO. At the 1 : 100 dilution used DMSO had no effect on the DEA/NO induced cGMP response (not shown). At the end of the exposure, individual slices or aliquots of the cell suspension were inactivated in boiling hypotonic buffer; protein was quantified using the bicinchoninic method and cGMP using radioimmunoassay (Garthwaite 1985; Garthwaite and Garthwaite 1987).

Data analysis

Results are given as the mean cGMP levels from n independently treated cell populations ± SEM (or SD where indicated), and analysed using the unpaired Student's t-test (two-tailed) or, where stated, analysis of variance using Dunnett's multiple comparison test. Significance was assumed when $p < 0.05$.

Immunocytochemistry

Suspensions and slices with or without various treatments (as described in the results) were fixed in paraformaldehyde (4%) in 0.1 M phosphate buffer, pH 7.4, for either 1 h (slices) or 20 min (cell suspensions) at room temperature (23°C). Cell suspensions were processed as previously described (Bellamy *et al.* 2000). Slices were cryoprotected by incubating in phosphate buffer containing 20% sucrose overnight at 4°C. Cryostat sections (10 μm) were cut and dried onto gelatine-coated slides. The sections were then

microwaved for 1 min. Slides (with adhering cell suspensions or sections) were rinsed with Tris-buffered saline containing 0.1% Triton X-100 and incubated with normal rabbit and horse sera for 30 min followed by an overnight incubation at 4°C with the primary antibodies, which were sheep anti-cGMP (1 : 8000), mouse anti-neurone-specific nuclear protein (NeuN, 1 : 100), mouse anti-glial fibrillary acidic protein (GFAP, 1 : 800), or mouse anti-microtubule associated protein 2 (MAP-2, 1 : 2000). MAP-2 was used to identify neurones in cell suspensions but because this is unsuitable for doing so in intact brain tissue (staining of the neuropil masks individual cells), NeuN was used to stain the slice sections. Slides were rinsed and incubated with secondary antibodies (anti-mouse FITC and anti-sheep TRITC) for 1 h at room temperature, mounted in Vectorshield with DAPI nuclear stain, and viewed under fluorescence optics (Figs 2a–c) or laser scanning confocal microscope (Leika Microsystems, Milton Keynes, UK; Figs 2d–e).

To determine the percentage of cells that accumulated cGMP, four separate striatal cell suspensions were prepared, exposed to DEA/NO for 30 s in the presence of EHNA (300 µM) and processed for immunocytochemistry as detailed above. At least three fields containing 80–150 cells were selected at random from each slide and the number of cells that were co-stained with cGMP and the nuclei marker DAPI were counted.

Simulation of cGMP accumulation in striatal neurones

The desensitizing profile of sGC activity was originally found in cerebellar astrocytes by mathematical deconvolution of a function fitted to cGMP accumulation over time (Bellamy *et al.* 2000). Subsequently, a more detailed analysis of these cells indicated that, at its simplest, the decline in sGC activity with time due to desensitization could be described by a single exponential function (Bellamy and Garthwaite 2001a). In this study, we have tested the suitability of this model to striatal neurones by simulating the cGMP accumulation over time with a combination of an exponentially declining rate of synthesis (v_s) and a substrate-linked (Michaelis–Menten) rate of degradation (v_d). The Michaelis–Menten parameters defining v_d were found as previously described (Bellamy and Garthwaite 2001b).

The system describing rate of cGMP accumulation, can be defined thus:

$$\frac{dP}{dt} = v_s - v_d,$$

$$v_s = (ae^{-kt} + c)$$

and

$$v_d = \left(\frac{V_pP}{K_p + P}\right)$$

where P = concentration of cGMP, V_p = apparent maximal rate of degradation, and K_p = apparent Michaelis constant. The initial rate of synthesis (maximum v_s; non-desensitized sGC) = $a + c$ and the final rate (minimum v_s; desensitized sGC) = c. The constant k determines the rate at which sGC progresses from maximum to minimum activity. The time course for cGMP accumulation under these conditions was simulated with a simple custom-written programme in Microsoft VISUAL BASIC 6™ (Microsoft MSN, London, UK) and overlaid on the experimental data.

Materials

The sheep anti-cGMP was a kind gift from Dr J. de Vente (Maastricht, Netherlands). Mouse NeuN, mouse GFAP and mouse MAP-2 antibodies were purchased from Chemicon (Temecula, CA, USA); secondary antibodies and Vectorshield were purchased from Vector laboratories (Orton Southgate, Peterborough, UK). DEA/NO was from Alexis Corporation (Bingham, Nottingham, UK), L-nitroarginine was from Tocris Cookson (Bristol, UK) and sildenafil was supplied by the Chemistry Division, Wolfson Institute for Biomedical Research. All other chemicals were from Sigma-Aldrich (Poole, Dorset, UK).

Results

Accumulation of cGMP in striatal preparations

For analysing the kinetics of the NO-cGMP pathway, cell suspensions are suitable preparations to use because diffusional delays are minimized and so target cells are exposed to the same NO concentrations simultaneously, and they can be inactivated speedily. The basal cGMP level in cell suspensions from the striatum incubated in the presence of the non-selective PDE inhibitor 3-isobutyl-1-methylxanthine (IBMX; 1 mM) was 3.3 ± 0.8 pmol/10^6 cells ($n = 7$). On exposure to DEA/NO (0.03–3 µM) for 30 s a concentration-dependent accumulation of cGMP occurred, attaining a maximum of about 60 pmol/10^6 cells at 1 µM; the EC$_{50}$ was approximately 0.1 µM (Fig. 1). Immunocytochemistry on cell suspensions stimulated with 1 µM DEA/NO (in the presence of a selective PDE 2 inhibitor; see below) indicated that a minor proportion of the constituent cells (6.7 ± 1.3% of the total; four separate striatal cell suspensions) accumulated cGMP markedly in response to NO (Fig. 2b). These cells were amongst those that were immunostained with MAP-2 (Fig. 2a) but they were unstained for the astrocyte marker
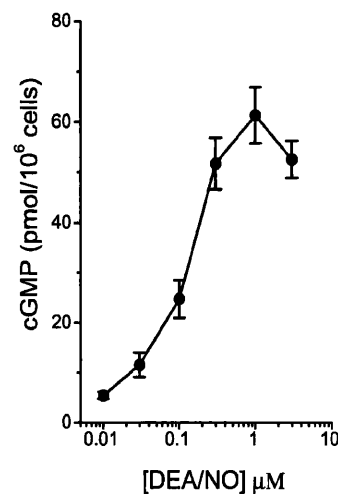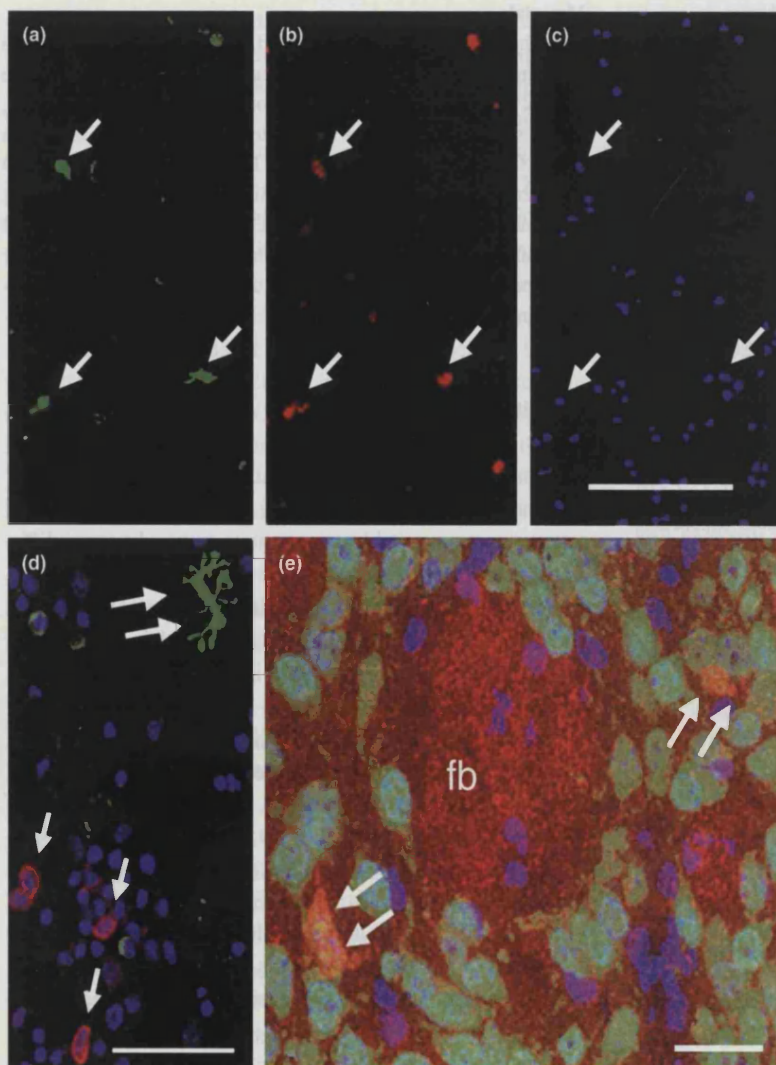

Fig. 1 Concentration-cGMP response curve for DEA/NO in striatal cell suspensions. The cells were exposed to the NO donor for 30 s in the presence of 1 mM IBMX; $n = 9$–12.

Fig. 2 Location of NO-stimulated cGMP accumulation in striatal tissue. (a–d) Striatal cell suspension following a 30-s exposure to DEA/NO (1 μм) in the presence of EHNA (300 μм) stained for MAP-2 (a) and cGMP (b); cell nuclei (DAPI stain) are shown in (c). In (d), cells are stained for GFAP (green), cGMP (red) and nuclei (blue); single arrows indicate cGMP-positive cells; double arrows indicate GFAP-positive astrocyte. (e) Immunofluorescent staining for NeuN (green) and cGMP (red) in a striatal slice exposed to DEA/NO (10 μм) for 2 min in the presence of IBMX (1 mм); co-stained cells (orange) are marked with double arrows. Nuclei are stained with DAPI (blue); fb, fibre bundle. Calibration bar = 100 μm (a–c) and 20 μm (d–e).

GFAP (Fig. 2d), indicating that the target cells were neurones. The cells accumulating cGMP were approximately spherical with a mean diameter of 7.7 ± 0.4 μm ($n = 18$). No cGMP immunostaining was observed in unstimulated cell suspensions (not shown).

To determine whether the presence of neurones responding in the cell suspensions to NO with an increase in cGMP might somehow be a non-physiological consequence of cell dissociation, checks were carried out on intact striatal slices. The mean cGMP level in unstimulated slices averaged 3.8 ± 0.5 pmol/mg protein ($n = 4$), and the level approximately doubled to 6.2 ± 0.7 pmol/mg protein ($n = 6$) after 10 min incubation with IBMX (1 mм), a response that reflects the activity of endogenous NO synthase (Griffiths *et al.* 2002). When the slices were exposed for 2 min to DEA/NO (10 μм, a maximally effective concentration; not shown) in the presence of IBMX, cGMP rose nearly 40-fold higher to 223 ± 30 pmol/mg protein ($n = 6$).
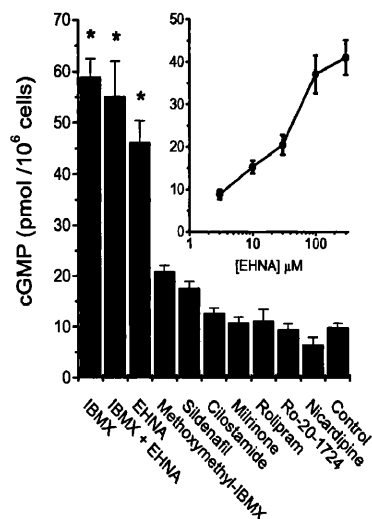
In unstimulated slices (incubated with 1 mм IBMX), no cGMP immunostaining was observed (not shown). On

exposure to 10 μм DEA/NO for 2 min high levels of cGMP staining were observed in bundles of fibres running through the striatum, and a lower level was seen in a network of varicose fibres (Fig. 2e). A small population of cell bodies stained brightly and these were identified as neurones (arrows in Fig. 2e). It is reasonable to assume that these are the same cells that respond to NO in the dissociated cell suspension.

Identification of active PDEs

So far, 11 distinct families of PDEs have been identified, with multiple isoforms each (Beavo 1995; Soderling and Beavo 2000). As the properties of the PDE are expected to participate in the shaping of cGMP signals, an attempt was made to identify the PDEs responsible for degrading cGMP in the striatal cells, using a pharmacological approach. Inhibitors selective for different families of PDE were screened by determining their ability to enhance cGMP accumulation in response to a 30-s exposure to DEA/NO (0.3 μм). In control cells (no PDE inhibitor) cGMP

accumulation was 9.8 ± 0.9 pmol/10^6 cells whereas, in the presence of the non-specific PDE inhibitor IBMX (1 mM) the response was 57 ± 4 pmol/10^6 cells. The PDE 1-selective inhibitors nicardipine (300 μM; Agullo and Garcia 1997) and 8-methoxymethyl-IBMX (300 μM; Ahn et al. 1989), the PDE 3-selective inhibitors cilostamide (100 μM; Manganiello et al. 1995) and milrinone (300 μM; Manganiello et al. 1995; Schudt et al. 1996a), the PDE 4-selective inhibitors rolipram and Ro-20–1724 (300 μM; Schudt et al. 1996b), and the PDE 5-selective inhibitor sildenafil (300 μM; Turko et al. 1999), all failed to augment cGMP accumulation significantly (Fig. 3). The only isoform-selective inhibitor that was effective was the PDE 2-selective compound erythro-9-(2-hydroxy-3-nonyl)adenine (EHNA, 300 μM; Michie et al. 1996), which elevated cGMP to levels not significantly different from those found with IBMX (Fig. 3). A concentration-response curve for EHNA (3–300 μM) indicated an apparent EC_{50} of around 30 μM and an apparent near-maximal effect at 300 μM (Fig. 3, inset) although, with a competitive inhibitor, complete inhibition cannot be achieved because of progressive competition by the build-up of cGMP. In contrast to findings in striatal slices (see above), none of the PDE inhibitors significantly influenced cGMP levels in cell suspensions not treated with DEA/NO (not shown). This presumably reflects the absence of a synaptic network in the cell suspension.
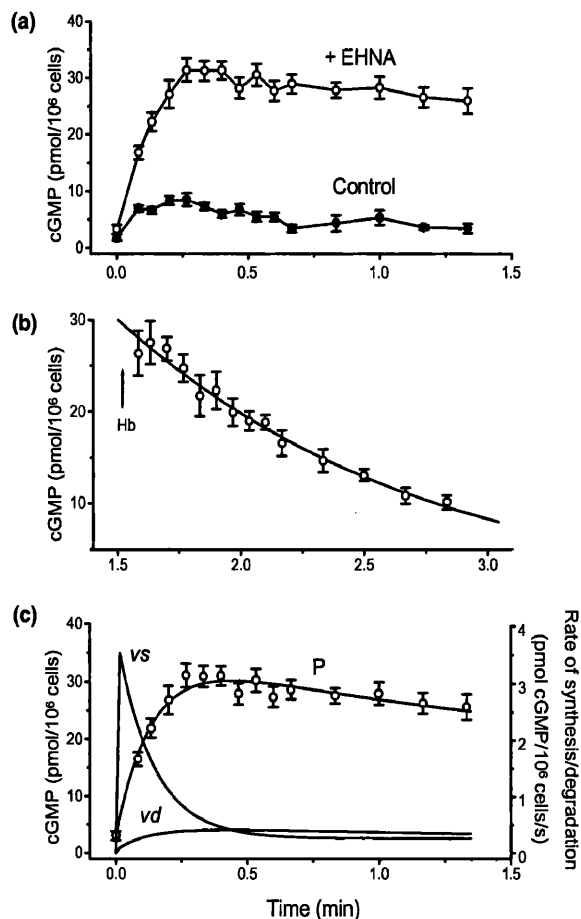
Kinetic analysis of cGMP synthesis and degradation

To investigate the kinetics of sGC and PDE in the striatal neurones, detailed time-courses of cGMP accumulation in response to a maximal concentration of DEA/NO (1 μM) were obtained in the presence and absence of EHNA (300 μM). In the presence of EHNA, cGMP rose rapidly to reach a transient plateau after 15 s (Fig. 4a). In untreated cells, the overall time course was similar but the cGMP levels throughout were much lower.

The profile of the cGMP accumulation reflects the difference between the rates of cGMP synthesis (v_s) and degradation (v_d). The first step in unravelling the contribution of v_s and v_d to the cGMP profile was to find the Michaelis–Menten parameters governing PDE activity. This was achieved by a method previously described (Bellamy and

Fig. 3 Effect of PDE inhibitors on NO-stimulated cGMP responses in striatal cell suspensions. Data are mean cGMP levels 30 s after addition of 0.3 μM DEA/NO ($n = 4$–9). All PDE inhibitors were tested at a concentration of 300 μM with the exception of IBMX (1 mM) and cilostamide (100 μM). *$p < 0.05$ versus control based on Dunnett's test. Inset: Concentration-response curve for EHNA on DEA/NO-stimulated cGMP accumulation ($n = 3$).

Fig. 4 Kinetic analysis of cGMP synthesis and degradation in striatal cell suspension. (a) Time courses of cGMP accumulation induced by DEA/NO (1 μM) in the presence (O) and absence (●) of the PDE inhibitor EHNA (300 μM; $n = 6$–7). (b) Decay of cGMP after addition of haemoglobin (10 μM) to striatal cells exposed to DEA/NO (1 μM) in the presence of EHNA ($n = 5$), fitted by the Michaelis–Menten equation. (c) Data for cGMP accumulation (o) from (a), are fitted assuming an exponentially declining rate of synthesis (v_s) and a rate of degradation (v_d) calculated from the Michaelis–Menten parameters obtained from the fit to the data in (b).

Garthwaite 2001b) wherein the NO-scavenging ability of haemoglobin (Hb) was exploited to arrest sGC activity abruptly following a 1-min exposure of cells to 1 μM DEA/ NO. After addition of Hb, cGMP synthesis ceases with a half-time of around 200 ms (Bellamy and Garthwaite 2001a) and the cGMP concentration in the cells then falls due to the action of PDEs. From the time course of the cGMP decline, the parameters defining PDE activity (i.e. the apparent Michaelis constant, K_p, and maximal velocity, V_p) can be found by iteration (Fernley 1974), allowing PDE activity to be calculated for any given level of cGMP.

In the striatal cells, PDE activity was too rapid to be discernible by this strategy in the absence of PDE inhibitors (see below). In the presence of 300 μM EHNA the decline in cGMP was greatly slowed, though not eliminated. The cGMP decline under these conditions could be satisfactorily fitted with the Michaelis–Menten equation (Fig. 4b) allowing the rate of cGMP degradation over the time-course of cGMP accumulation to be defined (Fig. 4c).

Earlier studies using cerebellar cell suspensions stimulated with NO have suggested that sGC activity declines exponentially with time, reflecting desensitization (Bellamy *et al.* 2000; Bellamy and Garthwaite 2001a). The suitability of this model in the striatal cell preparations was evaluated by simulating the cGMP responses to NO with an exponentially falling v_s and Michaelis–Menten-type degradation kinetics (see Experimental procedures). The simulations were over-laid on experimental data and provided a close fit to the cGMP accumulation in cells incubated with EHNA (Fig. 4c). The derived v_s was initially 3.5 pmol cGMP/10^6 cells/s and then it declined progressively to a 13-fold lower rate (0.26 pmol cGMP/10^6 cells/s) within around 30 s ($n = 7$). This is similar to the profile derived from rat cerebellar cells (Bellamy *et al.* 2000) suggesting that sGC expressed in the striatal neurones exhibits similar kinetics to the enzyme in cerebellar astrocytes.

Given the profile of sGC activity under conditions of PDE inhibition, the model can then be used to investigate if the profile of cGMP accumulation observed under control conditions (where the parameters for cGMP degradation cannot be measured directly) can be predicted. The simplest case is to assume that v_s is identical but v_d is enhanced in the absence of EHNA. However, when this situation was modelled by reducing the Michaelis–Menten parameter K_p (to simulate loss of a competitive inhibitor), no good fit was obtained regardless of the K_p value used (Fig. 5a).

One explanation for the inaccurate simulation is that some of the measured cGMP is not vulnerable to hydrolysis by PDE (e.g. due to export from the cell). To test this, Hb was added to arrest sGC activity 16 and 80 s after adding DEA/ NO (i.e. at the peak and plateau stages of the time course). At both times, cGMP declined rapidly to basal levels, indicating that it was subject to degradation by PDE throughout (Fig. 5b).
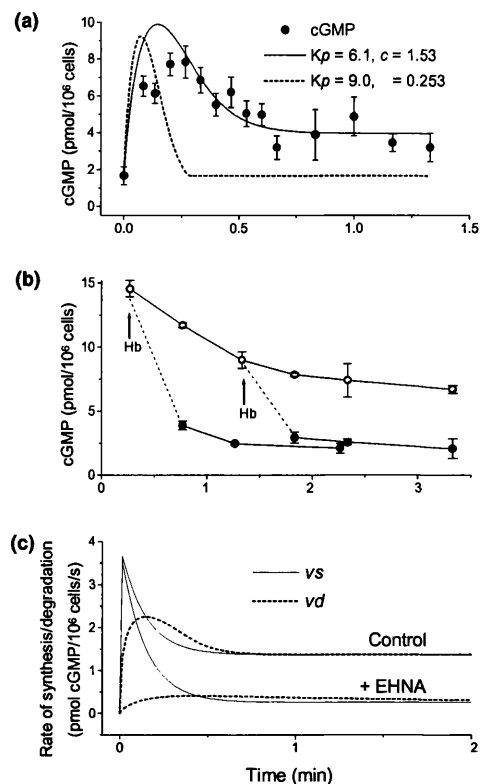
Fig. 5 Kinetic analysis of cGMP accumulation in the absence of PDE inhibition. (a) Data for the cGMP response to DEA/NO (●) are taken from Fig. 4(a). The broken line shows the best fit achieved by taking the profile of cGMP synthesis (v_s) and the value of the apparent maximal rate of cGMP degradation (V_p) giving the fit to the data in Fig. 4(c), but decreasing the apparent Michaelis constant (K_p) for cGMP degradation (corresponding to removal of a competitive inhibitor). Solid line shows the better fit obtained by altering both K_p and the maximum level of sGC desensitization (see Experimental procedures). (b) Vulnerability of cGMP to PDE activity. During the normal response to 1 μM DEA/NO (○), Hb (10 μM) was added (arrows) and cGMP levels subsequently followed (●); $n = 4$–6. (c) Comparison of the profiles of cGMP synthesis (v_s) and degradation (v_d) providing the best fits to experimental data obtained in the absence and presence of EHNA.

Consequently, in contrast to findings on cerebellar cells (Bellamy *et al.* 2000), the model fails to predict the control profile of cGMP accumulation. There are two simple reasons why the model may be inaccurate: if PDE activity does not follow simple Michaelis–Menten kinetics, or if sGC activity does not vary in an identical manner in the presence and absence of PDE inhibition. The former suggestion is not supported by the experimental data. First, the decline in cGMP after addition of Hb to EHNA-treated cells was well described by the Michaelis–Menten equation (Fig. 4b). It could be argued that at the lower levels of cellular cGMP attained under control conditions, the PDE activity could be lower than predicted, or it may change with time such that the value of v_d is initially high, but then falls to a lower level

during the steady-state cGMP plateau. However, the rapid fall in cGMP taking place when Hb was added during the plateau (Fig. 5b) indicates that PDE activity is (immeasurably) high. It follows that in order to maintain a steady-state cGMP concentration, sGC activity must remain equally high. This line of reasoning points us towards the alternate hypothesis, namely that the profile of sGC activity varies according to whether PDE is active or inhibited. In other words, sGC may not desensitize to the same degree under control conditions as when EHNA is present. This scenario can be simulated by increasing the minimum rate of cGMP synthesis to which sGC desensitizes (the constant 'c', see Experimental procedures). Such a situation provided a greatly improved fit to the experimental data (solid line, Fig. 5a), the profile of sGC activity generating the best fit being desensitization to a level a little over 50% of the peak activity instead of by more than 90% in the presence of EHNA (Fig. 5c).

Possible role of cGMP in sGC desensitization

The mechanism of sGC desensitization is not yet known. One possible reason for a lower degree of desensitization when PDE is not inhibited is that the cGMP concentration governs the degree of sGC desensitization. A way of examining this is to study the contrary property: recovery from desensitization.

The principle of the experiment is to activate sGC with DEA/NO for 2 min, and then deactivate sGC as usual with Hb. At the point of deactivation, sGC will be desensitized, and intracellular cGMP will be elevated. The concentration of cGMP subsequently falls. At various periods following deactivation, DEA/NO is reapplied at a concentration sufficient to overwhelm the Hb quench and reactivate sGC. The degree of recovery of sGC from desensitization (i.e. resensitization) can be deduced from the initial rate of cGMP accumulation after reapplication of DEA/NO.

This experiment is not feasible in striatal cells because the PDE activity is much too high, but it can be carried out in cerebellar cells where PDE activity is lower (Bellamy et al. 2000). In these cells, exposure to 1 μM DEA/NO led to cGMP accumulating to a plateau after 2 min, as before (Fig. 6a). Addition of Hb then triggered a decline in cGMP to basal levels that was fitted well by the Michaelis–Menten equation throughout the 10 min time course. Reapplication of DEA/NO (100 μM) after various intervals caused cGMP to accumulate once more and the rate of accumulation increased with increasing delays between sGC deactivation and reactivation. Complete resensitization occurred 8 min after deactivation (Fig. 6b), coincident with cGMP returning to basal levels. Analysis of the mean initial rate of cGMP accumulation 30 s after reactivation revealed that resensitization occurred with a half-time of around 1.5 min (Fig. 6a, inset).

To investigate if the resensitization rate was simply determined by the recovery time, or whether it was related mechanistically to the decline in cGMP concentration, the
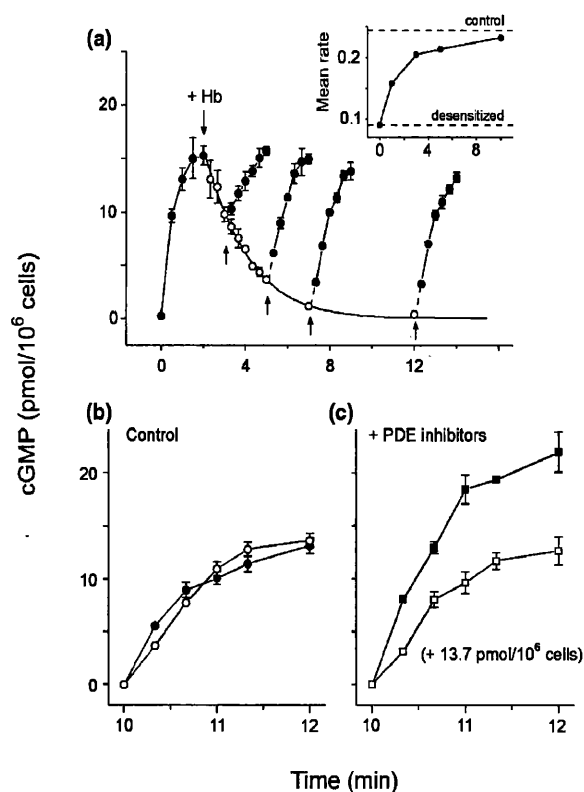
Fig. 6 Recovery of sGC from desensitization is linked to cGMP levels in cerebellar cells. (a) Cells were treated with 1 μM DEA/NO for 2 min to evoke sGC desensitization (●), before addition of 10 μM Hb (descending arrow). The subsequent decline in cGMP (O) was fitted with Michaelis–Menten kinetics (line). After various periods, DEA/NO was re-applied (ascending arrows) in a concentration (100 μM) producing sufficient NO to overcome the capacity of the haemoglobin. Inset, rate of recovery from desensitization expressed as mean rate 30 s after addition of 100 μM DEA/NO against time (min) after haemoglobin addition. (b) After 8 min following haemoglobin addition, cGMP has returned to basal levels, and the profile of cellular cGMP accumulation in response to 100 μM DEA/NO (O) is indistinguishable from control (●). (c) Cells preincubated with PDE inhibitors (300 μM sildenafil + 1 μM rolipram) retain elevated cGMP levels (13.7 pmol/10^6 cells) 8 min after haemoglobin addition, and the cGMP response to maximal DEA/NO (□) is decreased relative to control (■).

experiment was repeated in the presence of the appropriate PDE inhibitors (300 μM sildenafil and 1 μM rolipram). As expected, the decline in cGMP level following deactivation of sGC was slowed, such that after 8 min cGMP now remained elevated well above basal levels (13.7 ± 0.31 pmol/10^6 cells; $n = 3$). A time course of cGMP accumulation obtained at this point revealed that the rate and magnitude of the response was markedly reduced compared to control (Fig. 6c).

A role for (de)phosphorylation?

cGMP-dependent protein kinase (PKG) inhibits sGC activity in bovine chromaffin cells apparently via activation of

phosphatases (Ferrero *et al.* 2000) and changes in phosphorylation state are commonly utilized as a mechanism for receptor desensitization, including for the related membrane-bound guanylyl cyclases (Potter and Garbers 1994). Inhibition of sGC desensitization would be manifest as an accumulation of cGMP that is more linear with time and that becomes progressively larger than that observed in control cells. However, when cerebellar cells were incubated with a selective PKG inhibitor (KT5823), a broad-spectrum kinase inhibitor (staurosporine) or a broad-spectrum phosphatase inhibitor (calyculin A), the cGMP response to DEA/NO was not significantly affected at any time point examined (0, 20 s, 40 s, 1 min, 1.5 min and 2 min). Values for the 2 min time point, when any effect of increased sGC activity would have been greatest, are given in Table 1. The absence of any effect on cGMP accumulation could mask a balanced increase in both sGC and PDE activity. To test the effects of the inhibitors on PDE activity, Hb was added after 2 min stimulation with DEA/NO and cGMP levels measured 3 min later. In control cells, about 75% of the accumulated cGMP was hydrolysed during this period (Table 1), in agreement with other data (Fig. 6a). Calyculin or KT5823 had no effect on the residual cGMP whereas staurosporine increased it, suggesting PDE was inhibited to the extent that the proportion of cGMP hydrolysed (40%) was about half that observed in control cells (Table 1). This result is consistent with a recent report that the activity of PDE 5, which is the major PDE in the cerebellar cells (Bellamy and Garthwaite 2001b), is enhanced by phosphorylation (Mullershausen *et al.* 2001).

Discussion

This investigation of NO-cGMP signalling in the striatum has permitted the first analysis of the kinetics of this pathway in neuronal cells. Whilst there were some similarities with

Table 1 Effect of kinase and phosphatase inhibition on NO-evoked cGMP accumulation and PDE activity in cerebellar cell suspension

Inhibitor (1 μM)	cGMP accumulated	cGMP remaining 3 min after haemoglobin
None	16.3 ± 1.1 (16)	4.3 ± 0.3 (7)
KT5823	16.2 ± 0.8 (5)	4.8 ± 0.3 (2)[a]
Staurosporine	18.5 ± 1.4 (9)	11.2 ± 0.8 (6)*
Calyculin A	17.5 ± 1.1 (7)	3.5 ± 0.3 (4)

The inhibitors were added 10 min before addition of 1 μM DEA/NO. After a further 2 min, either the cells were inactivated and the accumulation of cGMP measured, or else haemoglobin (10 μM) was added to remove free NO and the cGMP level determined 3 min afterwards. Data are mean cGMP levels (pmol/mg protein) ± SEM or [a]SD. The numbers of independent determinations are given in parentheses. *$p < 0.05$ versus control (no inhibitor).

what had been observed previously in cerebellar cells, in which astrocytes are the target for NO, the several differences observed in the neurones are consistent with the idea that cell-to-cell variations in the sGC-cGMP section of the pathway can generate diverse outputs in response to a common incoming NO signal.

The general location of NO-stimulated cGMP in the striatal slices was similar to that reported before (Markerink-van Ittersum *et al.* 1997). The loss of the fibres on cell dissociation resulted in a subpopulation of cGMP-responsive cells, identified as neurones, being present in the cell suspensions. These are presumed to be the same neurones that were cGMP- and NeuN-positive in the intact slices. Their exact identity remains unknown but for the present purposes, given the restricted range of cell sizes, the similar intensities of cGMP immunostaining, and the absence of evidence for more than one PDE isoform at work, it is reasonable to treat them as a single population.

The first notable difference compared with cerebellar astrocytes is the PDE isoform that degrades the cGMP generated in response to NO. In the astrocytes, the predominant PDE is sensitive to sildenafil and zaprinast, suggesting it to be PDE 5 (Bellamy and Garthwaite 2001b), whereas in the striatal neurones, the effectiveness of EHNA indicated that PDE 2 performed this role. An EHNA-sensitive isoform also appears to participate importantly in cGMP hydrolysis in hippocampal slices stimulated with NO (van Staveren *et al.* 2001). PDE 2 is a cGMP-stimulated enzyme capable of hydrolysing both cGMP and cAMP. The affinities are similar (10 and 30 μM, respectively), as are the maximal velocities (Juilfs *et al.* 1999). In purified PDE 2 preparations, cGMP in submicromolar concentrations stimulates cAMP hydrolysis up to 50-fold suggesting that one function is to mediate cross-talk between cGMP- and cAMP-regulated pathways (Juilfs *et al.* 1999).

As there remained appreciable PDE activity in the striatal cells in the presence of a maximally effective EHNA concentration, it is possible that another isoform also participates. The pharmacological tests carried out suggested that PDE 1, 3, 4 and 5 are not significantly involved. Of those that are left, PDE 6 is apparently confined to the retina (Beavo 1995), PDE 7 and PDE 8 are selective for cAMP (Sasaki *et al.* 2000; Soderling and Beavo 2000), and PDE 11A appears to have little or no expression in the CNS (Yuasa *et al.* 2001). PDE 9A and 10A are found in the brain (Fujishige *et al.* 1999; Andreeva *et al.* 2001) and can hydrolyse cGMP but the lack of selective inhibitors makes their role difficult to evaluate. The residual PDE activity in the presence of high EHNA concentrations may alternatively be explained by the fact that the effectiveness of a competitive PDE inhibitor is inherently self-limiting: the more the inhibition, the more the inhibitor will be out-competed by the attendant build up of the cyclic nucleotide.

Another obvious difference between the cerebellar astrocytes and the target striatal neurones is the activity of the PDE. Thus, in the former, maximal PDE inhibition has relatively little effect on cGMP accumulation over the first minute or so of sGC stimulation (Bellamy et al. 2000) whereas in the striatal cells a large difference over the first 15 s was observed. To illustrate this quantitatively, the parameter V_p/K_p can be used as a measure of catalytic efficiency. From the simulation (Fig. 5a), the Michaelis–Menten parameters that best describe the cGMP profile in control cells are $V_p = 3.76$ pmol/10^6 cells/s, $K_p = 6.10$ pmol/10^6 cells. Thus V_p/K_p is 0.616 s^{-1}, a value 56-fold greater than for cerebellar astrocytes (Bellamy and Garthwaite 2001b).

Where the striatal neurones appeared similar to cerebellar astrocytes was in the desensitizing profile of sGC activity. Thus, analysis of the cGMP accumulation curve in the striatal cells in the presence of EHNA suggested that on addition of NO, sGC activity fell progressively over 30 s to a final rate of less than 10% of the initial activity. Interestingly, sGC desensitization is not seen in homogenized tissue or with the purified enzyme suggesting that it is not an intrinsic property of the protein but requires a cellular factor. Currently, the factor is unknown and there is very little information about its properties, although desensitization does appear to be NO concentration-dependent, at least at supramaximal NO concentrations (Bellamy and Garthwaite 2001b).

In the original description of this phenomenon (Bellamy et al. 2000), simply taking the profile of sGC activity derived in platelets when PDE was inhibited and applying it to a situation of normal PDE activity provided a good approximation of the experimental data. In the striatal neurones, however, the same strategy failed, demonstrating that this model of desensitization is an oversimplification. From simulations, a good approximation of the data could be obtained by linking the degree of sGC desensitization to the cGMP level so that sGC desensitization becomes less pronounced in normal neurones than in EHNA-treated neurones (where cGMP levels were fourfold higher). That the product of receptor or enzyme activity provides feedback inhibition is common in biology, and so it is an attractive mechanism to apply to sGC. The inability to study sGC desensitization in homogenates, however, makes it difficult to test in this case. As an alternative, we investigated NO-stimulated sGC activity during recovery from desensitization, at different starting cGMP levels. In the cells (cerebellar cells for convenience), the evidence suggested that the initial rate of sGC activity was inversely correlated with cGMP levels. Moreover, deliberately slowing down the decline in cGMP levels by PDE inhibition slowed down recovery of sGC activity. Thus, cGMP appears to maintain sGC in its desensitized state and therefore could also initiate and regulate the extent of desensitization, a hypothesis that would be compatible with the data on striatal cells. If so, an

additional factor would be necessary, because cGMP itself (up to 1 mM) does not inhibit purified sGC activity (Lee et al. 2000). Thus, sGC desensitization may be triggered by a build-up of cGMP, which acts through an inhibitory factor(s).

Interestingly, Mullerhausen et al. (2001) recently suggested that application of the sGC activity profile obtained in the presence of PDE inhibitors to the normal cGMP response is also inappropriate. They demonstrated that, in normal platelets, sGC remains similarly active throughout the time course of NO exposure, indicating lack of sGC desensitization. Evidence was obtained that the sag in the cGMP response that takes place with time was instead associated with up-regulation of PDE 5 activity, although no quantitative analysis was performed. Furthermore, it was speculated that the desensitizing profile of sGC activity observed in the presence of PDE inhibitors could be due to depletion of intraplatelet GTP levels, thus starving sGC of substrate. In cerebellar cells, however, we have shown that sGC desensitization is unaffected by wide variations in GTP utilization (Bellamy et al. 2000). Furthermore, for GTP depletion to account for the observed 90% reduction in sGC activity occurring on full desensitization, the intracellular GTP concentration would have to fall to around 3 μM, assuming the K_m of sGC to be 30 μM (Lewicki et al. 1982). From Mullerhausen et al. (2001), however, it appears that in platelets exposed to an NO donor in the presence of PDE inhibitors, there is still about 350 μM GTP, a concentration sufficient to sustain cGMP synthesis at near maximal possible rates.

Instead, the lack of sGC desensitization in normal platelets (no PDE inhibitor) observed by Mullerhausen et al. (2001) could be explained on the basis of the hypothesis proposed here, namely that cGMP regulates desensitization. In fact, this hypothesis explains all the data obtained so far in the three cell types examined. Thus, in normal platelets, cGMP levels are negligible following the short-lived peak and there is minimal sGC desensitization (Mullerhausen et al. 2001). In the normal striatal neurones, cGMP levels are intermediate and a model of intermediate desensitization fits the experimental data (Fig. 5a). In cerebellar astrocytes cGMP levels are high, and desensitization is pronounced (Bellamy et al. 2000). Finally, when PDE inhibitors are added to drive cGMP to high levels in platelets and striatal neurones, desensitization of sGC is substantial and similar in extent to that observed in cerebellar astrocytes in the absence of PDE inhibitors. Whilst the hypothesis accommodates the available data, it cannot be excluded that alterations in PDE activity with time (Mullerhausen et al. 2001) may also shape cGMP responses in some cells.

Concerning the identity of the desensitizing factor, an obvious candidate would be PKG. However, the profile of cGMP accumulation was unaffected by two different inhibitors of this enzyme, or by a phosphatase inhibitor. This, together with evidence that the inhibitors did not increase

PDE activity, suggests that protein phosphorylation or dephosphorylation are unlikely to be responsible for sGC desensitization. By analogy with other receptors, and with adenylyl cyclases and other guanylyl cyclases (Chern 2000), there may be multiple sGC-regulating factors awaiting identification and they may be different in different cells.

Acknowledgements

References

Agullo L. and Garcia A. (1997) Ca^{2+}/calmodulin-dependent cyclic GMP phosphodiesterase activity in granule neurons and astrocytes from rat cerebellum. *Eur. J. Pharmacol.* **323**, 119–125.

Ahn H. S., Crim W., Romano M., Sybertz E. and Pitts B. (1989) Effects of selective inhibitors on cyclic nucleotide phosphodiesterases of rabbit aorta. *Biochem. Pharmacol.* **38**, 3331–3339.

Almeida A., Heales S. J., Bolanos J. P. and Medina J. M. (1998) Glutamate neurotoxicity is associated with nitric oxide-mediated mitochondrial dysfunction and glutathione depletion. *Brain Res.* **790**, 209–216.

Andreeva S. G., Dikkes P., Epstein P. M. and Rosenberg P. A. (2001) Expression of cGMP-specific phosphodiesterase 9A mRNA in the rat brain. *J. Neurosci.* **21**, 9068–9076.

Beavo J. A. (1995) Cyclic nucleotide phosphodiesterases: functional implications of multiple isoforms. *Physiol. Rev.* **75**, 725–748.

Bellamy T. C. and Garthwaite J. (2001a) Sub-second kinetics of the nitric oxide receptor, soluble guanylyl cyclase, in intact cerebellar cells. *J. Biol. Chem.* **276**, 4287–4292.

Bellamy T. C. and Garthwaite J. (2001b) 'cAMP-specific' phosphodiesterase contributes to cGMP degradation in cerebellar cells exposed to nitric oxide. *Mol. Pharmacol.* **59**, 54–61.

Bellamy T. C., Wood J., Goodwin D. A. and Garthwaite J. (2000) Rapid desensitization of the nitric oxide receptor, soluble guanylyl cyclase, underlies diversity of cellular cGMP responses. *Proc. Natl Acad. Sci. USA* **97**, 2928–2933.

Calabresi P., Gubellini P., Centonze D., Sancesario G., Morello M., Giorgi M., Pisani A. and Bernardi G. (1999) A critical role of the nitric oxide/cGMP pathway in corticostriatal long-term depression. *J. Neurosci.* **19**, 2489–2499.

Centonze D., Pisani A., Bonsi P., Giacomini P., Bernardi G. and Calabresi P. (2001) Stimulation of nitric oxide-cGMP pathway excites striatal cholinergic interneurons via protein kinase G activation. *J. Neurosci.* **21**, 1393–1400.

Chern Y. (2000) Regulation of adenylyl cyclase in the central nervous system. *Cell. Signal.* **12**, 195–204.

Cherry J. A. and Davis R. L. (1999) Cyclic AMP phosphodiesterases are localized in regions of the mouse brain associated with reinforcement, movement, and affect. *J. Comp. Neurol.* **407**, 287–301.

Contestabile A. (2000) Roles of NMDA receptor activity and nitric oxide production in brain development. *Brain Res. Rev.* **32**, 476–509.

Dawson V. L., Dawson T. M., London E. D., Bredt D. S. and Snyder S. H. (1991) Nitric oxide mediates glutamate neurotoxicity in primary cortical cultures. *Proc. Natl Acad. Sci. USA* **88**, 6368–6371.

East S. J., Parry-Jones A. and Brotchie J. M. (1996) Ionotropic glutamate receptors and nitric oxide synthesis in the rat striatum. *Neuroreport* **8**, 71–75.

Fernley H. N. (1974) Statistical estimations in enzyme kinetics. The integrated Michaelis equation. *Eur. J. Biochem.* **43**, 377–378.

Ferrero R., Rodriguez-Pascual F., Miras-Portugal M. T. and Torres M. (2000) Nitric oxide-sensitive guanylyl cyclase activity inhibition through cyclic GMP-dependent dephosphorylation. *J. Neurochem.* **75**, 2029–2039.

Fujishige K., Kotera J. and Omori K. (1999) Striatum- and testis-specific phosphodiesterase PDE10A. *Eur. J. Biochem.* **266**, 1118–1127.

Furuyama T., Inagaki S. and Takagi H. (1993) Localizations of $\alpha 1$ and $\beta 1$ subunits of soluble guanylate cyclase in the rat brain. *Brain Res. Mol. Brain Res.* **20**, 335–344.

Garthwaite J. (1985) Cellular uptake disguises action of L-glutamate on *N*-methyl-D-aspartate receptors. *Br. J. Pharmacol.* **85**, 297–307.

Garthwaite J. (1991) Glutamate, nitric oxide and cell-cell signalling in the nervous system. *Trends Neurosci.* **14**, 60–67.

Garthwaite J. (2000) The physiological roles of nitric oxide in the central nervous system, in *Handbook of Experimental Pharmacology*, vol. 143 (Mayer B., ed.), pp. 259–275. Springer, Berlin.

Garthwaite J. and Garthwaite G. (1987) Cellular origins of cyclic GMP responses to excitatory amino acid receptor agonists in rat cerebellum *in vitro*. *J. Neurochem.* **48**, 29–39.

Gibb B. J. and Garthwaite J. (2001) Subunits of the nitric oxide receptor, soluble guanylyl cyclase, expressed in rat brain. *Eur. J. Neurosci.* **13**, 539–544.

Greenberg L. H., Troyer E., Ferrendelli J. A. and Weiss B. (1978) Enzymic regulation of the concentration of cyclic GMP in mouse brain. *Neuropharmacology* **17**, 737–745.

Griffiths C., Garthwaite J., Goodwin D. A. and Garthwaite J. (2002) Dynamics of nitric oxide during simulated ischaemia-reperfusion in rat striatal slices measured using an intrinsic biosensor, soluble guanylyl cyclase. *Eur. J. Neurosci.* **15**, 962–968.

Juilfs D. M., Soderling S., Burns F. and Beavo J. A. (1999) Cyclic GMP as substrate and regulator of cyclic nucleotide phosphodiesterases (PDEs). *Rev. Physiol. Biochem. Pharmacol.* **135**, 67–104.

Lee Y. C., Martin E. and Murad F. (2000) Human recombinant soluble guanylyl cyclase: expression, purification, and regulation. *Proc. Natl Acad. Sci. USA* **97**, 10763–10768.

Lewicki J. A., Brandwein H. J., Mittal C. K., Arnold W. P. and Murad F. (1982) Properties of purified soluble guanylate cyclase activated by nitric oxide and sodium nitroprusside. *J. Cyclic Nucleotide Res.* **8**, 17–25.

Manganiello V. C., Taira M., Degerman E. and Belfrage P. (1995) Type III cGMP-inhibited cyclic nucleotide phosphodiesterases (PDE3 gene family). *Cell. Signal.* **7**, 445–455.

Markerink-van Ittersum M., Steinbusch H. W. and de Vente J. (1997) Region-specific developmental patterns of atrial natriuretic factor- and nitric oxide-activated guanylyl cyclases in the postnatal frontal rat brain. *Neuroscience* **78**, 571–587.

Michie A. M., Lobban M., Muller T., Harnett M. M. and Houslay M. D. (1996) Rapid regulation of PDE-2 and PDE-4 cyclic AMP phosphodiesterase activity following ligation of the T cell antigen receptor on thymocytes: analysis using the selective inhibitors erythro-9-(2-hydroxy-3-nonyl)-adenine (EHNA) and rolipram. *Cell. Signal.* **8**, 97–110.

Mullershausen F., Russwurm M., Thompson W. J., Liu L., Koesling D. and Friebe A. (2001) Rapid nitric oxide-induced desensitization of the cGMP response is caused by increased activity of phosphodiesterase type 5 paralleled by phosphorylation of the enzyme. *J. Cell. Biol.* **155**, 271–278.

Polli J. W. and Kincaid R. L. (1994) Expression of a calmodulin-dependent phosphodiesterase isoform (PDE1B1) correlates with

brain regions having extensive dopaminergic innervation. *J. Neurosci.* **14**, 1251–1261.

Potter L. R. and Garbers D. L. (1994) Protein kinase C-dependent desensitization of the atrial natriuretic peptide receptor is mediated by dephosphorylation. *J. Biol. Chem.* **269**, 14636–14642.

Prast H. and Philippu A. (2001) Nitric oxide as modulator of neuronal function. *Prog. Neurobiol.* **64**, 51–68.

Reinhardt R. R. and Bondy C. A. (1996) Differential cellular pattern of gene expression for two distinct cGMP-inhibited cyclic nucleotide phosphodiesterases in developing and mature rat brain. *Neuroscience* **72**, 567–578.

Sasaki T., Kotera J., Yuasa K. and Omori K. (2000) Identification of human PDE7B, a cAMP-specific phosphodiesterase. *Biochem. Biophys. Res. Commun.* **271**, 575–583.

Schudt D. A., Dent G. and Rabe K. F. (1996a) cGMP-inhibitied phosphodiesterases (PDE-3), in *Phosphodiesterase Inhibitors*, pp. 89–109. Academic Press, London, UK.

Schudt D. A., Dent G. and Rabe K. F. (1996b) Interaction of PDE4 inhibitors with enzymes, in *Phosphodiesterase Inhibitors*, pp. 110–126. Academic Press, London, UK.

Soderling S. H. and Beavo J. A. (2000) Regulation of cAMP and cGMP signaling: new phosphodiesterases and new functions. *Curr. Opin. Cell Biol.* **12**, 174–179.

Southam E. and Garthwaite J. (1993) The nitric oxide-cyclic GMP signalling pathway in rat brain. *Neuropharmacology* **32**, 1267–1277.

van Staveren W. C., Markerink-van Ittersum M., Steinbusch H. W. and de Vente J. (2001) The effects of phosphodiesterase inhibition on cyclic GMP and cyclic AMP accumulation in the hippocampus of the rat. *Brain Res.* **888**, 275–286.

Trabace L. and Kendrick K. M. (2000) Nitric oxide can differentially modulate striatal neurotransmitter concentrations via soluble guanylate cyclase and peroxynitrite formation. *J. Neurochem.* **75**, 1664–1674.

Turko I. V., Ballard S. A., Francis S. H. and Corbin J. D. (1999) Inhibition of cyclic GMP-binding cyclic GMP-specific phosphodiesterase (Type 5) by sildenafil and related compounds. *Mol. Pharmacol.* **56**, 124–130.

Vincent S. R. and Kimura H. (1992) Histochemical mapping of nitric oxide synthase in the rat brain. *Neuroscience* **46**, 755–784.

Yan C., Bentley J. K., Sonnenburg W. K. and Beavo J. A. (1994) Differential expression of the 61 kDa and 63 kDa calmodulin-dependent phosphodiesterases in the mouse brain. *J. Neurosci.* **14**, 973–984.

Yuasa K., Ohgaru T., Asahina M. and Omori K. (2001) Identification of rat cyclic nucleotide phosphodiesterase 11A (PDE11A) Comparison of rat and human PDE11A splicing variants. *Eur. J. Biochem.* **268**, 4440–4448.

Properties of NO-activated guanylyl cyclases expressed in cells

[1]Barry J. Gibb, [1]Victoria Wykes & *,[1]John Garthwaite

[1]The Wolfson Institute for Biomedical Research, University College London, Gower Street, London WC1E 6BT

1 Physiological nitric oxide (NO) signal transduction occurs through activation of guanylyl cyclase (GC)-coupled receptors, resulting in cGMP accumulation. There are five possible receptors: four heterodimers ($\alpha1\beta1$, $\alpha2\beta1$, $\alpha1\beta2$, $\alpha2\beta2$) and a presumed homodimer ($v\beta2$). The present study investigated the kinetic and pharmacological properties of all these putative receptors expressed in COS-7 (or HeLa) cells.

2 All exhibited NO-activated GC activity, that of $\alpha1\beta1$ and $\alpha2\beta1$ being much higher than that of the $\beta2$-containing heterodimers or $v\beta2$. All were highly sensitive NO detectors. Using clamped NO concentrations, EC_{50} values were 1 nM for $\alpha1\beta1$ and 2 nM for $\alpha2\beta1$. With $\alpha1\beta2$, $\alpha2\beta2$ and $v\beta2$, the EC_{50} was estimated to be lower, about 8 nM.

3 All the GCs displayed a marked desensitising profile of activity. Consistent with this property, the concentration–response curves were bell-shaped, particularly those of the $\beta2$ heterodimers and $v\beta2$.

4 Confocal microscopy of cells transfected with the fluorescently tagged $\beta2$ subunit suggested targeting to the endoplasmic reticulum through its isoprenylation sequence, but no associated particulate GC activity was detected.

5 The NO-stimulated GC activity of all heterodimers and $v\beta2$ was inhibited by 1H-[1,2,4]oxadiazolo[4,3-a]quinoxalin-1-one and, except for $v\beta2$, was enhanced by the allosteric activator YC-1.

6 It is concluded that all the four possible heterodimers, as well as the putative $v\beta2$ homodimer, can function as high-affinity GC-coupled NO receptors when expressed in cells. They exhibit differences in NO potency, maximal GC activity, desensitisation kinetics and possibly subcellular location but, except for $v\beta2$, cannot be differentiated using existing pharmacological agents.
British Journal of Pharmacology (2003) **139**, 1032–1040. doi:10.1038/sj.bjp.0705318

Introduction

Nitric oxide (NO) functions as a diffusible messenger in almost all tissues and exerts most of its physiological effects by binding to its guanylyl cyclase (GC)-coupled receptors ($NO_{GC}Rs$). The ligand-binding site on the receptors is a specialised haem group, the occupation of which results in conformational changes that trigger GC activity and so the generation of cGMP from GTP. The ensuing accumulation of cGMP then engages various downstream targets, including protein kinases, phosphodiesterases and ion channels to bring about changes in cell function, such as smooth muscle relaxation, platelet disaggregation and synaptic plasticity (Mayer, 2000).

$NO_{GC}Rs$ appear to exist predominantly as heterodimers comprising one α and one β subunit, with the haem prosthetic group being attached to a histidine residue on the β subunit (Denninger & Marletta, 1999; Koesling & Friebe, 2000). Two types of α and two β subunits have so far been identified, providing a possible four different isoforms ($\alpha1\beta1$, $\alpha2\beta1$, $\alpha1\beta2$ and $\alpha2\beta2$). Only two have hitherto been shown to exist *in vivo* at the protein level: $\alpha1\beta1$, which is expressed widely and $\alpha2\beta1$,

which was originally identified in human placenta but which has now also been found in rat brain where it associates with synaptic scaffold proteins (Russwurm *et al.*, 2001). At the mRNA level, the $\alpha2$ subunit is widely expressed in the brain with a particular concentration in the cerebellum and hippocampus (Gibb & Garthwaite, 2001), two regions in which the NO-cGMP pathway contributes prominently to synaptic plasticity (Garthwaite, 2000). When studied as purified proteins, the $\alpha1\beta1$ and $\alpha2\beta1$ isoforms have appeared similar in terms of their maximal activity, sensitivity to the NO donor diethylamine/NO adduct (DEA/NO) and pharmacological characteristics (Russwurm *et al.*, 1998). Measured in this way, however, the potency of DEA/NO is a poor indicator of sensitivity to NO (Bellamy *et al.*, 2002) and so neither the absolute nor relative potencies of NO on the two receptors can be deduced from the results.

The $\beta2$ subunit has remained enigmatic. The cDNA was first identified in the kidney with lesser amounts in the liver (Yuen *et al.*, 1990), but recently $\beta2$ mRNA was also detected in the brain (Gibb & Garthwaite, 2001). Several attempts to obtain NO-stimulated GC activity in cells transfected with $\beta2$ together with other subunits have apparently been unsuccessful (Denninger & Marletta, 1999; Koesling & Friebe, 2000),

*Author for correspondence: E-mail: john.garthwaite@ucl.ac.uk

Table 1   Primers used to generate full-length GC cDNAs

PCR primers	Sequence 5'-3'	Accession
α1 (f)	GCAGGATCCAGGAACACCATGTTCTGCAGG	M57405
α1 (r)	AACACAGAAACAATGGCGGCTC	
β1 (f)	GCAGTCGACGACACCATGTACGGTTTTGTG	M22562
β1 (r)	GTTCTTTTTGCCCCACAAAGG	
α2 (f)	GGCGGATCCAGCATGTCTCGCAGGAAGATTTCATC	AF109963
α2 (r)	GGCGGATCCATCTCAGAGGCTAGTTTCTCGGAG	
β2 (f)	GGAAGATCTGTGTCCATGGAAGCCATTCTG	M57507
β2 (r)	GCGGGGATCCTTCTCGTGATCACAGCACCACAAC	
vβ2 (f)	GGGGGATCCACCATGTATGGATTCATCAACACCTGC	AY004153
vβ2 (r)	CCAAGTGTCCGCAGCATCCTGTC	AY004153
		M57507

Restriction sites are underlined and the ATG initiation codons are in bold. Disruption of the β2 isoprenylation consensus sequence was achieved by mutating the β2 stop codon to a glycine residue by altering the adenine indicated in bold to cytosine.

although there has been one report that the combination of α1 and β2 tagged with green fluorescent protein (GFP) was able to generate GMP when expressed transiently in COS-7 cells (Gupta *et al.*, 1997). Recently, the role of the β2 subunit has been further complicated by the discovery of a variant β2 (vβ2), containing an additional 60 amino acids at the N terminus, adjacent to the haem-binding domain. It has been claimed that this protein functions as a homodimer and that it has a 10-fold higher affinity for NO than the α1β1 heterodimer (Koglin *et al.*, 2001). This latter conclusion is in doubt because of the method used (Bellamy *et al.*, 2002). Furthermore, the physiological relevance of the vβ2 subunit remains questionable because GC activity required a high concentration (4 mM) of Mn^{2+} (rather than the usual Mg^{2+}), which does not exist in cells.

As with any signalling molecule, it is important to understand how the different receptors function when they are expressed within cells, but for the known and putative NO$_{GC}$Rs this remains largely unexplored. In cells from a brain region (the cerebellum), several properties of the operative receptor (probably the α1β1 isoform; Gibb & Garthwaite, 2001) were different from those reported for the α1β1 and α2β1 isoforms in cell-free systems (Bellamy *et al.*, 2000; Bellamy & Garthwaite, 2001). While some of these differences have now been reconciled (Bellamy *et al.*, 2002), one property that remains peculiar to GC in its natural environment is that it desensitises rapidly following addition of NO (Bellamy *et al.*, 2000; Bellamy & Garthwaite, 2001). In concert with varying phosphodiesterase activities, this profile of activity has been hypothesised to generate diverse cGMP signals, enabling the second messenger to engage different downstream targets in different cells. Whether desensitisation is peculiar to specific NO$_{GC}$Rs or is a general property of the receptor within cells has not been investigated. The aim of the present work was to analyse this and other properties of all the known and putative NO$_{GC}$Rs expressed in cells.

Methods

Materials

YC-1, DEA/NO and DETA/NO were from Alexis Biochemicals (Nottingham, U.K.); 1H-[1,2,4]oxadiazolo[4,3-a]quinoxalin-1-one (ODQ) and L-nitroarginine were from

Tocris (Avonmouth, U.K.); 3-isobutyl-1-methylxanthine (IBMX) and haemoglobin were from Sigma-Aldrich (Dorset, U.K.).

RT–PCR and cloning of GC subunits

Total RNA was prepared from fresh lung (for α1 and β1 subunits) or fresh kidney tissue (for β2 and vβ2) from 8-day-old Wistar rats (either sex). Trizol reagent (Sigma-Aldrich) was used according to the manufacturer's instructions to isolate the RNA. For α2, rat kidney poly A^{+} RNA was purchased from BD Biosciences (Oxford, U.K.). First-strand cDNA synthesis was performed using Thermoscript reverse transcriptase (Invitrogen Ltd, Paisley, U.K.) and 1–2 μg of total or poly A^{+} RNA per reaction. Platinum *Pfx* proofreading DNA polymerase was subsequently used to generate the PCR products from 5% of the reverse transcription reaction. The primers used are listed in Table 1 and PCR was performed as follows: α1, 95°C for 5 min followed by 30 cycles of 95°C for 30 s, 55°C for 30 s, 68°C for 2 min, followed by 10 min at 68°C; α2, 95°C for 5 min, 65°C for 1 min, 68°C for 3 min, followed by 40 cycles of 94°C for 30 s, 65°C for 30 s, 68°C for 2 min 15 s, followed by 10 min at 68°C; β1, 95°C for 5 min followed by 40 cycles of 94°C for 30 s, 55°C for 30 s, 68°C for 2 min 10 s followed by 10 min at 68°C; β2, 95°C for 5 min, followed by 40 cycles of 94°C for 30 s, 50°C for 30 s, 68°C for 2 min 10 s, followed by 10 min at 68°C; vβ2, 95°C for 5 min, followed by 40 cycles of 94°C for 30 s, 60°C for 30 s, 68°C for 30 s, followed by 5 min at 68°C. PCR products were cloned into the vector pCR2.1 using the TA-Cloning system (Invitrogen Ltd, Paisley, U.K.) and sequenced by MWG Biotech-UK, Ltd. Sequences were confirmed using BLAST at the NCBI website (http://www.ncbi.nlm.nih.gov/BLAST/). Full-length subunit cDNAs were subcloned into an expression vector derived from pECFP-C1 (BD Biosciences, Oxford, U.K.), pCMV, in which the fluorophore encoding sequence was removed by digestion with *Age*I and *Brs*GI, end repaired with T4 DNA polymerase (InVitrogen Ltd, Paisley, U.K.) and ligated overnight with T4 DNA ligase (New England Biolabs UK Ltd, Hertfordshire, U.K.).

Generation of full-length vβ2 subunit cDNA

RT–PCR was used to amplify a 278 bp region from the amino terminus of the vβ2 mRNA. Full-length vβ2 cDNA was

generated by exploiting the unique amino terminal XmnI restriction site common to both the β2 and vβ2 cDNA. The vβ2 PCR product was digested with both BamHI and XmnI and the resulting fragment spliced directly into the corresponding region of the pCMV/β2 plasmid via the BglII and XmnI sites.

Tagging the β2 subunit with enhanced yellow fluorescent protein (pEYFP)

RT–PCR was used to generate either full-length wild-type β2 subunit cDNA or full-length mutant β2 cDNA in which the carboxy terminal isoprenylation consensus sequence was ablated (see Table 1). Newly introduced BglII and BamHI restriction sites were used to introduce both cDNAs into the pEYFP vector in-frame, producing amino-terminally tagged β2 subunits.

Transfections and tissue culture

COS-7 cells were maintained in Dulbecco's modified Eagles medium containing 10% foetal bovine serum and $100\,U\,ml^{-1}$ of both penicillin and streptomycin (Invitrogen Ltd, Paisley, U.K.). Transfections were optimised and performed using Effectene Transfection Reagent (Qiagen U.K. Ltd, West Sussex, U.K.) according to the manufacturer's instructions. Transfected cells were left for 48 h prior to harvesting by trypsinisation. The transfection efficiency was routinely approximately 40%.

Determination of cGMP accumulation in transfected cells

For each experiment, cells from two or four 35 mm wells were pooled, spun at $1500 \times g$ for 5 min, the supernatant aspirated and the cells resuspended in 400 or $800\,\mu l$ of incubation medium (NaCl 130 mM, KCl 3 mM, $MgSO_4$ 1.2 mM, Na_2HPO_4 1.2 mM, Tris HCl 15 mM, $CaCl_2$ 2 mM, glucose 11 mM, IBMX 1 mM, and L-nitroarginine $100\,\mu M$, pH 7.4). DEA/NO was freshly prepared in 10 mM NaOH prior to use. ODQ and YC-1 were prepared as concentrated stock solutions in DMSO, such that the final concentration of DMSO in each experiment did not exceed 1%. Cell suspensions were preincubated at 37°C for 10 min in the presence of IBMX, with or without YC-1 or ODQ, before addition of DEA/NO for the required time (see figure legends). At the end of the experiment, aliquots of cells $(50\,\mu l)$ were inactivated by boiling in $200\,\mu l$ Tris-HCl 50 mM, EDTA 4 mM (pH 7.4) for 3 min. Levels of cGMP were determined by radioimmunoassay and protein levels by BCA assay (Perbio Science U.K. Ltd, Cheshire, U.K.). One set of control experiments used untransfected COS-7 cells, which showed no significant alteration in cGMP levels on exposure to DEA/NO (200 nM; 2 min), and no significant effect of YC-1 $(30\,\mu M)$ or ODQ $(1\,\mu M)$ in the absence or presence of DEA/NO. Controls for the activity of the heterodimers included transfecting COS-7 cells with cDNAs for each of the single subunits. No measurable increase in cGMP occurred on addition of DEA/NO (100–200 nM, 2 min exposure), indicating that the endogenous expression of any of the subunits is too low to contribute to the results.

Assay of soluble and particulate GC activity

Combinations of the GC subunits were cotransfected as described above. After 48 h, two wells were harvested and resuspended in $500\,\mu l$ ice-cold lysis buffer (Tris-HCl, 10 mM; DTT, 1 mM) and then sonicated briefly (four 0.5 s pulses) on ice. Sonicated samples were then centrifuged at $100,000 \times g$ for 1 h at 4°C. The supernatant fraction was stored on ice while the pellet was carefully resuspended in $500\,\mu l$ lysis buffer. Both fractions were assayed immediately for NO-activated GC activity as described (Bellamy et al., 2000).

Applying clamped NO concentrations

Clamped NO concentrations were achieved by allowing a dynamic equilibrium to exist between NO release from the donor DETA/NO and NO inactivation by haem in red blood cells (Bellamy et al., 2002). The red blood cells were resuspended at around 2 million cells ml^{-1} in incubation medium (as described above) with the addition of 0.5% bovine serum albumin (Sigma, Dorset, U.K.) and kept on ice. Before use, the red blood cells were warmed in a shaking water bath at 37°C for 1 min and then DETA/NO was added. After 2 min, when a steady-state NO concentration is established, COS-7 cells transfected with GC were added $(80\,\mu l\,ml^{-1})$, with mixing, from a suspension $(1\,mg\,protein\,ml^{-1})$ that had been preincubated for 10 min at 37°C in the presence of 1 mM IBMX and 0.5% bovine serum albumin. Aliquots of the mixture (50 or $100\,\mu l$) were withdrawn at various times and inactivated as above. In each experiment, the amplitude of the clamped NO concentration was measured (ISO-NOP, World Precision Instruments, Stevenage, U.K.) 2 min after addition of DETA/NO $(100–500\,\mu M)$.

Results

Responses of heterodimer combinations to DEA/NO

To investigate the comparative properties of $NO_{GC}R$ heterodimers in living cells, COS-7 cells were transfected with each of the four subunit combinations (α1β1, α2β1, α1β2 and α2β2) and exposed to DEA/NO which degrades with a half-life of 2.1 min at 37°C (pH 7.4), releasing the authentic NO radical. Receptor function was monitored by measuring the associated GC activity (i.e. the enzymatic activity of the NO-bound receptor). IBMX (1 mM) was present throughout to reduce cGMP breakdown by phosphodiesterases to negligible rates (see below) and L-nitroarginine was included to inhibit any NO synthase activity. Following a 2 min exposure, when the NO concentration is near its peak (Schmidt et al., 1997), cells transfected with all the four combinations generated cGMP. Concentration–response curves showed that α1β1 and α2β1 both produced high-amplitude cGMP responses, peaking at 500–800 pmol mg protein^{-1} (Figure 1a,c). In addition, the two isoforms appeared similarly sensitive to DEA/NO, the EC_{50} values both being about 5 nM. The β2 combinations were markedly less active, maximal cGMP accumulation being about 20 and 10 pmol mg protein^{-1} from α1β2 and α2β2, respectively. Moreover, sensitivity to DEA/NO was reduced compared with the corresponding β1-containing subunits, the EC_{50} values both being about 20 nM (Figure 1b,d). The responses of α2β2 and α1β2 peaked at 100 nM DEA/NO, but

the curves were distinctly bell-shaped, such that cGMP accumulation became progressively less at higher concentrations (Figure 1b,d).
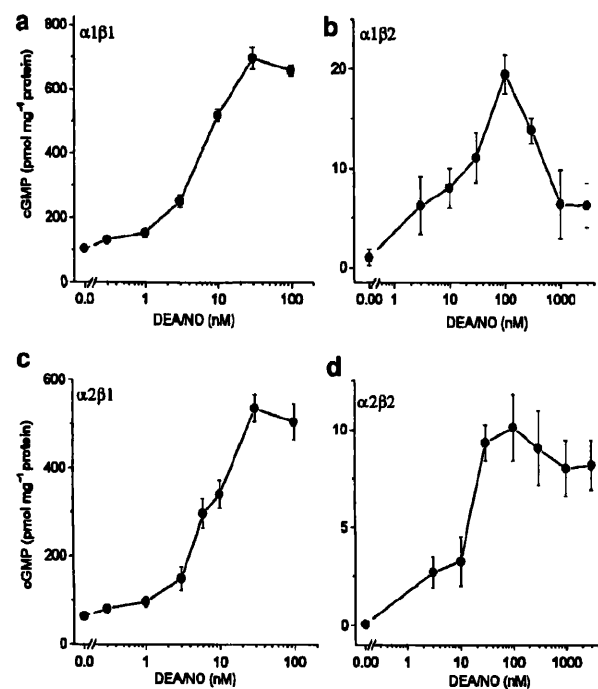
Figure 1 Sensitivity of the four possible heterodimeric GC-coupled NO receptors to DEA/NO. COS-7 cells cotransfected with different combinations of α and β subunits (as indicated) were exposed to different concentrations of DEA/NO for 2 min. Data are means $\pm$ s.e.m. ($n = 8$).

The activation kinetics of the different heterodimer combinations was examined using DEA/NO concentrations yielding maximal cGMP responses so as to avoid the variation in GC activity over time occurring at submaximal concentrations as a result of the continuously rising NO concentrations. On addition of 100 nM DEA/NO to cells expressing both $\alpha1\beta1$ and $\alpha2\beta1$, cGMP rose rapidly over the first 20 s, but then the rate of accumulation slowed and a plateau developed after 60–90 s (Figure 2a,c). In order to extract the kinetic profile of GC activity from these data, it is necessary to know the rate of cGMP breakdown and, if required, correct for it (Bellamy *et al.*, 2000). To do so, cells expressing $\alpha1\beta1$ were allowed to accumulate cGMP maximally by stimulating them with 100 nM DEA/NO for 2 min. Then 10 μM haemoglobin was added to remove free NO and cGMP followed over the next 2.5 min. The level of cGMP fell only slowly (e.g. it remained at $91 \pm 5\%$ of the prehaemoglobin level after 1 min and $83 \pm 3\%$ after 2 min; $n = 3$), indicating that phosphodiesterase activity in the presence of 1 mM IBMX was negligible over the relevant time period. This being so, the profile of sGC activity can be extracted from the cGMP accumulation data simply by fitting the data with a suitable function and then differentiating. As in previous studies on brain cells (Bellamy *et al.*, 2000), the data were well fitted by a hyperbolic function. The corresponding GC activity in the cells expressing $\alpha1\beta1$ and $\alpha2\beta1$ extracted in this way was essentially identical. It rose to a peak of over 20 pmol mg^{-1} protein s^{-1} and then sharply declined such that the activity was halved by 30 s and almost back to zero after 2 min (Figure 2a,c).

With the $\alpha1\beta2$ and $\alpha2\beta2$ subunit combinations, cGMP accumulated more gradually, but the rate still slowed after about 30 s. The corresponding GC profile indicated relatively
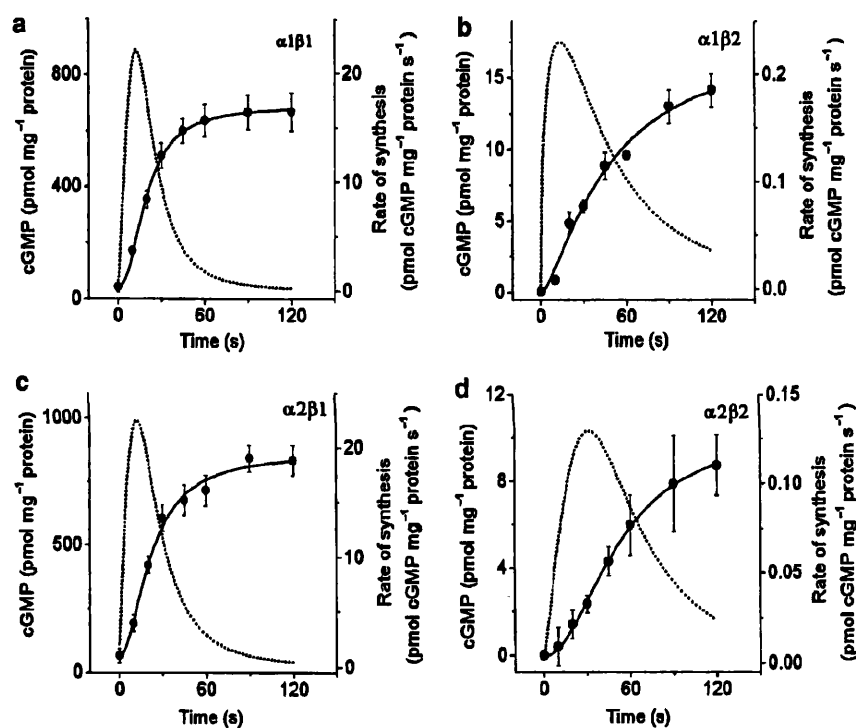
Figure 2 Activation kinetics of the four possible heterodimeric GC-coupled NO receptors on addition of DEA/NO. The cells were exposed to supramaximal concentrations of DEA/NO (100 nM for $\alpha1\beta1$, $\alpha2\beta1$ and $\alpha2\beta2$, 200 nM for $\alpha1\beta2$) at $t = 0$ and cGMP levels followed over time. Data are means $\pm$ s.e.m. ($n = 6$). Solid lines are hyperbolic fits to the data which, when differentiated, provide the underlying profiles of GC activity (broken lines, right axes).

low peaks of activity, approximately $0.2 \, pmol \, mg^{-1}$ protein s^{-1} for $\alpha1\beta2$ and $0.1 \, pmol \, mg^{-1}$ protein s^{-1} for $\alpha2\beta2$. Thereafter, the activity fell more slowly than with the $\beta1$-containing isoforms, the halftimes being about 60 s (Figure 2b,d).

Sensitivity of the $\alpha1\beta1$ and $\alpha2\beta1$ isoforms to clamped NO concentrations

The responsiveness of the GCs to DEA/NO may be an unreliable predictor of their absolute and relative sensitivities to NO, because the NO concentration changes with time (Bellamy et al., 2002). To address this problem, experiments were carried out using constant, known NO concentrations. Clamped concentrations were achieved using a method whereby NO release from the slow donor DETA/NO is allowed to become balanced by NO inactivation by red blood cells (Bellamy et al., 2002). Cells were then added to the pre-equilibrated mixture, but only small volumes can be added without perturbing the equilibrium significantly. This meant that, for the resulting cGMP levels to be measurable, the experiments were restricted to cells expressing the more active $\alpha1\beta1$ and $\alpha2\beta1$ heterodimers. A detailed measurement of the time course of cGMP accumulation in cells expressing the $\alpha1\beta1$ combination and exposed to 10 nM NO (Figure 3a) showed the shape to be similar to that found when a supramaximal DEA/NO concentration (100 nM) was applied to cells containing $\alpha1\beta1$ or $\alpha2\beta1$ (Figure 2a, c). The GC kinetics extracted from the data using the clamped NO concentration was more rapid, however, with the peak activity occurring within 2 s, followed by desensitisation to 50% of the maximum by about 12 s (Figure 3a).

Steady-state concentration–response curves were obtained for each of the receptors using a 1 min exposure to NO (Figure 3b). Both curves were maximum at 10 nM NO but were bell-shaped, such that higher concentrations (30–70 nM) generated lower cGMP levels. The threshold NO concentration in both cases was about 0.5 nM. Fitting the rising portions of the curves to the Hill equation indicated that the $\alpha1\beta1$ receptor had an EC_{50} of 1.2 ± 0.1 nM and a Hill coefficient of 1.8 ± 0.3, and the $\alpha2\beta1$ receptor an EC_{50} of 2.2 ± 0.2 nM and a Hill coefficient of 1.2 ± 0.1.

Activity of the $\nu\beta2$ subunit

Transfection of the $\nu\beta2$ subunit on its own into COS-7 cells resulted in cGMP accumulation in response to DEA/NO that was maximally about 13 pmol cGMP mg protein^{-1} and so was of comparable magnitude to the responses found with the $\beta2$ heterodimers (Figure 4a). Also, similar to these heterodimers, the concentration–response curve was bell-shaped and showed an EC_{50} of about 20 nM DEA/NO (Figure 4b). If the cells were cotransfected with $\alpha1$ or $\alpha2$, there was no discernable effect on $\nu\beta2$ activity (data not shown).

Analysis of the kinetics in $\nu\beta2$-transfected cells (Figure 4b) indicated a faster initial rise in cGMP than with the $\beta2$ heterodimers, with the plateau level being attained after about 30 s. Accordingly, the extracted GC profile rose sharply to peak at about 0.5 pmol mg protein^{-1} s^{-1} and then fell at a similar rate to that seen with the $\beta1$-containing isoforms.
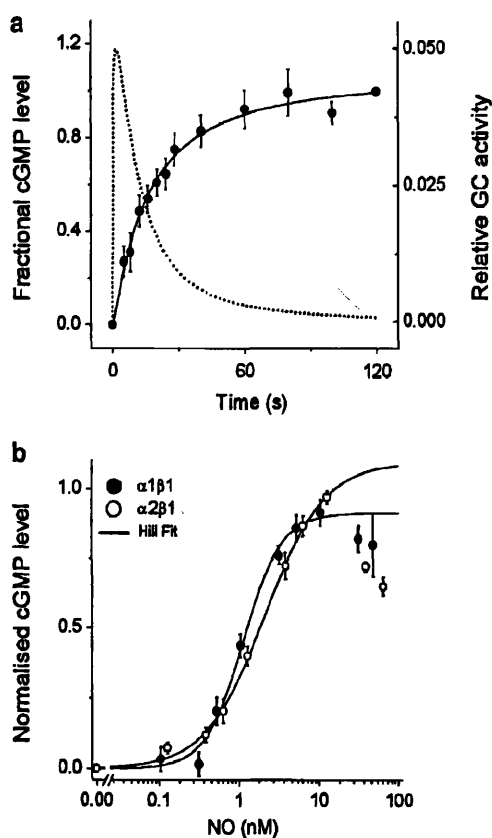

Figure 3 Kinetics of $\alpha1\beta1$ and $\alpha2\beta2$ NO$_{GC}$Rs exposed to clamped NO concentrations. In (a), COS-7 cells expressing the $\alpha1\beta1$ receptor were exposed to 10 nM NO at $t=0$ and then cGMP levels were followed over time. Each point is the mean$\pm$s.e.m. of data normalised to the cGMP level found after 120 s exposure, which in different experiments ranged from 400 to 700 pmol mg^{-1} protein ($n=6$). The solid line through the data is a fit to a hyperbolic function which, when differentiated, gives the indicated profile of GC activity (broken line; right axis). (b) Concentration–cGMP response curves for cells expressing the $\alpha1\beta1$ and $\alpha2\beta1$ receptors, as indicated. The cells were exposed to fixed NO concentrations for 1 min. The data are normalised to the maximum cGMP response observed in each experiment (range, 300–500 pmol mg^{-1} protein) and represent the means$\pm$s.e.m. ($n=6$–9). The solid lines are fits of the rising portions of the curves to the Hill equation.

Pharmacological properties

Two pharmacological tools are widely used to probe the involvement of NO$_{GC}$Rs in biological phenomena, the allosteric activator YC-1 (Friebe & Koesling, 1998), and the inhibitor ODQ (Garthwaite et al., 1995). Experiments were carried out to evaluate their activity towards the different GCs in cells. Under 'basal' conditions (no added NO), cGMP was highest (about 100 pmol mg protein^{-1}) in the cells expressing the $\alpha1\beta1$ and $\alpha2\beta1$ isoforms and exposure to YC-1 (30 μM) resulted in marked (five- to six-fold) increases, to levels normally attained on maximal NO stimulation (Figure 5a). Basal cGMP in the $\beta2$ combinations was about 10 pmol mg protein^{-1}. With $\alpha1\beta2$, YC-1 caused a two-fold elevation, whereas with $\alpha2\beta2$ no significant increase was observed. ODQ (1 μM) more than halved the basal level of cGMP in the cells expressing $\alpha1\beta1$ and $\alpha2\beta1$ but had no significant effect in cells containing $\alpha1\beta2$ or $\alpha2\beta2$ (Figure 5a).
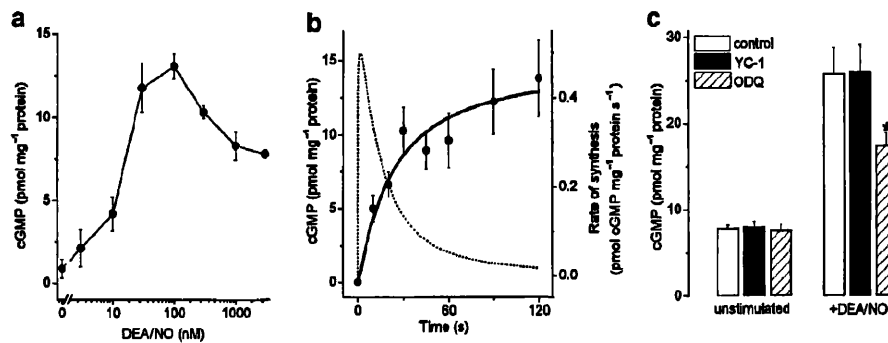
Figure 4 Properties of the $v\beta2$ subunit expressed in COS 7 cells. (a) The cells were exposed to different concentrations of DEA/NO for 2 min. Data are means ± s.e.m. ($n = 8$). (b) Cells were exposed to supramaximal concentrations of DEA/NO (100 nM) at $t = 0$ and cGMP levels followed over time. Data are means ± s.e.m. ($n = 6$). The solid line is a hyperbolic fit to the data which, when differentiated, provides the underlying profile of GC activity (broken line; right axis). (c) cGMP levels in cells that were unstimulated (three left panels) or stimulated with 100 nM DEA/NO (three right panels) in the absence or presence of YC-1 (30 μM) or ODQ (1 μM) as indicated. The preincubation period with YC-1 or ODQ was 10 min. Results are means ± s.e.m. ($n = 6$); *$P < 0.05$ versus DEA/NO alone (t-test).
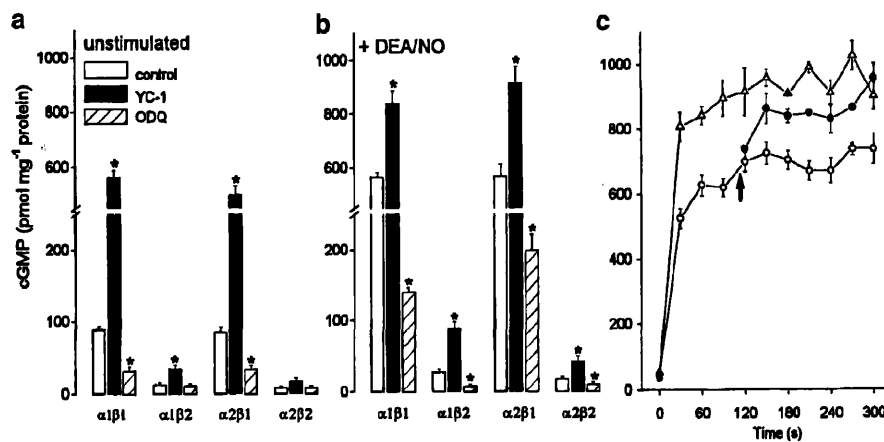
Figure 5 Pharmacological properties of the four possible heterodimeric GC-coupled NO receptors expressed in COS-7 cells. The data in (a) show the basal cGMP levels (open bars) and the effect of YC-1 (30 μM, filled bars) and ODQ (1 μM, hatched bars) in the absence of any added DEA/NO. *$P < 0.05$ versus basal cGMP levels. The data in (b) show the equivalent levels following exposure to supramaximal DEA/NO concentrations (100 nM for $\alpha1\beta1$, $\alpha2\beta1$ and $\alpha2\beta2$, 200 nM for $\alpha1\beta2$). *$P < 0.05$ versus DEA/NO alone. In all cases, the cells were preincubated for 10 min with YC-1 or ODQ; they were then sampled to obtain the data in (a) and then DEA/NO was added and the cells inactivated 2 min later for the data in (b). Results are means ± s.e.m. ($n = 6$); statistical significance was assessed by the Student's t-test. (c) Effect of YC-1 (100 μM) on cells expressing the $\alpha1\beta1$ receptor, added before ($t = -5$ s, open triangles) and after ($t = 115$, arrow, filled circles) DEA/NO-induced desensitisation of GC activity, compared to control (open circles). Data are means ± s.e.m. ($n = 6$).

YC-1 has only a very weak ability to activate GC in cells in the absence of NO (Schmidt et al., 2001; Bellamy & Garthwaite, 2002). The marked stimulatory effect of YC-1 and inhibitory effect of ODQ on cGMP in cells expressing $\alpha1\beta1$ and $\alpha2\beta1$ in the presence of an NO synthase inhibitor and in the absence of added NO indicated, nevertheless, that NO was present in active concentrations. To test this, haemoglobin (10 μM) was added to cells transfected with $\alpha1\beta1$. The basal cGMP was reduced by 65 ± 2% ($n = 3$). Within the same experiments, ODQ (1 μM) reduced the levels 68 ± 1% ($n = 3$) and no further reduction was observed with a combination of haemoglobin and ODQ (68 ± 1%; $n = 3$).

Under conditions of maximal GC stimulation by DEA/NO, YC-1 caused a further 40–100% increase in cGMP accumulation in all heterodimer combinations (Figure 5b). In addition, in cells expressing the $\alpha1\beta1$ isoform, addition of YC-1 at a time when the receptor is maximally desensitised (after 2 min exposure to DEA/NO) resulted in an additional burst of cGMP formation (Figure 5c) indicating that, as with the native

receptor (Bellamy & Garthwaite, 2002), YC-1 reverses GC desensitisation. ODQ inhibited the DEA/NO-stimulated cGMP accumulation in all combinations to 25–50% of control (Figure 5b).

Cells transfected with $v\beta2$ showed no change in basal cGMP levels following addition of either YC-1 or ODQ (Figure 4c) and, in the presence of 100 nM DEA/NO, both control cells and cells exposed to YC-1 generated the same (three-fold) increases in cGMP. Exposure to ODQ, however, reduced the NO-stimulated rise by about 50% (Figure 4c).

Subcellular location of the β2 subunit

Of the GC subunits, $\beta2$ and $v\beta2$ uniquely contain an isoprenylation consensus sequence (CVVL) at the carboxy terminal which, in principle, could target the enzyme to membranes (Yuen et al., 1990). In order to address this possibility, we tagged the amino terminal of the $\beta2$ subunit with EYFP and used confocal microscopy to study its
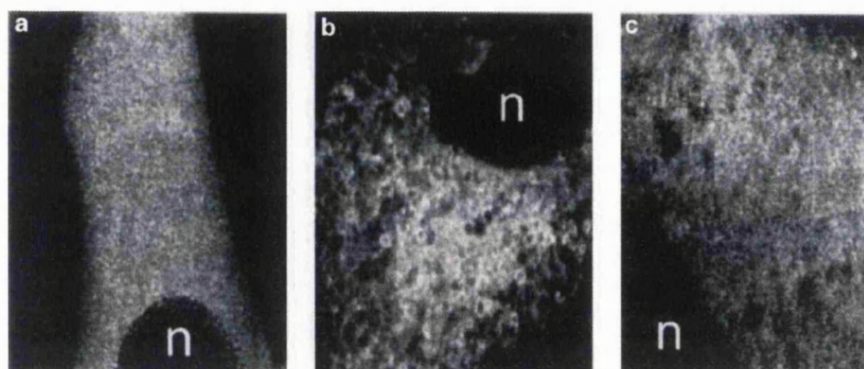
Figure 6 Confocal laser imaging of fluorescently tagged GC subunits in COS-7 cells. The panels show representative images of cells transfected with $\alpha1$-EYFP/$\beta1$ (a), $\alpha1$/EYFP-$\beta2$ (b) and $\alpha1$/EYFP-$\beta2$ with a mutated isoprenylation sequence (c). Nuclei are labelled '*n*'.

Table 2 Partitioning of GC activity

COS-7		$\alpha1\beta1$	$\alpha1\beta2$	*Mutated $\alpha1\beta2$*	$\alpha1$ only
Supernatant	37 ± 1	31316 ± 2813	457 ± 16	434 ± 11	62 ± 1
Pellet	46 ± 1	2879 ± 205	66 ± 1	64 ± 3	27 ± 1

Results are expressed as pmol cGMP mg^{-1} total protein. Samples were stimulated by exposure to $10\,\mu M$ DEA/NO for 10 min at 37°C ($n = 5$).

intracellular location when cotransfected with $\alpha1$ into COS-7 cells. For comparison, the EYFP-tagged $\alpha1$ was cotransfected with $\beta1$. The $\alpha1$-EYFP/$\beta1$ cotransfected cells displayed an even fluorescence throughout the cytoplasm, with apparent exclusion from the nuclei (Figure 6a). In the $\alpha1$/EYFP-$\beta2$ cotransfected cells, the nucleus was similarly nonfluorescent, but the protein appeared to be associated with a membranous complex within the cytoplasm (Figure 6b). To determine the role of the isoprenylation consensus sequence in this localisation, an EYFP-tagged mutant of $\beta2$ lacking this sequence was generated. Cotransfection of this mutated EYFP-$\beta2$ with $\alpha1$ resulted in a loss of apparent association with intracellular membranes and, instead, a diffuse cytosolic distribution resembling that of $\alpha1$/EYFP-$\beta1$ (Figure 6c). These localisation studies were all repeated in HeLa cells, with essentially identical results (data not shown), indicating that the findings with COS-7 cells are not cell specific.

When the cells transfected with $\alpha1\beta1$ or $\alpha1\beta2$ were homogenised and GC activity in supernatant and particulate fractions assayed, it appeared predominantly in the supernatant in both cases and no difference was observed whether the isoprenylation sequence in $\beta2$ was mutated or not (Table 2).

Discussion

That cells expressing the two established heterodimeric NO$_{GC}$Rs, $\alpha1\beta1$ and $\alpha2\beta1$, generated large cGMP responses was as predicted (Russwurm *et al.*, 1998). More surprising was that the $\alpha1\beta2$ and $\alpha2\beta2$ combinations both possessed NO-stimulated GC activity, although their maximal activities were relatively low. In several tests, transfection of HeLa cells with $\alpha1$ or $\alpha2$ together with $\beta2$ did not result in measurable DEA/NO-evoked cGMP accumulation (B.J. Gibb & J. Garthwaite,

unpublished observation), suggesting that cell-specific factors may be required for active $\beta2$ heterodimers. In this respect, it may be relevant that COS-7 cells are derived from the kidney, which contains the most abundant message for $\beta2$ (Yuen *et al.*, 1990). Moreover, EYFP tagging indicated that the $\beta2$ subunit associated with an intracellular membranous complex by virtue of its isoprenylation sequence. This complex had the typical appearance of the endoplasmic reticulum in COS-7 cells (Shakur *et al.*, 2001). Although no particulate activity attributable to membrane association through the isoprenylation sequence was detected in cell lysates, it may be that, as with cGMP-inhibited phosphodiesterase (PDE3) in these cells (Shakur *et al.*, 2001), the association with the endoplasmic reticulum is weak and easily disrupted. In contrast to the apparent localisation of the $\beta2$ subunit, the $\alpha2\beta1$ can associate with synaptic proteins in the brain (Russwurm *et al.*, 2001) and $\alpha1\beta1$ appears to attach to the cell membrane in response to a rise in Ca^{2+} (Zabel *et al.*, 2002), so that all possible GC isoforms may be differentially localised in cells.

The absence of measurable GC activity of the $v\beta2$ protein in extracts of Sf9 cells, except in the presence of high Mn^{2+} concentrations or when the isoprenylation site was mutated (Koglin *et al.*, 2001), questions its physiological significance. Our finding that it is active on its own in COS-7 cells suggests that it could form a functional homomer in the absence of Mn^{2+} (or mutation). The maximal cGMP response in cells expressing $v\beta2$ was comparable to that of the $\alpha1\beta2$ and $\alpha2\beta2$ heterodimers, indicating that they all possess similar GC activity. Although relatively low, the $10-20$ pmol mg protein^{-1} formed by $v\beta2$ or the $\beta2$ combinations corresponds to an average intracellular cGMP concentration in the low micromolar range (assuming $10\,\mu l$ cell volume mg protein^{-1}). If applicable to normal cells, this is well in the range needed to activate cGMP-dependent protein kinases.

All GC subunits expressed in cells were highly sensitive NO detectors, the EC$_{50}$ values for DEA/NO being about 5 nM ($\alpha1\beta1$, $\alpha2\beta1$) or 20 nM ($\alpha1\beta2$, $\alpha2\beta2$, $v\beta2$). These values are 1–2 orders of magnitude lower than those typically found for DEA/NO using standard GC assays on cell lysates or purified proteins (Russwurm *et al.*, 1998; Koglin *et al.*, 2001), but the EC$_{50}$ values reported by these assays are poor indicators of the sensitivity of the receptors to NO (Bellamy *et al.*, 2002). Using clamped NO concentrations, we found the EC$_{50}$ values of $\alpha1\beta1$ and $\alpha2\beta1$ to be 1 and 2 nM respectively and the maximal

responses to occur at about 10 nM. These values are compatible with the data using DEA/NO once the profile of NO release is considered. Assuming that the stoichiometry of NO release is 1.6 (Griffiths & Garthwaite, 2001) and that NO is consumed by autoxidation (Schmidt *et al.*, 1997), with 5 nM DEA/NO (approximately the EC_{50} for both heterodimers), the average NO concentration over the 2 min exposure is 2 nM; at the maximum for DEA/NO (30 nM), it is 13 nM. Thus, use of DEA/NO during the relatively short exposures can provide quite an accurate index of sensitivity to NO.

When constant NO concentrations are applied to the purified $\alpha 1\beta 1$ receptor, the EC_{50} (4 nM) is about three-fold higher than that found in cells expressing this isoform. This difference is predicted by GC desensitisation in cells truncating the concentration–response curve (Bellamy & Garthwaite, 2001). Furthermore, the apparent Hill slope in the cells expressing the $\alpha 1\beta 1$ isoform (1.8) was similar to that reported for the purified protein (Bellamy *et al.*, 2002) suggesting that the receptor in cells also exhibits at least two NO-binding sites. Whether this also applies to the $\alpha 2\beta 1$ receptor (apparent Hill slope of 1.2) is ambiguous. Studies on the purified protein, where the complication of desensitisation is eliminated, are needed to evaluate this possibility.

All the recent evidence, therefore, converges to position the potency of NO for its $\beta 1$-containing heterodimeric receptors in the very low nM range, which is far from the value of 250 nM (Stone & Marletta, 1996) that has generally been considered correct. The high sensitivity of the $\alpha 1\beta 1$ and $\alpha 2\beta 1$ receptors to NO is further attested by the finding that the 'basal' cGMP levels in COS-7 cells expressing these isoforms in the absence of endogenous or added NO were about 70% reduced by the NO scavenger haemoglobin or the GC inhibitor ODQ. Presumably, the environment was contributing biologically active concentrations of NO (Friebe *et al.*, 1996) which, from the concentration–response curves (Figures 1a,c and 3b), would be in the 0.5–1 nM range. This source of NO is not usually considered to contribute to results obtained *in vitro* but, we suggest, should be in the future.

Concerning the $\beta 2$-containing heterodimers and the presumed $v\beta 2$ homomer, analysis of the data using DEA/NO (as above) suggests that NO is about four-fold less potent (EC_{50} ~8 nM) than on the $\beta 1$ varieties. This contradicts the conclusion, made on the basis of the potency of DEA/NO in standard GC assays, that the $v\beta 2$ homomer is 10-fold more sensitive to NO than the $\alpha 1\beta 1$ receptor (Koglin *et al.*, 2001).

A prominent feature of native $NO_{GC}Rs$ in cerebellar cells is that they desensitise rapidly (Bellamy *et al.*, 2000; Bellamy & Garthwaite, 2001). This behaviour is typical of most neurotransmitter receptors but, in the case of $NO_{GC}Rs$, is not seen in cell-free preparations. It is apparently also not obvious in intact platelets under conditions where phosphodiesterases maintain cGMP at low levels (Mullershausen *et al.*, 2001), possibly because cGMP itself regulates receptor desensitisation (Wykes *et al.*, 2002). When expressed in COS-7 cells all the heterodimer combinations, and $v\beta 2$ on its own, desensitised. With a clamped NO concentration (10 nM), the speed of

desensitisation of the $\alpha 1\beta 1$ receptor was similar to that measured in the cerebellar cells (Bellamy & Garthwaite, 2001). With $\alpha 1\beta 2$, $\alpha 2\beta 2$, and to a lesser extent $v\beta 2$, desensitisation appeared somewhat slower, but the lower potency of NO for these GCs means that the buildup of NO to threshold concentrations and above will necessarily be slower than with the $\beta 1$ heterodimers, which may contribute to the slower apparent desensitisation kinetics. The bell-shaped concentration–response curves observed for all GCs (most obviously with $\alpha 1\beta 2$ and $v\beta 2$) is characteristic of rapidly desensitising receptors (Raman & Trussell, 1992; Paternain *et al.*, 1998). The finding that the $\beta 2$-containing GCs desensitise similarly to the $\alpha 1\beta 1$ and $\alpha 2\beta 1$ isoforms, despite the absolute activities of the $\beta 2$-containing GCs being at least 50-fold lower, adds to the already considerable evidence (Bellamy *et al.*, 2000; Bellamy & Garthwaite, 2002) that desensitisation is not simply caused by depletion of GTP substrate (cf Mullershausen *et al.*, 2001).

YC-1 and ODQ had their predicted effects on the $\alpha 1\beta 1$ and $\alpha 2\beta 1$ receptors, but neither agent had been tested previously on the $\beta 2$ heterodimers or on the presumed $v\beta 2$ monomer. Our finding that YC-1 enhanced the NO-stimulated activity of both heterodimers indicates that they are also equipped with a functional YC-1-binding site. As YC-1 synergises with NO (Friebe *et al.*, 1998), the lesser (or not significant) effect of this compound on the corresponding basal cGMP levels, compared with the $\beta 1$-containing receptors, can be explained by the $\beta 2$ heterodimers being intrinsically less sensitive to NO (see above) such that the ambient (environmental) NO concentration is too low to have much effect even in the presence of YC-1. The inhibitor ODQ, which oxidises the GC haem group (Garthwaite *et al.*, 1995; Schrammel *et al.*, 1996), affected the $\beta 2$-containing GCs similarly to the $\beta 1$-containing GC isoforms, suggesting that this approach is unlikely to be useful in differentiating between different GCs. The only agent found to discriminate between GCs was YC-1, which failed to influence NO-stimulated GC activity in cells expressing $v\beta 2$. This finding supports the proposal that the YC-1-binding site is located within the α subunits (Friebe *et al.*, 1999; Koglin *et al.*, 2002).

In conclusion, all the putative $NO_{GC}Rs$ when expressed heterologously possess NO-stimulated GC activity and are extremely sensitive to this diffusible messenger. They can be split into two broad groups: the $\beta 1$-containing heterodimeric receptors, which possess high GC activity and the lowest EC_{50}s for NO (1–2 nM), and the $\beta 2$-containing GCs which have lower GC activity and higher EC_{50}s (about 8 nM). All the GCs share a strongly desensitising profile of activity and, apart from a lack of effect of YC-1 on the presumed $v\beta 2$ monomer, are indistinguishable by existing pharmacological interventions. The expression of the $\beta 2$ subunits *in vivo* requires investigation.

References

BELLAMY, T.C. & GARTHWAITE, J. (2001). Sub-second kinetics of the nitric oxide receptor, soluble guanylyl cyclase, in intact cerebellar cells. *J. Biol. Chem.*, **276**, 4287–4292.

BELLAMY, T.C. & GARTHWAITE, J. (2002). Pharmacology of the nitric oxide receptor, soluble guanylyl cyclase, in cerebellar cells. *Br. J. Pharmacol.*, **136**, 95–103.

BELLAMY, T.C., GRIFFITHS, C. & GARTHWAITE, J. (2002). Differential sensitivity of guanylyl cyclase and mitochondrial respiration to nitric oxide measured using clamped concentrations. *J. Biol. Chem.*, **277**, 31801–31807.

BELLAMY, T.C., WOOD, J., GOODWIN, D.A. & GARTHWAITE, J. (2000). Rapid desensitization of the nitric oxide receptor, soluble guanylyl cyclase, underlies diversity of cellular cGMP responses. *Proc. Natl. Acad. Sci. U.S.A.*, **97**, 2928–2933.

DENNINGER, J.W. & MARLETTA, M.A. (1999). Guanylate cyclase and the NO/cGMP signalling pathway. *Biochim. Biophys. Acta*, **1411**, 334–350.

FRIEBE, A. & KOESLING, D. (1998). Mechanism of YC-1-induced activation of soluble guanylyl cyclase. *Mol. Pharmacol.*, **53**, 123–127.

FRIEBE, A., MALKEWITZ, J., SCHULTZ, G. & KOESLING, D. (1996). Positive effects of pollution? *Nature*, **382**, 120.

FRIEBE, A., MULLERSHAUSEN, F., SMOLENSKI, A., WALTER, U., SCHULTZ, G. & KOESLING, D. (1998). YC-1 potentiates nitric oxide- and carbon monoxide-induced cyclic GMP effects in human platelets. *Mol. Pharmacol.*, **54**, 962–967.

FRIEBE, A., RUSSWURM, M., MERGIA, E. & KOESLING, D. (1999). A point-mutated guanylyl cyclase with features of the YC-1-stimulated enzyme: implications for the YC-1 binding site? *Biochemistry*, **38**, 15253–15257.

GARTHWAITE, J. (2000). The physiological roles of nitric oxide in the central nervous system. In: *Nitric Oxide*. ed. Mayer, B. pp. 259–275. Berlin: Springer.

GARTHWAITE, J., SOUTHAM, E., BOULTON, C.L., NIELSEN, E.B., SCHMIDT, K. & MAYER, B. (1995). Potent and selective inhibition of nitric oxide-sensitive guanylyl cyclase by 1H-[1,2,4]oxadiazolo[4,3-a]quinoxalin-1-one. *Mol. Pharmacol.*, **48**, 184–188.

GIBB, B.J. & GARTHWAITE, J. (2001). Subunits of the nitric oxide receptor, soluble guanylyl cyclase, expressed in rat brain. *Eur. J. Neurosci.*, **13**, 539–544.

GRIFFITHS, C. & GARTHWAITE, J. (2001). The shaping of nitric oxide signals by a cellular sink. *J. Physiol. (Lond.)*, **536**, 855–862.

GUPTA, G., AZAM, M., YANG, L. & DANZIGER, R.S. (1997). The β2 subunit inhibits stimulation of the α1/β1 form of soluble guanylyl cyclase by nitric oxide Potential relevance to regulation of blood pressure. *J. Clin. Invest.*, **100**, 1488–1492.

KOESLING, D. & FRIEBE, A (2000). Enzymology of soluble guanylyl cyclase. In: *Nitric Oxide*. ed. Mayer, B. pp. 93–109. Berlin: Springer.

KOGLIN, M., STASCH, J.P. & BEHRENDS, S. (2002). BAY 41-2272 activates two isoforms of nitric oxide-sensitive guanylyl cyclase. *Biochem. Biophys. Res. Commun.*, **292**, 1057–1062.

KOGLIN, M., VEHSE, K., BUDAEUS, L., SCHOLZ, H. & BEHRENDS, S. (2001). Nitric oxide activates the β2 subunit of soluble guanylyl cyclase in the absence of a second subunit. *J. Biol. Chem.*, **276**, 30737–30743.

MAYER, B. (ed) (2000). *Nitric Oxide*. Berlin: Springer.

MULLERSHAUSEN, F., RUSSWURM, M., THOMPSON, W.J., LIU, L., KOESLING, D. & FRIEBE, A (2001). Rapid nitric oxide-induced desensitization of the cGMP response is caused by increased activity

of phosphodiesterase type 5 paralleled by phosphorylation of the enzyme. *J. Cell. Biol.*, **155**, 271–278.

PATERNAIN, A.V., RODRIGUEZ-MORENO, A., VILLARROEL, A. & LERMA, J. (1998). Activation and desensitization properties of native and recombinant kainate receptors. *Neuropharmacology*, **37**, 1249–1259.

RAMAN, I.M. & TRUSSELL, L.O. (1992). The kinetics of the response to glutamate and kainate in neurons of the avian cochlear nucleus. *Neuron*, **9**, 173–186.

RUSSWURM, M., BEHRENDS, S., HARTENECK, C. & KOESLING, D. (1998). Functional properties of a naturally occurring isoform of soluble guanylyl cyclase. *Biochem. J.*, **335**, 125–130.

RUSSWURM, M., WITTAU, N. & KOESLING, D. (2001). Guanylyl cyclase/PSD-95 interaction: targeting of the NO-sensitive α2β1 guanylyl cyclase to synaptic membranes. *J. Biol. Chem.*, **276**, 44647–44652.

SCHMIDT, K., DESCH, W., KLATT, P., KUKOVETZ, W.R. & MAYER, B. (1997). Release of nitric oxide from donors with known half-life: a mathematical model for calculating nitric oxide concentrations in aerobic solutions. *Naunyn Schmiedeberg's Arch. Pharmacol.*, **355**, 457–462.

SCHMIDT, K., SCHRAMMEL, A., KOESLING, D. & MAYER, B. (2001). Molecular mechanisms involved in the synergistic activation of soluble guanylyl cyclase by YC-1 and nitric oxide in endothelial cells. *Mol. Pharmacol.*, **59**, 220–224.

SCHRAMMEL, A., BEHRENDS, S., SCHMIDT, K., KOESLING, D. & MAYER, B. (1996). Characterization of 1H-[1,2,4]oxadiazolo[4,3-a]quinoxalin-1-one as a heme-site inhibitor of nitric oxide-sensitive guanylyl cyclase. *Mol. Pharmacol.*, **50**, 1–5.

SHAKUR, Y., TAKEDA, K., KENAN, Y., YU, Z.X., RENA, G., BRANDT, D., HOUSLAY, M.D., DEGERMAN, E., FERRANS, V.J. & MANGANIELLO, V.C. (2001). Membrane localization of cyclic nucleotide phosphodiesterase 3 (PDE3). Two N-terminal domains are required for the efficient targeting to, and association of, PDE3 with endoplasmic reticulum. *J. Biol. Chem.*, **275**, 38749–38761.

STONE, J.R. & MARLETTA, M.A. (1996). Spectral and kinetic studies on the activation of soluble guanylate cyclase by nitric oxide. *Biochemistry*, **35**, 1093–1099.

WYKES, V., BELLAMY, T.C. & GARTHWAITE, J. (2002). Kinetics of nitric oxide-cyclic GMP signalling in CNS cells and its possible regulation by cyclic GMP. *J. Neurochem.*, **83**, 37–47.

YUEN, P.S., POTTER, L.R. & GARBERS, D.L. (1990). A new form of guanylyl cyclase is preferentially expressed in rat kidney. *Biochemistry*, **29**, 10872–10878.

ZABEL, U., KLEINSCHNITZ, C., OH, P., NEDVETSKY, P., SMOLENSKI, A., MULLER, H., KRONICH, P., KUGLER, P., WALTER, U., SCHNITZER, J.E. & SCHMIDT, H.H. (2002). Calcium-dependent membrane association sensitizes soluble guanylyl cyclase to nitric oxide. *Nat. Cell Biol.*, **4**, 307–311.

A New and Simple Method for Delivering Clamped Nitric Oxide Concentrations in the Physiological Range: Application to Activation of Guanylyl Cyclase-Coupled Nitric Oxide Receptors

CHARMAINE GRIFFITHS, VICTORIA WYKES, TOMAS C. BELLAMY, and JOHN GARTHWAITE

The Wolfson Institute for Biomedical Research, University College London, London, United Kingdom (C.G., V.W., J.G.); and Division of Neurophysiology, National Institute for Medical Research, Mill Hill, London, United Kingdom (T.B.)

Received June 25, 2003; accepted August 27, 2003   This article is available online at http://molpharm.aspetjournals.org

ABSTRACT

The signaling molecule nitric oxide (NO) could engage multiple pathways to influence cellular function. Unraveling their relative biological importance has been difficult because it has not been possible to administer NO under the steady-state conditions that are normally axiomatic for analyzing ligand-receptor interactions and downstream signal transduction. To address this problem, we devised a chemical method for generating constant NO concentrations, derived from balancing NO release from a NONOate donor with NO consumption by a sink. On theoretical grounds, 2-4-carboxyphenyl-4,4,5,5-tetramethylimidazoline-1-oxyl-3-oxide (CPTIO) was selected as the sink. The mixture additionally contained urate to convert an unwanted product of the reaction (NO_2) into nitrite ions. The method enabled NO concentrations covering the physiological range (0–100 nM) to be formed within approximately 1 s. More-over, the concentrations were sufficiently stable over at least several minutes to be useful for biological purposes. When applied to the activation of guanylyl cyclase-coupled NO receptors, the method gave an EC_{50} of 1.7 nM NO for the protein purified from bovine lung, which is lower than estimated previously using a biological NO sink (red blood cells). The corresponding values for the $\alpha 1\beta 1$ and $\alpha 2\beta 1$ isoforms were 0.9 nM and 0.5 nM, respectively. The slopes of the concentration-response curves were more shallow than before (Hill coefficient of 1 rather than 2), questioning the need to consider the binding of more than one NO molecule for receptor activation. The discrepancies are ascribable to limitations of the earlier method. Other biological problems can readily be addressed by adaptations of the new method.

Nitric oxide (NO), synthesized from the amino acid L-arginine, functions as a signaling molecule throughout the body, in which it elicits diverse effects such as smooth muscle relaxation, platelet disaggregation, and synaptic plasticity. Physiological NO signal transduction occurs through the activation of intracellular guanylyl cyclase (GC)-coupled receptors, leading to cGMP formation (Denninger and Marletta, 1999; Koesling and Friebe, 2000). Depending on its concentration and/or other experimental conditions, however, biological effects can be exerted through other pathways, including the binding of NO to cytochrome *c* oxidase, resulting in the inhibition of mitochondrial respiration (Brown, 1999), reaction with other radicals (e.g., with superoxide ions to give reactive peroxynitrite anions), and the production of nitro-

sating species after the reaction of NO with oxygen (Beckman and Koppenol, 1996; Augusto et al., 2002). The extent to which these other reactions contribute to the biology of NO in vivo remains uncertain. Nevertheless, the spectrum of possible effects of NO in vitro can make the interpretation of experimental findings difficult, particularly when NO is applied in constantly changing concentrations, as happens with the current methods of delivery.

NO can be dispensed from concentrated anaerobic solutions, but on dilution into aerobic solutions used in the laboratory, it is consumed by reaction with oxygen (autoxidation) at a rate proportional to the square of its concentration (Ford et al., 1993). Alternatively, NO can be provided by donors, of which the so-called NONOates are preferred because they degrade to release NO with predictable kinetics (Morley and Keefer, 1993), and different NONOates with widely differing half-lives (1.8 s to 20 h) are commercially available. When added to biological media, however, the NO concentration increases (at a rate governed by the half-life)

ABBREVIATIONS: NO, nitric oxide; CPTIO, 2-4-carboxyphenyl-4,4,5,5-tetramethylimidazoline-1-oxyl-3-oxide; DEA/NO, diethylamine/nitric oxide adduct; DETA/NO, diethylenetriamine/nitric oxide adduct; GC guanylyl cyclase; SPER/NO, spermine/nitric oxide adduct; DTT, dithiothreitol; NOC, nitric oxide-amine complex.

and then decreases as the autoxidation rate exceeds the NO release rate (Schmidt et al., 1997). Moreover, autoxidation itself creates problems because it leads to the generation of reactive nitrosating agents (e.g., NO_2 and N_2O_3), and the rate of autoxidation at a given NO concentration will be approximately 10-fold higher in the hyperoxic environment in which cells are maintained in vitro than it would be in vivo (Ford et al., 1993; Augusto et al., 2002).

Clearly, methods are needed for applying NO in the controlled manner that would be axiomatic for meaningful studies of the biology of other signaling molecules. To try to address this problem, an apparatus for maintaining "clamped" NO concentrations has been designed (Zhelyas-kov and Godwin, 1999), but it is complex, expensive to construct, and unsuited to most biological applications. In principle, steady NO concentrations can be achieved by marrying a constant rate of NO production with an appropriate rate of inactivation. We recently exploited this concept by using red blood cells as biological NO sinks, which allowed for the determination of the absolute and relative sensitivities of the purified lung GC-coupled receptor and mitochondrial respiration to NO (Bellamy et al., 2002). Nevertheless, the method has several limitations, including the following: 1) having to prepare a washed red blood cell suspension for each experiment; 2) a slow increase of the NO level to plateau concentrations (60 s) so that, for rapid kinetics experiments, additions need to be made to a pre-equilibrated mixture in a small enough volume not to disturb the equilibrium, which limits the scope of the technique; 3) even a small leakage of free hemoglobin could compromise the experiment, because free hemoglobin inactivates NO at a much higher rate than when the protein is packaged in red blood cells (Liu et al., 1998); and 4) possible interference from bioactive substances taken up into, or released from, the red blood cells.

To address these and other limitations we sought to devise a cell-free method for generating steady NO concentrations covering the presumed physiological range (0–100 nM). This was achieved satisfactorily using the combination of a NONOate donor and the chemical NO scavenger CPTIO. When used to address one key issue in NO biology, namely the sensitivity of the GC-coupled receptors to NO, the new method gave results that differed in important ways from those obtained previously using red blood cells to provide the clamped NO concentration.

Materials and Methods

Materials. SPER/NO, DEA/NO, DETA/NO and CPTIO were all obtained from Alexis Corporation (Bingham, Nottingham, UK). All other reagents were obtained from Sigma Chemical (Poole, Dorset,

UK). NO donor stock solutions were made in 10 mM NaOH and kept on ice until use. Uric acid (30 mM) was dissolved in 60 mM NaOH and kept at room temperature. Stocks of CPTIO (20 mM) and superoxide dismutase (100,000 U/ml) were prepared in water and stored on ice until use. Ferrous oxyhemoglobin was prepared as described previously (Martin et al., 1985).

Measurement of NO. NO concentrations were recorded in buffer (1 ml) incubated in a sealed, stirred vessel (at 37°C) equipped with an NO electrode (Iso-NO; World Precision Instruments, Stevenage, Hertfordshire, UK). The rate of NO release from SPER/NO was measured by the addition of 10 μM of the donor to 50 mM Tris-HCl buffer containing 1000 U/ml superoxide dismutase (pH 7.4 at 37°C). After the 15 to 30 s required for the electrode response to settle (see *Results*), the measured NO concentration increased linearly for approximately another 60 s until autoxidation became significant as the NO concentration exceeded 250 nM. The NO release rate was obtained by measuring the gradient between 30 and 60 s after the addition of the donor.

Measurement of NO-Evoked GC Activity. Experiments were carried out in 50 mM Tris-HCl buffer supplemented with 1000 U/ml superoxide dismutase, 300 μM uric acid, 3 mM $MgCl_2$, 0.1 mM EGTA, 0.01 mM DTT, 0.05% bovine serum albumin, and 1 mM GTP, pH 7.4 at 37°C, and, except when DEA/NO was used, CPTIO (200 μM unless specified otherwise). When cell extracts were assayed, the buffer also contained 5 mM creatine phosphate and 200 μg/ml of creatine kinase. Receptor protein purified from bovine lung (soluble guanylyl cyclase; Alexis) was diluted in a buffer, pH 7.4, containing 50 mM Tris-HCl, 1 mM DTT, and 0.5% bovine serum albumin to give a stock concentration of 5 μg/ml, which was stored on ice and subsequently diluted 1:100 into assay buffer maintained at 37°C. NO donor was added, and aliquots of the reaction mix were removed at intervals and inactivated in boiling buffer (50 mM Tris, 4 mM EDTA). To examine individual receptor isoforms, COS-7 cells were transfected with combinations of either the α1 and β1 subunits or the α2 and β1 subunits (both rat) as described previously (Gibb et al., 2003) and maintained for 48 h before harvesting by trypsinization. The cells were pooled, pelleted at 1500g for 5 min, and resuspended at 3 mg protein/ml in ice-cold lysis buffer, pH 7.4, containing 50 mM Tris-HCl, 0.1 mM DTT, and a protease inhibitor cocktail (complete mini EDTA-free; Roche Diagnostics, East Sussex, UK). After the addition of glycerol (to give 5%), the homogenate was frozen until use. The NO-evoked GC activity of the two isoforms was compared directly. The homogenates were thawed, stored on ice, and diluted 1:10 into assay buffer pre-equilibrated at 37°C. SPER/NO was added to achieve varying steady-state NO concentrations, and 2 min later, aliquots of the reaction mixture were removed and inactivated as described above. cGMP levels were quantified by radioimmunoassay. Data are given as means $\pm$ S.E.M., and results were analyzed using an unpaired Student's t test (two-tailed).

Mathematical Modeling. The chemical reactions on which the NO delivery method depends were incorporated into a mathematical model using the rate constants listed in Table 1. The model consisted of the following differential equations, where x is the number of moles of NO released per mole of SPER/NO:

TABLE 1

Reactions considered in the model

For the autoxidation reaction (reaction 5), the concentration of O_2 was assumed to be 185 μM (that of an air-equilibrated solution).

Reaction No.	Reaction	Rate Constant	Reference
1	SPER/NO → SPER + NO·	$k_1 = 2.96 \times 10^{-4} s^{-1}$	Keefer et al., 1996
2	NO· + CPTIO → CPTI + NO_2	$k_2 = 1.6 \times 10^4 M^{-1} s^{-1}$	Present study
3	NO_2 + NO· → N_2O_3	$k_3 = 1.1 \times 10^9 M^{-1} s^{-1}$	Hogg et al., 1995; Ford et al. 2002
4	NO_2 + NO_2 → N_2O_4	$k_4 = 4.5 \times 10^8 M^{-1} s^{-1}$	Hogg et al., 1995; Augusto et al., 2002
5	2NO· + O_2 → 2NO_2	$k_5 = 13.6 \times 10^6 M^{-2} s^{-1}$	Schmidt et al., 1997
6	NO_2 + urate → NO_2^- + urate· + H^+	$k_6 = 2 \times 10^7 M^{-1} s^{-1}$	Augusto et al., 2002; Ford et al., 2002

$$\frac{d[SPER/NO]}{dt} = -k_1[SPER/NO]$$

$$\frac{d[NO]}{dt} = k_1[SPER/NO]x - k_2[CPTIO][NO] - k_3[NO_2][NO]$$

$$- k_5[O_2][NO]^2$$

$$\frac{d[NO_2]}{dt} = k_2[CPTIO][NO] - k_3[NO_2][NO] - 2k_4[NO_2]^2$$

$$- k_6[urate][NO_2] + k_5[O_2][NO]^2$$

$$\frac{d[CPTIO]}{dt} = -k_2[CPTIO][NO]$$

$$\frac{d[urate]}{dt} = -k_6[urate][NO_2]$$

The equations were solved numerically using the adaptive Runge-Kutta algorithm in Mathcad (version 2001i; Adept Scientific, Letchworth, Herts, UK). Calculation of the NO concentrations registered by the electrode was carried out by multiplying the derived NO concentration by the factor $[1 - exp(-k_e t)]$, where k_e is the rate constant of the electrode (0.116 s^{-1}) (Griffiths and Garthwaite, 2001).

Results

Theoretical Considerations. To obtain clamped NO concentrations after release from a donor, the following simple consecutive reaction scheme can be considered:

$$Donor \xrightarrow{k_a} NO \xrightarrow{k_b} products$$
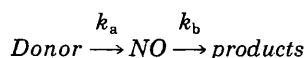
The equation describing the change in NO concentration over time is

$$[NO] = x[Donor]\frac{k_a}{k_b - k_a}(e^{-k_a t} - e^{-k_b t}) \qquad (1)$$

where x represents the number of moles of NO released per mole of donor. For an effectively constant rate of NO release (required to achieve steady NO concentrations), the donor must decompose slowly relative to the duration of the experiment. For the present purposes, NO concentrations that were steady over the time scale of a few minutes were desired, so SPER/NO, which has a half-life of 39 min at 37°C (Keefer et al., 1996), was selected. The corresponding rate constant for NO release from SPER/NO (k_a) is 2.96 × 10^{-4} s^{-1}.

To achieve rapid steady-state, the k_b value needs to be much greater than k_a, but not too large or the resulting NO concentrations would be too low to exert biological effects. When $k_b \gg k_a$, the steady-state NO concentration is given by

$$[NO] = \frac{k_a}{k_b} \times [SPER/NO] \qquad (2)$$

A k_b value on the order of 1 s^{-1} (imposing on NO a half-life of 0.7 s) would give rapid attainment of steady state (roughly within the mixing time of an experiment conducted manually) and would provide NO concentrations in the nanomolar range when micromolar concentrations of SPER/NO are added. Such a value of k_b renders insignificant any loss of NO

through autoxidation (e.g., at 100 nM NO, autoxidation would consume NO at a rate of only 25 pM/s, giving an NO half-life of 66 min). The sink needs to have the capacity to consume NO over the requisite time scale without significant exhaustion. With 100 μM SPER/NO and assuming $x = 1$ (see below), the initial rate of NO release (and consumption) would be approximately 1.8 μM/min, so sink concentrations in the 100 μM range are required. These considerations indicate that the sink needs to consume NO with a bimolecular rate constant of around 10^{-4}M^{-1}s^{-1}.

The nitronyl nitroxides 2-phenyl-4,4,5,5-tetramethylimidazoline-1-oxyl-3-oxide and its carboxylated derivative (CPTIO) are stable radicals that scavenge NO at approximately the required rate (Akaike et al., 1993). We chose to use CPTIO, the less cell-permeant of the two, to reduce possible unwanted intracellular effects when used with intact cells (although, to our knowledge, none has yet been described). Despite the NO being largely consumed extracellularly, the resulting extracellular and intracellular NO concentrations would be in dynamic equilibrium because of the fast rate of NO diffusion in lipid and aqueous environments. The reaction between NO and CPTIO forms the NO$_2$ radical, which is undesirable because it is a reactive oxidizing species that undergoes various reactions, including rapid combination with other radicals such as NO (Augusto et al., 2002). Therefore, NO$_2$ needs to be scavenged. Urate, an endogenous antioxidant (Becker, 1993) that converts NO$_2$ into NO$_2^-$ ($k = 2 \times 10^7$ M^{-1}s^{-1}) (Ford et al., 2002), was used for the purpose.

To analyze the reactions quantitatively, a more complex mathematical model was constructed using the rate constants given in Table 1. According to the model, with an initial CPTIO concentration of 200 μM, the addition of 300 μM SPER/NO results in a rapid increase of the NO concentration to 15 nM and the NO$_2$ concentration to 3 nM, both being stable over several minutes (Fig. 1). The inclusion of urate at the concentration found in plasma (300 μM) (Becker, 1993) leads to a doubling of the NO concentration (eliminat-
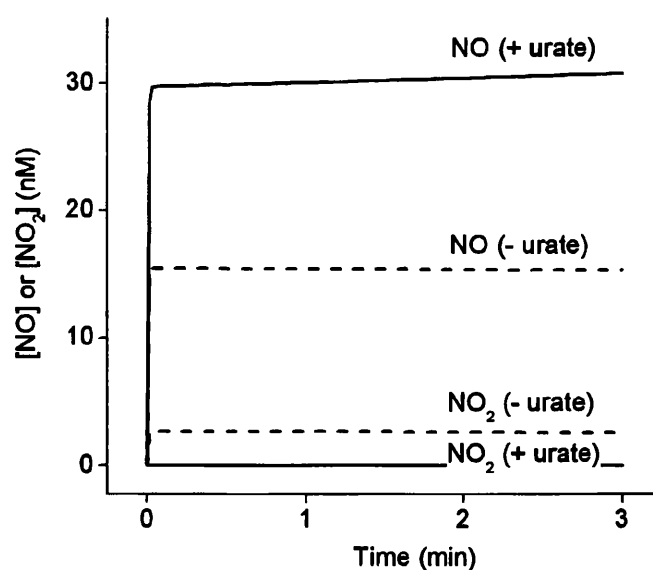
Fig. 1. Predicted profiles of the NO and NO$_2$ concentrations obtained by mixing 300 μM SPER/NO with 200 μM CPTIO in the absence (broken lines) and presence (solid lines) of 300 μM urate using the kinetic model described under *Materials and Methods*.

ing loss caused by a reaction with NO_2) and a reduction in the NO_2 concentration to 16 pM. Although included in the model for the sake of completion, the reaction of NO with O_2 is negligible compared with the reaction with CPTIO. In the presence of urate, therefore, the complex model reduces to the simple scheme outlined above (eqs. 1 and 2), providing that there is no significant depletion of NO donor or CPTIO. The mixture of urate, CPTIO, and SPER/NO (with the addition of 1000 U/ml of superoxide dismutase to scavenge any superoxide ions that would otherwise react with NO) was used for the experimental tests.

Evaluation of the Method for Delivering Clamped NO Concentrations. By measuring the initial rate of increase of the NO concentration after the addition of SPER/NO, the NO release rate was found to be 19.1 ± 0.8 nM NO/min/µM SPER/NO ($n = 3$). Assuming a SPER/NO half-life of 39 min, this value signifies 1.08 mol of NO released per mole of SPER/NO (x in eqs. 1 and 2 and in the more complex model). It is important to note that the rate of NO release from NONOates (including SPER/NO) can vary between different batches and between different suppliers (results not shown). Equation 2 predicts a linear relationship between the steady-state NO concentration and the donor concentration. To test this, SPER/NO was added in a range of concentrations, and the resulting profile of the NO concentration was measured using an electrochemical probe. The probe responds too slowly to register the rising phase accurately (see below), but increasing the SPER/NO concentration between 100 and 1000 µM produced graded increases in steady-state NO concentration from 10 to 100 nM (Fig. 2a). The amplitude of the plateau NO concentration (measured as the average recorded between 45 and 75 s after addition of SPER/NO) was directly proportional to the SPER/NO concentration (Fig. 2b). From the gradient of the line (10^{-4} M NO/M SPER/NO) and an x value of 1.08, the value of k_b comes to 3.2 s^{-1}. Dividing this pseudo-first-order rate constant by the CPTIO concentration (200 µM) gives a rate constant for the reaction of CPTIO with NO of 1.6×10^4 M^{-1}s^{-1} at 37°C, a value compatible with the published value of 1.01×10^4 M^{-1}s^{-1} at 25°C (Akaike et al., 1993).

A k_b value of 3.2 s^{-1} implies that 95% of the plateau NO concentration would be attained 1 s after the addition of SPER/NO (Fig. 2c), which is much faster than indicated by the electrode (Fig. 2a). If the time constant of the electrode (8.6 s) (Griffiths and Garthwaite, 2001) was incorporated into the model (see *Materials and Methods*), the shape of the recorded response was well approximated (Fig. 2c), suggesting that the sluggishness of the electrode accounts for the slow recorded rise time.

To explore the limitation of the method with respect to the time over which clamped NO concentrations can be maintained, recordings were made for more prolonged periods. With 100 µM SPER/NO, the NO concentration (initially approximately 10 nM) remained low for at least 50 min (Fig. 2d). With 300 µM SPER/NO, NO remained fairly steady for 10 to 15 min (at 30–40 nM) but then rose at a progressively increasing rate. With 1000 µM SPER/NO, the secondary increase in NO concentration was accelerated to the extent that there was initially more of a shoulder than a plateau (Fig. 2d). The recorded profiles of the NO concentration resemble those predicted by the more complex model (Fig. 3a), which suggests that the time over which NO can be main-
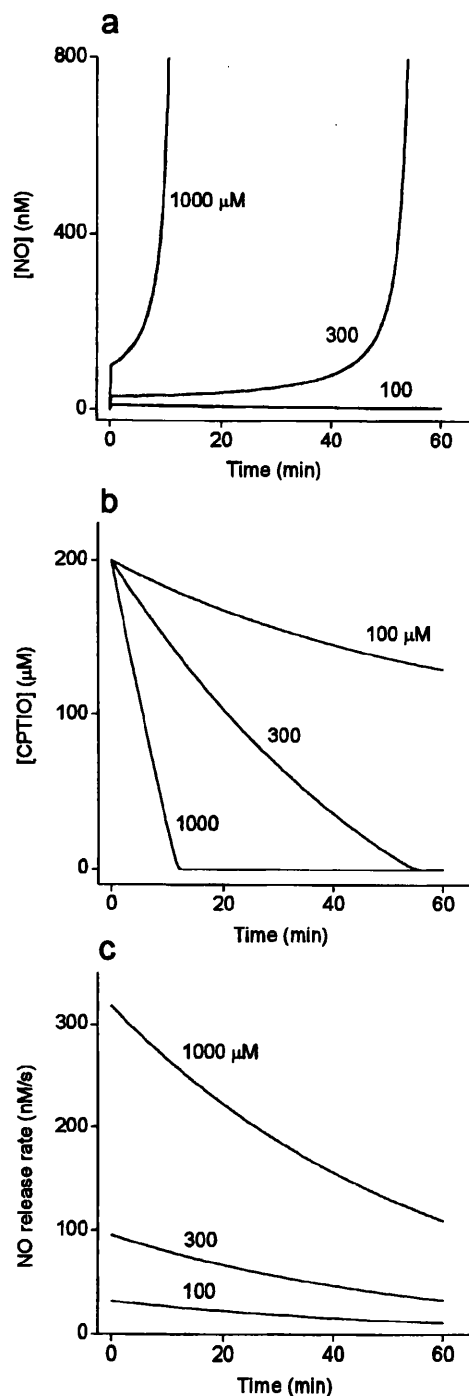
tained is a function both of the CPTIO concentration, which declines as it is used up (Fig. 3b), and the NO release rate, which reduces as the donor decomposes (Fig. 3c). At high SPER/NO concentrations, the former predominates, and as the CPTIO becomes depleted, the NO concentration eventually increases steeply (until curtailed by autoxidation to the low micromolar range) (data not shown). At low SPER/NO concentrations, on the other hand, the decreasing rate of NO release results in a gradually diminishing NO concentration. For example, at 100 µM SPER/NO, NO is predicted to decrease from 10 to 5.5 nM over 1 h. The measurement of such a change, however, is beyond the capability of the recording apparatus (Fig. 2d) whose quantifiable limit of detection is approximately 10 nM, depending on the particular electrode being used.

Application of the Method to Activation of GC-Coupled NO Receptors. To explore the usefulness of the method for biological purposes, we first investigated the kinetics of activation by NO of its GC-coupled receptor purified
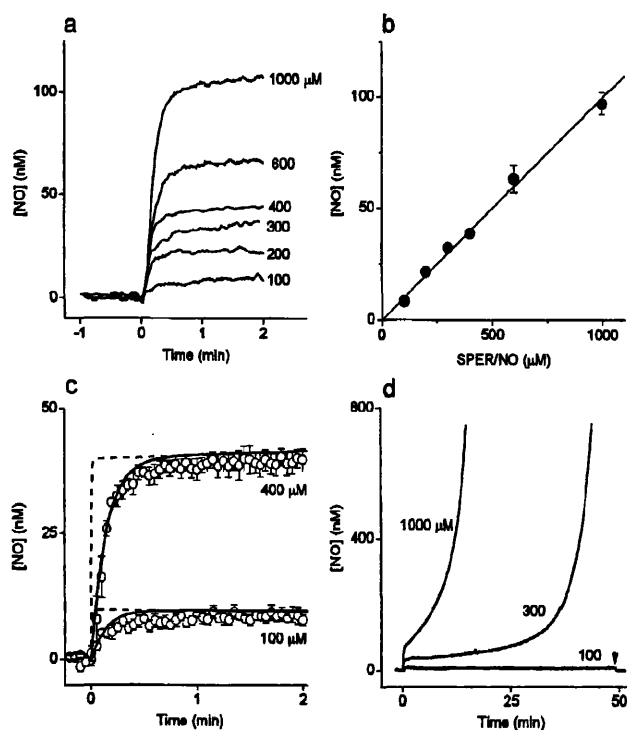
Fig. 2. Experimentally determined profiles of the NO concentrations resulting from the addition of SPER/NO in different concentrations to a mixture of 200 µM CPTIO and 300 µM urate. a, SPER/NO (100–1000 µM) was added at time = 0. The traces are representative of at least three individual experiments and were smoothed by adjacent averaging (5-s bins). b, amplitude of the steady-state NO concentration (measured as the average concentration between 45 and 75 s after the addition of SPER/NO) at different SPER/NO concentrations. Data are means ± S.E.M. ($n =$ 3–6) and are fitted by a linear function, which gives a slope of 10^{-4} M NO/M SPER/NO. c, comparison of the measured NO concentration profile obtained by adding 100 or 400 µM SPER/NO (data are means ± S.E.M., $n = 3$–4) with the profile predicted by the theoretical model with (solid line) or without (broken line) correction for the electrode response time. d, NO profiles over prolonged time intervals after the addition of 100, 300, and 1000 µM SPER/NO. In the case of 100 µM SPER/NO, hemoglobin (10 µM) was added at the arrowhead to remove NO. Records are single traces from one experiment. With 300 µM SPER/NO, the precise time at which NO started its secondary (almost vertical) ascent varied from test to test, even in the same experiment; this presumably reflects the cumulative effect of small variations in the initial CPTIO concentration and NO release rate on the time at which the CPTIO becomes exhausted (see Fig. 3).
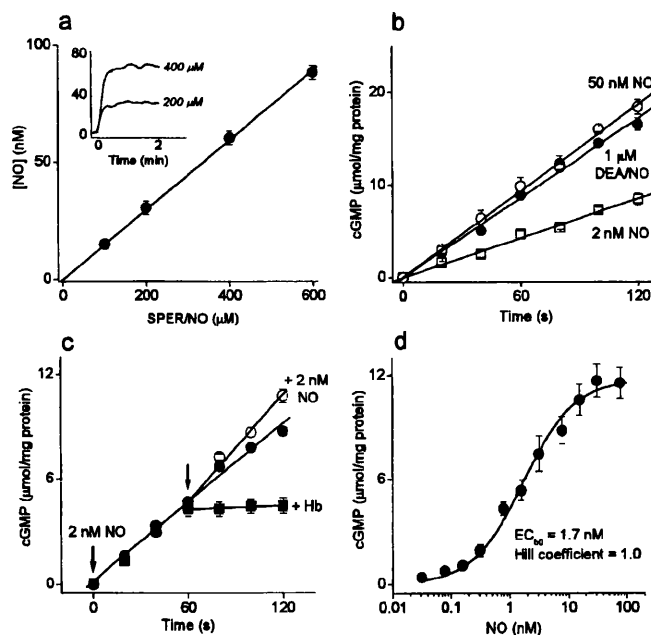
from bovine lung. Despite the more complex reaction mixture used for measuring GC activity (see *Materials and Methods*), the SPER/NO-CPTIO couple generated stable NO concentrations over a 2-min period that were linearly related to the SPER/NO concentrations (Fig. 4a). The slight difference in the slope compared with the simple buffer used previously (Fig. 2b) is probably attributable to the use of different

batches of both SPER/NO and CPTIO. NO concentrations in the GC reaction mixture were unaffected by the addition of receptor protein (data not shown).

Possible untoward effects of the new approach were investigated by comparing the time course of GC activity over 2 min at a maximally effective NO concentration produced by the SPER/NO-CPTIO couple (50 nM; see below) with that occurring on the addition of a supramaximal concentration of a donor used frequently in the past, DEA/NO (1 μM). The GC activity in each case was linear with time, and the slopes were not significantly different (approximately 10 μmol of cGMP/mg of protein/min; $P > 0.05$) (Fig. 4b). With DEA/NO, receptor activity cannot be monitored usefully at submaximal concentrations because the NO concentration changes rapidly and continuously (Bellamy et al., 2002). In contrast, using the SPER/NO-CPTIO couple, GC activity remained linear with time at the low NO concentration of 2 nM (Fig. 4b). The addition of a further 2 nM NO after 1 min increased the rate from 4.4 to 6.4 μmol/mg of protein/min, whereas addition of hemoglobin to scavenge NO led to an immediate cessation of GC activity (Fig. 4c), indicating that if any biologically significant variation in the NO concentration had occurred over time, it would have been detected.

Fig. 3. Predicted profiles of the NO concentration (a), the CPTIO concentration (b), and the NO release rate (c) after the addition of 100, 300, and 1000 μM SPER/NO for comparison with the experimental data shown in Fig. 2d. The curves were derived from the model described under *Materials and Methods*.

Fig. 4. Activation of the GC-coupled NO receptor under steady-state conditions. a, the mean NO concentrations present 45 to 75 s after the addition of SPER/NO in a range of concentrations to GC assay buffer containing CPTIO (200 μM) are plotted against the SPER/NO concentration and fit with a linear function. Data are means $\pm$ S.E.M. ($n = 4$). Inset, representative traces of the NO concentration profile with 200 and 400 μM SPER/NO, smoothed by adjacent averaging (5-s bins). b, time course of cGMP production by the receptor protein after exposure either to a SPER/NO-CPTIO mixture giving steady-state NO concentrations of 2 nM ($\square$) and 50 nM (O) or to 1 μM DEA/NO ($\bullet$). Data are fit with a linear function and are the means $\pm$ S.E.M. of three independent runs. c, cGMP accumulation after exposure of the receptor protein to 2 nM NO without further addition ($\bullet$) or with addition after 60 s (arrow) of either 25 μM hemoglobin (Hb) ($\blacksquare$) or a further 2 nM NO (O). Data are means $\pm$ S.E.M. ($n = 11$–12). d, equilibrium concentration-response curve for NO on the GC activity of the purified receptor protein. Data (means $\pm$ S.E.M., $n = 4$) were obtained after a 2-min exposure to a range of NO concentrations generated by adding various SPER/NO concentrations to a reaction mixture containing 200 μM CPTIO. Data are fit to the Hill equation, giving an EC$_{50}$ of 1.7 nM and a Hill coefficient of 1.0.

The concentration-response relationship was studied using 2-min exposures. The curve had a threshold of approximately 0.1 nM NO and displayed maximal activity at approximately 20 nM (Fig. 4d). It was well fitted by the Hill equation, with an EC_{50} of 1.7 nM and a Hill coefficient of 1.0.

With such low NO concentrations being effective, it is necessary to question whether the depletion of ligand through receptor binding could have distorted the results. Assuming a molecular mass of 150 kDa for GC and a single heme binding site on each protein (Denninger and Marletta, 1999; Koesling and Friebe, 2000), the total concentration of available binding sites at the protein concentration used (50 ng/ml) amounts to 0.33 nM, which is approximately 3-fold higher than the lowest effective NO concentration for GC activation (Fig. 4d). With normal methods of ligand application, therefore, ligand depletion would be significant and would have to be accounted for. To examine this issue using the present method of NO delivery, we incorporated reversible receptor binding into the model and assumed that the resultant GC activity was dependent on the concentration of the NO-bound species (see Fig. 5 legend for parameters). At 0.33 nM receptor, there would be negligible ligand depletion because the amount bound to the receptor is rapidly restored by NO release from the donor (Fig. 5a). Significant slowing of the attainment of the steady-state NO concentration and a resulting underestimate of GC activity is predicted to occur only with the receptor at concentrations 100-fold higher or more (Fig. 5, a and b).

To check that the concentration-response curve obtained for the purified receptor (Fig. 4b) was not peculiar to the use of SPER/NO as the donor, we evaluated the combination of diethylenetriamine/NO (DETA/NO; half-life = 20 h) and CP-TIO for the same purpose. To avoid the use of excessive DETA/NO concentrations, the concentration of CPTIO was decreased to 50 μM, allowing steady-state NO concentrations to be achieved in 4 s. As with SPER/NO, there was a linear relationship between the concentrations of DETA/NO and NO, the gradient being 4.6×10^{-5} M NO/M DETA/NO (data not illustrated). When the mixture was used to investigate the concentration-response curve for NO on purified lung GC (2-min exposure), the results (EC_{50} = 1.4 nM, Hill coefficient = 1.0; data not illustrated) were indistinguishable from those obtained using SPER/NO.

The established GC-coupled NO receptors are $\alpha\beta$ heterodimers, and the lung may contain both known isoforms, $\alpha1\beta1$ and $\alpha2\beta1$, with the former predominating (Mergia et al., 2003). Accordingly, the response of the purified lung protein may be a composite one. To examine the sensitivity of the separate isoforms to NO, they were expressed in COS-7 cells, and the NO-evoked GC activity was followed in cell lysates. The resultant maximal activity of the two isoforms was similar (Fig. 6, a and b). Moreover, the EC_{50} values for NO were also comparable (0.9 nM for $\alpha1\beta1$ and 0.5 nM for $\alpha2\beta1$). The slopes of both curves were described by a Hill coefficient of 1.1.

Discussion

Methodological Considerations. The method described here for delivering clamped NO concentrations is simple to use and requires chemicals that are available commercially, so it should find wide applications in NO research in which,

until now, it has been very difficult to administer this key signaling molecule in a manner that would be taken for granted in corresponding studies of other chemical messengers. There are, nevertheless, a number of real and potential limitations.

First, it is necessary to consider the biological reactivity of the ingredients and products other than NO. CPTIO has frequently been used as an NO scavenger to test for its participation in various biological phenomena, and we are unaware of any unrelated side effects. SPER/NO belongs to the much-used class of NONOate donor, but the carrier molecule, spermine, is an endogenous polyamine with biological activity (Bachrach et al., 2001). The rate of NO release from SPER/NO may also depend on constituents of the medium and on donor concentration (Davies et al., 2001), although we have not yet observed such inconsistencies (Figs. 2 and 4) and have obtained identical results with another donor (DETA/NO) not reported to exhibit this anomalous behavior (Davies et al., 2001). Other NONOates such as NOC-5 or NOC-12
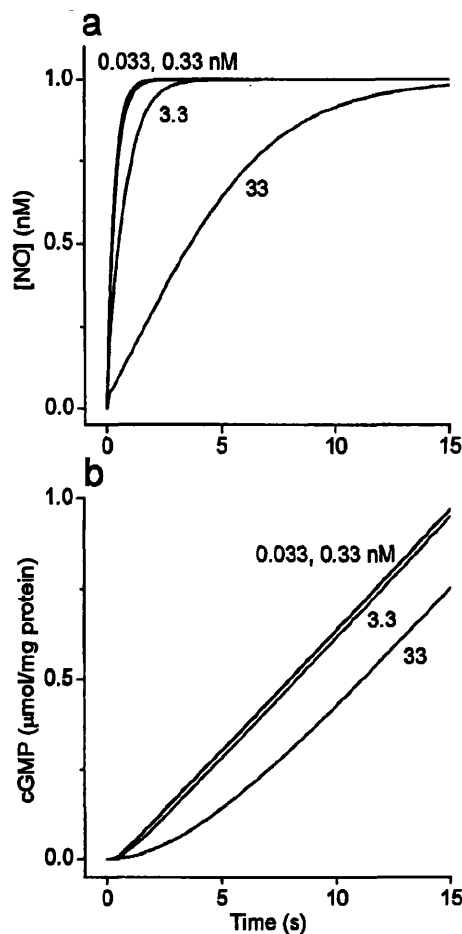
Fig. 5. Evaluation of the effect of ligand depletion on the measured activity of the GC-coupled NO receptor. NO delivery was modeled using 10 μM SPER/NO and 200 μM CPTIO, giving a steady-state NO concentration of 1 nM (see *Materials and Methods*). To investigate the depletion of NO through receptor binding, we assumed that NO binds with a bimolecular rate constant of 2.5×10^9 $M^{-1}s^{-1}$ (Zhao et al., 1999) and dissociates from the NO receptor complex with a rate constant of 3.7 s^{-1} (Bellamy and Garthwaite, 2001), giving an apparent K_d of 1.5 nM. The profiles of the NO concentration at receptor concentrations of 0.033 to 33 nM are shown in a. In each case, the corresponding profile of GC activity (b) was calculated by assuming that cGMP is formed from the NO receptor complex at a maximal rate (when all the receptors are occupied) equivalent to 10 μmol/mg of protein/min (Fig. 4b).
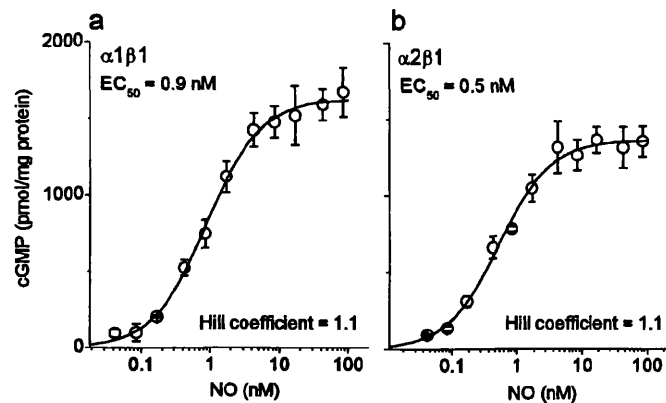
with half-lives of 25 and 100 min, respectively, could be used instead (http://www.dojindo.com/newprod/1/no/nodonors/nocsb.html). To deplete NO_2, urate was used at the concentration found in plasma (Becker, 1993) and so it can be regarded as a physiological ingredient. The fate and reactivity of the resulting urate radicals, however, are unclear, and it seems wise to limit their production. Finally NO_2^-, produced by the reaction of NO_2 with urate, will be formed at the same rate at which CPTIO is consumed. The NO_2^- concentration range found in human bodily fluids is 0.5 to 210 μM (Augusto et al., 2002), and it is relatively unreactive at neutral pH and therefore unlikely to create problems. Because of an overall lack of anticipated side effects, we recently used the method to analyze the kinetics of the NO-cGMP-phosphorylation pathway in suspensions of intact platelets (E. Mo, H. Amin, and J. Garthwaite., unpublished results) without encountering any problems.

Second, the method is limited in the range and duration of the NO concentrations obtainable. These two parameters are linked to the concentration and half-life of the donor and to the capacity of the sink. The immediate aim was to have a method that delivers fixed NO concentrations rapidly and maintains them over a time scale of minutes. With the combination of the donor and sink concentrations chosen, this objective was met for NO concentrations up to 100 nM. At this upper limit, the NO concentration was not constant but increased at a sufficiently slow rate to remain usable. For other types of experiments, exposures to NO of longer than a few minutes may be desirable. In this case, a donor with a longer half-life, such as DETA/NO (half-life 20 h), would be preferred. In this scenario, it is unlikely that the final NO concentration needs to be attained as rapidly as described here, so both donor and sink can be diluted to reduce the chemical flux. To illustrate the scope of such an application, Fig. 7 displays the predicted profile of the NO concentration obtained with a combination of 2 μM CPTIO and 3 to 10 μM DETA/NO. The time required for the initial equilibration of the NO concentration is approximately 2 min. With 3 μM DETA/NO, NO can be maintained at nearly 1 nM for at least 10 h, whereas at lower DETA/NO concentrations, the NO concentration decreases slowly as the donor decays. With 6
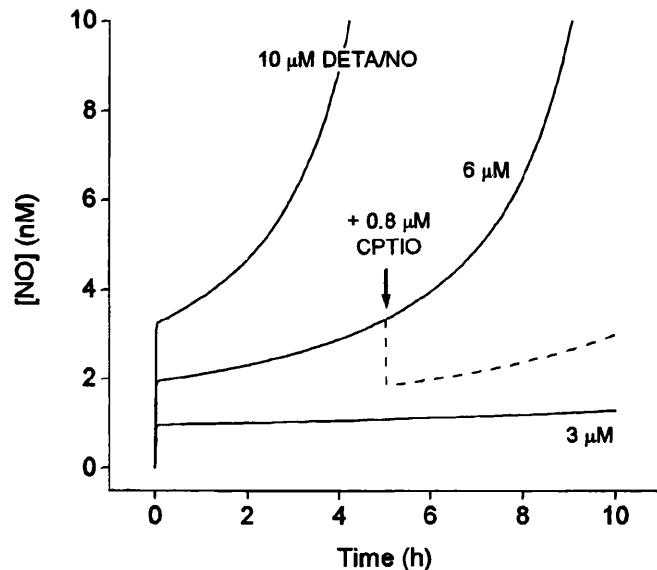
μM DETA/NO, the NO concentration is reasonably stable (2–3 nM) for approximately 5 h, but with 10 μM, the usable duration falls to approximately 1 h (3–4 nM NO). The duration can be extended quite easily by timely supplementation with fresh CPTIO, as illustrated for 6 μM DETA/NO in Fig. 7. Using essentially the same method, therefore, long exposures to physiological NO concentrations could be achieved.

The third methodological issue is variability. The precise value of the NO concentration obtained, and its duration, relies critically on the purity of the CPTIO and the release rate of NO from the donor. As mentioned earlier (see Results), we have noticed significant variation in the rate of NO released from NONOates depending on the particular batch and supplier used. In addition, the rate of decomposition of the NONOates depends on both temperature and pH (Davies et al., 2001). For this reason, it is essential that the pH of the buffers is adjusted at the temperature used for the experiment and that the buffers have a sufficient capacity to tolerate the addition of alkaline solutions (used to dissolve uric acid and the NONOates) or the production of protons (by the reaction of NO_2 with urate) without a change in pH. Finally, it should be noted that some cells can avidly consume NO (Griffiths and Garthwaite, 2001), which may necessitate the calibration of the NO delivery system in the presence of the cells under study.

Activity of GC-coupled NO Receptors Under Steady-State Conditions. In the past, a lack of control over NO concentrations has led to widely differing estimates of the potency of NO on its GC-coupled receptors. An initial estimate of the EC_{50} value, derived from the addition of NO from concentrated solutions, was ≤250 nM (Stone and Marletta, 1996), and the similar potency found for the NONOate DEA/NO in standard GC assays (approximately 300 nM)

Fig. 7. Theoretical NO concentration profiles over periods of hours produced by a combination of 2 μM CPTIO (instead of the usual 200 μM) and 3, 6, and 10 μM of the NONOate DETA/NO, which has a half-life of 20 h. In the case of 6 μM DETA/NO, the effect of adding a CPTIO supplement (0.8 μM) after 5 h (arrow) is illustrated by the broken line. Although at this time CPTIO is predicted to be 50% depleted, less than 50% of the starting concentration is needed to restore the NO concentration because the donor is also partially degraded. Curves were generated using the model described under *Materials and Methods*.

Fig. 6. Equilibrium concentration-response curves for NO on the GC activity of the $\alpha 1\beta 1$ (a) and $\alpha 2\beta 1$ (b) receptor isoforms in lysates of transfected COS-7 cells. Data (means ± S.E.M., $n = 3$) were obtained after a 2-min exposure to a range of NO concentrations generated by adding various SPER/NO concentrations to a reaction mixture containing 200 μM CPTIO. Data are fit to the Hill equation, giving EC_{50} values of 0.9 nM for $\alpha 1\beta 1$ and 0.5 nM for $\alpha 2\beta 1$ and a Hill coefficient of 1.1 for both.

(Russwurm et al., 1998) sustained the concept that physiological NO signaling involved NO concentrations in the 100 nM range. By monitoring the profile of NO release during the course of such assays, however, we found that a measured EC_{50} value of 300 nM for DEA/NO is compatible with the true potency of NO being in the low nanomolar range that had been suggested by a series of studies on intact cells from the brain (Bellamy et al., 2002). Furthermore, by using red blood cells to maintain constant NO concentrations, we obtained an EC_{50} of 4 nM for the purified lung receptor (Bellamy et al., 2002), suggesting that the high potency of NO in cells did not reflect some peculiarity of the protein in an intracellular environment. In addition, the slope of the concentration-response curve was unexpectedly steep (Hill coefficient of 2) which, if correct, would have important mechanistic implications for receptor activation in that it implies cooperative binding of two or more molecules of NO to each receptor.

Re-examination of this issue in the present study using the new NO delivery system supports the potency of NO for its receptor in lung being in the low nM range, although the actual EC_{50} value (~1.5 nM) was approximately 2-fold lower than that obtained using the red blood cell method (Bellamy et al., 2002). More importantly, the Hill coefficient was of the value (1) predicted for a single NO binding site. The discrepancy is best attributed to differences in the methodology and, in particular, to the former use of red blood cells. Any lysis of cells in the suspension would result in the release of free hemoglobin, which binds and inactivates NO far more avidly than when encapsulated in red blood cells (Liu et al., 1998). Although there was no evidence for free hemoglobin at the NO concentrations that were measurable ($\geq$5–10 nM) significant cell lysis (calculated to be 0.1% or greater) would preferentially impact the lower NO concentrations that could not be measured. Should this occur, the lower half of the concentration-response curve, which relied on predicted NO concentrations, would be artificially steepened, giving rise to an overestimate of the Hill coefficient. Such an effect would also explain the higher EC_{50} value obtained beforehand.

There had been no previous examination of the relative or absolute NO sensitivity of the individual $\alpha1\beta1$ and $\alpha2\beta1$ receptor isoforms in cell-free preparations. Concentration-response curves to DEA/NO were reported to be similar (Russwurm et al., 1998), but this result is equivocal (Bellamy et al., 2002). Nevertheless, a direct comparison using the new method indicated that the EC_{50} values for NO are closely comparable with each other (approximately 1 nM) and with the value obtained for the purified receptor protein from lung. We had previously found similar absolute potencies of NO toward the two isoforms when expressed in COS-7 cells (Gibb et al., 2003), but these estimates were complicated by receptor desensitization and bell-shaped concentration-response curves observed with the receptors in intact cells.

In conclusion, the kinetic parameters for activation of the GC-coupled NO receptor derived in this study are likely to be more reliable than those determined previously using the red blood cell method. The modified parameters obtained will simplify the development of models of receptor activation

because they eliminate the need for incorporating cooperative binding of NO to its receptor. More generally, the results support the usefulness of the new method for delivering physiological concentrations of NO to biological preparations in a reliable and reproducible manner, which should assist the analysis of NO signal transduction.

References

Akaike T, Yoshida M, Miyamoto Y, Sato K, Kohno M, Sasamoto K, Miyazaki K, Ueda S, and Maeda H (1993) Antagonistic action of imidazolineoxyl N-oxides against endothelium-derived relaxing factor/.NO through a radical reaction. *Biochemistry* **32:**827–832.

Augusto O, Bonini MG, Amanso AM, Linares E, Santos CC, and De Menezes SL (2002) Nitrogen dioxide and carbonate radical anion: two emerging radicals in biology. *Free Radic Biol Med* **32:**841–859.

Bachrach U, Wang YC, and Tabib A (2001) Polyamines: new cues in cellular signal transduction. *News Physiol Sci* **16:**106–109.

Becker BF (1993) Towards the physiological function of uric acid. *Free Radic Biol Med* **14:**615–631.

Beckman JS and Koppenol WH (1996) Nitric oxide, superoxide, and peroxynitrite: the good, the bad and the ugly. *Am J Physiol* **271:**C1424–C1437.

Bellamy TC and Garthwaite J (2001) Sub-second kinetics of the nitric oxide receptor, soluble guanylyl cyclase, in intact cerebellar cells. *J Biol Chem* **276:**4287–4292.

Bellamy TC, Griffiths C, and Garthwaite J (2002) Differential sensitivity of guanylyl cyclase and mitochondrial respiration to nitric oxide measured using clamped concentrations. *J Biol Chem* **277:**31801–31807.

Brown GC (1999) Nitric oxide and mitochondrial respiration. *Biochim Biophys Acta* **1411:**351–369.

Davies KM, Wink DA, Saavedra JE, and Keefer LK (2001) Chemistry of the diazeniumdiolates. 2. Kinetics and mechanism of dissociation to nitric oxide in aqueous solution. *J Am Chem Soc* **123:**5473–5481.

Denninger JW and Marletta MA (1999) Guanylate cyclase and the NO/cGMP signalling pathway. *Biochim Biophys Acta* **1411:**334–350.

Ford E, Hughes MN, and Wardman P (2002) Kinetics of the reactions of nitrogen dioxide with glutathione, cysteine and uric acid at physiological pH. *Free Radic Biol Med* **32:**1314–1323.

Ford PC, Wink DA, and Stanbury DM (1993) Autoxidation kinetics of aqueous nitric oxide. *FEBS Lett* **326:**1–3.

Gibb BJ, Wykes V, and Garthwaite J (2003) Properties of NO-activated guanylyl cyclases expressed in cells. *Br J Pharmacol* **139:**1032–1040.

Griffiths C and Garthwaite J (2001) The shaping of nitric oxide signals by a cellular sink. *J Physiol (Lond)* **536:**855–862.

Hogg N, Singh RJ, Joseph J, Neese F, and Kalyanaraman B (1995) Reactions of nitric oxide with nitronyl nitroxides and oxygen: prediction of nitrite and nitrate formation by kinetic simulation. *Free Radic Res* **22:**47–56.

Keefer LK, Nims RW, Davies KM, and Wink DA (1996) "NONOates" (1-substituted diazen-1-ium-1, 2-diolates) as nitric oxide donors: convenient nitric oxide dosage forms. *Methods Enzymol* **268:**281–293.

Koesling D and Friebe A (2000) Enzymology of soluble guanylyl cyclase, in *Nitric Oxide* (Mayer B ed) pp 93–109, Springer, Berlin.

Liu X, Miller MJ, Joshi MS, Sadowska-Krowicka H, Clark DA, and Lancaster JR Jr (1998) Diffusion-limited reaction of free nitric oxide with erythrocytes. *J Biol Chem* **273:**18709–18713.

Martin W, Villani GM, Jothianandan D, and Furchgott RF (1985) Selective blockade of endothelium-dependent and glyceryl trinitrate-induced relaxation by hemoglobin and by methylene blue in the rabbit aorta. *J Pharmacol Exp Ther* **232:**708–716.

Mergia E, Russwurm M, Zoidl G, and Koesling D (2003) Major occurrence of the new $\alpha_2\beta_1$ isoform of NO-sensitive guanylyl cyclase in brain. *Cell Signal* **15:**189–195.

Morley D and Keefer LK (1993) Nitric oxide/nucleophile complexes: a unique class of nitric oxide-based vasodilators. *J Cardiovasc Pharmacol* **22 (Suppl 7):**S3–S9.

Russwurm M, Behrends S, Harteneck C, and Koesling D (1998) Functional properties of a naturally occurring isoform of soluble guanylyl cyclase. *Biochem J* **335:**125–130.

Schmidt K, Desch W, Klatt P, Kukovetz WR, and Mayer B (1997) Release of nitric oxide from donors with known half-life: a mathematical model for calculating nitric oxide concentrations in aerobic solutions. *Naunyn Schmiedeberg's Arch Pharmacol* **355:**457–462.

Stone JR and Marletta MA (1996) Spectral and kinetic studies on the activation of soluble guanylate cyclase by nitric oxide. *Biochemistry* **35:**1093–1099.

Zhao Y, Brandish PE, Ballou DP, and Marletta MA (1999) A molecular basis for nitric oxide sensing by soluble guanylate cyclase. *Proc Natl Acad Sci USA* **96:**14753–14758.

Zhelyaskov VR and Godwin DW (1999) A nitric oxide concentration clamp. *Nitric Oxide* **3:**419–425.

Address correspondence to: Dr. John Garthwaite, The Wolfson Institute for Biomedical Research, University College London, Gower Street, London, WC1E 6BT, United Kingdom. E-mail: john.garthwaite@ucl.ac.uk

SPECIAL REPORT

Membrane-association and the sensitivity of guanylyl cyclase-coupled receptors to nitric oxide

[1]Victoria Wykes & *,[1]John Garthwaite

[1]The Wolfson Institute for Biomedical Research, University College London, Gower Street, London WC1E 6BT

Nitric oxide (NO) signal transduction occurs through guanylyl cyclase-coupled receptors, which exist in both cytosolic and membranous locations. It has recently been reported from experiments using heart tissue that the membrane-associated receptor has enhanced sensitivity to NO. Owing to its potential importance, we tested this finding using a method of applying NO in known, constant concentrations. The results showed that the concentration–response curves for receptor activation in cytosolic and membrane preparations of two different tissues (cerebellum and platelets) were indistinguishable. In all cases, half-maximal activation required about 1 nM NO and the curves had Hill coefficients of close to 1. The differential sensitivity reported for the heart is attributed to NO being scavenged by myoglobin in the cytosol, but not in the membrane fraction.
British Journal of Pharmacology (2004) 141, 1087–1090. doi:10.1038/sj.bjp.0705745

Introduction Nitric oxide (NO) functions as a signalling molecule in almost all tissues of the body and regulates diverse processes, including blood vessel dilatation, platelet function, and the induction of long-term changes in the strength of central synaptic transmission (Moncada et al., 1991; Garthwaite & Boulton, 1995). The established mechanism for physiological NO signal transduction in these and other processes is through guanylyl cyclase (GC)-linked receptors. The resulting increase in intracellular cGMP can engage multiple downstream targets, including kinases, ion channels, and phosphodiesterases, to elicit various biological effects. The known GC-coupled receptors are $\alpha\beta$-heterodimers of which two isoforms, $\alpha1\beta1$ and $\alpha2\beta1$, are widely expressed at the mRNA and protein levels (Friebe & Koesling, 2003). So far, the two isoforms have appeared functionally and pharmacologically similar, whether studied in intact cells or in cell lysates (Friebe & Koesling, 2003; Gibb et al., 2003; Griffiths et al., 2003). However, complexity might arise from differences in subcellular location. In this respect, early data showed that NO-evoked GC activity was present in varying amounts in the soluble (cytosolic) and insoluble (particulate) fractions of several tissues (Arnold et al., 1977) and recent evidence indicates that the $\alpha1\beta1$ receptor translocates to membranes in response to a Ca^{2+} signal (Zabel et al., 2002), whereas, in the brain, the $\alpha2\beta1$ isoform is targeted to membrane-linked synaptic scaffold proteins (Russwurm et al., 2001).

From a study using heart tissue, an association with membranes was reported to sensitise the receptors to NO (Zabel et al., 2002). If correct, this conclusion might be important because it could provide a device for modulating cellular responsiveness to NO and/or for concentrating

NO signal transduction into discrete subcellular domains analogous to those mediating conventional synaptic transmission. The result was based on differences in the concentrations of the NO donor, diethylamine/NO adduct (DEA/NO) needed to evoke GC activity in cytosol and membrane fractions. DEA/NO degrades to release NO with a half-life of 2.1 min (37°C). The amplitude, shape, and duration of the resulting NO concentration profile, however, is dependent on several factors, including pH and the rate of consumption of NO. Without rigorous checks, therefore, a shift in the DEA/NO concentration–response curve is difficult to interpret (Bellamy et al., 2002). Accordingly we have evaluated the veracity of the result using a method for delivering NO in known, fixed concentrations (Griffiths et al., 2003).

Methods *Tissue preparation* Adult female Sprague–Dawley rats (Charles River, Margate, U.K.) were anaesthetised with pentobarbitone (60 mg kg^{-1}, i.p.) as approved by the British Home Office and the local ethics committee. The animals were perfused through the left ventricle with PBS until the returning buffer ran clear. The cerebella and/or hearts were swiftly removed and immersed in ice-cold PBS. Adhering connective tissue and visible vasculature were discarded under a dissecting microscope and the tissues were then cut into 1 mm cubes using a McIlwain tissue chopper, before being frozen on dry ice and homogenised (while frozen) using a stainless-steel mortar and pestle, both precooled in dry ice. The heart tissue was resuspended at 3–4 hearts per 5 ml in ice-cold buffer A, which contained (mM): NaCl (137), MgCl$_2$ (0.5), NaH$_2$PO$_4$ (0.55), KCl (2.7), HEPES (25), glucose (5.6) and a protease inhibitor cocktail (complete mini EDTA-free; Roche, East Sussex, U.K.), pH 7.4. The cerebellar tissue was resuspended (at 3 per 5 ml) in buffer as before (Bellamy et al., 2000), except that the DTT concentration was reduced 10-fold to avoid problems

---

*Author for correspondence; E-mail: john.garthwaite@ucl.ac.uk

of NO consumption (Bellamy et al., 2002). The preparations were then centrifuged for 5 min at 500 g to remove cellular debris.

To obtain platelets, whole blood was collected from four adult Sprague–Dawley rats into acid citrate dextrose solution (12.5%) and centrifuged at 300 g for 10 min. The platelet-rich plasma was withdrawn and recentrifuged to eliminate residual red and white blood cells. The supernatant was centrifuged for 10 min at 2000 g and the platelet pellet was resuspended in buffer A at a final concentration of 1 mg protein ml^{-1}. The platelets were lysed by addition of an equal volume of ice-cold distilled water containing the protease inhibitor cocktail and 0.2 mM DTT, followed by sonication. The lysate was kept on ice.

Approximately 3 ml of each homogenate was centrifuged for 1 h at 100,000 g at 4°C. The supernatants (cytosols) were removed and kept on ice and the pellets (crude membrane fractions) were resuspended in the corresponding homogenisation buffers to a fifth to a tenth of the original homogenate volume. The protein concentrations were measured using the bicinchoninic acid method; for platelets and cerebellum, these values were measured in samples prepared in parallel but lacking DTT (which interferes with the protein assay).

Measurement of GC activity The activity of the GC-coupled receptors in the different preparations was measured by exposing them to constant concentrations of NO, using a new method (Griffiths et al., 2003) in which NO release from a NONOate donor, in this case spermine/NO adduct (Alexis Biochemicals, Nottingham, U.K.), is balanced by NO consumption by a chemical scavenger 2-4-carboxyphenyl-4,4,5,5-tetramethylimidazoline-1-oxyl-3-oxide (CPTIO; Alexis Biochemicals). Aliquots of the tissue fractions were diluted 1:10 into an assay buffer containing 50 mM Tris-HCl, 3 mM MgCl$_2$, 0.1 mM EGTA, 0.01 mM DTT, 0.05% BSA, 1 mM GTP, 0.2 mg ml^{-1} creatine kinase, 5 mM creatine phosphate, 1 mM 3-isobutyl-1-methylxanthine, 200 μM CPTIO, 1000 U ml^{-1} superoxide dismutase, and 300 μM uric acid (pH 7.4 at 37°C). Spermine/NO adduct was added from concentrated stock solutions (in 10 mM NaOH) to achieve varying steady-state NO concentrations (achieved within about 1 s) and, 2 min later, 100 μl of the reaction mix was removed and inactivated by addition to 200 μl of boiling hypotonic buffer (50 mM Tris HCl, 4 mM EDTA). cGMP was measured using radioimmunoassay. Results are given as the mean cGMP levels from '*n*' independent estimations $\pm$ s.e.m. Each concentration-response curve was fitted to the Hill equation (in the Origin™ version 6.1; Aston Scientific Ltd, Stoke Mandeville, U.K.) to obtain values of the EC$_{50}$ and Hill coefficient. Averaged data were analysed for significance using the unpaired Student's *t*-test (two-tailed). To scrutinise the results obtained by Zabel et al. (2002), the GC reaction mixture was changed to the one they used (with 1000 U ml^{-1} superoxide dismutase as an additional ingredient) and DEA/NO was used as the donor. The methods otherwise were as detailed above, except that the tissue fractions were diluted 1:100 into the reaction mixture and aliquots were sampled for cGMP determination at 1 min intervals for a total of 10 min.

NO measurement NO concentrations were recorded in buffer A (1 ml) supplemented with 1000 U ml^{-1} superoxide dismutase

and incubated in a sealed, stirred vessel (37°C) equipped with an NO electrode (Iso-NO, World Precision Instruments, Stevenage, U.K.).

Results We initially selected tissue from a brain region (the cerebellum) in which the NO-cGMP pathway is highly expressed (Garthwaite & Boulton, 1995). NO elicited GC activity in both cytosolic and membrane fractions of the cerebellum, with the former dominating (Figure 1a). Concentration–response curves were constructed using NO delivered in known, constant concentrations (Griffiths et al., 2003). In both fractions, the threshold NO concentration required to stimulate GC activity was 50–100 pM and the maximum response occurred at about 10 nM (Figure 1a). The concentrations giving half-maximal activity (the EC$_{50}$ values) were very similar (0.94$\pm$0.09 nM in the cytosol and 1.09$\pm$0.15 nM in the membranes, $n=4$; $P>0.4$), as were the Hill slopes (1.1$\pm$0.1 and 0.9$\pm$0.1; $P>0.2$). Accordingly, when normalised, the two curves were superimposable (Figure 1b).

In case the cerebellum behaved unusually, the experiments were repeated using blood platelets, a well-known target for NO (Schwarz et al., 2001). The concentration-response curves for cytosol and membrane fractions were again closely similar (Figure 2a,b). The respective EC$_{50}$ values (0.90$\pm$0.12 nM and 1.23$\pm$0.04 nM; $n=3$–4) were not significantly different from each other ($P>0.07$), nor from the corresponding values in the cerebellum ($P>0.7$ and 0.4). The Hill coefficients (1.2$\pm$0.2 and 1.1$\pm$0.03) were also no different from each other ($P>0.6$) or from the cerebellar values ($P>0.3$ and 0.1).

The experiments leading to the general conclusion that membrane association sensitises the receptors to NO were conducted on the rat heart (Zabel et al., 2002). In view of the above negative findings, we began to investigate the possibility that the phenomenon might be peculiar to this organ. However, it soon became evident that such an undertaking would be compromised. A homogenate of three rat hearts (previously perfused thoroughly *in situ* to wash out red blood cells) in 5 ml buffer was used to prepare concentrated membrane and cytosol fractions. The membrane fraction was
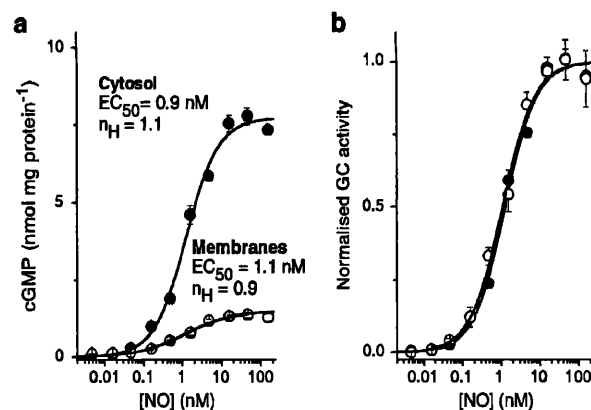
Figure 1 Comparison of the sensitivity of GC-coupled NO receptors in membrane and cytosol fractions of rat cerebellum. (a) Raw concentration–cGMP response curves for NO in cytosol and membrane fractions; $n=3$–4. The solid lines fit the data to the Hill equation; n_H signifies the Hill coefficient. (b) The same data normalised to the maximal GC activity in each case (derived from the Hill fits). Protein concentrations were 140 μg ml^{-1} (cytosol) and 290 μg ml^{-1} (membranes).
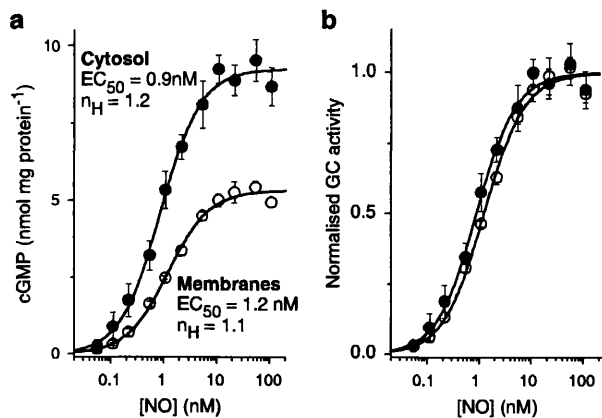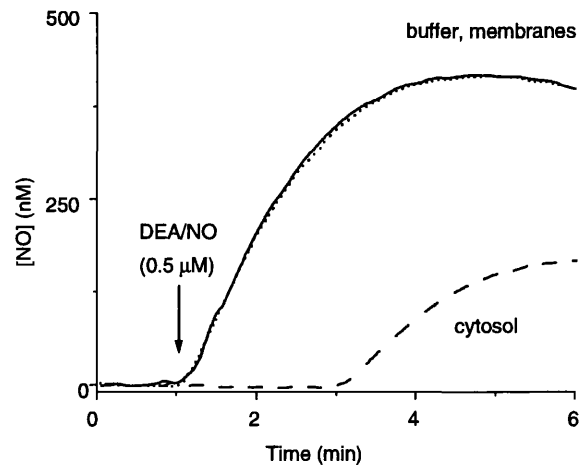
Figure 2 Comparison of the sensitivity of GC-coupled NO receptors in membrane and cytosol fractions of rat platelets. (a) Raw concentration–cGMP response curves for NO in cytosol and membrane fractions; $n = 4$. The solid lines fit the data to the Hill equation; n_H signifies the Hill coefficient. (b) The same data normalised to the maximal GC activity in each case (derived from the Hill fits). Protein concentrations were $13\,\mu g\,ml^{-1}$ (cytosol) and $40\,\mu g\,ml^{-1}$ (membranes).

Figure 3 Consumption of NO by heart cytosol. Data are recordings of the NO concentration profiles over time resulting from addition of DEA/NO ($0.5\,\mu M$; arrow) in buffer alone (solid line), or buffer containing the membrane fraction (dotted line) or the cytosolic fraction (dashed line) from rat heart. The traces are means of two runs and were smoothed by adjacent averaging (10 s bins). Protein concentrations were $130\,\mu g\,ml^{-1}$ (cytosol) and $50\,\mu g\,ml^{-1}$ (membranes).
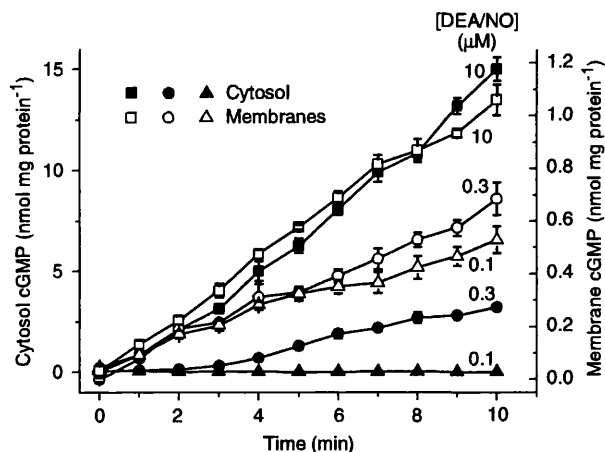
its usual milky-white colour, but the cytosol was bright red-pink due to the presence of myoglobin, a cytosolic protein expressed in sufficient abundance to give the heart its gross colour (Garry et al., 1998). NO reacts very rapidly with myoglobin, forming nitrate and metmyoglobin (Eich et al., 1996); consequently, the presence of significant quantities of myoglobin in the cytosol will reduce the amount of NO available for activating GC-coupled receptors. Hence, more NO would have to be added to match the degree of receptor activation taking place in the absence of myoglobin.

In order to evaluate this simple explanation for the results of Zabel et al. (2002), recordings were first made of the NO concentration profiles following addition of DEA/NO, the donor used to supply NO in the previous experiments. The DEA/NO concentration selected ($0.5\,\mu M$) was one evoking approximately half-maximal activation of GC-coupled NO receptors in the heart cytosol preparations during a 10 min incubation (Zabel et al., 2002). In buffer, the NO concentration rose to a peak of approximately 400 nM after about 3 min (Figure 3). Unfortunately, the dilution of heart cytosol used in the study of Zabel et al. was not disclosed, but when DEA/NO was added to a 1 : 100 dilution of the cytosol (giving a final protein concentration equivalent to that used for assaying GC activity in the cerebellar cytosol), NO was undetectable for about 2 min. Afterwards, the concentration rose to reach a plateau about three-fold lower than in buffer. On the other hand, when the test was repeated on the membrane fraction (similarly diluted), the NO profile was the same as in the buffer.

The method of assaying GC activity used by Zabel et al. was then applied to the heart fractions, except that the activity was followed at 1 min intervals for 10 min rather than at only a single time point (10 min). With a maximal DEA/NO concentration ($10\,\mu M$; Zabel et al., 2002), cGMP accumulated fairly linearly over the 10 min period in both fractions, with the GC activity being more than 10-fold higher in the cytosol than in the membranes (Figure 4). In the membranes, DEA/NO concentrations spanning the EC_{50} value reported by Zabel et al.

Figure 4 DEA/NO-induced cGMP accumulation in heart membranes and cytosol. The data show cGMP levels over time in response to addition of DEA/NO at the indicated concentrations to membranes or cytosol from rat heart; $n = 4$. Protein concentrations were $86\,\mu g\,ml^{-1}$ (cytosol) and $66\,\mu g\,ml^{-1}$ (membranes).

(2002), namely 0.1 and $0.3\,\mu M$, gave cGMP levels after 10 min that were, respectively, about 50 and 70% of the maximum. In the cytosol, the corresponding levels at this time were lowered to about 0 and 22%. These relative values are all closely similar to those reported by Zabel et al. (although, unfortunately, they did not disclose the absolute values). Inspection of earlier time points at the $0.3\,\mu M$ concentration, however, showed that, in the membranes, there was near-maximal GC activity over the first 2 min (when the rate of NO release is highest), followed by a decline. In contrast, in the cytosol, there was no measurable GC activity for the same initial period, with a slow rise occurring afterwards. Measurement of the NO concentration under the same conditions gave the

same result as before (Figure 3): on addition of DEA/NO (0.3 μM), NO rose immediately in the diluted membranes but was undetectable for about 2 min in the diluted cytosol (results not illustrated).

Discussion From the two different tissues examined in detail, we conclude that there is no discernable alteration in NO sensitivity of membrane-associated *versus* cytosolic GC-coupled receptors and that previous evidence that the two differ is spurious because, in the tissue examined (heart), the exposures to NO in the two fractions were different.

The concentration of myoglobin in the heart is about 200 μmoles (kg wet weight)$^{-1}$ (Godecke *et al.*, 1999) from which it can be estimated that the diluted cytosol used in our experiments would contain the protein in the upper 100 nM range. At the concentration of DEA/NO tested in Figure 3 (0.5 μM), NO would be released at an initial rate of about 2.8 nM s^{-1} (assuming a half-life of 2.1 min and 1 mole of NO released per mole of DEA/NO; Schmidt *et al.*, 1997). To scavenge NO for the period observed (2 min) would require 250 nM myoglobin, a concentration well within the range predicted to be present, even allowing for some of the protein being in its oxidised, unreactive, form (metmyoglobin). A similar period of NO consumption was observed at a lower DEA/NO concentration (0.3 μM) in another experiment (the one whose cGMP results are reported in Figure 4), which is explained by the protein concentration also being lower (see legends to Figures 3 and 4): assuming a proportionate

reduction in myoglobin concentration (to 165 nM) it can be calculated that NO released from 0.3 μM DEA/NO would be grounded for 2 min, as was observed. The same myoglobin concentration would consume all NO releasable from 0.1 μM DEA/NO.

The presence of such a powerful NO scavenger means, of course, that the receptor cannot become activated until the scavenger is exhausted, which explains why, in the heart cytosol, there was no GC activity for 2 min following addition of 0.3 μM DEA/NO and no activity at all during a 10 min exposure to 0.1 μM DEA/NO whereas, with no scavenger (in the heart membranes), these same concentrations were sufficient to evoke half-maximal, or greater, net GC activity. Unfortunately, the problem imposed by myoglobin in the heart cytosol would also apply to the other NO delivery method used here for the cerebellum and platelets (NO reacts with myoglobin 1000-fold faster than with CPTIO); a method for removing myoglobin is needed to conduct the experiment meaningfully.

Rather than regulate their sensitivity to NO, the subcellular distribution of the GC-coupled NO receptors may reflect a physical compartmentation of the signal transduction cascade, although the possibility that functional differences exist when the proteins are in their normal cellular environment *in vivo* cannot be excluded.

References

ARNOLD, W.P., MITTAL, C.K., KATSUKI, S. & MURAD, F. (1977). Nitric oxide activates guanylate cyclase and increases guanosine 3':5'-cyclic monophosphate levels in various tissue preparations. *Proc. Natl. Acad. Sci. U.S.A.*, **74**, 3203–3207.

BELLAMY, T.C., GRIFFITHS, C. & GARTHWAITE, J. (2002). Differential sensitivity of guanylyl cyclase and mitochondrial respiration to nitric oxide measured using clamped concentrations. *J. Biol. Chem.*, **277**, 31801–31807.

BELLAMY, T.C., WOOD, J., GOODWIN, D.A. & GARTHWAITE, J. (2000). Rapid desensitization of the nitric oxide receptor, soluble guanylyl cyclase, underlies diversity of cellular cGMP responses. *Proc. Natl. Acad. Sci. U.S.A.*, **97**, 2928–2933.

EICH, R.F., LI, T., LEMON, D.D., DOHERTY, D.H., CURRY, S.R., AITKEN, J.F., MATHEWS, A.J., JOHNSON, K.A., SMITH, R.D., PHILLIPS JR, G.N. & OLSON, J.S. (1996). Mechanism of NO-induced oxidation of myoglobin and hemoglobin. *Biochemistry*, **35**, 6976–6983.

FRIEBE, A. & KOESLING, D. (2003). Regulation of nitric oxide-sensitive guanylyl cyclase. *Circ. Res.*, **93**, 96–105.

GARRY, D.J., ORDWAY, G.A., LORENZ, J.N., RADFORD, N.B., CHIN, E.R., GRANGE, R.W., BASSEL-DUBY, R. & WILLIAMS, R.S. (1998). Mice without myoglobin. *Nature.*, **395**, 905–908.

GARTHWAITE, J. & BOULTON, C.L. (1995). Nitric oxide signaling in the central nervous system. *Annu. Rev. Physiol.*, **57**, 683–706.

GIBB, B.J., WYKES, V. & GARTHWAITE, J. (2003). Properties of NO-activated guanylyl cyclases expressed in cells. *Br. J. Pharmacol.*, **139**, 1032–1040.

GODECKE, A., FLOGEL, U., ZANGER, K., DING, Z., HIRCHENHAIN, J., DECKING, U.K. & SCHRADER, J. (1999). Disruption of myoglobin in mice induces multiple compensatory mechanisms. *Proc. Natl. Acad. Sci. U.S.A.*, **96**, 10495–10500.

GRIFFITHS, C., WYKES, V., BELLAMY, T.C. & GARTHWAITE, J. (2003). A new and simple method for delivering clamped nitric oxide concentrations in the physiological range: application to activation of guanylyl cyclase-coupled nitric oxide receptors. *Mol. Pharmacol.*, **64**, 1349–1356.

MONCADA, S., PALMER, R.M. & HIGGS, E.A. (1991). Nitric oxide: physiology, pathophysiology, and pharmacology. *Pharmacol. Rev.*, **43**, 109–142.

RUSSWURM, M., WITTAU, N. & KOESLING, D. (2001). Guanylyl cyclase/PSD-95 interaction: targeting of the NO-sensitive alpha2-beta1 guanylyl cyclase to synaptic membranes. *J. Biol. Chem.*, **276**, 44647–44652.

SCHMIDT, K., DESCH, W., KLATT, P., KUKOVETZ, W.R. & MAYER, B. (1997). Release of nitric oxide from donors with known half-life: a mathematical model for calculating nitric oxide concentrations in aerobic solutions. *Naunyn Schmiedebergs Arch. Pharmacol.*, **355**, 457–462.

SCHWARZ, U.R., WALTER, U. & EIGENTHALER, M. (2001). Taming platelets with cyclic nucleotides. *Biochem. Pharmacol.*, **62**, 1153–1161.

ZABEL, U., KLEINSCHNITZ, C., OH, P., NEDVETSKY, P., SMOLENSKI, A., MULLER, H., KRONICH, P., KUGLER, P., WALTER, U., SCHNITZER, J.E. & SCHMIDT, H.H. (2002). Calcium-dependent membrane association sensitizes soluble guanylyl cyclase to nitric oxide. *Nat. Cell Biol.*, **4**, 307–311.